

UNCLASSIFIED

AD NUMBER

AD889169

LIMITATION CHANGES

TO:

Approved for public release; distribution is unlimited.

FROM:

Distribution authorized to U.S. Gov't. agencies only; Test and Evaluation; NOV 1971. Other requests shall be referred to Army Electronics Command, Fort Monmouth, NJ 07703.

AUTHORITY

USAEC ltr 28 Apr 1972

THIS PAGE IS UNCLASSIFIED

AD889169L

Final Report

Covering the Period 1 September 1962 through 15 February 1970

RESEARCH ENGINEERING AND SUPPORT FOR TROPICAL COMMUNICATIONS

By: G. H. HAGN G. E. BARKER

*Distribution limited to U.S. Gov't. agencies only;
Test and Evaluation; 24 NOV 1971. Other requests
for this document must be referred to*

*U.S. ARMY ELECTRONICS COMMAND
FORT MONMOUTH, NEW JERSEY 07703*

Attn: AMSEL - RD-DO

*CONTRACT DA 36-039-AMC-00040(E)
Order No. 5384-PM-63-91*

Sponsored by

*ADVANCED RESEARCH PROJECTS AGENCY
ARPA ORDER 371*



STANFORD RESEARCH INSTITUTE
Menlo Park, California 94025 · U.S.A.

DISCLAIMER NOTICE

**THIS DOCUMENT IS THE BEST
QUALITY AVAILABLE.**

**COPY FURNISHED CONTAINED
A SIGNIFICANT NUMBER OF
PAGES WHICH DO NOT
REPRODUCE LEGIBLY.**



STANFORD RESEARCH INSTITUTE
Menlo Park, California 94025 U.S.A.

Final Report

February 1970

Covering the Period 1 September 1962 through 15 February 1970

RESEARCH ENGINEERING AND SUPPORT FOR TROPICAL COMMUNICATIONS

By: G. H. HAGN G. E. BARKER

Prepared for:

U.S. ARMY ELECTRONICS COMMAND
FORT MONMOUTH, NEW JERSEY 07703

CONTRACT DA 36-039-AMC-00040(E)
Order No. 5384-FM-63-91

SRI Project 4240

Approved by:

R. F. DALY, Director
Telecommunications Department

E. J. MOORE, Executive Director
Engineering Systems Division

Sponsored by

ADVANCED RESEARCH PROJECTS AGENCY
ARPA ORDER 371

"PRECEDING PAGE BLANK-NOT FILMED".

ABSTRACT

This report summarizes the results of the technical and scientific research effort on radio communications in the tropical environment conducted by the Stanford Research Institute under the SEACORE Program of the Advanced Research Projects Agency's Project AGILE [Contract DA 36-039 AMC-00040(E)]. The work included studies of HF ionospheric propagation and prediction; MF and HF atmospheric radio noise; HF and VHF propagation through tropical terrain including forests (jungle), paddy fields, and mountains; modeling and measurement of the directivity patterns of antennas emersed in forests; and the testing of selected communications equipments in the tropical environment.

"PRECEDING PAGE BLANK-NOT FILMED".

CONTENTS

ABSTRACT	iii
LIST OF ILLUSTRATIONS	ix
LIST OF TABLES	xvii
ACKNOWLEDGMENTS	xix
I INTRODUCTION	1
A. Historical Review	1
1. Prefacing Remarks	1
2. Laboratory Facility in Bangkok, Thailand . . .	2
3. Technical and Scientific Work.	4
B. Project Organization and Task Structure	6
C. Organization of Current Report.	7
II SUMMARY OF MAJOR TECHNICAL AND SCIENTIFIC FINDINGS . . .	11
A. Task A: Antenna-Environment and Antenna-System Investigations.	11
B. Task B: Ionospheric and Frequency-Spectrum Investigations.	13
C. Task C: System Test Format and Procedure Investigations.	15
III TASK A: ANTENNA-ENVIRONMENT AND ANTENNA-SYSTEM INVESTIGATIONS	17
A. Mathematical Model of Antennas in Forest Environment	17
1. Objective.	17
2. Background	17
3. The Forest-Slab Model.	19
4. Parametric Sensitivity Test.	22

B.	Measurements of Vegetation and Ground	
1.	Constants	30
2.	Vegetation Constants	30
2.	Ground Constants	47
C.	Full-Scale Antenna Pattern Measurements	54
1.	Objective.	54
2.	Background	54
3.	Measurement Technique.	61
4.	Results of Measurements at HF.	62
5.	Measurement Results at VHF	73
6.	Summary.	76
D.	Comparison of Measured Antenna Radiation Patterns in Forests with Model Predictions	79
1.	Objective.	79
2.	Background	79
3.	HF Antennas.	80
4.	VHF Antennas	85
5.	Summary.	85
E.	Antenna Relative-Gain Measurements with Vertical- Incidence Sounders.	88
1.	Objectives	88
2.	Background	89
3.	Measurement Technique.	90
4.	Results.	92
5.	Summary.	101
F.	Antenna Impedance Results	105
1.	Objective.	105
2.	Background	105
3.	HF Results	106
4.	VHF Results.	118
G.	VHF Xeledop System Loss Measurements.	120
1.	Manpack Xeledop System Loss Measurements . .	120
2.	Results.	121
3.	Balloon-Borne Xeledop Tests.	123
4.	Results.	123
H.	Single-Tree Studies	123
1.	Objectives	123
2.	Background	124
3.	Signal Level and Antenna Impedance Tests . .	125
4.	Scatter Pattern of an Isolated Tree.	127
5.	Use of a Tree as a Shunt-Fed, Grounded Vertical Antenna	127

IV	TASK B: IONOSPHERIC AND FREQUENCY-SPECTRUM INVESTIGATIONS	131
A.	Frequency Prediction.	131
1.	foF2 Predictions at Bangkok.	131
2.	Ionospheric Sounding Tests in Thailand over Oblique Paths from 230 to 1320 km.	138
B.	Ionospheric Signal Strength	144
1.	HF Propagation and Communication Tests in Thailand over Oblique Paths from 40 km to 1320 km.	144
2.	Dipole Orientation Effects	155
C.	Special Ionospheric Studies	163
1.	Faraday Rotation Studies	163
2.	Sudden Ionospheric Disturbances.	169
3.	Magnetic and Ionospheric Storms.	170
4.	Solar Eclipse Observation.	172
5.	Anomalous Ionospheric Reflections.	174
D.	Noise and Interference.	179
1.	ARN-3 Studies.	179
2.	Ratio of Signal-Plus-Noise to Noise on HF Field-Expedient Antennas	191
3.	Lightning-Flash Counter Studies.	193
4.	Interference Considerations.	198
V	TASK C: SYSTEM TEST FORMAT AND PROCEDURE INVESTIGATIONS	201
A.	Early Tests with HF Manpack Radios.	201
1.	Objective.	201
2.	Background	201
3.	Results.	202
B.	Tests with VHF Manpack Radios	205
1.	Forest Test near Bang Sapan, Thailand.	205
2.	Delta Tests near Bangkok, Thailand	206
3.	Forest Tests near Rayong, Thailand	207
4.	Forest and Varied-Terrain Tests near Chumphon, Thailand	209
5.	Antenna Substitution Tests with AN/PRC-25.	211
C.	Definition of Range of VHF Manpack Radios	212
1.	Objective.	212
2.	Background	212
3.	Results.	213

VI	RECOMMENDATIONS	215
A.	Technical Recommendations	215
B.	Future Work	215
Appendix A--DESCRIPTIONS OF FORESTED MEASUREMENT SITES IN THAILAND		219
Appendix B--PROJECT PERSONNEL		227
Appendix C--TECHNICAL REPORTS PREPARED UNDER THIS CONTRACT		233
REFERENCES		251
DISTRIBUTION LIST		255
DD Form 1473		

ILLUSTRATIONS

Figure I-1	Photograph of MRDC-EL in Bangkok.	3
Figure I-2	Map showing Thailand Field Sites.	5
Figure I-3	Project Flow Chart--By Task	9
Figure III-1	Nomenclature and Coordinates for Idealized Lossy Dielectric Slab Model	20
Figure III-2	Effective Antenna Length for Various Antenna Heights in Clearing and Forest.	24
Figure III-3	Effective Antenna Length as a Function of Height above Good Ground--Zenith.	25
Figure III-4	Effective Antenna Length as a Function of Antenna Height above Good Ground--Horizon . . .	26
Figure III-5	Effective Antenna Length at Zenith and Horizon as a Function of Forest Height-- $h_a = 0.03 \lambda$. . .	28
Figure III-6	Effective Antenna Length at Zenith and Horizon as a Function of Forest Dielectric Constant-- $h_a = 0.125 \lambda$	29
Figure III-7	Relative Power Distribution in the Vicinity of a 300- Ω Open-Wire Transmission Line	32
Figure III-8	Comparison of Measured Median Values of ϵ'_{ri} and δ'_1 at Five Thailand Sites	35
Figure III-9	Comparison of Median σ_1 and α_1 Measured in Undergrowth at Five Sites	36
Figure III-10	Lateral Wave Attenuation Constant Computed from OWL Measurements--as a Function of Frequency. . .	39

Figure III-11 Lateral Wave Attenuation Constant Computed as a Function of Frequency with Constant Conductivity.	41
Figure III-12 Lateral Wave Attenuation Constant Computed as a Function of Frequency, with Variable Conductivity.	42
Figure III-13 Permittivity as a Function of Willow Sample Weight.	45
Figure III-14 Variation of Attenuation Constant and Conductivity as a Function of Willow Sample Weight.	46
Figure III-15 Map of MF Ground Conductivity in Central, Eastern, and Northeastern Thailand (units in mmho/m)	50
Figure III-16 Median Surface Conductivity of Ground at Selected Sites in Thailand.	52
Figure III-17 Median Surface Ground Permittivity Measured at Selected Sites in Thailand.	53
Figure III-18 Sketches of Antennas Measured with the HF Airborne Xeledop.	56
Figure III-19 Measured Radiation Pattern of the 8 MHz, 23' High Unbalanced Dipole at Almanor--E _θ at 8 MHz.	63
Figure III-20 Measured Radiation Pattern of the 8 MHz, 23' High Unbalanced Dipole at Almanor--E _θ at 8 MHz.	64
Figure III-21 Measured Radiation Pattern of the 8 MHz, 23' High Unbalanced Dipole at Almanor--Power at 8 MHz	65
Figure III-22 Estimated Absolute Gain Versus Elevation Angle for the 8 MHz, 23' High Unbalanced Dipole Antenna at Lodi and Ban Mun Chit.	67
Figure III-23 Comparison of Measured Radiation Patterns of the Monopole Antennas at Lodi, Almanor, and Ban Mun Chit--E _θ at 6 MHz	68

Figure III-24 Estimated Absolute Gain Versus Elevation Angle for the Monopole Antennas at Lodi, Almanor, and Ban Mun Chit--E _θ at 6 MHz	69
Figure III-25 Measured Radiation Pattern of the 6 MHz 5:1 Inverted L Antenna at Ban Mun Chit--Power at 6 MHz	71
Figure III-26 Measured Radiation Pattern of the 6 MHz 30° Slant Wire Antenna at Ban Mun Chit--Power at 6 MHz	72
Figure III-27 Measured Amplitude Versus Azimuth Angle of 50-MHz VHF Antennas in a Eucalyptus Grove--8° Elevation	74
Figure III-28 Measured Amplitude Versus Azimuth Angle of 100-MHz VHF Antennas in a Eucalyptus Grove--8-Elevation	75
Figure III-29 Comparison of Measured and Calculated Effective Lengths for Dipole in Forest and in Open.	81
Figure III-30 Comparison of Measured and Calculated Median Radiation Patterns for the 16-ft High 6 MHz Unbalanced Dipole in the Foliage at Ban Mun Chit--E _θ at 6 MHz	83
Figure III-31 Comparison of Measured and Calculated Median Radiation Pattern for the 16-ft High 6 MHz Unbalanced Dipole in the Foliage at Ban Mun Chit--E _θ at 6 MHz	84
Figure III-32 Comparison of Measured and Calculated Median Radiation Pattern for the 75 MHz Unbalanced Dipole in the Forest at Ban Mun Chit--E _θ at 75 MHz	86
Figure III-33 Comparison of Measured and Calculated Median Radiation Pattern for the 75 MHz Unbalanced Dipole in the Forest at Ban Mun Chit--E _θ at 75 MHz	87
Figure III-34 Sketches of Special Dipole Configurations for Relative Gain Measurements.	91

Figure III-35 Relative Dipole Gain as a Function of Antenna Length.	99
Figure III-36 Comparison of Computed and Measured Dipole Gain Toward the Zenith as a Function of Antenna Height in Clearing and Forest	100
Figure III-37 Typical Relative Response Toward the Zenith of 6-MHz Field-Expedient Antenna	102
Figure III-38 Measured Dipole Gain Toward the Zenith as a Function of Antenna Height--At Several Sites. . .	103
Figure III-39 Measured Impedance of 8-MHz Horizontal Dipole in Clearing and Forest--as a Function of Frequency	107
Figure III-40 Measured Impedance of 6-MHz Horizontal Dipole in Clearing and Forest--as a Function of Length. . .	109
Figure III-41 Measured Impedance of 6-MHz Horizontal Dipole in Clearing and Forest--as a Function of Height.	110
Figure III-42 Measured Resistance of Balanced and Unbalanced 6-MHz Horizontal Dipoles in Clearing and Forest--as a Function of Height	111
Figure III-43 Measured Impedance of 6-MHz 30° Slant Wire in Clearing and Forest--as a Function of Frequency	113
Figure III-44 Measured Impedance of 6-MHz 5:1 Inverted L in Clearing and Forest--as a Function of Frequency	115
Figure III-45 Measured Impedance of 15.6-ft Monopole in Clearing and Forest--as a Function of Frequency .	116
Figure III-46 Measured Impedance of Tuned 15.6-ft Monopole in Clearing and Forest--as a Function of Frequency .	117
Figure III-47 Effect of Rubber Plantation on Received Signal as MPX is Carried into Forest	122

Figure III-48	Samples of the Received Signals in the Preliminary Study of the Scattering Properties of an Isolated Tree	126
Figure III-49	Measured and Calculated Input Impedance of 100-MHz $\lambda/2$ Dipole Versus Distance from Trees (height = 6.56 feet)	128
Figure III-50	Comparison of the Theoretical and Experimental Scatter Patterns of an Isolated Tree and Mast . .	129
Figure IV-1	Comparison of Observed and Predicted Monthly Median foF2 for a Typical Month	133
Figure IV-2	Median and Quartile Values of Error Function of ESSA foF2 Predictions from 1964 through 1967. . .	134
Figure IV-3	C-2 Versus Granger foF2 Readings at Bangkok, Thailand.	136
Figure IV-4	Percent of Time the Operating Frequency exceeds MOF on a Path of Length Less Than 50 km	137
Figure IV-5	Map of Sounder Sites in Thailand.	139
Figure IV-6	Results of Oblique-Incidence Ionospheric Soundings	142
Figure IV-7	MOF Factor as a Function of Local Time.	143
Figure IV-8	Block Diagram of CW Experiment Receiving and Recording System.	145
Figure IV-9	CW Received Signal Strength at Prachuab	147
Figure IV-10	Envelope Correlation Coefficient of Signals Received at Prachuab	147
Figure IV-11	CW Received Signal Strength at Nakon Sawan. . . .	148
Figure IV-12	Envelope Correlation Coefficient of Signals Received at Nakon Sawan	148

Figure IV-13	CW Received Signal Strength at Chiengmai	149
Figure IV-14	Envelope Correlation Coefficient of Signals Received at Chiengmai	149
Figure IV-15	S/N Ratio on Paths 2, 3, and 4 as a Function of Local Time	150
Figure IV-16	Time Delay Spread on Paths 2, 3, and 4 as a Function of Local Time.	152
Figure IV-17	Doppler Spread on Paths 2, 3, and 4 as a Function of Local Time.	153
Figure IV-18	Character Error Rate on Path 2 as a Function of Local Time.	154
Figure IV-19	QL and QT Regions	158
Figure IV-20	Ayudhaya: 1.7 MHz CW, All Transmitting/ Receiving Antenna Combinations.	159
Figure IV-21	Nakornpathom: 5 MHz CW, All Transmitting/ Receiving Antenna Combinations.	160
Figure IV-22	Example of Results of Polarization Diversity Test--Ayudhaya to Bangkok	162
Figure IV-23	Diurnal Variation of Electron Content and F-Layer Peak Electron Density and Solar Flux-- Descending Passes	165
Figure IV-24	Seasonal Variation of Peak Electron Content . .	167
Figure IV-25	Latitudinal Variation of Electron Content . . .	167
Figure IV-26	Diurnal Variation of Equivalent Slab Thickness and Mean Scale Height--Ascending and Descending Passes.	168
Figure IV-27	Percentage Change of foF2 During Ionospheric Storms.	173
Figure IV-28	Diurnal Variation of Percent of Time foEs at Bangkok Exceeds 3 MHz--September 1963 through May 1965.	176

Figure IV-29	foE_s and Percent Occurrence of Sporadic E at Local Noon as a Function of Latitude in Thailand.	177
Figure IV-30	Mass Plot of foE_s as a Function of Frequency of the C-2 and Granger Sounders at Bangkok.	178
Figure IV-31	Percent Occurrence of Spread F and Sporadic E at Songkhla, February 1967.	180
Figure IV-32	Quarterly Time Block Median of Noise Power (F_{am}) Observed at Laem Chabang during the Period March 1966 Through February 1968	184
Figure IV-33	Quarterly Time-Block Median of Noise Voltage Deviation (V_{dm}) Observed at Laem Chabang during the Period March 1966 Through February 1968	185
Figure IV-34	Month-Hour Values of Effective Antenna Noise Factor for 5.0-MHz Trapped Dipoles at Laem Chabang	186
Figure IV-35	Comparison of ARN-2 Monopole and Trapped Dipole Observed Noise with CCIR Report 322 Predictions, Laem Chabang, Thailand, Winter, 1967-1968	189
Figure V-1	Comparison of Performance of Sets Using Dipole, Slant-Wire, and Whip Antennas--All Tests in Thailand (Spring and Summer, 1963).	203
Figure V-2	Communication Success as a Function of Range for HC-162 (AN/PRC-74) in Mountain and Varied-Terrain	204
Figure V-3	Intelligibility Versus Distance for AN/PRC-35 (XC-3)--65 MHz.	214

"PRECEDING PAGE BLANK-NOT FILMED".

TABLES

Table III-1 Summary of Measured HF Antenna Pattern Data Available in STRs 10, 25, and 35.	57
Table III-2 Summary of Measured VHF Antenna Pattern Data Available in STRs 19 and 39D.	60
Table III-3 Relative Gain and Jungle Loss for 6.05-MHz Antennas at Ban Mun Chit	93
Table III-4 Relative Gain Data for 6-MHz Antennas at Chumphon.	96
Table III-5 Relative Gain Data for 4-MHz Antennas at Chumphon.	97
Table III-6 Relative Gain Data for 8-MHz Antennas at Chumphon.	97
Table III-7 Average Reflection Coefficients for Three Trees . .	127
Table IV-1 Sounder Site Operating Schedule	140
Table IV-2 Distribution of Difference (Δ) Between Observed and Predicted Noise Powers.	188
Table V-1 Characteristics and Effective Ranges for Radio Sets Tested in Delta.	208
Table V-2 Typical Improvement in AN/PRC-25 System Gain Obtained by Changing from Short to Long Whips . . .	212

"PRECEDING PAGE BLANK-NOT FILMED".

ACKNOWLEDGMENTS

Many organizations and individuals have contributed to the success of the SRI SEACORE program. Considerable effort was required to plan, coordinate, and carry out this complex project. It would be impossible to acknowledge properly all of the numerous assistances we have received. It is our pleasure to attempt to document and acknowledge the most significant of these contributions.

At the head of the list are the ARPA-AGILE Communications Program Managers (Washington, D.C.): Col. H. E. Tabor, Col. J. L. Jones, Col. G. J. Ackerland, and Col. T. W. Doeppner, under whose overall supervision the SEACORE program was conducted. Working closely with ARPA as contract service agent were the personnel of the U.S. Army Electronics Command (USAECOM), Fort Monmouth, New Jersey, under whose guidance the program has been conducted. The special attention and constant support given to this work by Mr. R. A. Kulinyi and his staff (especially the Contracting Officer's Technical Representatives, Mr. H. L. Kitts, and Mr. R. N. Herring, and also Mssrs. M. Acker, D. Dence, and K. Murphy) is especially appreciated.

In Thailand acknowledgment is due the Military Research and Development Center (MRDC), which includes representatives of the Thai Ministry of Defense and the ARPA. In particular, the support of the Commanding Generals of MRDC, Gen. Singchai Mensuta, RTA; Air Marshal Manob Suriya, RTAF; and Gen. Prasert Mokhaves, RTA; and the Communications Program Manager, Capt. Prapat Chandaket, RTN; and the other Thai personnel working on the communications program, including Commander Paibul Nacaskul, RTN; and Wing Commander Termpoon Kovattana, RTAF, is appreciated.

The ARPA (Bangkok) personnel included the Field Unit Directors Mr. T. W. Brundage and Dr. R. D. Holbrook, and Communication Program Managers Col. J. Scoggin, Lt. Col. P. Collom, Col. J. L. Jones, and Lt. Col. E. B. Howard. The assistance in Bangkok of Mr. C. W. Bergman of ARPA and Lt. Col. J. A. Kranz, Capt. K. M. Irish, and Lt. Col. J. Valenti of USAECOM during the initial phase of the work and Mr. R. K. Yee of ARPA and Lt. Col. A. P. Sidon of USAECOM during the final phases also is appreciated.

The responsiveness of the Sylvania Electronics Defense Laboratory, Mountain View, California, in providing the laboratory to SRI specification on a very short time scale is acknowledged--especially the efforts of Mr. C. Sibley and Mr. W. Bush.

The SRI and subcontractor personnel who carried out the work are listed in Appendix B.

I INTRODUCTION

A. Historical Review

1. Prefacing Remarks

Under Project AGILE, the Advanced Research Projects Agency (ARPA) of the U.S. Department of Defense has been providing research and engineering support to selected developing countries friendly to the United States. In the summer of 1962, the ARPA asked the U.S. Army Electronics Research and Development Laboratory (USAERDL), Fort Monmouth, New Jersey,* and the Stanford Research Institute (SRI), Menlo Park, California, to establish an electronics laboratory in Bangkok, Thailand, under a part of Project AGILE called SEACORE--a loose acronym for Southeast Asia Communication Research. The SRI SEACORE work had two objectives: first, to establish and operate a laboratory facility in Bangkok, Thailand, and assist Thai personnel toward the end goals of providing the Thai government with a research and development capability in communications/electronics; and second, in the course of this work, to perform research on various radio communication problems of mutual interest to Thailand and the United States.

The establishment of the laboratory facility in Bangkok will be discussed briefly, but the main purpose of this report is to summarize the results of the scientific and technical research work performed while the laboratory was under SRI directorship.

* The U.S. Army Electronics Research and Development Laboratory was later named the U.S. Army Electronics Laboratory and subsequently renamed the U.S. Army Electronics Command (USAECOM).

2. Laboratory Facility in Bangkok, Thailand

The laboratory facility was designed by SRI during the fall of 1962, built by the Sylvania Electronics Defense Laboratory in Mountain View, California, under contract to USAERDL, and shipped to Thailand in the spring of 1963. The main laboratory building consisted of three 8-ft x 8-ft x 28-ft air-conditioned shelters connected to form a tee (T). Four transportable air-conditioned field shelters were also provided, as well as power-generating equipment, and an extensive assortment of electronic test equipment providing a measurement capability from dc well into the microwave part of the spectrum.

The laboratory was installed at a temporary location in the Bangkapi section of Bangkok at 59 Petchburi Road extension. In addition to the T-van, the facility consisted of an adjacent generator house and a leased three-story office building. In August 1963 the U.S. Army Radio Propagation Agency, Fort Monmouth, New Jersey, provided a C-2 sounder for study of the equatorial ionosphere. Additional land was leased for an antenna farm, and the C-2 was installed adjacent to the T-van. Subsequently, one side of the T was filled in to form a store-room--see Figure I-1, a recent photograph. The present T-van complex (exclusive of the office building and C-2 sounder) provides about 2,000 square feet of usable floor space. Plans currently are being made for a permanent laboratory facility at another site in or near Bangkok.

The laboratory, originally a part of the joint Thai-U.S. agency called the Combat Development and Test Center (CDTC), had its official opening on 4 October 1963. The CDTC was established to conduct research and development in the tropical environment; consequently, the name was changed to the Military Research and Development Center (MRDC) early in 1964. The laboratory has been called the MRDC Electronics Laboratory (MRDC-EL) since that time.

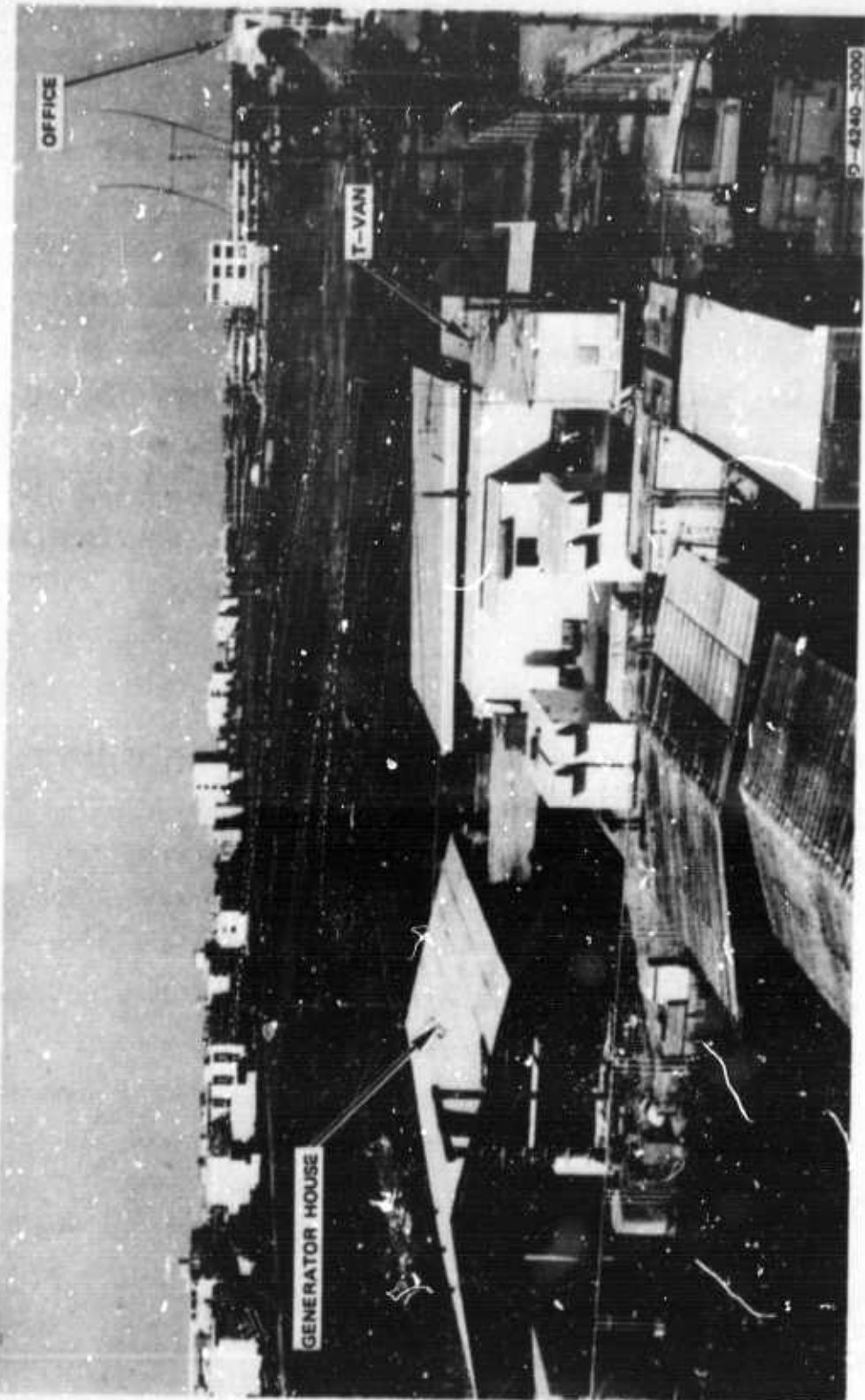


FIGURE I-1 PHOTOGRAPH OF MRDC-EL IN BANGKOK

The MRDC-EL was operated under SRI direction through 1967 (see Appendix B for staff listing). The development of the laboratory and its work during this initial phase have been described in the Semi-annual Reports prepared under Contract DA 36-039 AMC-00040(E), and in Final Report 1, Vol. 1 (see Appendix C).* The first phase of a transfer of the responsibility for the MRDC-EL to the Thai began in January 1968 under Contract DAAB 07-68-C-0194 (SRI Project 7163). Since that time SRI has played only a consultative and administrative role. Through the summer of 1969, three SRI staff members were consultants to the Thai Director and his staff on problems they are pursuing such as HF point-to-point communications, inter-village communications, etc. Since that time two SRI staff members have been assisting the MRDC-EL, and this effort is continuing under Contract DAAH-1-70-C-0550 (SRI Project 8326).

3. Technical and Scientific Work

The technical and scientific work in Thailand began in 1963--even before the arrival of the laboratory facility--with the testing of selected manpack radios. During the course of the project, work was performed on many different tasks (see Section I-B) at the MRDC-EL in Bangkok and at numerous remote sites (see Figure I-2). Field work in Thailand was completed in 1967, and analysis of most of the data obtained has been accomplished and the results reported in Special Technical Reports (see Appendix C). Several of these reports are still in preparation with USAECOM support under Contract No. DAAB 07-070-C-0220 (SRI Project 8663).

* References to reports on this contract will be made as discussed in Section 1-C and Appendix C. References to other material are given at the end of this report.



FIGURE I-2 MAP SHOWING THAILAND FIELD SITES

B. Project Organization and Task Structure

The SRI SEACORE effort originally was divided into three tasks. Task I (Operations Analysis Program) dealt with communications-oriented operations research and analysis. The results of this part of the program have been summarized in the Task I Final Report (dated December 1966) and will not be discussed further in this report. Task II (Scientific and technical Investigations) dealt with establishing the MRDC Electronics Laboratory and with the various scientific and technical tasks undertaken by the MRDC-EL in Bangkok and the SRI Communication Laboratory in Menlo Park, California. Task III (CONUS Support) dealt with supporting the MRDC-EL. The purpose of this report is to summarize the results obtained under Task II (and Task III, which was merged with Task II early in the program).

During the course of the SRI SEACORE work, the efforts under Task II were grouped under various subtasks, and these subtasks were continually reviewed and redefined as the program developed. The final set of Technical Guidelines (dated 20 May 1966) divided the work between three tasks:

Task A--Antenna Environment and Antenna System Investigations

Task B--Ionospheric and Frequency Spectrum Investigations

Task C--System Test Format and Procedure Investigations.

All of the work performed under the original Task II will be summarized
in this report under this final task structure.

* It should be noted that the work indicated in the 20 May 1966 Technical Guidelines under Task C was not funded and hence was not undertaken. This task heading is relatively descriptive of some of the work performed under other (earlier) subtasks, and it will be used in this report for the purpose of discussing such work.

A detailed flow chart has been prepared to assist the reader in following the Task II work progress chronologically in the context of this structure (see Figure I-3). Each block in the chart indicates a significant step in the work, and the corresponding report numbers are given at the bottom of each block. Those blocks which are not connected to others represent technical tasks performed as direct support to MRDC. This chart, together with the list of reports, provides a guide and reference to the work performed on this contract.

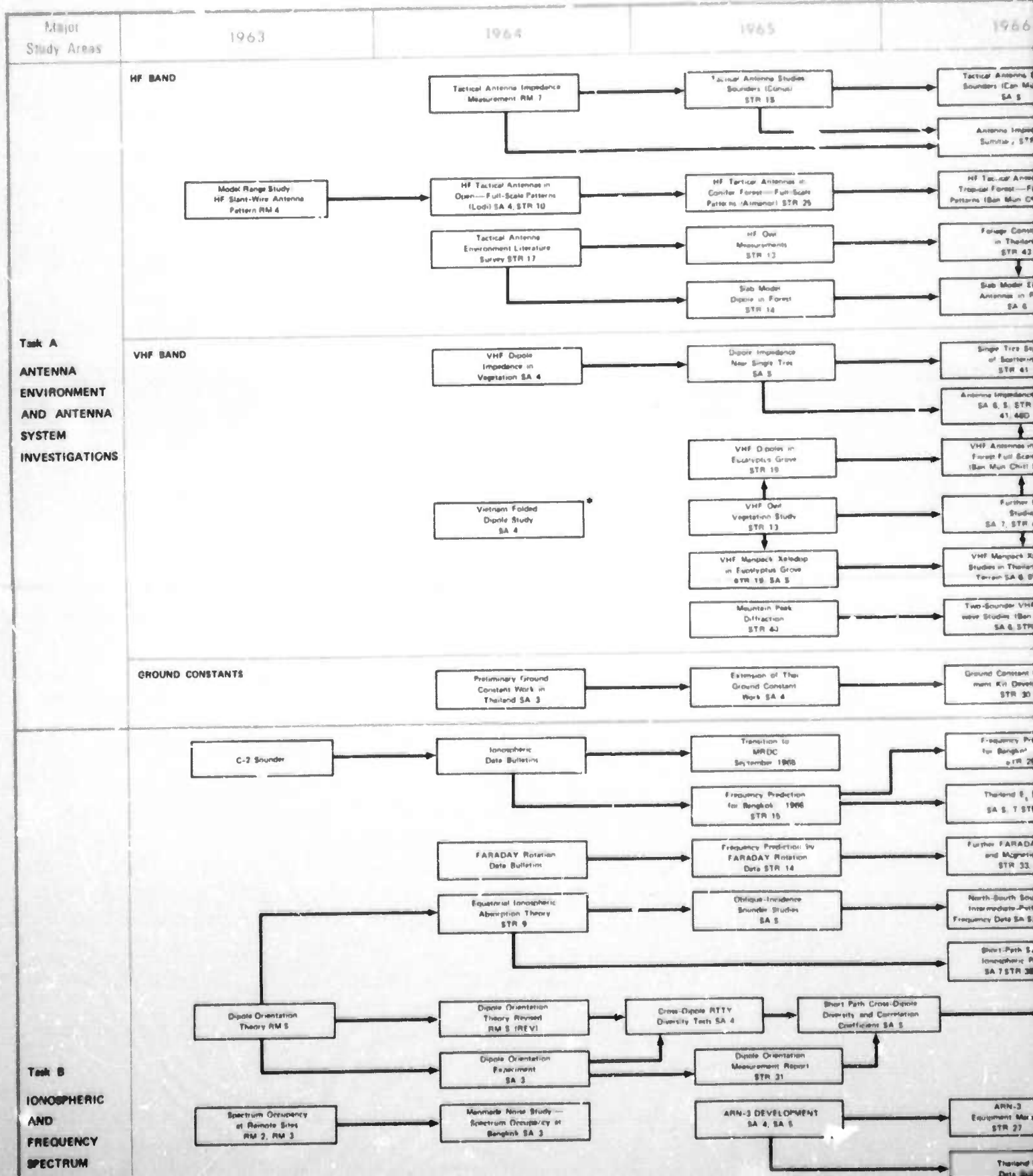
C. Organization of Current Report

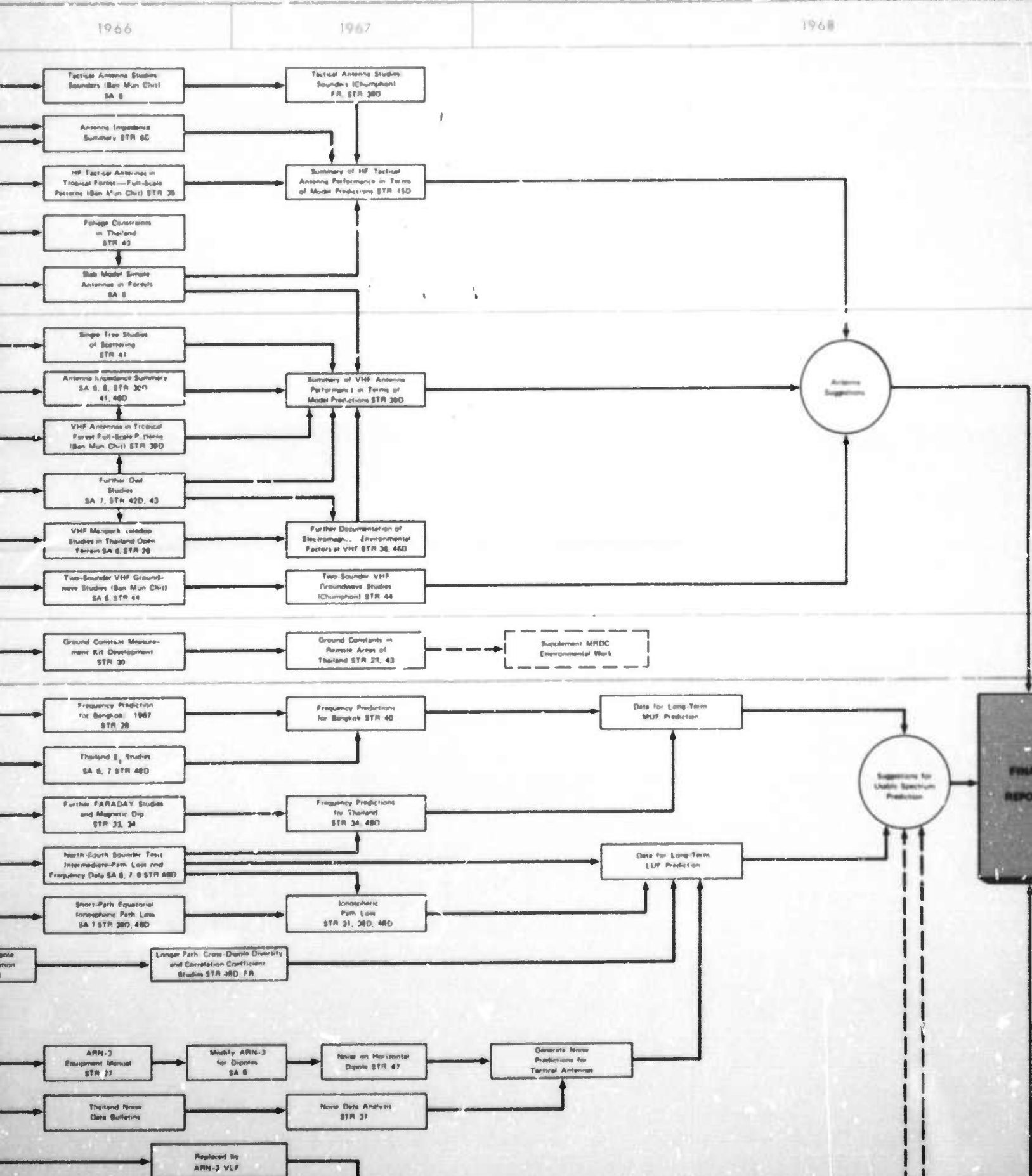
The major technical and scientific results are summarized in Section II. The remainder of this report is organized along the lines of the final task structure, with Sections III, IV, and V summarizing the results obtained under Tasks A, B, and C, respectively.

Numerous reporting techniques and report categories have been employed on this project, and they are described in Appendix C--which includes a list of the reports. References in the text of this report to Research Memoranda (RM's), Special Technical Reports (STR's), and Semiannual Reports (SAR's) prepared on this contract will be made by simply giving the report number in parenthesis (e.g., STR 1). Applicable reports also will be referenced in this manner at the beginning of each major subsection.

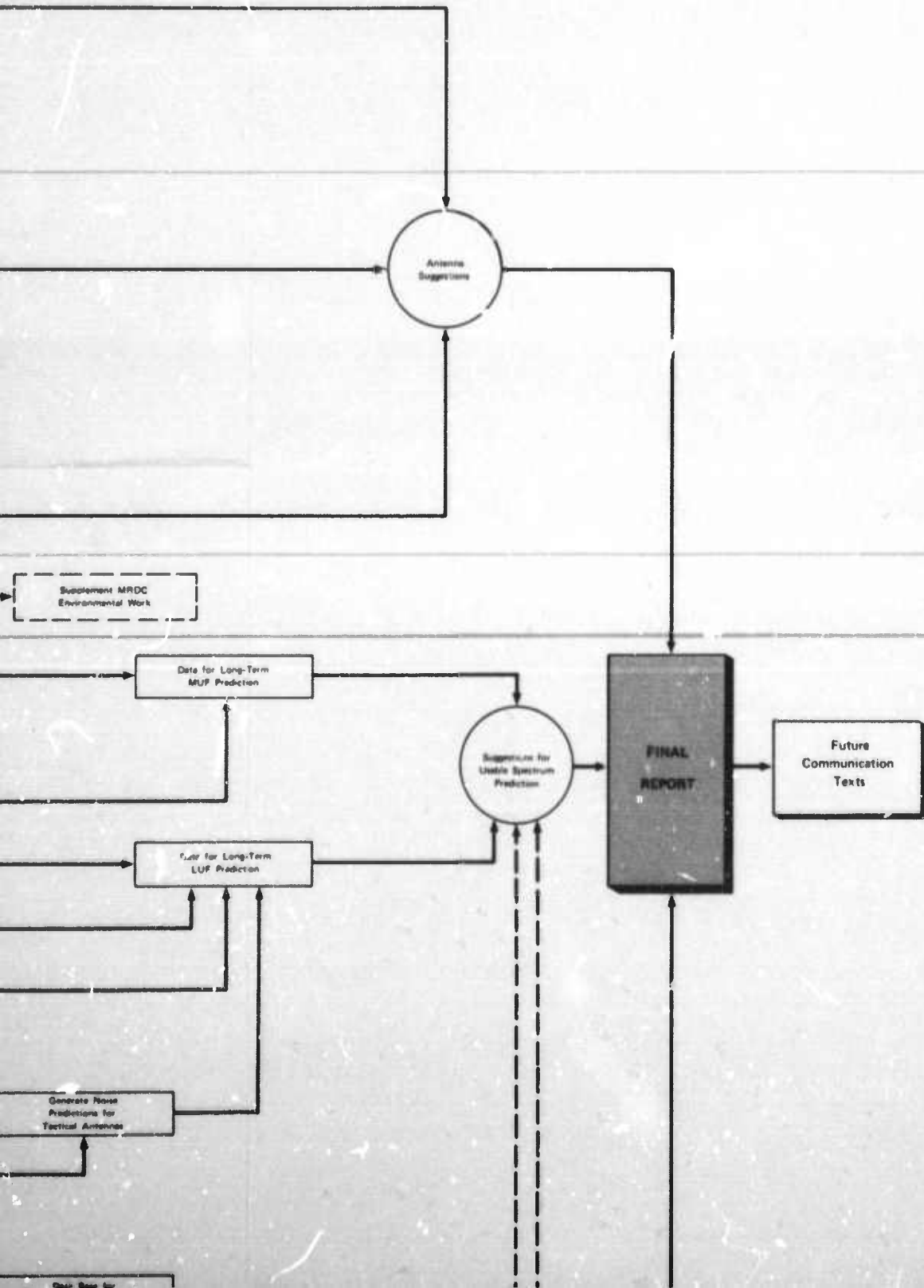
"PRECEDING PAGE BLANK-NOT FILMED"

1

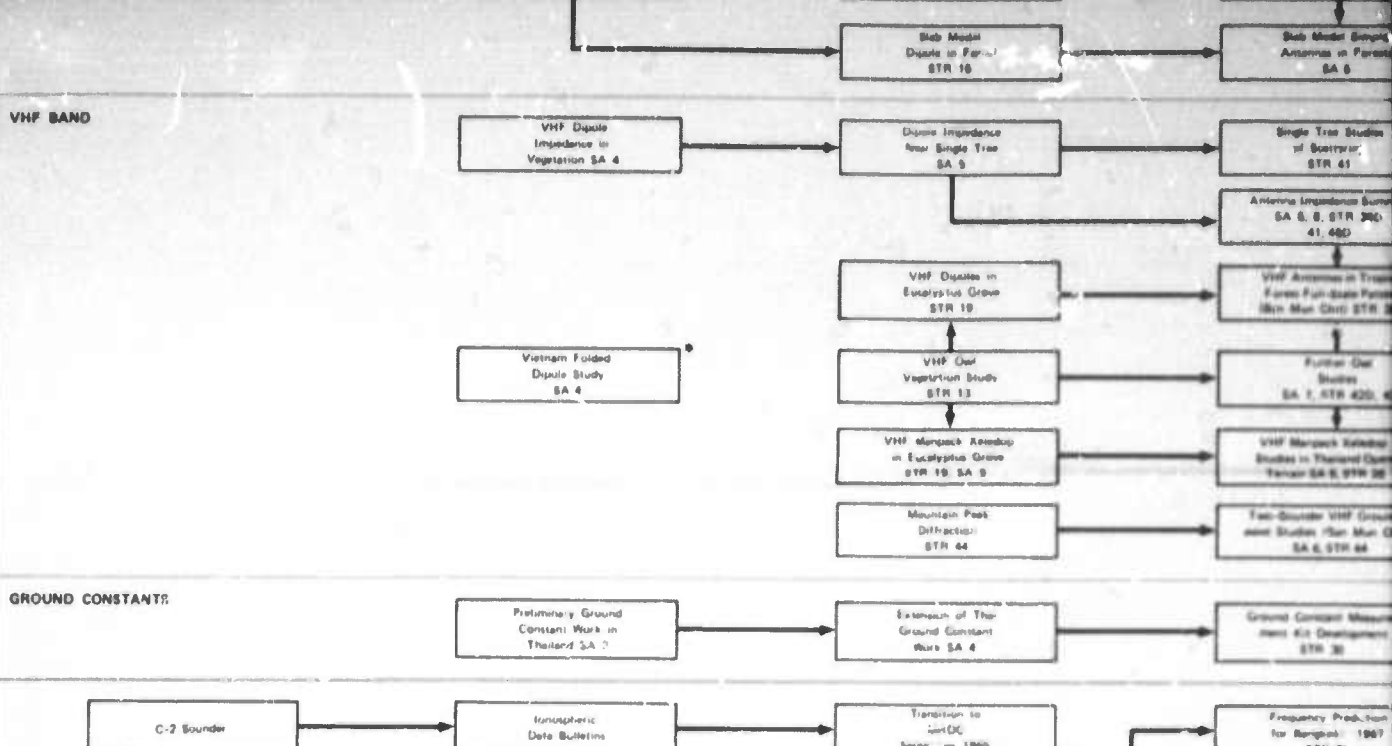




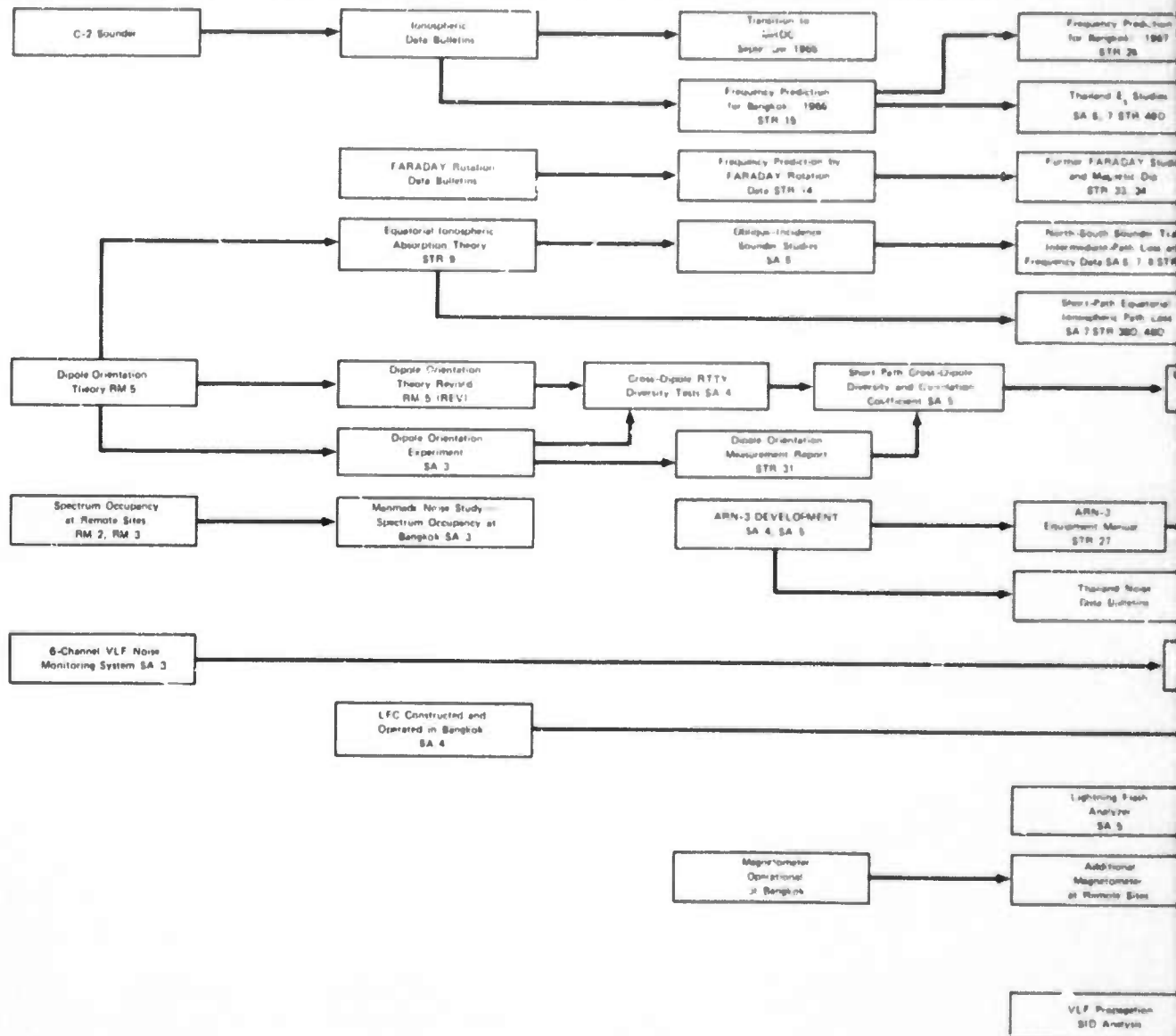
1968



Task A
ANTENNA ENVIRONMENT AND ANTENNA SYSTEM INVESTIGATIONS

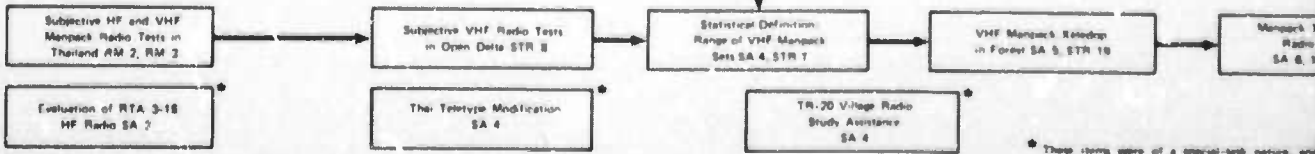


Task B
IONOSPHERIC AND FREQUENCY SPECTRUM INVESTIGATIONS

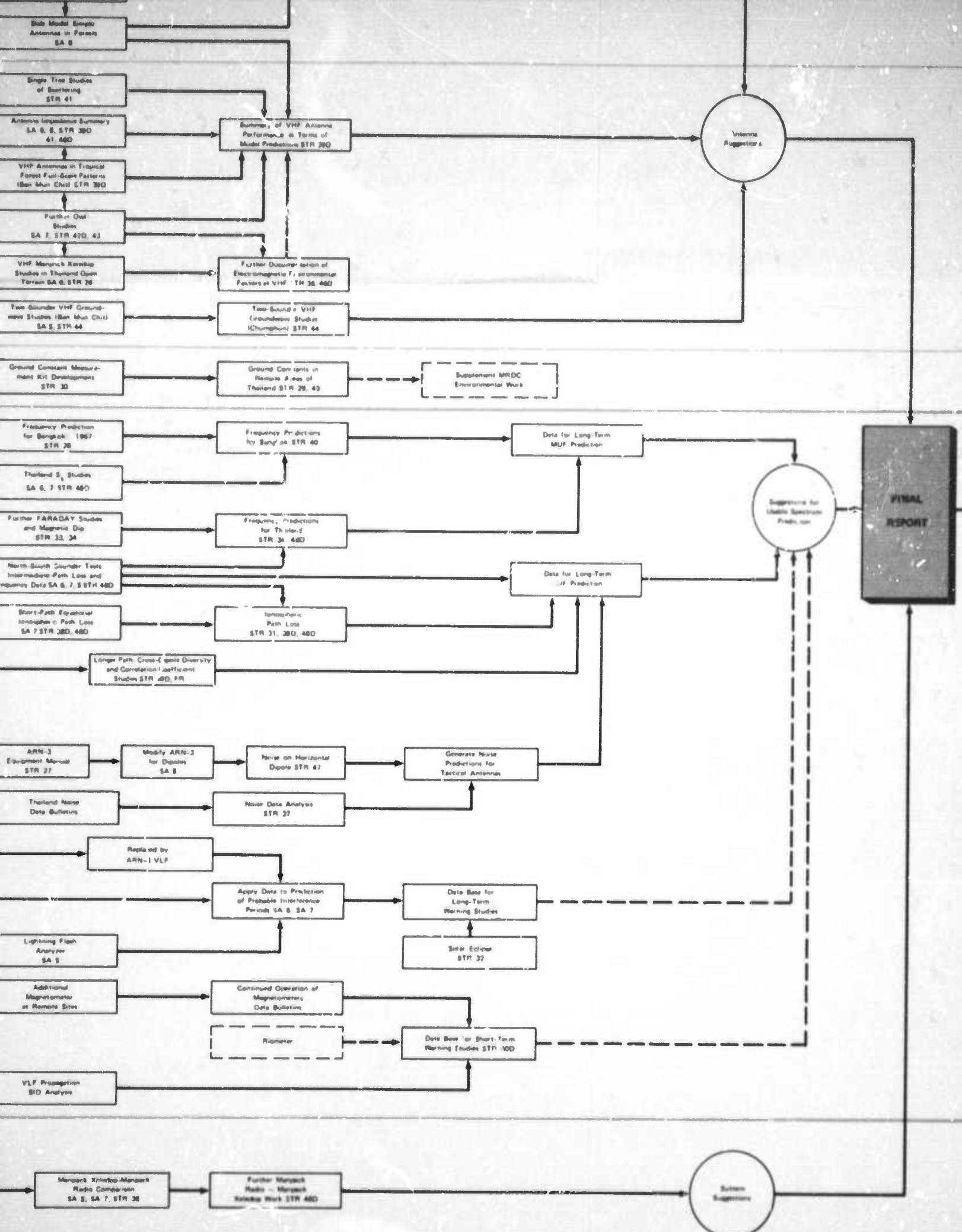


Task C
SYSTEM TEST FORMAT AND PROCEDURE INVESTIGATIONS

NOTE: Task C as described in the Technical Guidelines (20 May 1966) was not actually undertaken. The items shown on this chart under Task C represent past work most logically grouped under this general task heading.



* These items were of a special-task nature, and



a special-task nature, and were not part of the on-going program.

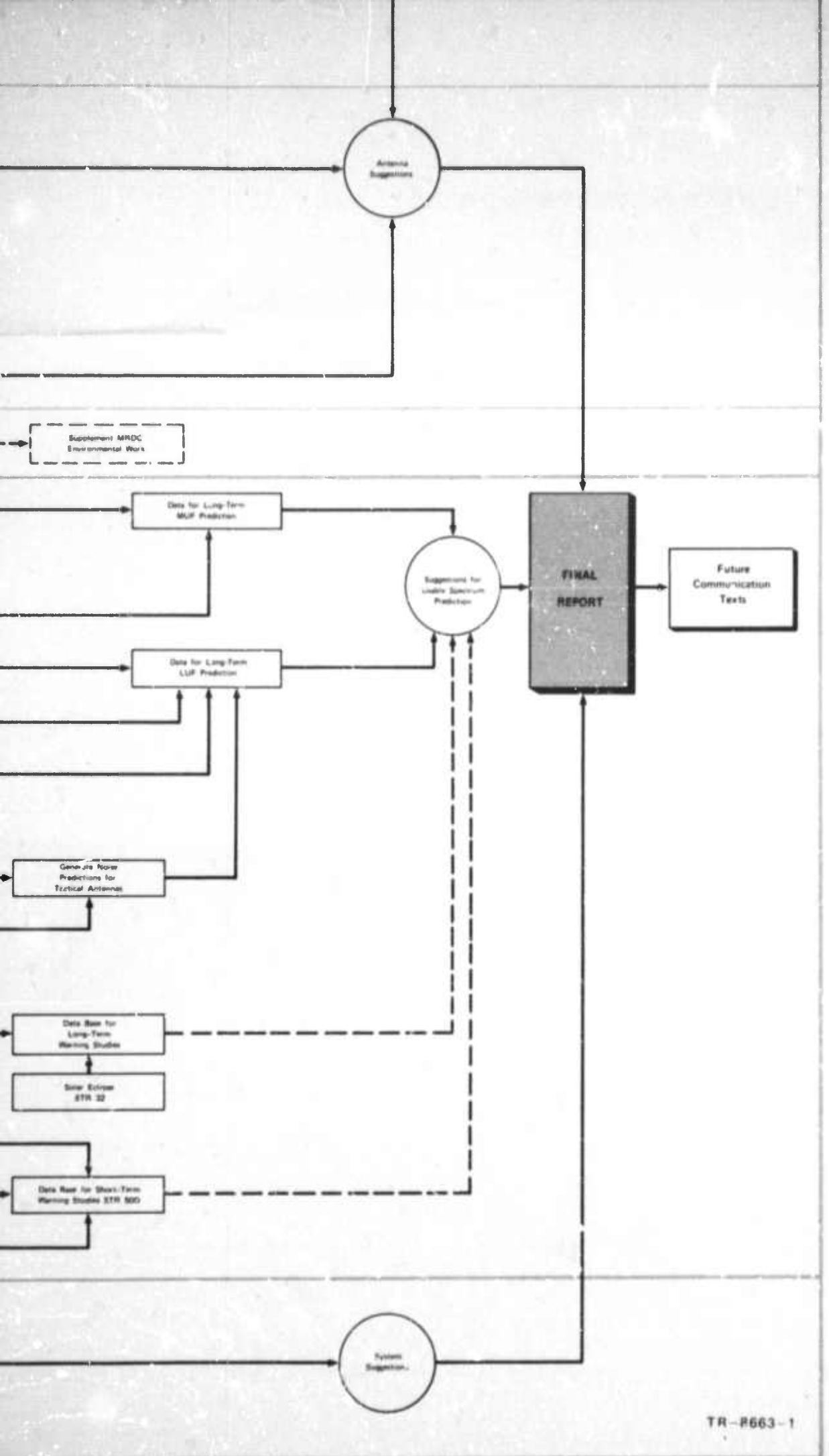


FIGURE I-3 PROJECT FLOW CHART— δ Y TASK

TR-R663-1

"PRECEDING PAGE BLANK-NOT FILMED".

II SUMMARY OF MAJOR TECHNICAL AND SCIENTIFIC FINDINGS

A. Task A: Antenna-Environment and Antenna-System Investigations

1. The 3-layer slab model of a forest environment developed on this contract is useful for predicting the average performance of HF antennas in forests and can be used for limited applications on VHF antennas in forests. The model is more accurate at HF and it does not account for the detailed variations due to scattering effects which become important for frequencies above about 10 MHz--especially for vertical polarization. More work is required to incorporate the scattering effects on a statistical basis.

The model correctly predicts that the most significant variable controlling dipole gain toward the zenith is the height of the antenna above ground and that at low elevation angles, the height of the forest is also significant in determining dipole gain. The model also correctly predicts an increase in low-angle gain in the broadside direction when the dipole is in the forest.

2. The center-fed half-wave horizontal dipole is the best field-expedient antenna for use on short HF skywave paths (50 miles or less), and this antenna need be elevated only to $\lambda/10$ above ground to be within about 3 dB of the maximum gain (which occurs for a dipole height of about $\lambda/8$ rather than the commonly assumed height of $\lambda/4$).

3. Open-wire transmission line (OWL) techniques developed under this contract are useful for measuring the electrical characteristics of forests and ground to provide input data for mathematical modeling of antenna performance. Measurements from the OWLs have shown that the

foliage can be approximated by a slab of $\mu_r = 1.0$ and ϵ_r between 1.01 and 1.06.

4. Full-scale antenna measurement techniques developed by SRI were employed on this contract. The results of these measurements showed that the radiation patterns of full-scale antennas should be measured to fully understand the effects of environment on antenna performance. Measurements showed that the E_θ (vertical polarization response of the measured antennas) was affected by the forest more than the E_ϕ (horizontal polarization) response. The maximum directivity of the measured monopole antennas occurred at higher elevation-angles when the antennas were measured at forested sites than when measured in open areas.

Measurements of the radiation patterns of VHF antennas in forested environments indicated strong scattering created by the foliage and it was necessary to process (smooth) the data statistically in order to interpret the data in terms of model predictions.

5. Vertical-incident ionospheric sounders were employed to measure the relative gain of field-expedient antennas and from these measurements and model data, estimates of the absolute gains of these antennas were derived. Measurements employing these techniques showed that the elements of a half-wavelength dipole antenna can sag approximately 45° relative to horizontal before 1 dB of gain toward the zenith is lost (provided the feed point is elevated greater than $\lambda/10$). The half-wavelength dipole antenna was shown to be the most effective radiator for propagation toward the zenith; followed by the inverted L, the slant wire, and the monopole or whip which was the least efficient.

6. Measurements of the feed-point impedance of the various field-expedient antennas were performed. The impedance of a simple field-expedient antenna typically increases as the antenna is moved from

clearing to forest, and the antenna will resonate at a slightly lower frequency in the forest. The impedance bandwidth of a half-wave horizontal dipole antenna increased when it was moved from a clearing to a forest, whereas the measured impedance bandwidth of a monopole sometimes decreased when it was moved from a clearing to a forest.

B. Task B: Ionospheric and Frequency Spectrum Investigations

1. The ESSA predictions of vertical-incidence critical frequency are the best available for the vicinity of Thailand and these predictions of monthly median values typically are accurate to within about 1 MHz. These predictions may be applied directly to compute the maximum usable frequency (MUF) for oblique-incidence paths up to about 200 miles. For longer paths, oblique-incidence predictions of the "MU" factor given in this report should be used.

2. A preferred orientation (magnetically north-south) was predicted and observed to exist for linearly polarized antennas (e.g., dipoles) when used on certain short skywave paths in the vicinity of the geomagnetic dip equator (which passes through the Malay Peninsula south of Bangkok and the Mekong River delta south of Saigon). Signal enhancements of 6 dB or more were commonly observed on short paths (less than 50 miles) when using north-south alignment at both terminals regardless of the path bearing, but for paths of about 150 miles or greater the traditional broadside orientation produced the greater received signals. The signals received on adjacent north-south and east-west dipoles were uncorrelated (except when sporadic E was present) on paths of up to about 800 miles, and "orientation diversity" appears to be attractive for use with diversity receivers.

3. The signal-to-noise ratio on simple, field-expedient antennas tends to be determined more by relative gain for the desired signal than

by the noise discrimination properties of these antennas. There seems to be very little difference in the noise currents induced in HF antennas placed in forests and those placed in adjacent cleared areas, and the noise on horizontal dipoles is relatively independent of dipole alignment.

4. Observations of MF and HF atmospheric radio noise over a two-year period indicate that the generally accepted noise maps (CCIR Report 322) do not predict enough noise for Thailand by about 10 dB, but the data are in agreement with the CCIR Report 322 diurnal variation of noise power. Local electrical storms in Thailand (as detected with lightning flash counters) can increase the average noise level in the lower part of the HF band by as much as 20 dB. The British Electrical Research Association (ERA) counter was considered the best for documenting the occurrence of local storms, and the results of the counter studies correlated well with local meteorological activity.

5. The time-delay spread of pulses propagated ionospherically on oblique paths out to about 800 miles was observed to be between 1 and 4 ms, and Doppler spreads of a CW signal of 0.4 Hz to 1.4 Hz were observed on these same paths. S/N and interference rather than time-delay spread or Doppler spread seemed to limit the performance of the AN/MRC-95 radio teletype on short paths in Thailand. For high S/N, the observed time-delay spreads probably cause errors due to frequency selective fading. This effect could be minimized by reducing the frequency shift of this equipment and this deserves more study.

6. Beacon satellite transmissions are useful in determining

- (a) The total electron content between a satellite and a ground receiving site,

* International Radio Consultative Committee of the International Telecommunication Union, Geneva, Switzerland

- (b) The vertical incidence (v.i.) critical frequency vs. latitude to within about 10 percent, and
- (c) The magnetic dip angle (when multiple receiving sites are employed).

C. Task C: System Test Format and Procedure Investigations

1. Subjective tests with HF manpack radios in Thailand showed:

- (a) The necessity for flexibility in changing frequency to avoid interfering signals.
- (b) The feasibility and need of using HF skywave where groundwave was not usable for communications with manpack radios in forested or mountainous terrain over paths exceeding a few miles.
- (c) The superiority of the center-fed horizontal dipole over the slant wire, and of the slant wire over the whip antenna for use on short HF skywave paths.

2. Subjective tests with VHF manpack radios in forests near the range limit of the set showed:

- (a) The improvement in performance obtained by elevating the antenna.
- (b) Improvement in performance by bending a whip over (away from the set) to approximate a horizontal antenna.

(c) Improvement in performance often could be obtained by moving around in an area of only about 20-ft radius to find a location of higher signal strength. Difficulty in using VHF (FM) sets while moving, which often could be remedied by stopping at a position of higher signal strength.

3. The need for a meaningful definition of the range of a VHF manpack radio in statistical terms was observed and such a definition (based upon propagation statistics and voice-intelligibility tests) was formulated.

III TASK A: ANTENNA-ENVIRONMENT AND ANTENNA-SYSTEM INVESTIGATIONS

A. Mathematical Model of Antennas in Forest Environment (STR 16)

1. Objective

The objective of the antenna-forest model work was to develop a mathematical model for predicting the electromagnetic fields in the region above a forest due to transmitting antennas located in the forest. Applications are to HF skywave communications and to HF and VHF air-to-ground communications.

2. Background

Very little was known about the effects of living vegetation upon antenna performance or upon radio-wave propagation when the SEACORE work began in 1962 (see STR 17, a literature survey). Only limited amounts of data were available for the case of ground-to-ground propagation in jungles,^{*1,2} and Jansky and Bailey (J&B) was tasked by the U.S. Army Signal Corps and ARPA to obtain extensive additional data of this type in Thailand as part of the SEACORE effort.³ Jansky and Bailey also were to work on the mathematical modeling for the ground-to-ground case as it pertained to interpretation of their data. No data were available for the HF skywave or HF and VHF ground-to-air (or air-to-ground) cases, and SKI was tasked to obtain such data in CONUS and in Thailand and to

* The term forest probably is preferable to jungle, however, both are used interchangably in this report.

[†] References are listed at the end of the report.

analyze the results in the context of a mathematical model. The SRI theoretical effort was limited to determining the fields at a significant distance above the forest caused by a transmitting antenna located in the forest and, by reciprocity, the inverse case (i.e., transmitting antenna located far above the jungle and the receiving antenna located in the jungle).

Pounds and LaGrone⁴ were the first to consider the macroscopic effects of living vegetation from an electromagnetic standpoint, and they proposed to consider the forest as a dissipative (lossy) dielectric slab. This approach also was used by Lippmann,⁵ who considered ground-to-ground propagation in a jungle from the network theory point of view. As part of this project, Taylor addressed himself to the HF skywave problem (STR 16). He employed the lossy-slab model of a forest region to compute the far-field (in air) directivity and gain of Hertzian dipoles located in the forest part of a three-layer (air-jungle-ground) slab. Sachs and Wyatt⁶ first successfully used the slab model to explain the J&B ground-to-ground results in terms of a lateral wave propagating in air along the air-forest interface. Subsequently, this approach has been successfully employed by Tamir⁷ and others⁸⁻⁹ for predicting the radio system loss (or basic transmission loss) for both ground-to-ground and air-to-ground systems operating in the equatorial forested environment.

The remainder of this section will summarize the results of Taylor's theoretical work on this contract with application to the SRI airborne pattern measurements as discussed in Sections III-C and III-D and to the height-gain measurements discussed in Section III-E.

3. The Forest-Slab Model

a. Nomenclature

As discussed above, the slab model approximates the forest as a multilayer dielectric sandwich (see Figure III-1 for slab and antenna nomenclature). The uppermost region is the space above the forest, characterized by ϵ'_{ro} and μ_{ro} (both unity), the relative permittivity and permeability of free space. The i layers below this region are layers of forest ($i = 1$) and ground ($i = 2$) characterized by their complex refractive indices, n_i , where $n_i^2 = \epsilon_{ri}$, and where the respective relative complex dielectric constants, ϵ_{ri} , are given by:

$$\epsilon_{ri} = \epsilon'_{ri} - j\epsilon''_{ri} = \epsilon'_{ri} - j60\sigma_i \lambda_0 = \epsilon'_{ri} (1-j\delta_i)$$

where the loss tangent, δ_i , is defined by

$$\delta_i = \frac{\epsilon''_{ri}}{\epsilon'_{ri}} = \frac{\sigma_i}{\omega \epsilon_o \epsilon'_{ri}}$$

and σ_i is the conductivity, λ_0 is the free-space wavelength at radian frequency ω , and ϵ_o is the permittivity of free space (all in MKS units). Each region is assumed to be homogeneous and to possess the magnetic permeability of free space (μ_o).

b. Assumptions

The simplicity of the model permits a reasonably rigorous analysis, but certain assumptions must be made. The assumption of a flat surface on the top probably is justifiable when one considers that the surface roughness is small compared to the wavelength--at least in the lower part of the HF band. An actual forest is not homogeneous, and it will not act as if it were homogeneous for tree spacings greater than

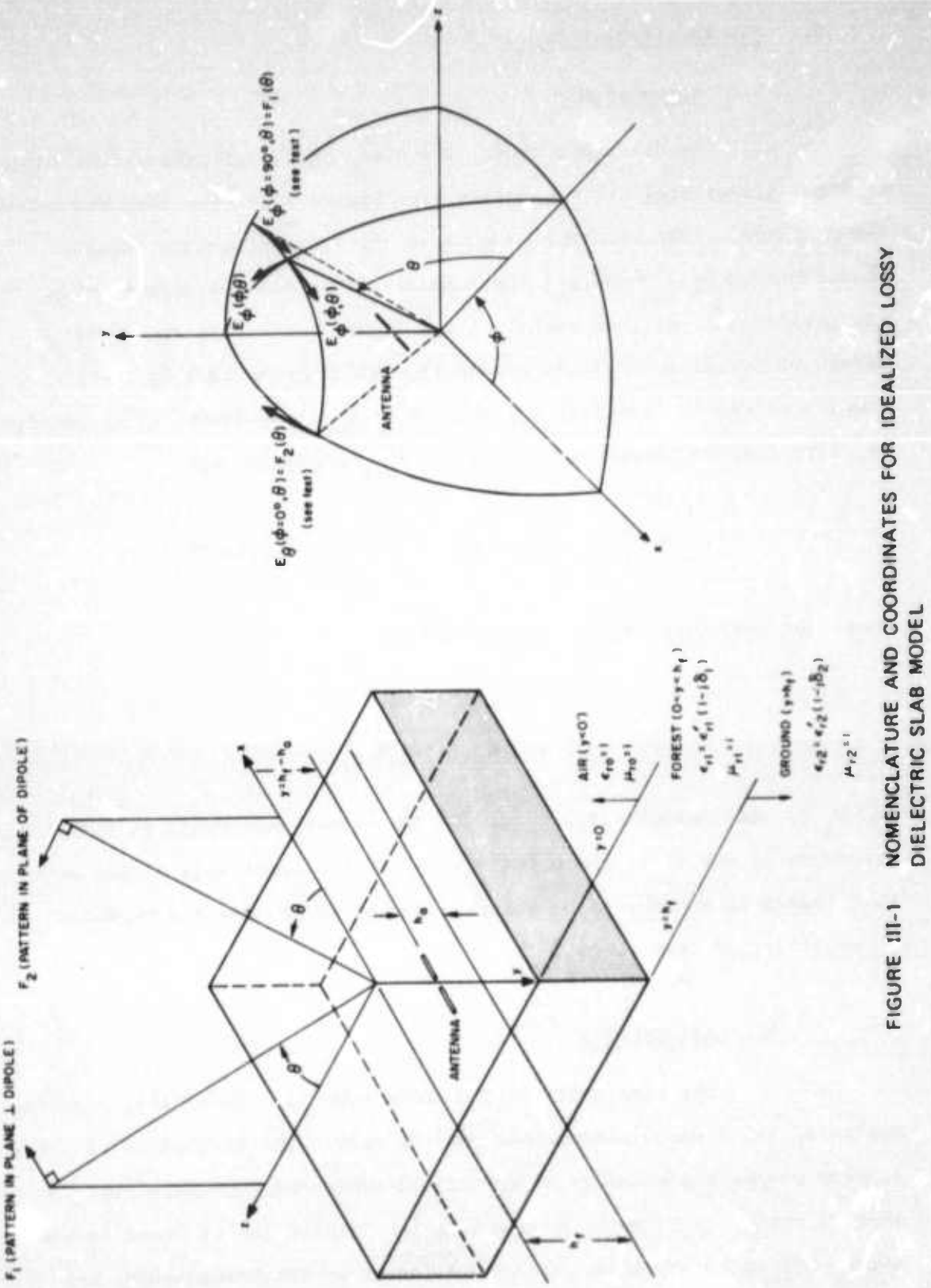


FIGURE III-1 NOMENCLATURE AND COORDINATES FOR IDEALIZED LOSSY DIELECTRIC SLAB MODEL

about $\lambda/20$. Also, the effective conductivity in the vertical direction probably is greater than the effective conductivity in the horizontal direction (STR 19), causing an actual forest to be anisotropic.

c. Definition of F_1 and F_2 and Relationship to E_θ and E_ϕ

The dipole far-field radiation patterns in STR 16 and in this section are presented in terms of F functions where F is the ratio of the effective length of a short electric dipole (with no end loading) in the forest slab, to one-half the actual length of the short dipole in free space. The relationship between the F functions for a horizontal dipole and the E-field coordinates of Figure III-1(a) is:

- (1) Pattern in the plane normal to the dipole (for polarization normal to the plane of incidence)

$$F_1(\theta) = |E_z|$$

- (2) Pattern in the plane of the dipole (for polarization in the plane of incidence)

$$F_2(\theta) = |E_x|$$

Once $F_1(\theta)$ and $F_2(\theta)$ are determined from the model equations of STR 16, the functions $E_\phi(\theta, \psi)$ and $E_\theta(\theta, \psi)$ as depicted in Figure III-1(b)--the directivity pattern parameters measured with the airborne pattern-measurement system--can be found by using the relationships:

$$E_\phi(\theta, \psi) \cong F_1(\theta, \psi) = F_1(\theta) \sin \psi \quad 0^\circ \leq \psi \leq +90^\circ$$

and

$$E_\theta(\theta, \psi) \cong F_2(\theta, \psi) = F_2(\theta) \cos \psi \quad -90^\circ \leq \psi \leq +90^\circ$$

where

θ = elevation angle*

ϕ = azimuth angle relative to the dipole axis.

A program was developed to provide contours of the calculated E_θ and E_ϕ radiation patterns. This program determines at what azimuth angle the relative -3, -6, -9, and -12 dB contours intersect a given elevation angle. The resulting contours of constant response can then be plotted to provide a contour map of computed relative signal strength similar to those produced from the measured data. Computed contours are presented in Section III-D for comparison with measured results.

4. Parametric Sensitivity Test

There are many factors that affect the radiation pattern of an elementary dipole antenna placed in a forest. It is not feasible to compute radiation patterns for all parameter combinations of interest. Therefore, the results discussed here were obtained by choosing typical values of each model parameter and then varying them, one at a time, around this value. The parameters considered were:

- (1) Antenna height
- (2) Forest height
- (3) Real part of the relative dielectric constant of the forest

* In this report (and in STRs 10, 25, 35, and 45D) θ is used to denote the elevation angle, whereas θ was the zenith angle (90° minus the elevation angle) in STR 16.

- (4) Loss tangent of the forest
- (5) Real part of the relative dielectric constant of the earth
- (6) Loss tangent of the earth.

a. Effect of Antenna Height (h_a)

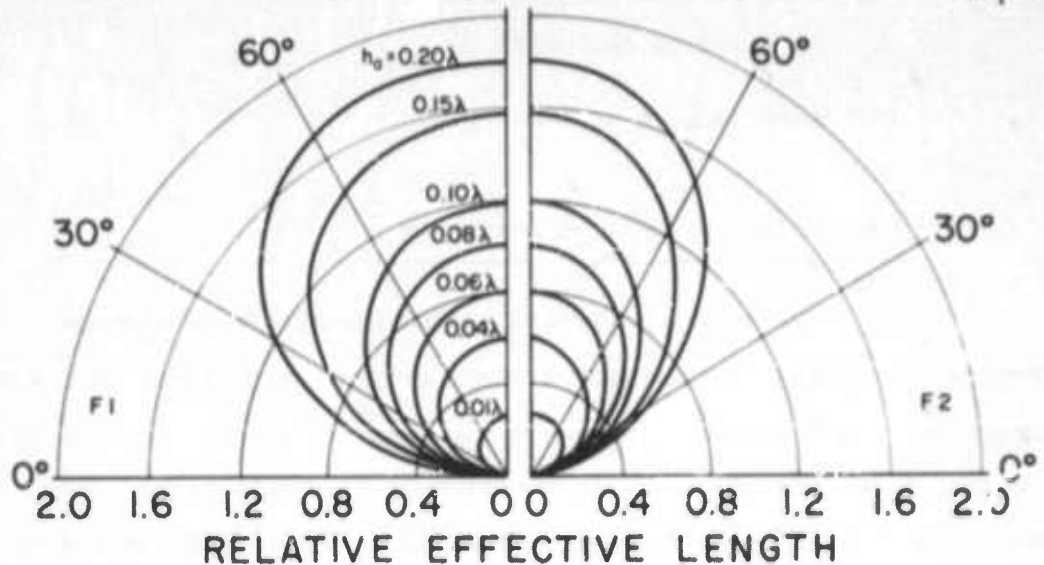
The most significant of the parameters considered here is the height of the antenna above ground. It affects both the effective length of the antenna-slab combination and the input resistance, and therefore, changes the gain function quite drastically. Also, it is one of the few factors that can be readily controlled in the field.

Figure III-2 present polar plots of $F_1(\theta)$ and $F_2(\theta)$ with antenna height in wavelengths as a parameter. Figure III-2(a) is for the case of no forest; Figure III-2(b) is for an antenna in a dense forest. To emphasize the importance of raising the antenna above the ground, the same data are presented in a different way in Figures III-3 and III-4. Here F , the field-imaging function, is plotted as a function of antenna height for two specific angles, one at the zenith and one very near the horizon (grazing incidence). Figure III-3 shows that the forest has little effect on radiation toward the zenith. The antenna height determines whether the low-angle radiation is stronger off the ends of the elements (F_2) or broadside to the elements (F_1). The vertically polarized radiation off the ends predominates at very low antenna heights (see Figure III-4). It should be noted that the effects of antenna height upon antenna impedance (and hence upon efficiency) are not included in Figures III-2 through III-4 (this topic is discussed in STR 16 and in Section III-E of this report).

GROUND $\epsilon'_{r2} = 20$
 $\delta_2 = 5$

ELEVATION
ANGLE, θ
90° 90°

NO FOREST $\epsilon'_{r1} = 1$
 $\delta_1 = 0$
 $h_f = 0$



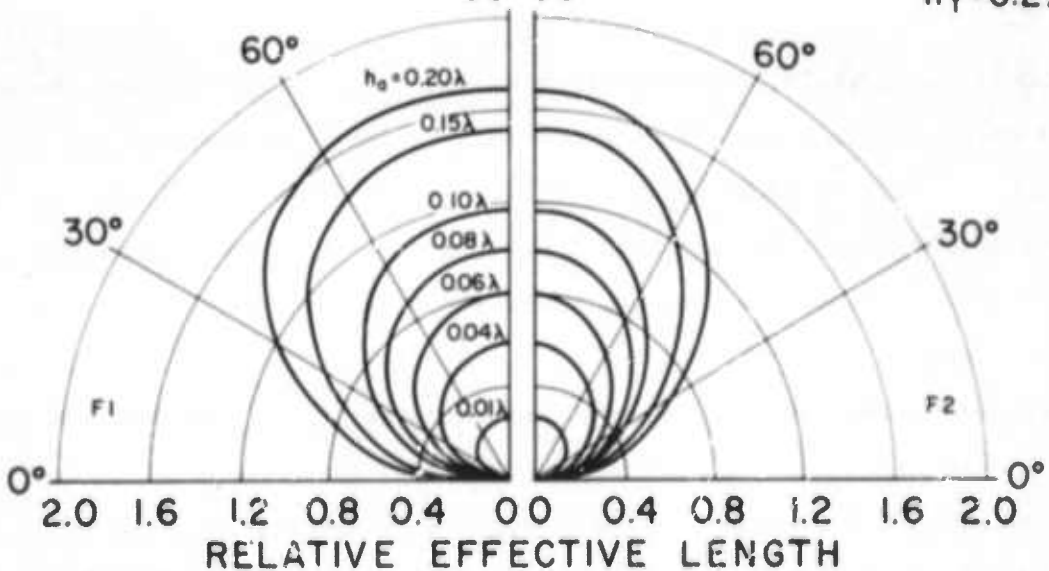
PATTERN IN PLANE \perp DIPOLE

PATTERN IN PLANE OF DIPOLE

GROUND $\epsilon'_{r2} = 20$
 $\delta_2 = 5$

ELEVATION
ANGLE, θ
90° 90°

FOREST $\epsilon'_{r1} = 1.2$
 $\delta_1 = 0.1$
 $h_f = 0.2\lambda$



PATTERN IN PLANE \perp DIPOLE

PATTERN IN PLANE OF DIPOLE

D-4240-900S

FIGURE III-2 EFFECTIVE ANTENNA LENGTH FOR VARIOUS ANTENNA HEIGHTS
IN CLEARING AND FOREST

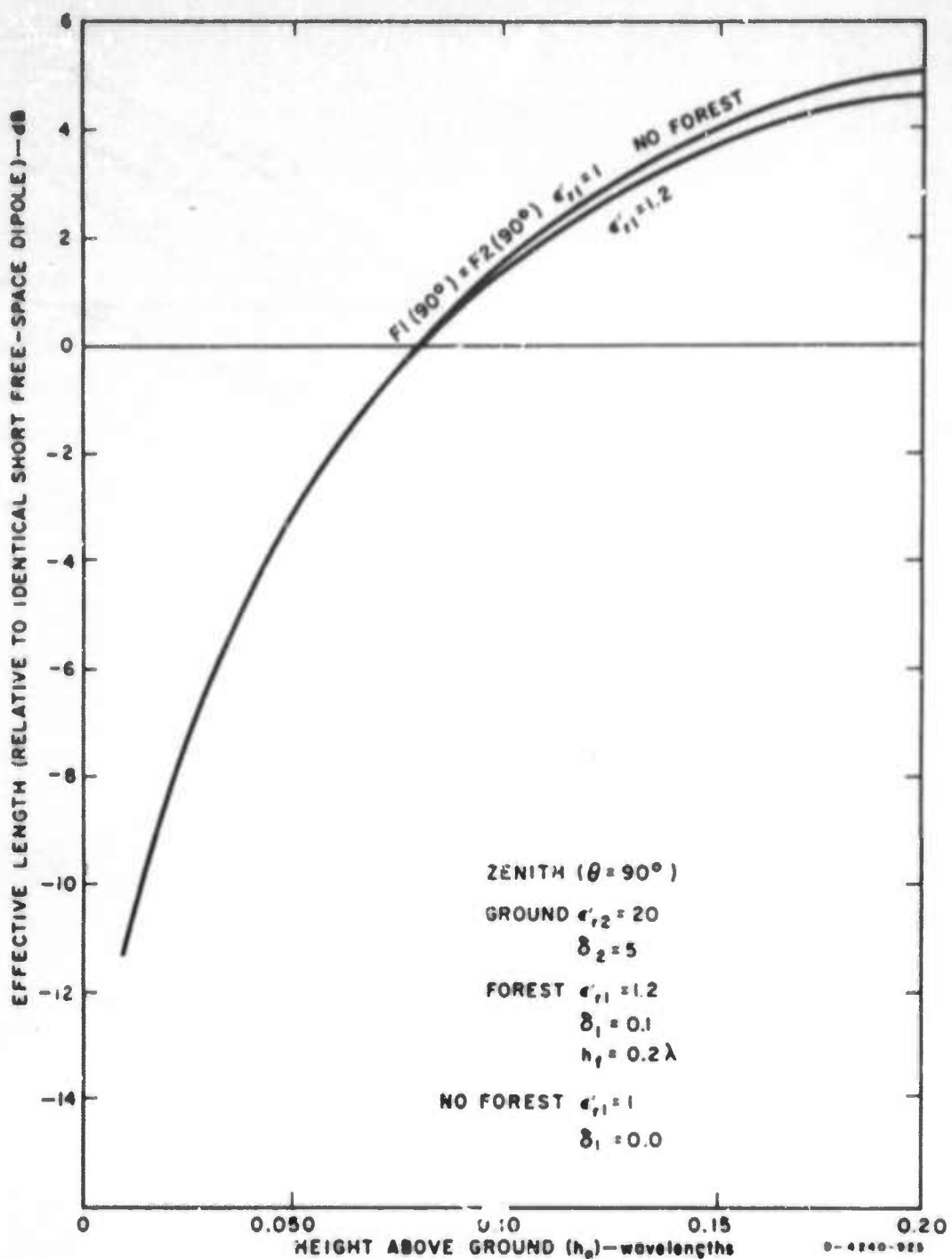


FIGURE III-3 EFFECTIVE ANTENNA LENGTH AS A FUNCTION OF HEIGHT ABOVE GOOD GROUND—ZENITH

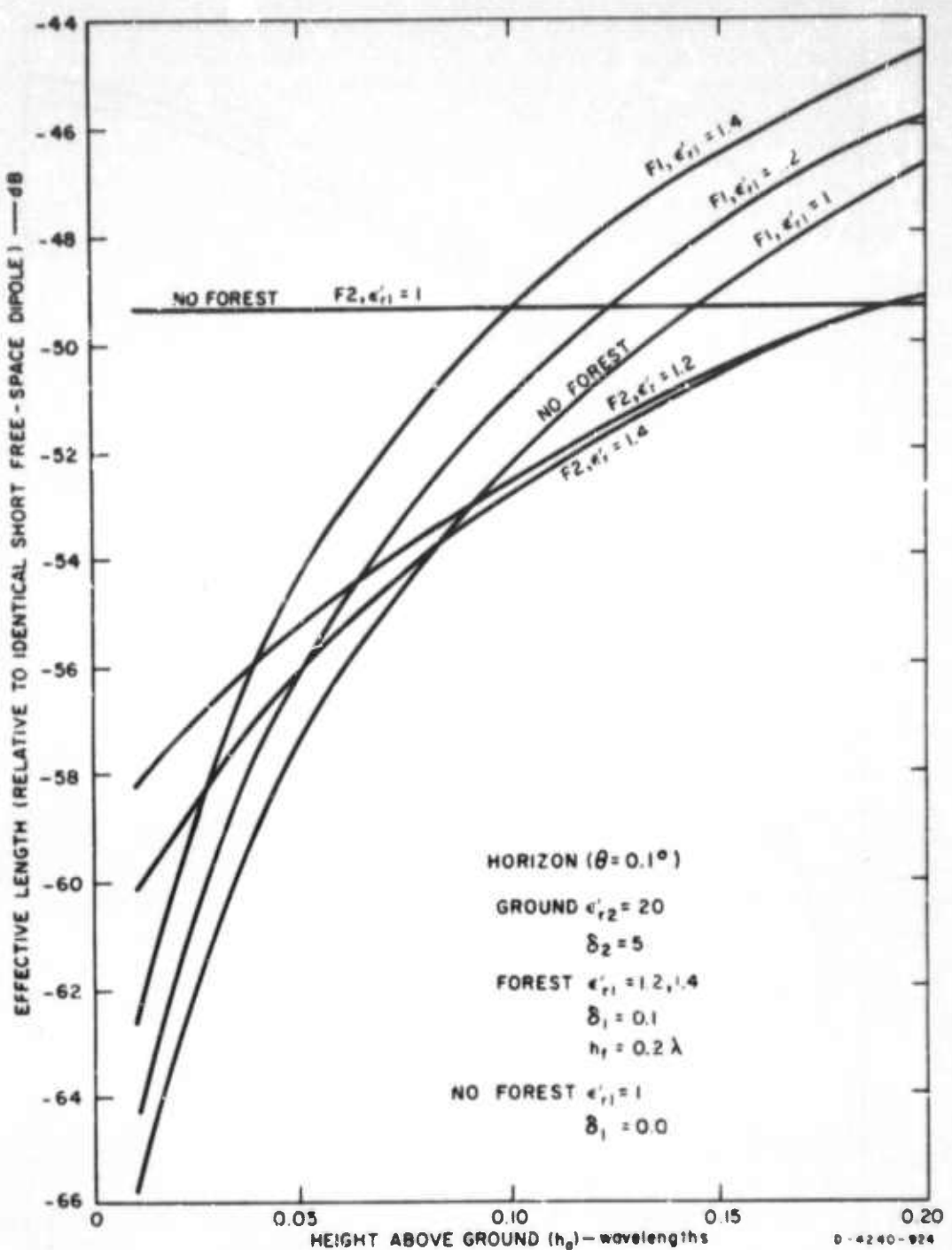


FIGURE III-4 EFFECTIVE ANTENNA LENGTH AS A FUNCTION OF ANTENNA HEIGHT ABOVE GOOD GROUND—HORIZON

b. Effect of the Forest Height (h_f)

Figure III-5 shows the effect of forest height (in wavelengths) on the patterns. The high-angle radiation is affected only slightly, while the low-angle radiation is affected rather markedly--as much as 10 dB relative to the no-forest case for this example. The vertically polarized signal off the ends of the dipole at low elevation angles (F_2) decreases as forest height increases, while the horizontally polarized signal broadside to the antenna (F_1) increases with forest height.

c. Effect of the Dielectric Constant of the Forest (ϵ'_{rl})

High-angle radiation (above about 30° elevation angle) is relatively independent of the dielectric constant of the forest as is low-angle radiation off the ends of the dipole (F_2). Low-angle radiation broadside to the dipole (F_1) is more dependent on ϵ'_{rl} --especially for the greater forest heights--and increases as ϵ'_{rl} increases (see Figure III-6).

d. Effect of the Loss Tangent of the Forest (δ_1)

The effect of δ_1 on F_1 and F_2 for both high- and low-angle radiation is negligible.

e. Effect of Ground Constants (ϵ'_{r2} and δ_2)

Neither ϵ'_{r2} or δ_2 of typical ground are significant variables.

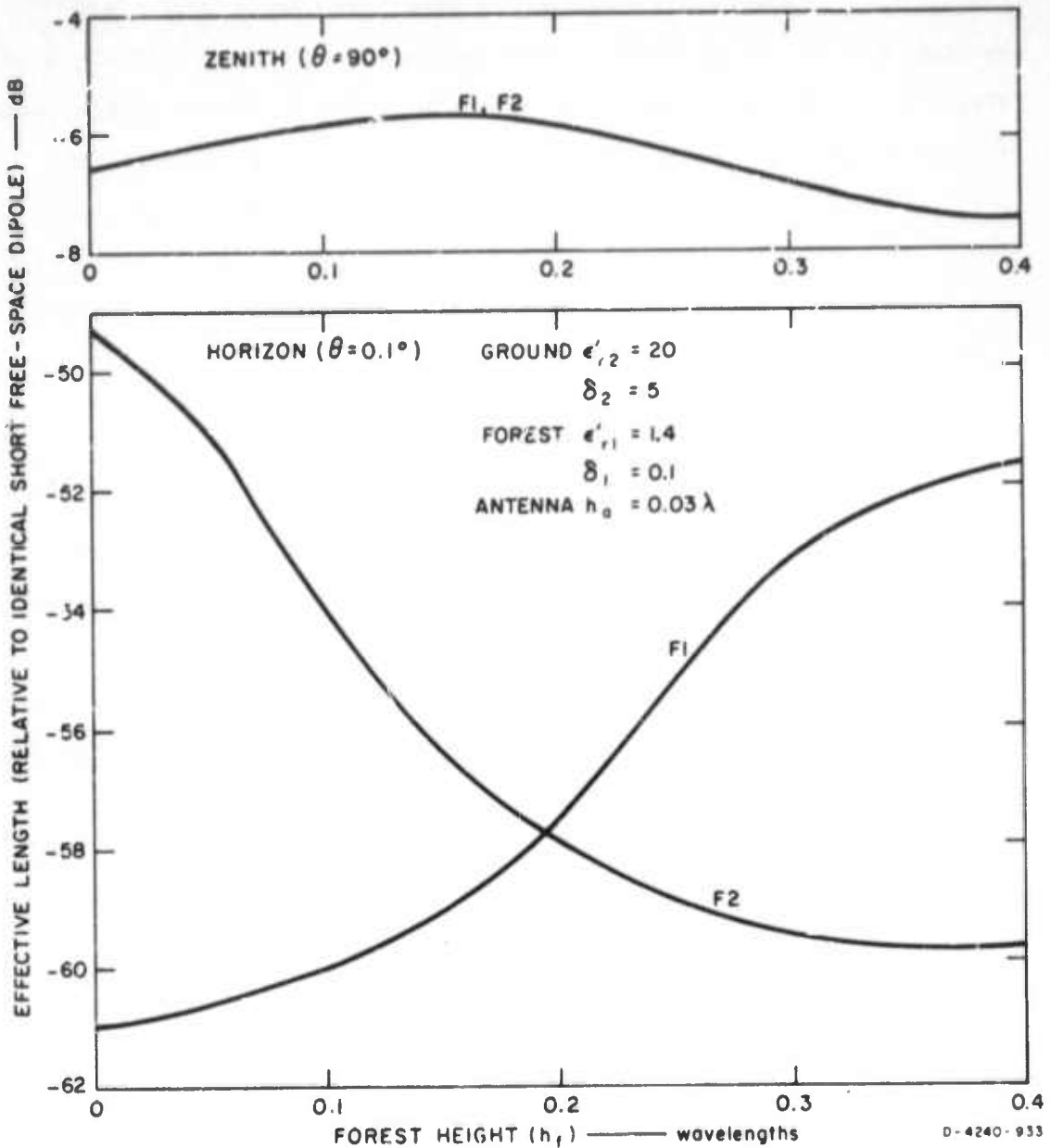


FIGURE III-5 EFFECTIVE ANTENNA LENGTH AT ZENITH AND HORIZON AS A FUNCTION OF FOREST HEIGHT— $h_a = 0.03\lambda$

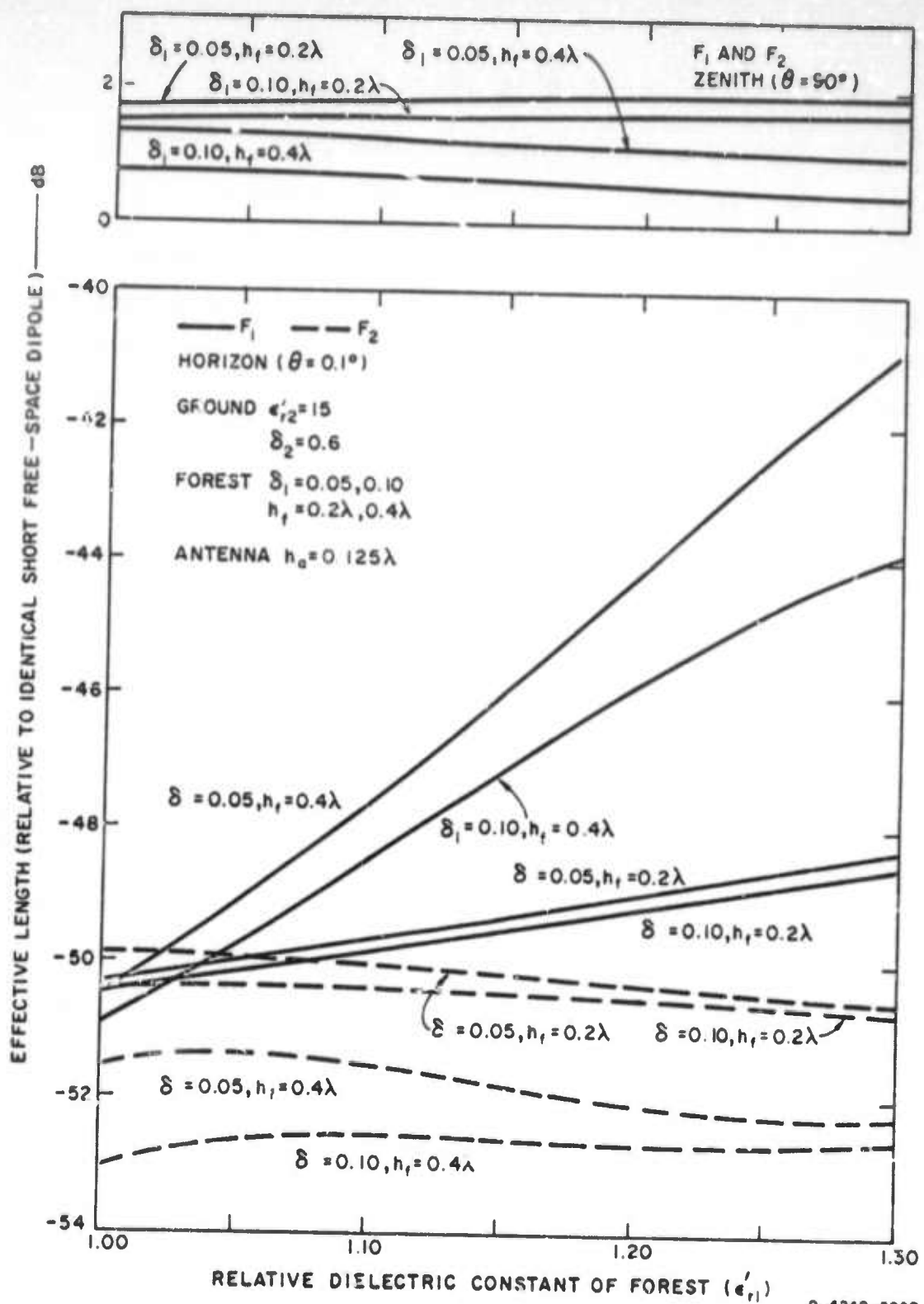


FIGURE III-6 EFFECTIVE ANTENNA LENGTH AT ZENITH AND HORIZON AS A FUNCTION OF FOREST DIELECTRIC CONSTANT— $h_a = 0.125\lambda$

B. Measurements of Vegetation and Ground Constants

1. Vegetation Constants (STRs 13, 42D, 43)

a. Objective

In order to use the lossy-dielectric-slab model of a forest (see Section III-A), the macroscopic electrical properties of the forest (conductivity, permittivity, and permeability) must be known. Open-wire transmission line (OWL) probes offer one method of measuring these properties. The objective of this section is to discuss the use of OWL probes for measuring the electrical properties of forests and to summarize the measured results obtained.

b. Background

The macroscopic electrical properties of the forest, considered as a homogeneous and isotropic dielectric, can be adequately described for our purposes by two parameters, the complex relative dielectric constant, ϵ_{rl} , and the complex relative permeability, μ_{rl} . The two parameters can be computed from the characteristic impedance, Z_c , and the propagation constant, γ_1 , of a transmission line in which the space around the conductors is filled with the material in question. The problem of finding ϵ_{rl} and μ_{rl} , then, reduces to the problem of finding the characteristic impedance and propagation constant of the transmission line in air and in the forest. These values can be obtained from measurements of the input impedance of the line using one of two methods: the short-circuit-termination, open-circuit-termination method or the variable-length, fixed-termination method (STRs 13, 42D, 43).

c. Limitations of the OWL Probes

1. Inhomogeneity Limitations

We desire to use the probes to measure the average value of the dielectric constant in a forest--probably an inhomogeneous region. The averaging volume is determined by how the power carried in the transmission-line wave is distributed about the line. The relative power distribution vicinity of a 300-ohm line* is shown in Figure 111-7 where it can be noted that 95 percent of the power passes through a circle of radius 1-1/2 times the line spacing centered on a line midway between the conductors. This confinement of the power is adequate to permit isolation of the sensing region of the transmission line in a forest from the ground and the air above the forest and yet allow vegetation in the region between the conductors, while utilizing conductors of practical size.

2. Anisotropy Limitations

One would expect to be able to resolve anisotropic effects if the field about the probe were predominantly linearly polarized and most of the power was contributed by the principal component. The field about a two-wire line is linearly polarized everywhere, but the resultant field varies in direction from point to point. Upon detailed examination, it is apparent that a balanced two-wire transmission line constructed of cylindrical conductors is not a satisfactory instrument for determining the macroscopic anisotropic properties of dielectrics (STR 42D).

*The power is distributed even closer to the conductors for lines of higher characteristic impedance.

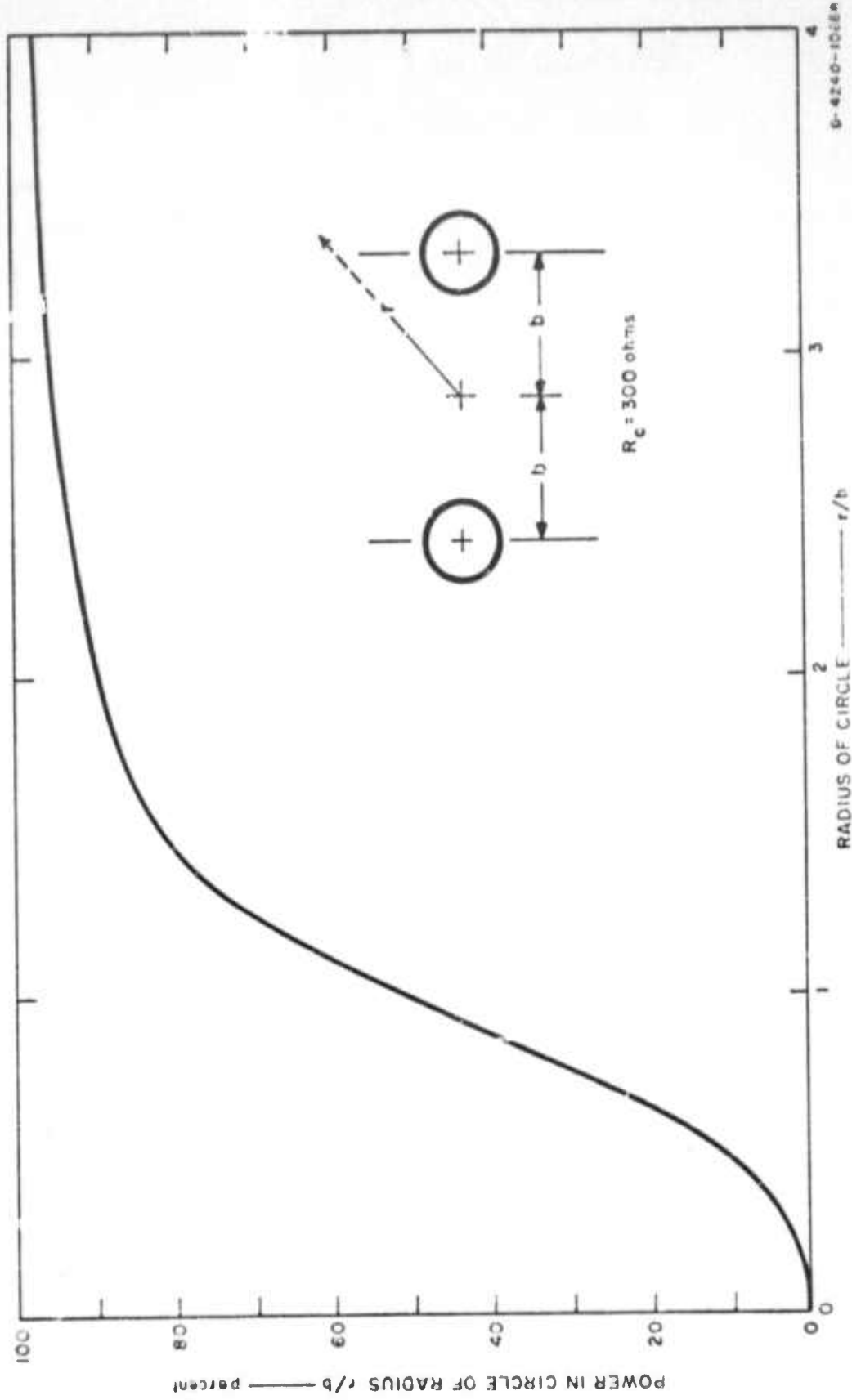


FIGURE III-7 RELATIVE POWER DISTRIBUTION IN THE VICINITY OF A 300- Ω OPEN-WIRE TRANSMISSION LINE

3. Scatterer Limitations

A real forest is not a continuous slab of dielectric material, but rather it is composed of groups of discrete scatterers (tree trunks, branches, etc.). The question then arises: How well can a group of randomly spaced discrete scatterers be represented in the slab model by only two parameters--the complex dielectric constant and the complex permeability? To answer this question, the effect of scatterers near a two-wire transmission line was investigated experimentally at the laboratory at the University of South Carolina and in the field (see STR 42D). Dry and wet wooden bars and aluminum rods were used individually and in groups to simulate in the laboratory the effects of tree trunks and/or branches. The measurements on individual scatterers yield equivalent circuits of the scatterers as lumped-constant loads at the location of the scatterer along the line. These equivalent circuits then were used to compute the effects of a random distribution of such scatterers and to infer the effective macroscopic electrical properties of a volume containing these scatterers. Measurements were made on random distributions of these scatterers for comparison with the computed values. Measurements on freshly cut vegetation (tree branches) and living vegetation were made to check the reasonableness of the simulation. Also, computations were made as a check on the validity of representing a transmission line with discrete capacitive scatterers (shunt capacitors) as a line with a higher dielectric constant and no shunt capacitors (see Appendix D of STR 42D). The real part of the relative dielectric constant was found to increase linearly with the number of scatterers per wavelength placed along the line, and the real part of the relative permeability remained essentially unity.

The conclusion of this study (STR 42D) was that a forest that consists of an ensemble of scatterers can be represented by a slab with a single macroscopic descriptor, the complex dielectric constant. Therefore, OWL probes are useful for estimating the macroscopic electrical properties of a volume containing living vegetation--even when significant scatterers (e.g., tree trunks) are present--although the results of OWL measurements must be interpreted with care. It is important to sample and average (or otherwise smooth the results such as by computing the median value) in order to obtain a reasonable estimate of the effective slab constant.

d. Lines Used for Measurements

Several three-hundred-ohm lines were constructed for use at HF and VHF. The HF line was made from 20-ft sections of 10-cm-diameter aluminum irrigation pipes, whereas the VHF line was constructed of 1.6-cm-diameter brass tubing plated with silver. These lines are discussed in detail in STRs 13 and 43.

e. Results with OWL Probes

The majority of the results were obtained in undergrowth with the small brass line, because the pipe line was cumbersome and difficult to set up. The approach with the smaller line was to sample on a matrix grid and obtain a statistical sample of the desired slab constants. The median results from five sites in Thailand* are plotted in Figures III-8 and III-9. The σ scale on Figure III-9 is the "through-the-slab" attenuation constant (see the discussion of the

* Detailed descriptions of these sites are given in STR 43 and in various MRDC-ES reports. A brief description is given in Appendix C.

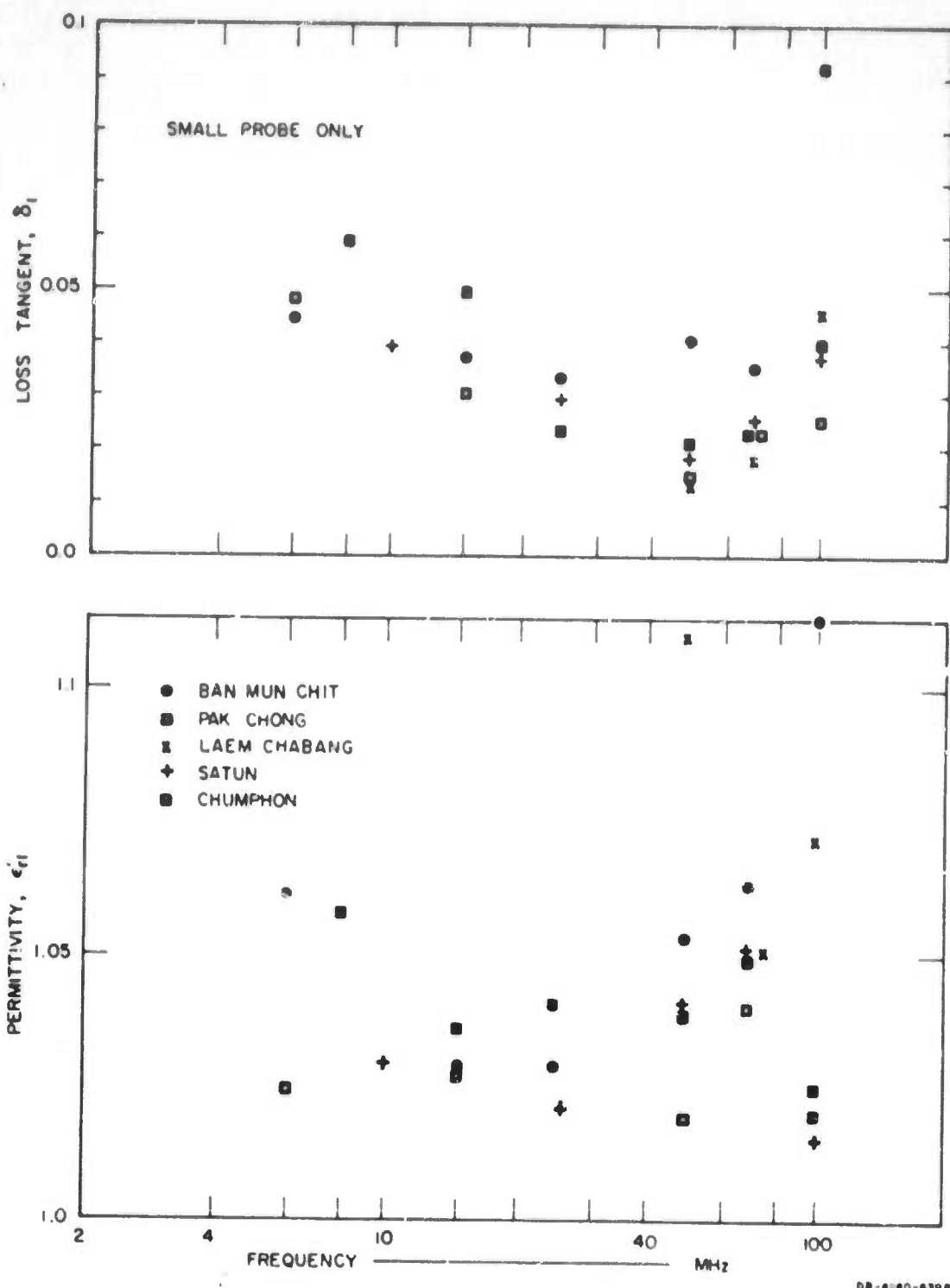


FIGURE III-8 COMPARISON OF MEASURED MEDIAN VALUES OF ϵ_r AND δ_t AT FIVE THAILAND SITES

DB-4240-639A

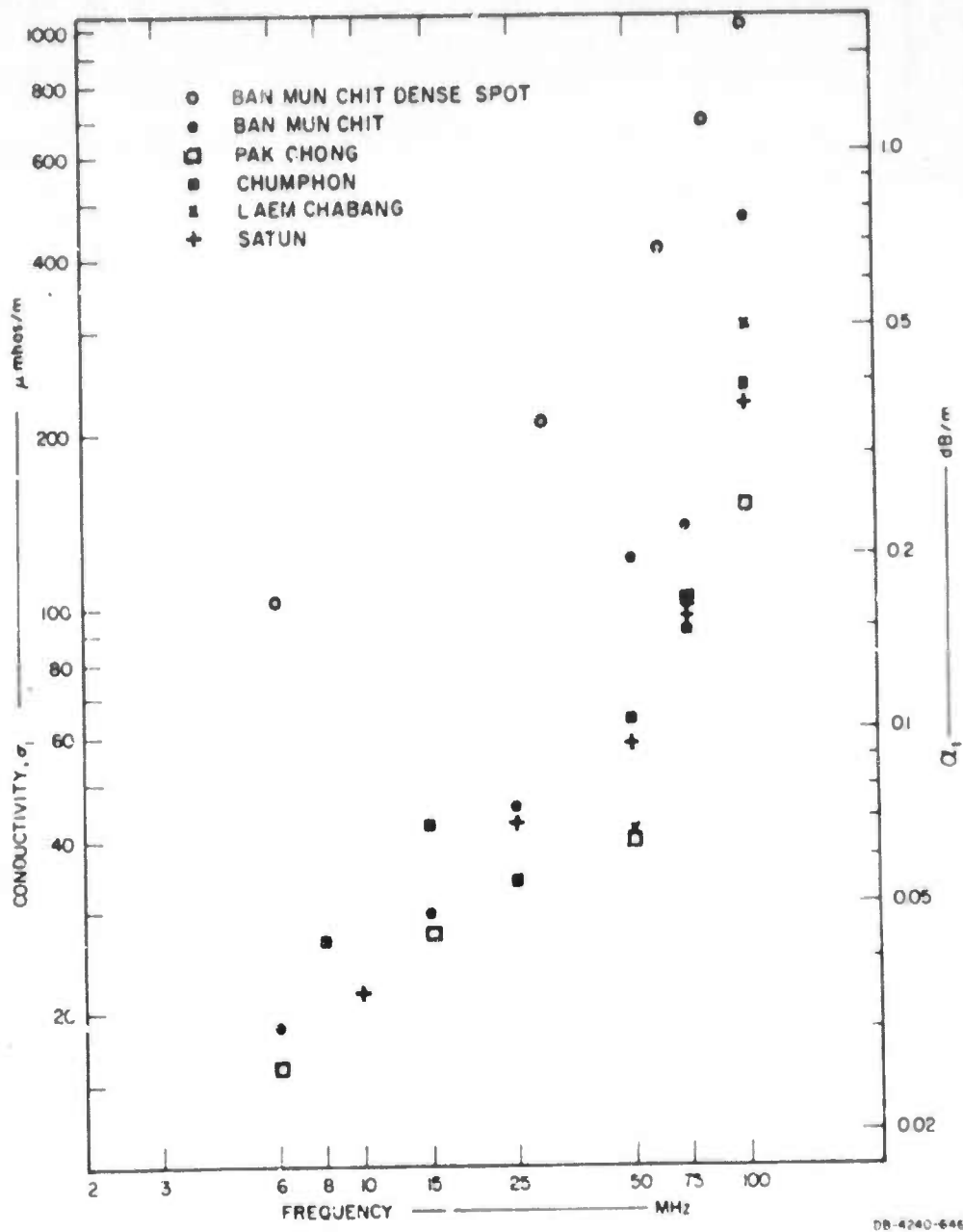


FIGURE III-9 COMPARISON OF MEDIAN σ_1 AND α_1 MEASURED IN UNDERGROWTH AT FIVE SITES

"lateral-wave" attenuation constant in the following section). Some of the conductivity values at 75 and 100 MHz may be too high due to probe limitations (see especially the loss tangent data),^{*} but the values observed in the frequency range 6 through 50 MHz probably are reasonable estimators of the equivalent slab parameters. The conductivity curve labeled Ban Mun Chit dense spot was generated from data taken in the most dense vegetation found at any of the Thailand sites and is included as an example of an isolated pocket of very dense foliage. The values from the other sites are surprisingly similar even though the forest sites yielding these data appeared quite different to the eye. The spread of the Thailand OWL data is discussed in STR 43, but it may be remarked that only rarely did the individual observed values of ϵ'_{rl} and μ'_{rl} fall outside the bounds (which include measurement error):

$$0.9 < \epsilon'_{rl} < 1.2$$

$$0.8 < \mu'_{rl} < 1.1 .$$

It should be noted, however, that a limitation in the manner in which the probes were used probably caused the median values of μ'_{rl} to differ from unity on the low side and caused the average values of ϵ'_{rl} to be biased slightly high (see Appendix E in STR 42D). The most probable

* The loss tangent data generally exhibited a decreasing trend with increasing frequency from 6 through 50 MHz: $\delta \approx 0.12 f^{-1/2}$ MHz. But from 50 to 100 MHz the loss tangent generally increased with increasing frequency; and, since the conductivity dominates the expression for loss tangent, it is possible that the OWL-measured conductivity values are too high at 75 and 100 MHz.

value of μ'_{rl} is 1.0, and a reasonable estimate of ϵ'_{rl} for use in the slab model is between 1.01 and 1.06.

f. Discussion of the Use of Vegetation Electrical Constants in Lateral Wave Computations

The measured values of the macroscopic electrical parameters for the forest can be used to compute α_L , the slab attenuation constant for the lateral wave,* which is required to calculate antenna height-gain functions for the ground-to-ground case.⁷

$$\alpha_L = 8.686(2\pi/\lambda_0) \operatorname{Im} \left\{ \frac{n^2 - 1}{n^2 + 1} \right\}^{1/2} \text{ dB/m}$$

where λ_0 is the free-space wavelength in meters, and $n_i = (\epsilon'_{rl} - j60\pi\lambda_0)^{1/2}$ is the complex refractive index of the forest. Computed values of α_L in dB/meter are given as a function of frequency in Figure III-10. There is quite a bit of scatter at a given frequency, but nevertheless there is a reasonable amount of agreement between the values obtained at the different sites. For frequencies below 75 MHz a reasonable approximate expression for α_L as a function of frequency is:

$$\alpha_L \approx 0.009f_{\text{MHz}} + 0.1 \quad \text{in dB/m.}$$

At 100 MHz the values are consistently higher than the trend indicated by the other values, and these values appear suspect. Apparently the conductivity values deduced from the line measurements were high by about a factor of 2.

* Note that this attenuation constant differs from the "through-the-slab" attenuation constant given in Figure III-9.

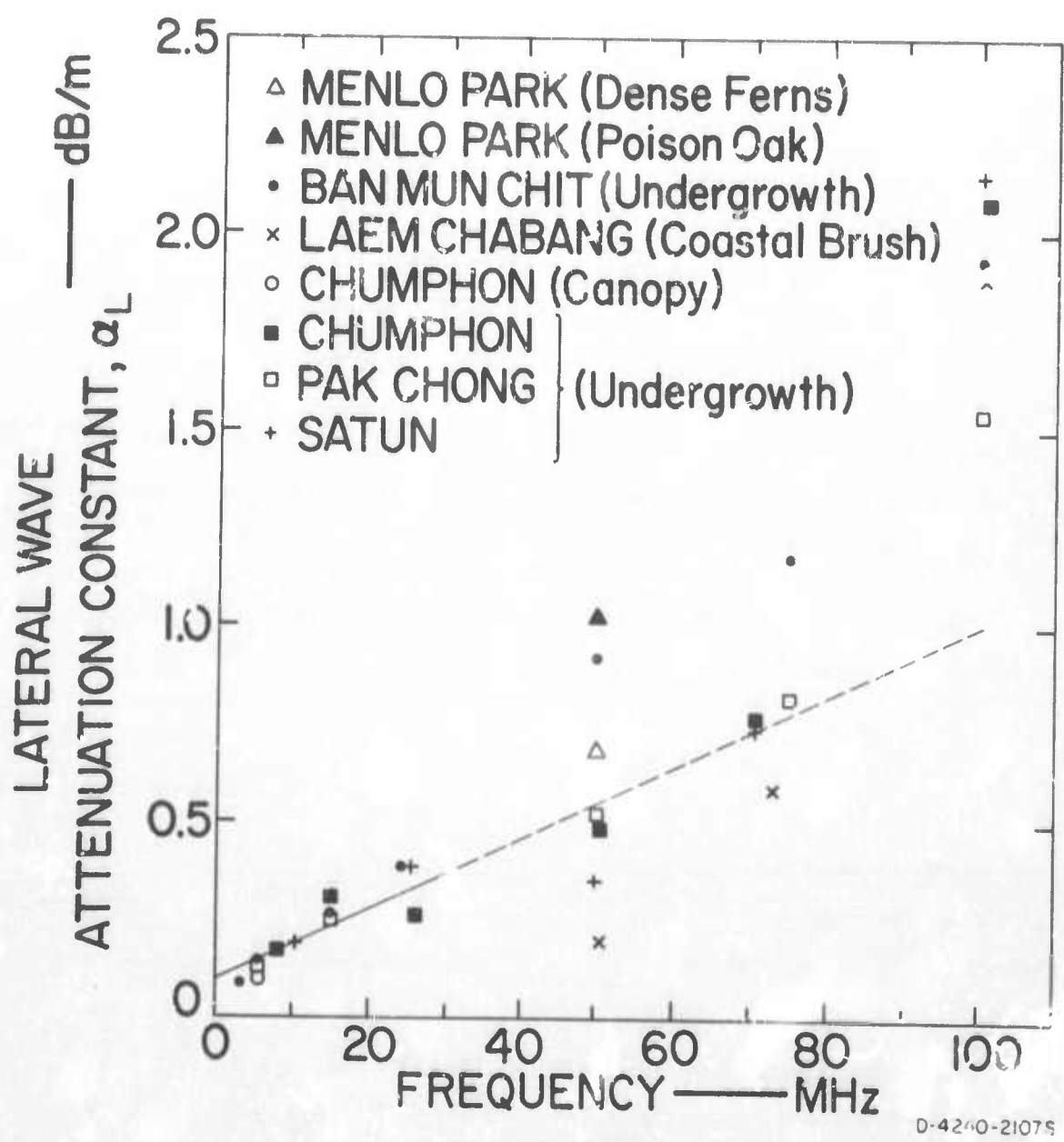


FIGURE III-10 LATERAL WAVE ATTENUATION CONSTANT COMPUTED FROM OWL MEASUREMENTS—AS A FUNCTION OF FREQUENCY

Let us consider the effect of conductivity on α_L . (see Figure III-11). For these computations, ϵ'_{rl} was held constant at 1.038--a typical value in the frequency range 5 to 75 MHz. Notice that at a given frequency α_L increases as σ_1 increases, and becomes independent of frequency for frequencies higher than some limiting frequency, f_L (e.g., $f_L \approx 10$ MHz for $\sigma_1 = 10^{-5}$ mho/m, 30 MHz for $\sigma_1 = 3 \times 10^{-5}$ mho/m, and 60 MHz for $\sigma_1 = 6 \times 10^{-5}$ mho/m, etc.) Computed values of α_L for the Pak Chong site and also the approximate linear expression for α_L versus frequency are shown for comparison. While the computations of α_L with constant ϵ'_{rl} and σ_1 are useful to show the effects of these variables, the OWL data indicate that computations based upon the assumption of σ_1 increasing with increasing frequency (and ϵ'_{rl} constant) should be more typical of actual α_L variation with frequency.

A reasonable fit to the conductivity values of Figure III-9 in the range 5 to 75 MHz is given by

$$\sigma_1 \approx 0.45 \times 10^{-5} \left(f_{\text{MHz}} \right)^{0.7} \quad \text{in mho/m} .$$

Let us use this expression for σ_1 and calculate α_L for various values of ϵ'_{rl} . The results of such a calculation are shown in Figure III-12. Notice that a larger value of ϵ'_{rl} at a given frequency corresponds to a smaller value of α_L . The approximate linear expression for α_L and the OWL-measured data from Pak Chong again are shown for comparison with the parametric curves, and the trends are quite similar.

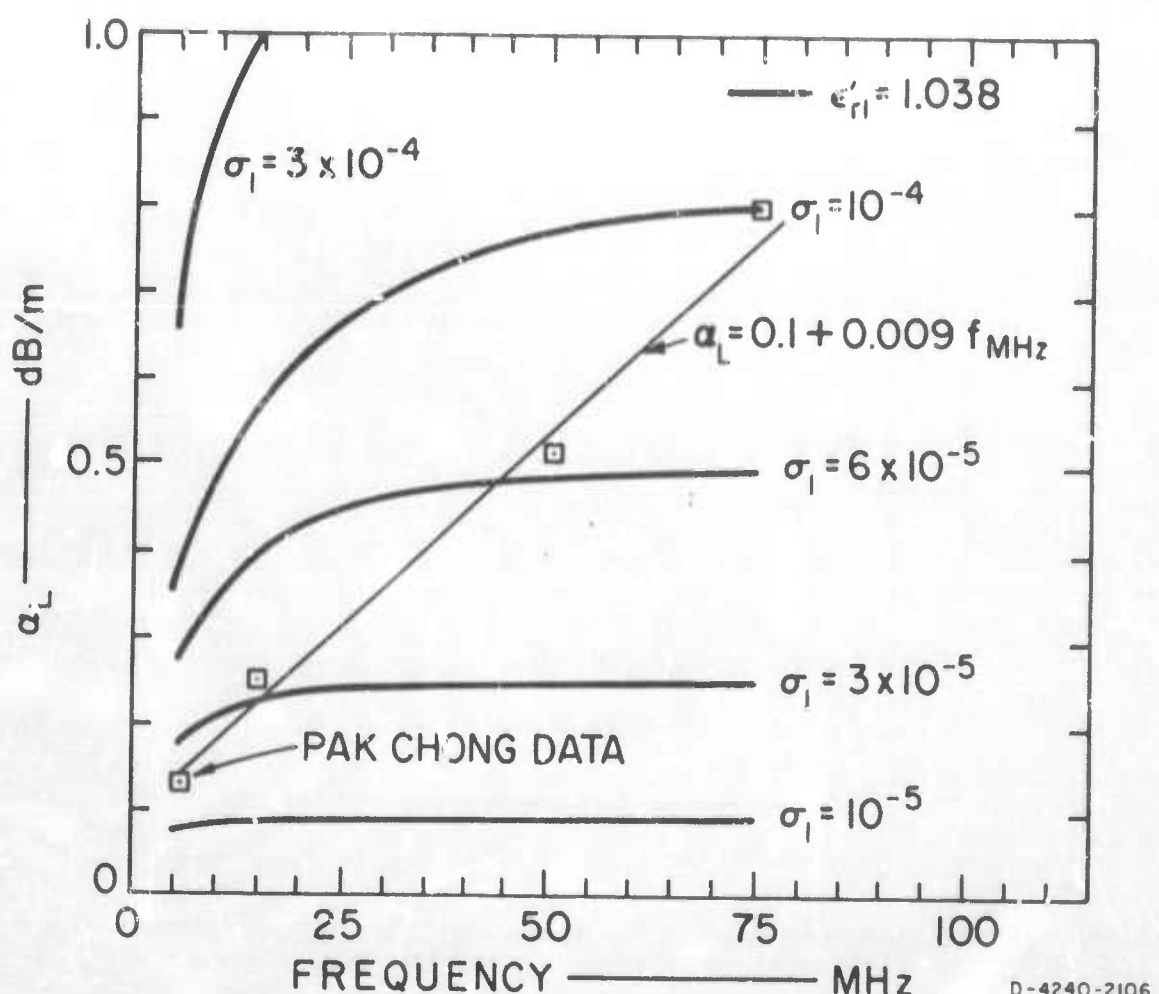


FIGURE III-11 LATERAL WAVE ATTENUATION CONSTANT COMPUTED AS A FUNCTION OF FREQUENCY, WITH CONSTANT CONDUCTIVITY

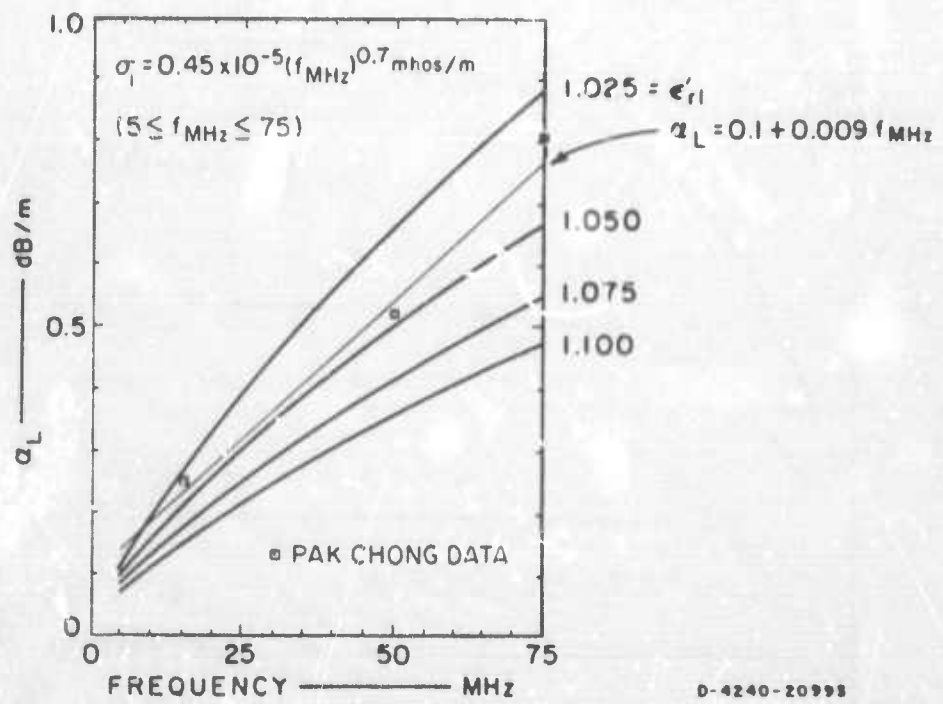


FIGURE III-12 LATERAL WAVE ATTENUATION CONSTANT COMPUTED AS A FUNCTION OF FREQUENCY, WITH VARIABLE CONDUCTIVITY

g. Intrinsic Conductivity of Vegetation as Inferred from a Biodensity Experiment

The biomass * concept expressed originally by Dr. L. T. Burcham¹⁰ and employed in Thailand by Mr. S. Sabhasri and Dr. L. E. Wood¹¹ led us to perform measurements at three sites, which we termed "biodensity" experiments. These experiments consisted of placing freshly cut vegetation in a dry wooden hopper mounted on a drayage scale and measuring the sample weight and the input impedance of the small (VHF) OWL inserted into the middle of the cut vegetation as a function of time after cutting. By observing the weight change, and subtracting out the weight of the wooden hopper, it was possible to relate the macroscopic electric properties of the cut vegetation (computed from the impedance readings) to the weight of the vegetation as a function of time after cutting. An estimate of the volume of the sample permitted a conversion from sample weight to biodensity. Knowing the height of the uncut vegetation one could convert biomass to biodensity by dividing the biomass by the height of the uncut vegetation (and an appropriate constant). Thus, one could theoretically convert biomass data to electrical constant estimates. While the relationship between the biomass concept and radio propagation in forests has not been worked out to the point of being useful, except as a gross technique for differentiating between forests, † these experiments did yield some interesting results.

* Biomass is defined as the weight per unit area (e.g., tons/acre) of the biological matter (primarily vegetation).

† Biomass data (when accompanied by data on forest height and tree spacing) might be useful when trying to estimate the macroscopic electrical properties of forests for which we have no radio propagation data (OWL, height gain, or path loss), but it does not appear to be directly useful from the standpoint of predicting the performance of radio equipments.

Figure 111-13 shows the relative dielectric constant of a sample of freshly cut willows as a function of sample weight. The relationship is linear in each case for all but the lowest values (driest condition). The average attenuation constant for the OWL is shown in Figure 111-14 as a function of sample weight for the same sample. Also shown is the effective conductivity of the fraction of the sample volume occupied by bioplasm (mostly water)--as inferred from the sample dimensions and the weight change. These latter data indicate an intrinsic RF conductivity of the willow bioplasm prior to cutting of about 3×10^{-2} mho/m. Notice that this intrinsic conductivity tends to increase as the weight (and hence fraction of remaining water) decreases to about 800 lbs--analogous to the action in a salt drying pond--even though the attenuation constant of the line is monotonically decreasing. Presumably the oscillatory variations observed for small sample weights are caused by the diurnal cycle of local humidity which is super-imposed upon the drying process (and less noticeable at earlier times after cutting when the change in water content due to this cycle is a smaller fraction of the total water content).

A similar experiment was repeated at Ban Mun Chit, Thailand. The sample was invaded by a colony of ants and, about 38 hours after cutting the sample actually exhibited a weight gain! It was concluded that this type of experiment is not too practical in the tropical environment. Nevertheless, it was possible to estimate the intrinsic conductivity of the bioplasm at 0.025 to 0.05 mho/m. In spite of the difficulties with this type of experiment another try was made at Chumphon, Thailand. The results of that test indicated an intrinsic conductivity of about 0.03 to 0.06 mho/m.

The results obtained in Thailand are reasonably consistent with the result of the willow test in California, and indicate

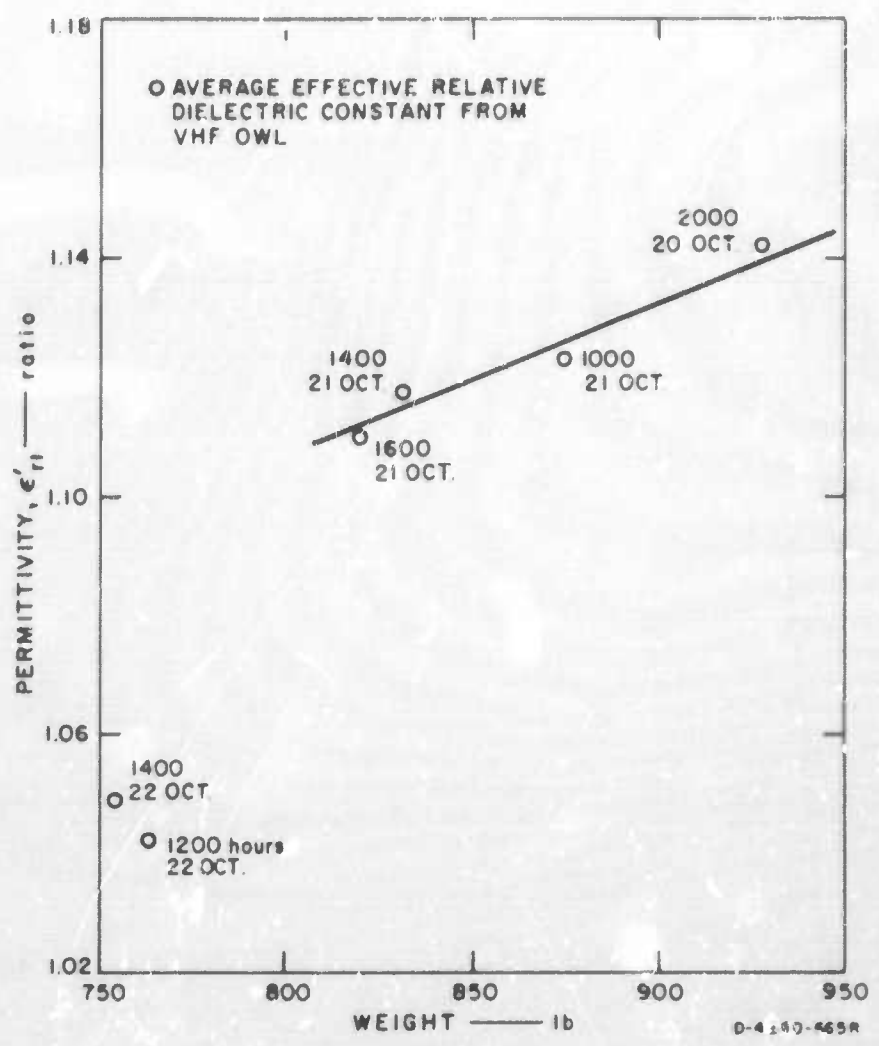


FIGURE III-13 PERMITTIVITY AS A FUNCTION OF WILLOW SAMPLE WEIGHT

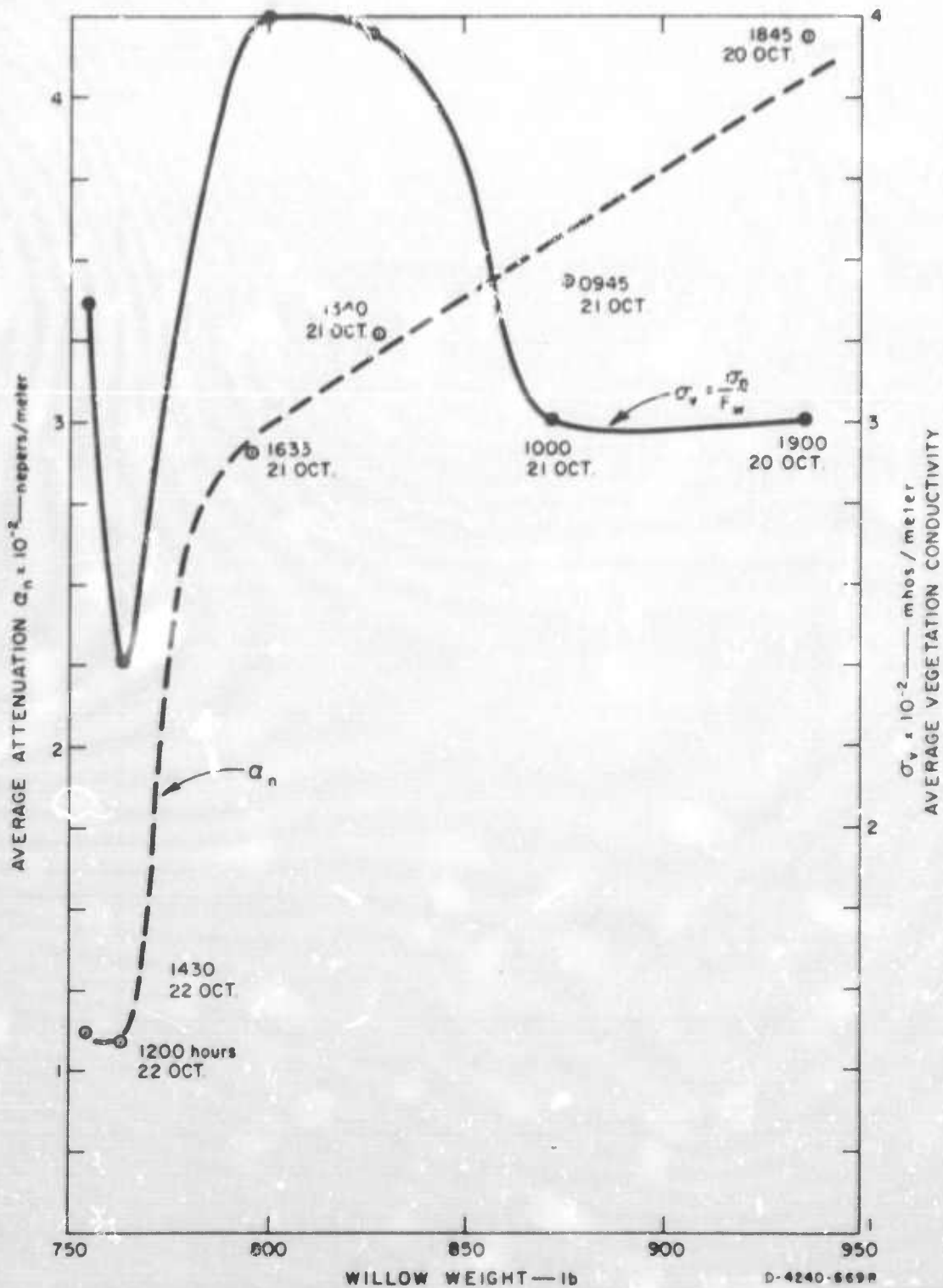


FIGURE III-14 VARIATION OF ATTENUATION CONST. AND CONDUCTIVITY AS A FUNCTION OF WILLOW SAMPLE WEIGHT

that the intrinsic conductivity of living vegetation is the order of 0.04 mho/m. It might be noted in passing that Dickinson,¹² using an even more indirect method, estimated the HF intrinsic conductivity of eucalyptus stems at 0.24 mho/m. Hence, we might conclude that the intrinsic conductivity of the bioplasm of living vegetation probably is between 0.01 and 1.0 mho/m at HF and VHF.

2. Ground Constants (STRs 29, 30, 43)

a. Objectives

The main reason for measuring ground electrical constants is to obtain values for use in mathematical models to predict antenna performance and propagation loss between transmitting and receiving antennas.

b. Background

This problem can be considered to consist of two parts: (1) measurements performed to document an environment with a view toward determining the usefulness of certain mathematical models, and (2) measurements performed to obtain input data for mathematical models of proven usefulness with a view toward equipment design, system performance estimates, etc. Measurements were made under this program toward both of these basic objectives.

A review of the various techniques for ground-constant measurements was made at the beginning of this project (STR 17), and the following techniques were identified:

- (1) Field-strength decrease versus distance method
- (2) Wave-tilt method

- (3) Capacitor dielectric methods
- (4) Reflection coefficient methods
- (5) DC (and audio frequency) probe methods
- (6) RF probe methods
- (7) Antenna impedance methods.

The field-strength-decrease-versus-distance method consists of comparing measured field-strength data with propagation curves derived from a rigorous mathematical formulation, and is useful for obtaining an estimate of the effective conductivity of the ground over areas with linear dimensions of several tens of kilometers. This method is most useful for frequencies in the lower part of the HF band and below, and for regions free of vegetation and major surface perturbations. Measurements in the MF band were made using this technique in central, eastern, and northeastern Thailand (STR 29).

The wave-tilt method consists of relating the tilt of the resultant electric-field vector at the air-ground interface (produced by a vertically polarized transmitting antenna located on the ground some distance away) to the real part of the relative dielectric constant of the ground as derived from a rigorous mathematical formulation.

Capacitor dielectric methods require transfer of the soil to the capacitor, with probable change in compaction of the sample, loss of moisture, and miscellaneous bother. This method was rejected in favor of in situ techniques.

Reflection-coefficient methods, though promising for determining effective ground constants (or surface impedance) of irregular terrain, require a systems approach that becomes costly when properly instrumented and carried out. These methods were not used in this program.

A special effort was made to investigate methods which could be employed for in situ measurements in forested terrain (STR 30). The wave-tilt method was ruled out because of scatter from the trees* (STRs 19, 25, 35, 40, and 41). The technique of curve fitting path-loss data to mathematical model calculations was ruled out because present models for propagation in forested terrain incorporate ground constants only as a relatively insignificant effect.⁶ Indeed, simple models that neglect the presence of the ground entirely have been used successfully to describe wave propagation over forested terrain between antennas not too near the ground-vegetation interface.⁷ RF probe techniques^{2,3} (STRs 30, 43) appear the most practical approach to determining the constants of surface ground beneath living trees, and DC or audio frequency probe techniques (STRs 10, 30) appear the most practical for determining to what depths the surface values can be extrapolated. Antenna impedance methods require further mathematical development, but show promise for providing useful supplementary information on ground conductivity (see STR 30).

c. Results

The results of conductivity measurements made using the field-strength-decrease-with-distance method in central, eastern, and northeastern Thailand on 820 kHz and 1455 kHz (STR 29) are summarized in the map of Figure III-15. The areas over which these values probably apply--as indicated by the solid boundary lines--were determined from

* Subsequently, it was learned that propagation was supported primarily by a lateral wave when the separation between the transmitting and receiving sites is greater than a few tens of one kilometer.⁶ The interpretation of data from a standard wave-tilt measuring setup (such as that described in STR 29) obtained in a lateral-wave field in a forest would require more study.



DB-1240-269

FIGURE III-15 MAP OF MF GROUND CONDUCTIVITY IN CENTRAL, EASTERN, AND NORTHEASTERN THAILAND (UNITS IN mmho/m)

maps of soil type, geology, and topography. The range of values shown includes the variation with season (dry season and rainy season), with the higher conductivities generally occurring during the rainy season.

Measurements of ϵ'_{r2} were made at approximately 42 sites in eastern and northeastern Thailand using the wave-tilt method at 27 MHz (STR 29). These measurements were made during the dry season, but there were occasional showers during the period of measurement. When these occurred it was necessary to wait until the surface soil had dried before applying the wave-tilt method. The observed values ranged from 4 to 48 with the lower values in the plateau areas and the higher values in the river valleys.

Open-wire transmission-line probes (RF probes) were used at six sites in Thailand to measure ϵ'_{r2} and σ_z (STR 43). Measurements were taken beneath living vegetation at all sites except the open paddy field at Bangkok. At Laem Chabang, on the Gulf of Thailand, data were obtained on the open sandy beach and beneath coastal brush growing nearby. At the Chumphon site, on the Malay Peninsula (near the Isthmus of Kra), data were obtained at two sites in an open, cleared area and at two sites beneath the rain forest. It should be noted that there was standing water at each sample station at this site except Chumphon Forest II. Data also were obtained on ground constants beneath the vegetation at the Pak Chong and Satun sites used by Jansky and Bailey to make path loss measurements and beneath the vegetation at Ban Mun Chit where SRI made tests on antenna-vegetation effects with the Xeledop systems and ionospheric sounder systems. These results are summarized in Figures III-16 and III-17. In general, conductivity was greater when moisture content was greater, and the trend of variation with frequency revealed less increase with frequency for the higher moisture contents. Permittivity was

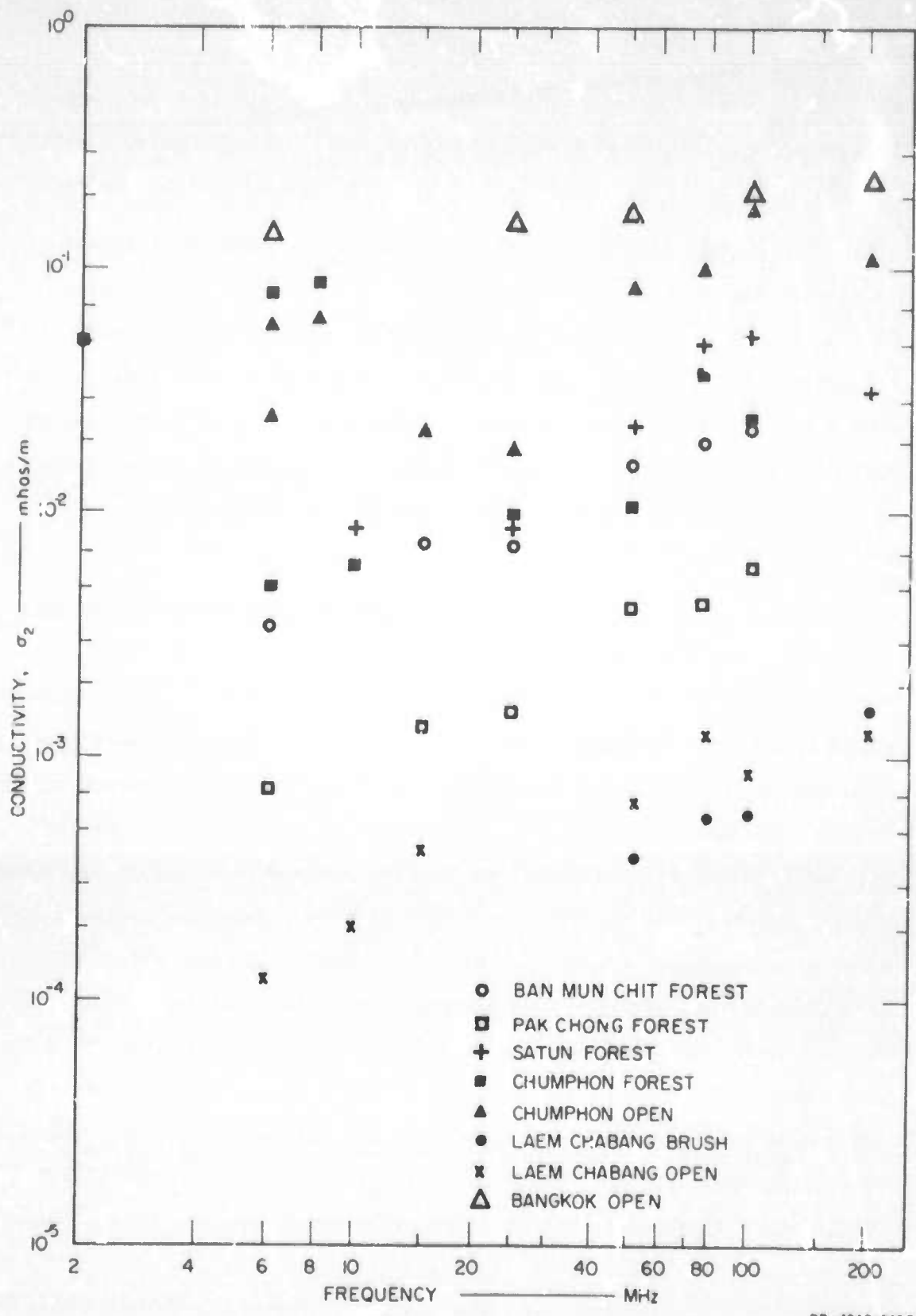


FIGURE III-16 MEDIAN SURFACE CONDUCTIVITY OF GROUND AT SELECTED SITES IN THAILAND

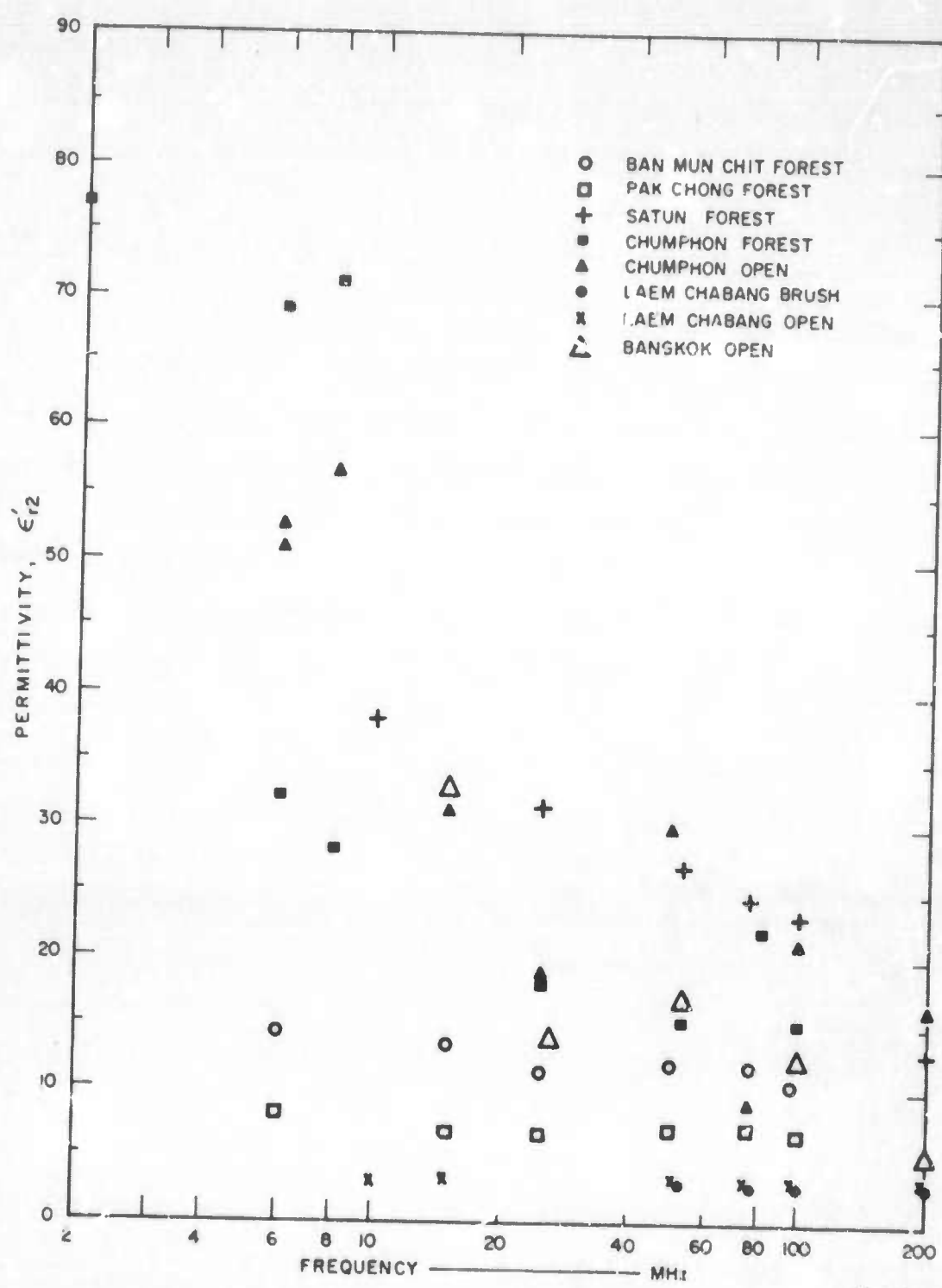


FIGURE III-17 MEDIAN SURFACE GROUND PERMITTIVITY MEASURED AT SELECTED SITES IN THAILAND

lower when moisture content was lower; but the trend was for ϵ'_{r2} to decrease as the measurement frequency increased, with less variation with frequency for the lower moisture contents.

C. Full-Scale Antenna Pattern Measurements (STRs 10, 25, 35, 39D, 45D)

1. Objective

The radiation patterns of full-scale field-expedient HF and VHF antennas were measured in several environments in order to gain a better understanding of the effects of tropical forests on antennas and propagation. The data from these measurements were also used to verify the mathematical model described in Section III-A. Of primary interest was the determination of the effect of tropical forests on HF sky-wave and HF and VHF air-to-ground propagation.

2. Background

The radiation patterns and gains of simple antennas operating under ideal conditions (i.e., perfect ground, balanced feed lines, etc.) have been thoroughly studied, but at the beginning of this work relatively little information was available on the performance of these antennas when they were operated in less than ideal conditions--as is necessary in general practice (STR 17). Of particular interest was the effect of tropical forests and unbalanced feed lines on the radiation patterns and feed-point impedance (see Section III-F) of these antennas.

In order to measure the radiation patterns of full-scale antennas, the airborne Xeledop (an acronym denoting "Transmitting Elementary Dipole with Optional Polarization") system was developed by Stanford Research Institute and was used on this contract to measure the radiation patterns of HF and VHF antennas.

HF radiation patterns were measured while the antennas were located in the following environments:

- (1) Over an open, flat terrain near Lodi, California (STR 10)
- (2) In a U.S. conifer forest near Almanor, California (STR 25)
- (3) In a dry evergreen forest near Ban Mun Chit, Thailand (STR 35).

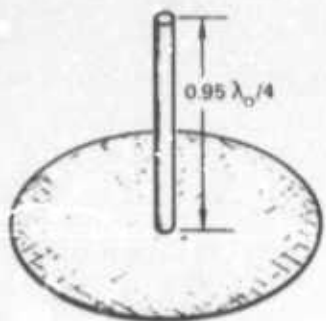
The results from these measurement sites were compared, and a comparison of the measured and calculated patterns was made (STR 45D).

Sketches of the HF antennas measured at the three sites--Lodi, Almanor, and Ban Mun Chit--are presented in Figure III-18, and a summary of the HF antenna radiation pattern data available is given in Table III-1. Detailed descriptions of the measurement sites and measurement antennas can be found in the Special Technical Reports describing the individual measurements (STRs 10, 25, and 35). Only selected examples of these data will be presented in this section.

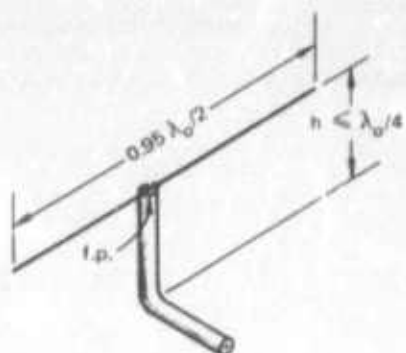
VHF measurements were performed at two sites, as follows:

- (1) Preliminary measurements were conducted in a eucalyptus grove near Newark, California (STR 19).
- (2) More comprehensive measurements were conducted in a dry evergreen forest near Ban Mun Chit, Thailand (STR 39D).

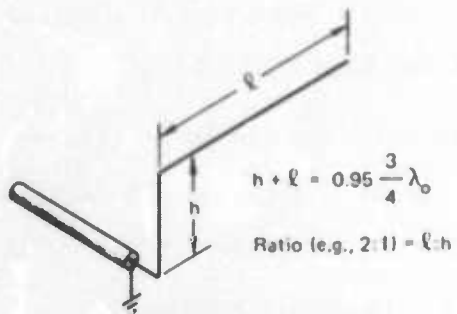
A summary of the VHF radiation pattern data available from the two measurement sites is presented in Table III-2.



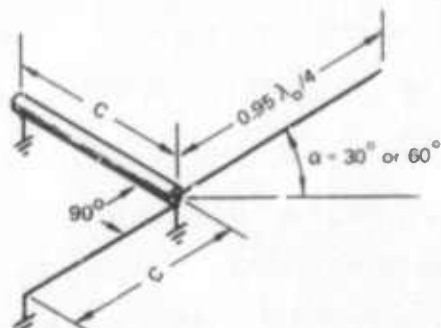
(a) MONPOLE OR WHIP



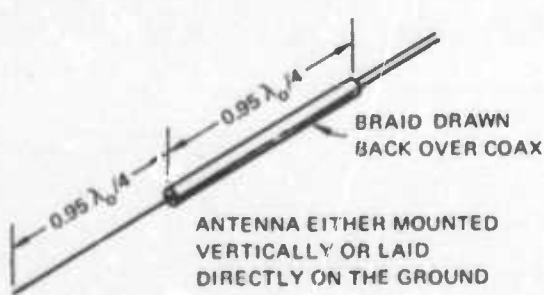
(b) DIPOLE—BALUN INSTALLED
AT FEEDPOINT (f.p.) FOR
BALANCED DIPOLES



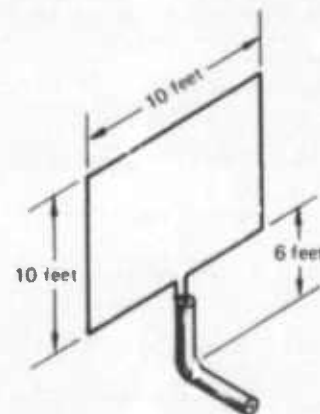
(c) INVERTED L



(d) SLANT WIRE



(e) SLEEVE DIPOLE



(f) LOOP

TA-310522-4

FIGURE III-18 SKETCHES OF ANTENNAS MEASURED WITH THE HF AIRBORNE XELEDOP

Table III-1

SUMMARY OF MEASURED HF ANTENNA PATTERN DATA AVAILABLE IN STR 10, 25, and 35

Antenna Type	f_o (MHz)	f_m (MHz)	Data Available		
			Lodi (STR 10)	Almanor (STR 25)	Ban Mun Chit (STR 35)
Balanced Dipole with Ground Screen in Clearing-- 41-ft High	6.0	3.0			θ, e, p
		4.0			θ, e, p
		6.0			θ, e, p
		8.0			θ, e, p
Balanced Dipole in Clearing-- 41-ft High	6.0	3.0			θ, e, p
		4.0			θ, e, p
		6.0			θ, e, p
		8.0			θ, e, p
Unbalanced Dipole in Clearing-- 41-ft High	6.0	3.0			θ, e, p
		4.0			θ, e, p
		6.0			θ, e, p
		8.0			θ, e, p
Balanced Dipole in Forest-- 41-ft High	6.0	6.0			θ, e, p
Unbalanced Dipole in Forest-- 41-ft High	6.0	3.0			θ, e, p
		4.0			θ, e, p
		6.0			θ, e, p
		8.0			θ, e, p
Unbalanced Dipole in Forest-- 16-ft High	6.0	6.0			θ, e, p
Unbalanced Dipole in Forest-- 8-ft High	6.0	6.0			θ, e, p
2-ft-High Unbalanced Dipole	6.0	2.0	θ	θ	
		4.0	θ	θ, e, p	θ, e, p
		6.0	θ, e	θ, e, p	θ, e, p
		8.0			θ, e, p
		10.0	θ, e	θ, e, p	
23-ft-High Unbalanced Dipole	8.0	2.67	θ, e		
		5.0	θ, e	θ, e, p	
		8.0	θ, e	θ, e, p	θ, e, p
		15.0	θ, e	θ, e, p	
Balanced Dipole over Ground Screen-- 16.4 ft High	15.0	4.0	θ	θ	θ, e, p
		5.0	θ	θ	
		6.0	θ	θ	θ, e, p
		8.0	θ	θ	θ, e, p
		10.0	θ	θ	
		12.0	θ		θ, e, p
		15.0	θ	θ	θ, e, p

* Symbols for patterns are as follows: θ is vertical polarization response, e is horizontal polarization response and P is power response.

The design frequency of the antenna is denoted by f_o and the measurement frequency is f_m .

Table III-1 (Continued)

Antenna Type	f_o (MHz)	f_m (MHz)	Data Available		
			Lodi (STR 10)	Almanor (STR 25)	Ban Mun Chit (STR 35)
Sleeve Dipole	5.0	5.0		θ, ϵ, P	
		8.0		θ, ϵ, P	
Sleeve Dipole	6.0	6.0			θ, ϵ, P
J&B-Type 80-ft-High Balanced Dipole	6.0	6.0			θ, ϵ, P
J&B-Type 40-ft-High Balanced Dipole	6.0	6.0			θ, ϵ, P
J&B-Type 40-ft-High Balanced Dipole	12.0	12.0			θ
Monopole in Clearing	6.0	6.0			θ
Monopole on Edge of Clearing	6.0	4.0			θ
		6.0			θ
		8.0			θ
Monopole in Forest	6.0	4.0			θ
		6.0			θ
		8.0			θ
Monopole	15.0	2.0	θ	θ	
		2.67	θ	θ	
		4.0	θ	θ	
		5.0	θ	θ	
		6.0	θ	θ	
		8.0	θ	θ	
		10.0	θ	θ	
		15.0	θ	θ	
J&B-Type 80-ft-High Vertical	2.0	2.0			θ
J&B-Type 40-ft-High Vertical	6.0	6.0			θ
J&B-Type 20-ft-High Vertical	12.0	12.0			θ
2:1 Inverted L	6.0	3.0			θ, ϵ, P
		4.0			θ, ϵ, P
		6.0			θ, ϵ, P
		8.0			θ, ϵ, P
2:1 Inverted L	8.0	2.67	θ, ϵ	θ	
		5.0		θ, ϵ, P	
		8.0	θ, ϵ	θ, ϵ, P	θ, ϵ, P
5:1 Inverted L	6.0	4.0			θ, ϵ, P
		6.0			θ, ϵ, P
		8.0			θ, ϵ, P
5:1 Inverted L	10.0	4.0		θ, ϵ, P	
		6.0		θ, ϵ, P	
		10.0	θ, ϵ	θ, ϵ, P	θ, ϵ, P
30° Slant Wire	4.0	2.0	θ	θ, ϵ, P	
		4.0	θ, ϵ	θ, ϵ, P	θ, ϵ, P
		6.0	θ, ϵ	θ, ϵ, P	θ, ϵ, P

Table III-1 (Concluded)

Antenna Type	f_o (MHz)	f_m (MHz)	Data Available		
			Lodi (STR 10)	Almanor (STR 25)	Ban Mun Chit (STR 35)
30° Slant Wire	6.0	3.0			θ, *, P
		4.0			θ, *, P
		6.0			θ, *, P
		8.0			θ, *, P
60° Slant Wire	5.0	5.0	θ, *		
		15.0	θ, *		
Loop in Clearing	6.0	6.0			θ, *, P
Loop in Forest	6.0	6.0			θ, *, P
Long Wire	6.0	3.0			θ, *, P
		4.0			θ, *, P
		6.0			θ, *, P
		8.0			θ, *, P

Table III-2

**SUMMARY OF MEASURED VHF ANTENNA PATTERN DATA
AVAILABLE IN STRs 19 AND 39D***

Antenna Type	f _o and f _m (MHz)	Data Available [*]		
		Newark	Ban Mun Chit	
Horizontal unbalanced dipole in the clearing	50		θ, ε	
Horizontal unbalanced dipole in the forest	50	θ, ε	θ, ε	
Horizontal folded dipole in the forest	50		θ, ε	
Vertical sleeve dipole in the clearing	50		θ, ε	
Vertical sleeve dipole in the forest	50	θ, ε	θ	
Vertical folded dipole in the forest	50		θ, ε	
Horizontal unbalanced dipole in the clearing	75		θ	
Horizontal unbalanced dipole in the forest	75	θ, ε	θ, ε	
Horizontal balanced dipole in the forest	75		θ, ε	
Horizontal dipole with balun in the forest	75		θ, ε	
Vertical sleeve dipole in the clearing	75		θ, ε	
Vertical sleeve dipole in the forest	75	θ, ε	θ, ε	
Horizontal unbalanced dipole in the clearing	100		θ, ε	
Horizontal unbalanced dipole in the forest	100	θ, ε	θ, ε	
Horizontal balanced dipole in the forest	100		θ, ε	
Vertical sleeve dipole in the clearing	100		θ, ε	
Vertical sleeve dipole in the forest	100	θ, ε	θ, ε	
Vertical balanced dipole in the forest	100		θ, ε	

* Only linear plots of amplitude as a function of azimuth angle and sample statistical estimators of the data are presented in STR 19, whereas contour plots and statistical estimators of the measured data will be presented in STR 39D.

* Pattern data are summarized as follows: θ is vertical polarization, and ε is horizontal polarization.

3. Measurement Technique

The instrumentation and data processing of the antenna measurements are only briefly described in this and the following sections. A more detailed description can be found in the reports describing the measurements (STRs 10, 19, 25, 35, 39D, and 45D), and in the open literature.¹⁴

The Xeledop transmitter is the primary component of the antenna pattern-measurement system. Two of these transmitters were constructed--one for HF (2 to 30 MHz) and the other for VHF (50 to 100 MHz). Either of these multiple-frequency transmitters is towed behind an aircraft on approximately 300 ft of dielectric rope. All of the electronics and batteries for the transmitters are contained in a central sphere. Arms extending from the sphere are fed as a balanced dipole antenna, whose total length is always less than one-half wavelength for the frequencies used. Thus, the directivity pattern of the Xeledop is approximately that of a Hertzian dipole for all measurement frequencies. The Xeledops can be towed to transmit either horizontally (E_ϕ) or vertically (E_θ --when corrected for the transmitting dipole pattern) polarized waves. The electrical symmetry of the Xeledops is such that the radiated polarization depends only upon its physical orientation, and its radiated power remains constant for either polarization.

The signals transmitted by the Xeledop are received by the measurement antennas and recorded, along with information on the location of the towing aircraft, in an instrumentation van at the measurement field site.

The measurement data are then processed to produce an azimuthal equal-area projection (contour plot) of the measured signal strength. In the case of the VHF measurements, it was necessary to process the data

statistically in order to provide a more understandable and useful presentation of the data.

4. Results of Measurements at HF

The pattern-measurement technique does not readily provide absolute gains since the radiated power from the Xeledop was not determined. (The transmitters in the Xeledop were either replaced or retuned between measurement sites.) Consequently, the relative gains of these antennas cannot be compared among sites by using only the data available from the pattern measurements. Therefore, the primary discussion in this section will pertain to the effects of the forests on the directivity patterns of these antennas. A more complete discussion of the absolute gains of these antennas will be presented in Section III-E and in STR 45D.

Examples of the azimuthal equal-area projections used in STRs 10, 25, 35, and 45D to present the pattern-measurement data are presented in Figures III-19 through III-21. These are patterns of the 8-MHz, 23-ft-high unbalanced dipole antenna when it was measured in the conifer forest at Almanor, California. Figure III-19 shows the E_ϕ (horizontal polarization) response of the antenna and Figure III-20 shows the E_θ (vertical polarization) response of the antenna. The measured maximum responses of this antenna to the two polarizations were within 0.5 dB of each other ($E_\phi/E_\theta = 0.5$ dB)--remember that the maximum E_ϕ response is at 90° and 270° from the axis of the dipole and the maximum E_θ response occurs on the axis of the dipole. The E_ϕ and E_θ data were combined using Poynting's theorem ($P = |E_\phi|^2 + |E_\theta|^2$), and combined with measurement data obtained from flying an orthogonal grid pattern above the antenna to provide the power pattern or optimum-reception

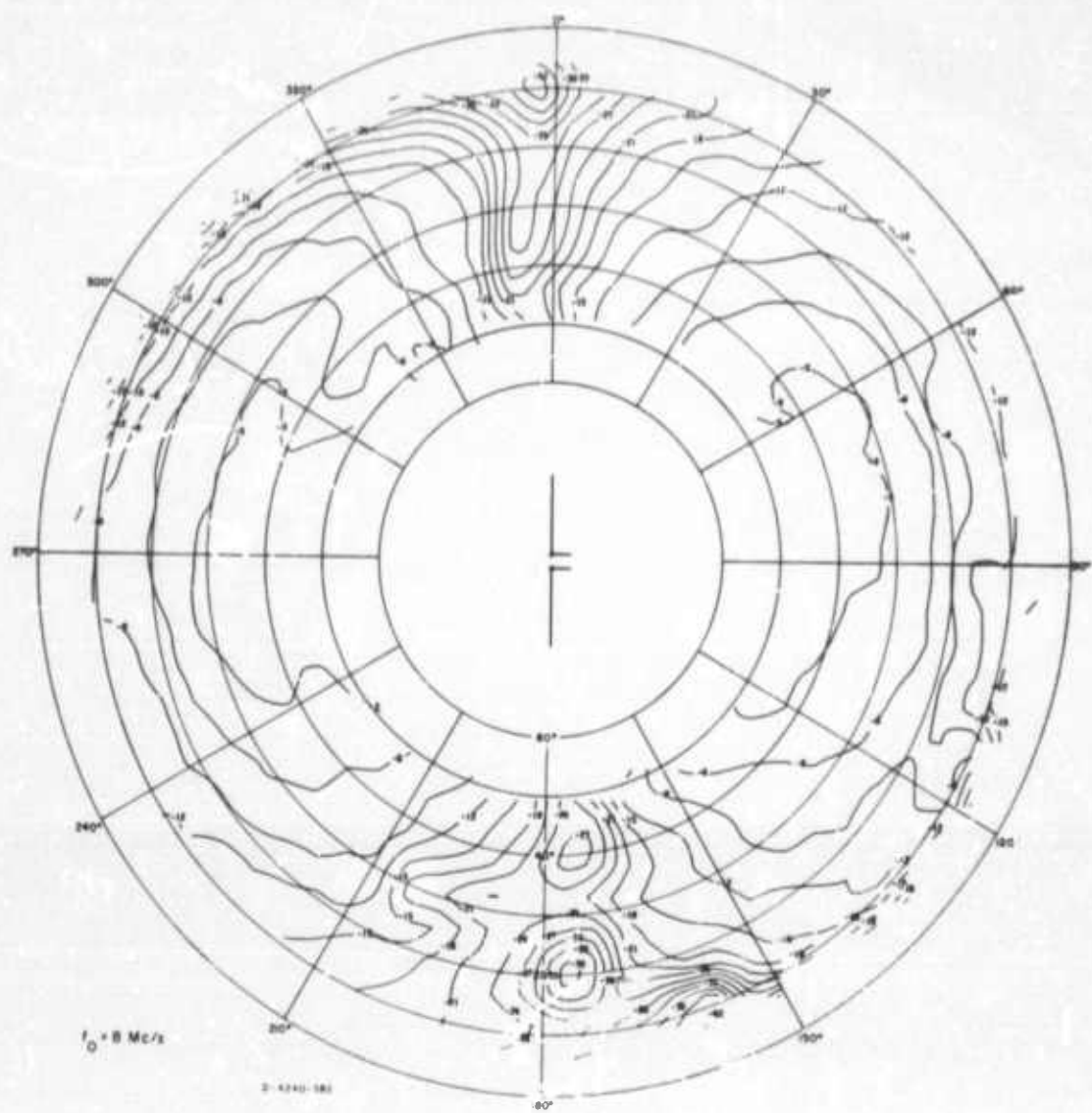


FIGURE III-19 MEASURED RADIATION PATTERN OF THE 8 MHz, 23-FOOT HIGH UNBALANCED DIPOLE AT ALMANOR— E_ϕ AT 8 MHz

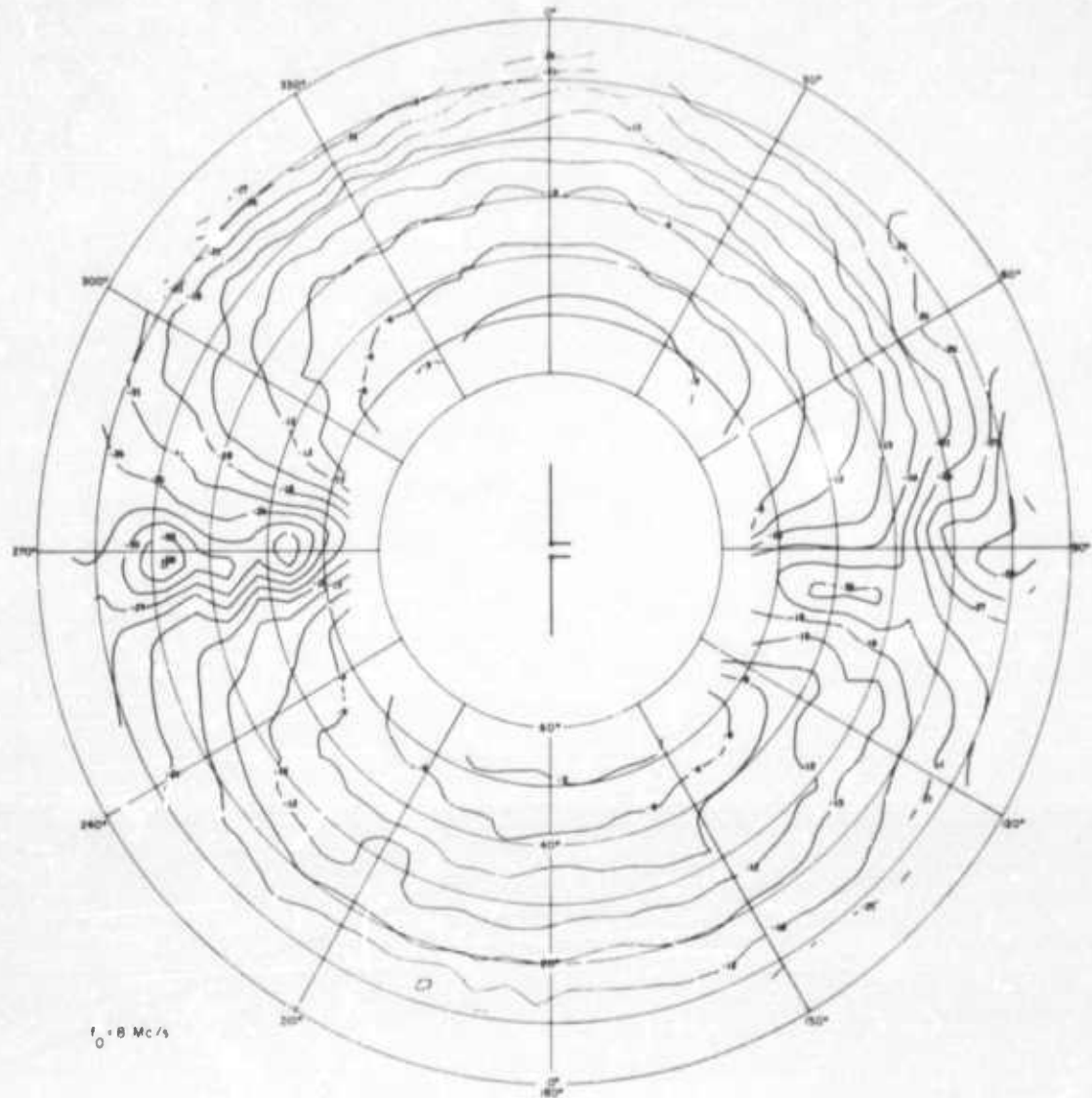


FIGURE III-20 MEASURED RADIATION PATTERN OF THE 8 MHz, 23-FOOT HIGH UNBALANCED DIPOLE AT ALMANOR— E_0 AT 8 MHz

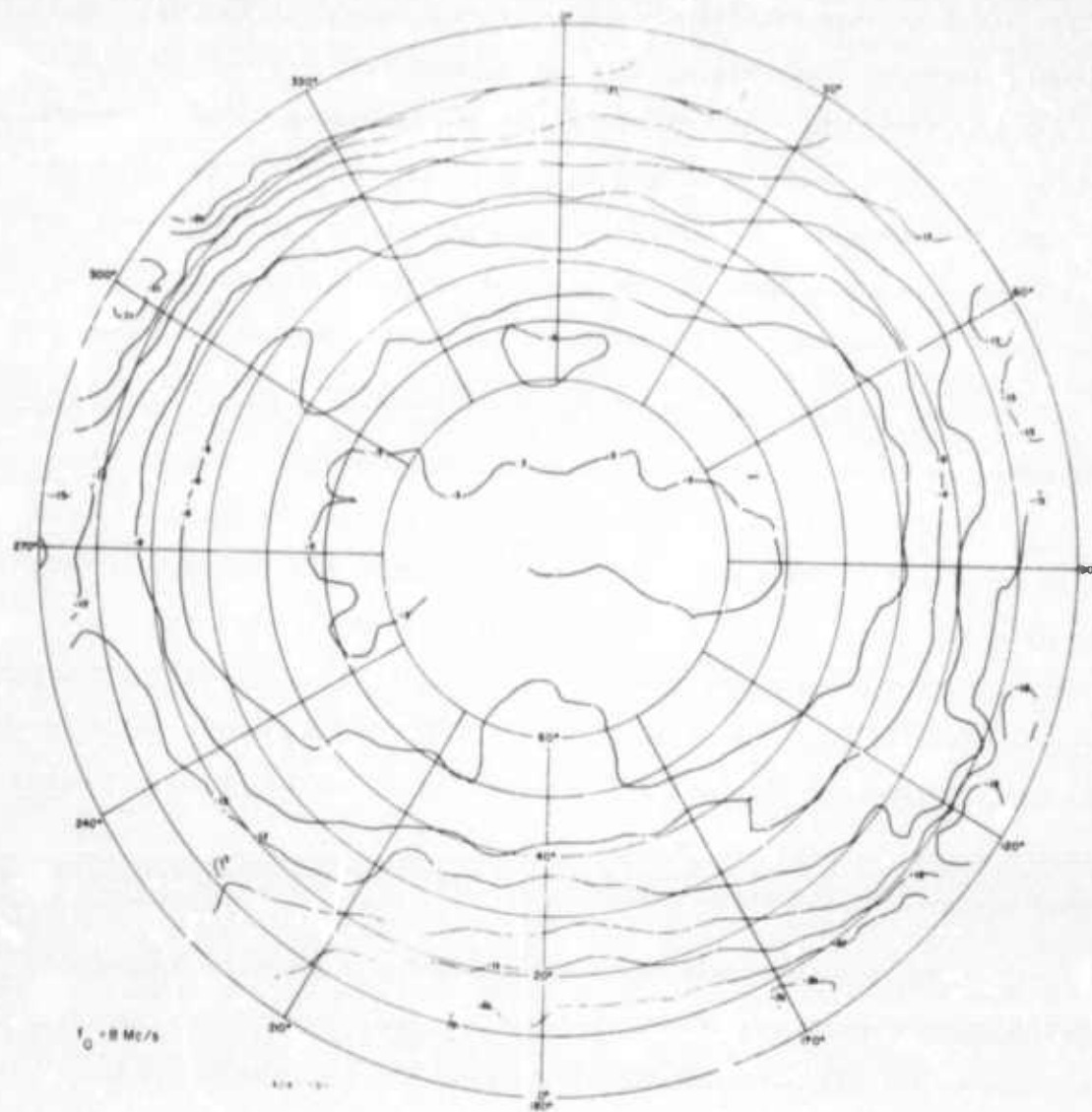


FIGURE III-21 MEASURED RADIATION PATTERN OF THE 8 MHZ, 23-FOOT HIGH UNBALANCED DIPOLE AT ALMANOR—POWER AT 8 MHZ

response pattern of the antenna as shown in Figure III-21.* Figure III-21 shows that the power pattern of this dipole is almost omnidirectional at high elevation angles. Figure III-22 is an elevation plane pattern of this antenna that was derived from the contour plots of the measured data. The absolute gain was estimated using the model of Section III-A, and the accuracy of these gains are estimated to be ± 3 dB. This figure shows an increase in gain for E_θ but not for E_ϕ at low elevation angles when the antenna was placed in the forest at Ban Mun Chit--as predicted by the mathematical model (see Figure III-29).

The monopole antennas were basically 15-MHz quarter-wavelength vertical elements over 50-ft-diameter wire-mesh ground screens. When the antennas were measured on 6 MHz at Ban Mun Chit, matching networks were installed to improve the antenna efficiency, but this should have no effect on the relative directivity patterns of the antennas. A contour plot comparing the directivity of the E_θ response of the monopole at the three sites is shown in Figure III-23. The elevation angle of the maximum response of this antenna increased when the antenna was located in the forest at Almanor, but it remained relatively omnidirectional when measured at the three sites.

The absolute gain was estimated for the monopole measured in the forest at Ban Mun Chit and the data for Lodi and Almanor was normalized to the Ban Mun Chit data to compare the performance of the antennas at the three sites, as shown in Figure III-24. The absolute gains in this figure are estimated to be accurate to 3 dB for an electrically short monopole. The figure shows that the elevation angle of

*A description of the measurement of the power patterns of full-scale antennas and the interpretation of the data for applications at the receiving end of the communication link is presented in STR 25.

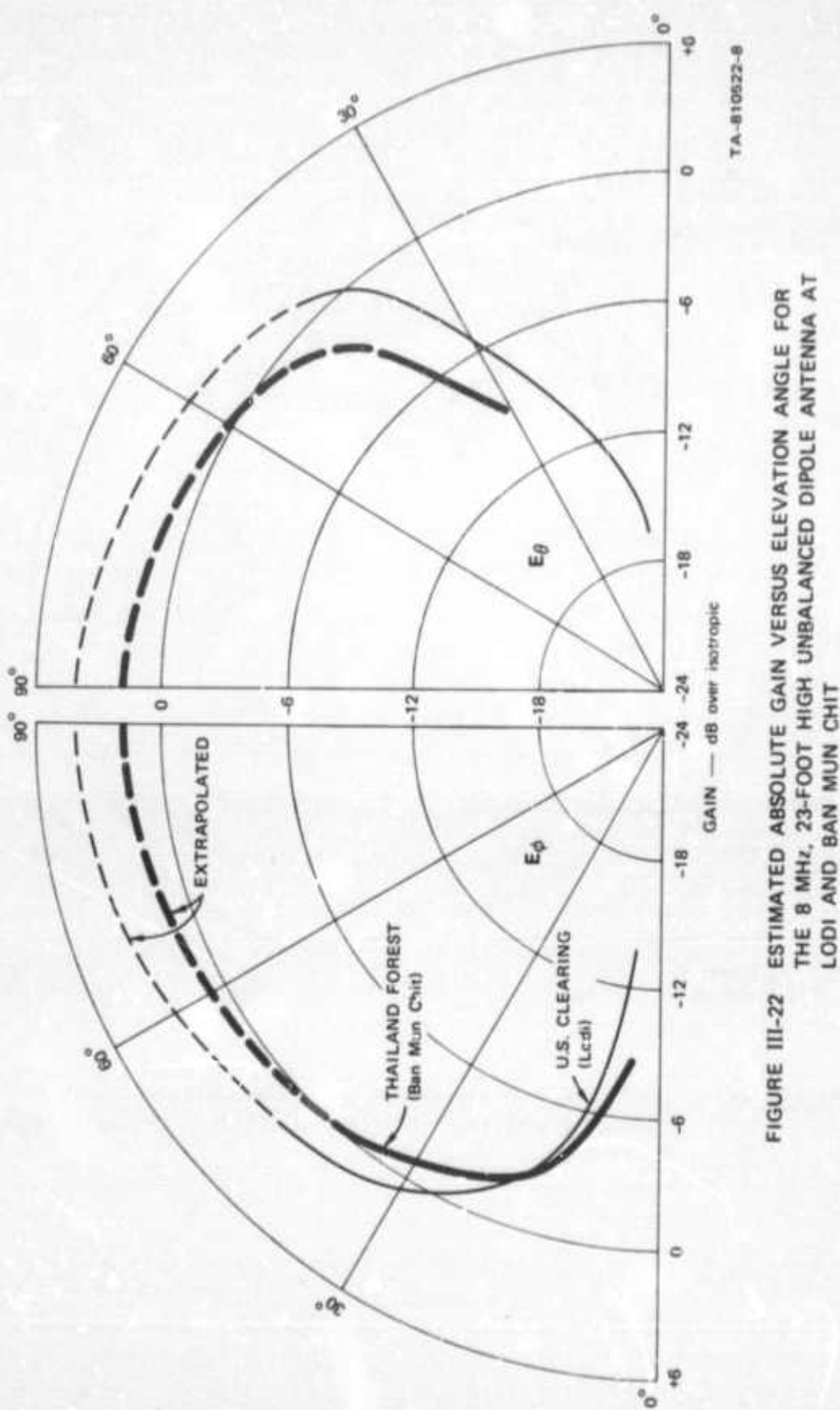


FIGURE III-22 ESTIMATED ABSOLUTE GAIN VERSUS ELEVATION ANGLE FOR THE 8 MHZ, 23-FOOT HIGH UNBALANCED DIPOLE ANTENNA AT LODI AND BAN MUN CHIT

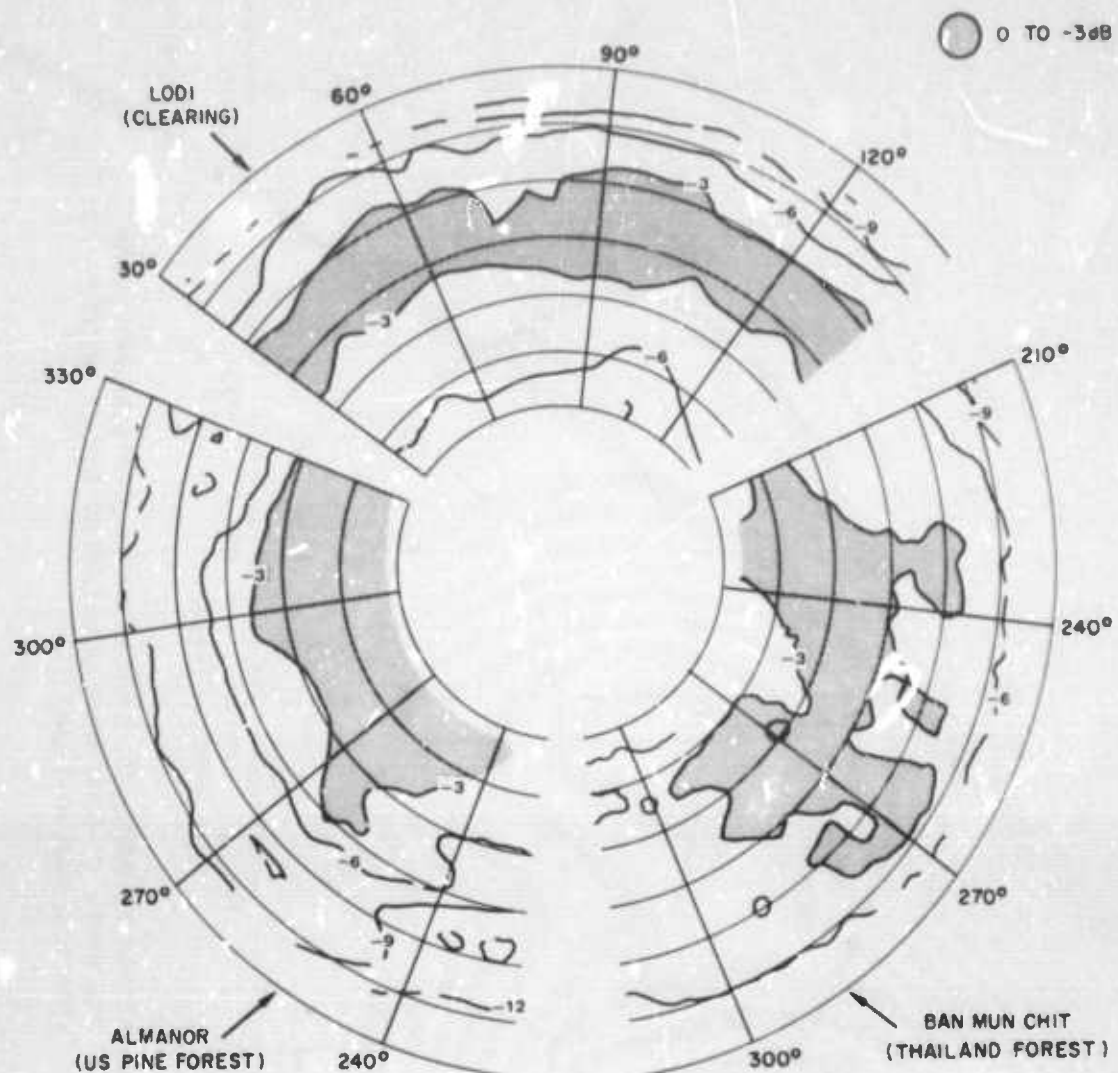


FIGURE III-23 COMPARISON OF MEASURED RADIATION PATTERNS OF THE MONPOLE ANTENNAS AT LODI, ALMANOR, AND BAN MUN CHIT—
 E_θ AT 6 MHz

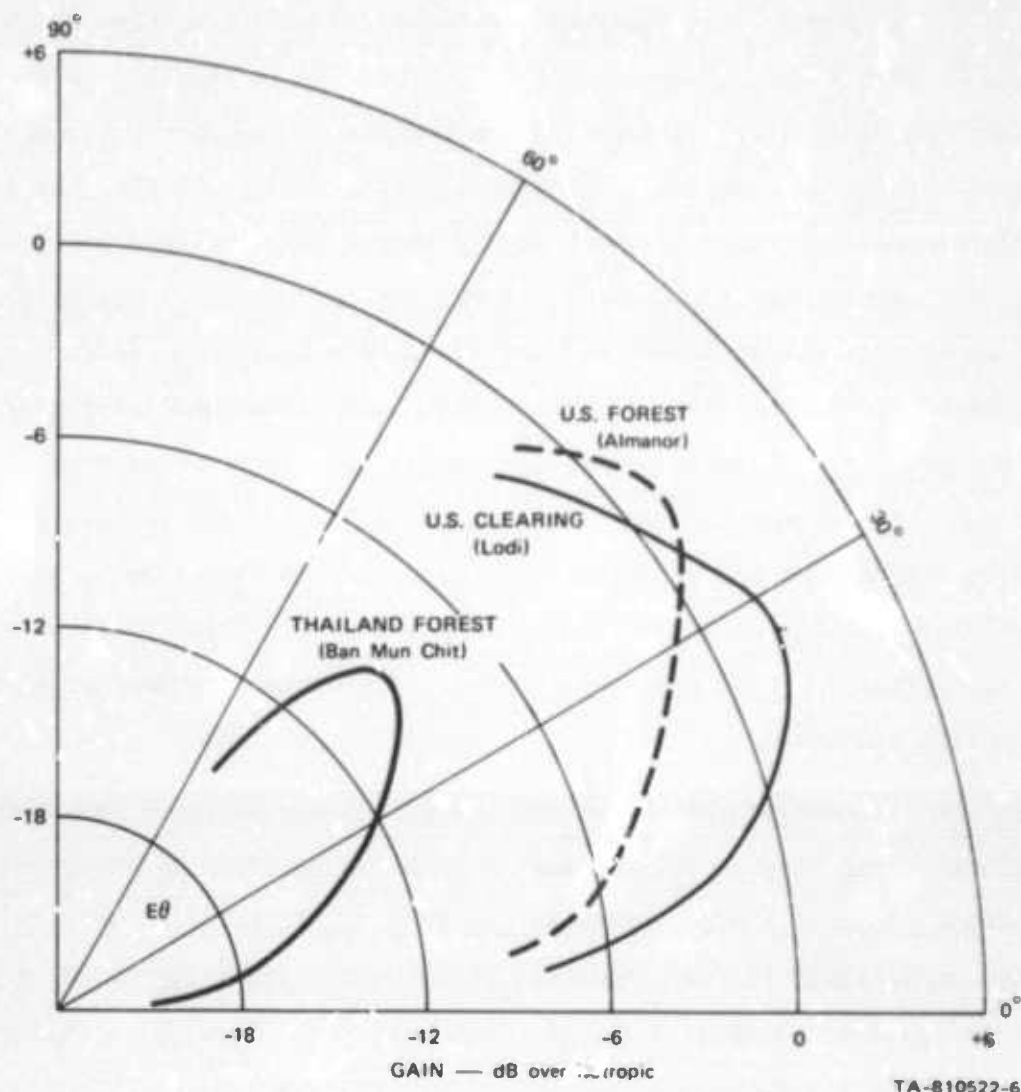


FIGURE III-24 ESTIMATED ABSOLUTE GAIN VERSUS ELEVATION ANGLE FOR THE MONOPOLE ANTENNAS AT LODI, ALMANOR, AND BAN MUN CHIT— E_θ AT 6 MHz

the maximum response increased and the gain of the antenna decreased when the antenna was measured at the forested sites.

At 8 MHz, perturbations were observed in the pattern of the monopole when it was measured at Almanor, whereas it remained relatively omnidirectional at Lodi and Ban Mun Chit. The perturbations in the pattern of the antenna at Almanor occurred through 15 MHz, but it remained omnidirectional through 15 MHz when it was measured at Lodi. No measurements were performed at 15 MHz at Ban Mun Chit. The pattern breakup at Almanor at 8 MHz, but not at Ban Mun Chit, can possibly be explained by the fact that the tree trunks were about half as far apart at Ban Mun Chit. Although there are no data available above 8 MHz at Ban Mun Chit (except VHF data--see Section III-D-5--that exhibit fairly extreme breakup of the patterns of similar antenna structures), it appears reasonable to assume that the pattern would start to break up at approximately 16 MHz, assuming this criterion is dependent primarily upon tree spacing.

Two configurations of the inverted-L antenna were measured: a 2:1 inverted L and a 5:1 inverted L. The E_ϕ patterns of these antennas resemble those of a dipole antenna, whereas the E_θ patterns deviate from those of a dipole in that they have a stronger response in the direction of the vertical element of the antenna. The power pattern of the 6-MHz, 5:1 inverted L antenna measured at Ban Mun Chit is shown in Figure III-25.

The power pattern for the 6-MHz 30° slant-wire antenna measured at Ban Mun Chit (Figure III-26) shows that the radiation of this antenna primarily consists of the E_θ component--mostly in the direction of the counterpoise and away from the direction of the sloping wire. It often is erroneously assumed by field operators that the directivity of this antenna is in the direction of the slanting element. The directivity

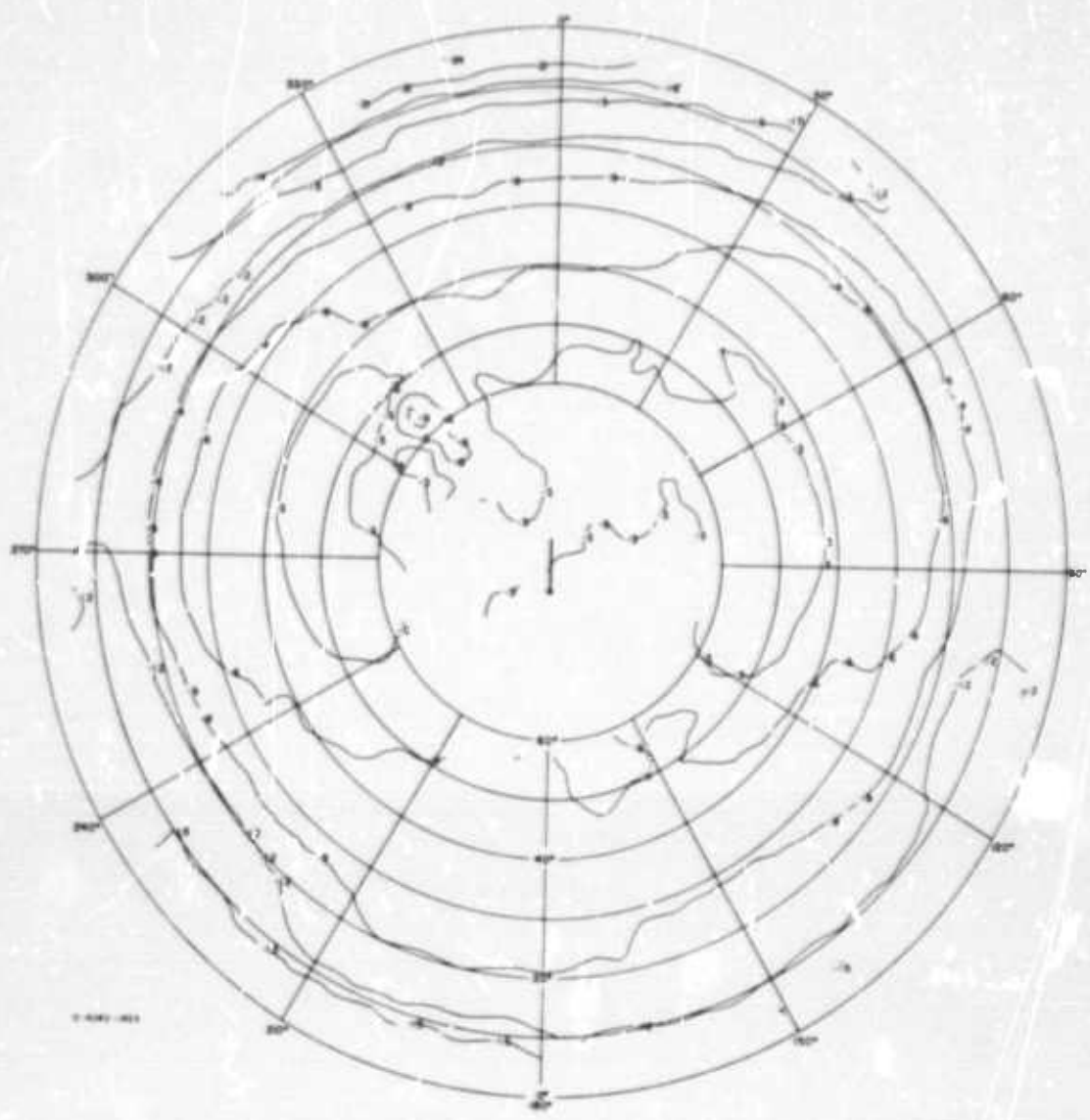


FIGURE III-25 MEASURED RADIATION PATTERN OF THE 6 MHz 5:1 INVERTED L ANTENNA AT BAN MUN CHIT—POWER AT 6 MHz

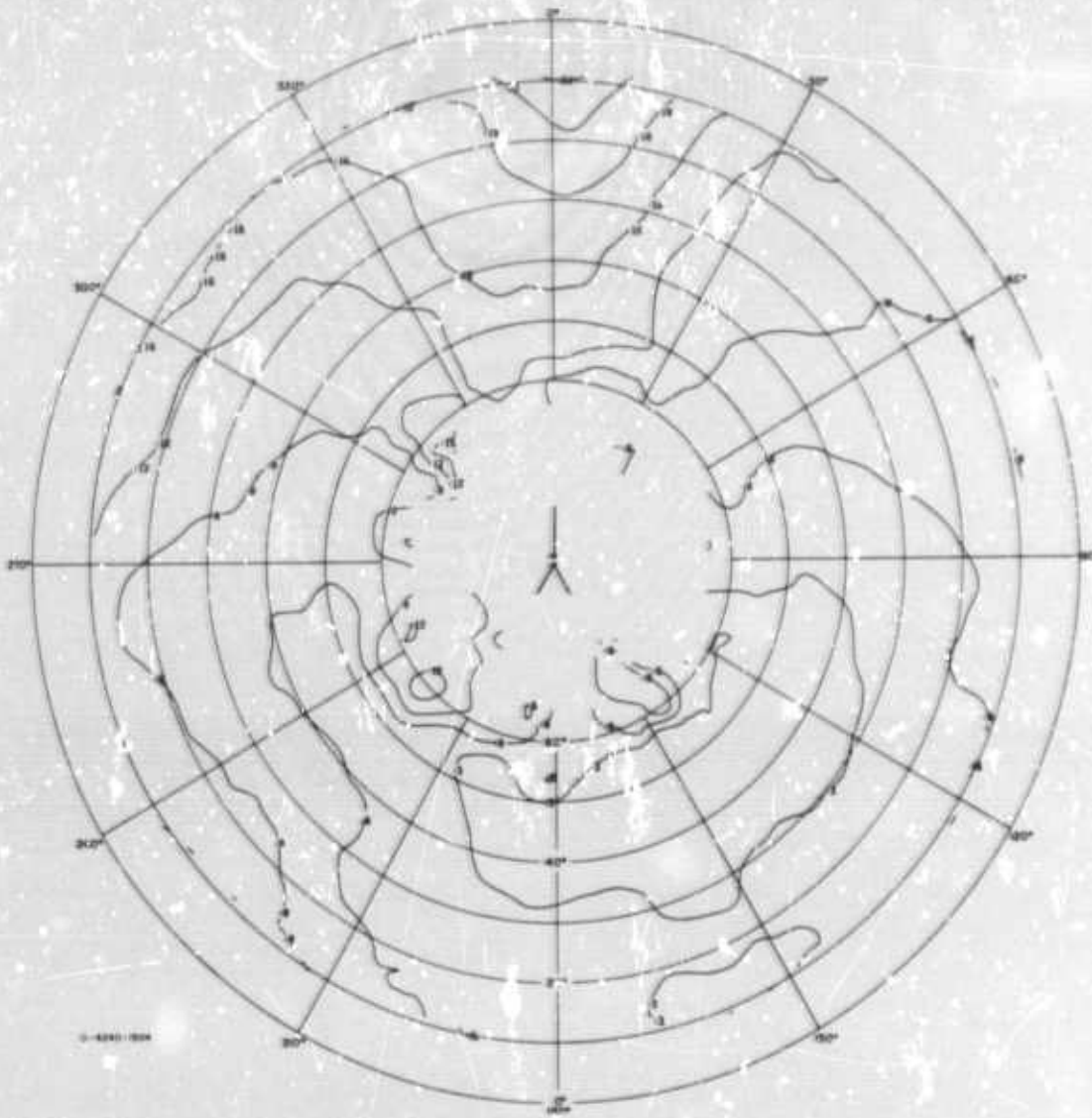


FIGURE III-26 MEASURED RADIATION PATTERN OF THE MHz 30° SLANT WIRE ANTENNA AT BAN MUN CHIT—POWER AT 6 MHz

of the slant-wire antenna should be considered when the antenna is installed in a communication link.

5. Measurement Results at VHF

VHF antenna pattern measurements were conducted at two sites--in a eucalyptus grove near Newark, California (STR 19) and in a Thailand tropical forest at Ban Mun Chit (STR 39D). The measurements in Newark were only preliminary measurements conducted primarily to evaluate the VHF field instrumentation and to gain a better understanding of the data-processing requirements for the more comprehensive measurements to be conducted later in Thailand.

Examples of the pattern data from the eucalyptus grove are presented in Figures III-27 and III-28. These data show the primary polarization response of the 50- and 100-MHz horizontal and vertical dipoles for one of the elevation angles that was measured. Because of the significant variation in signal strength that was observed for a small angular change in azimuth (particularly for low-elevation-angle measurements with vertically polarized antennas) it was decided to process the data statistically in order to provide a more meaningful and useful presentation of the data.

Statistical processing was performed only on the data from the vertical antennas, since these were omnidirectional in the absence of a scattering medium and exhibited the greatest perturbation in the presence of the trees. A parameter that provides an indication of how the signal would change for air-to-ground communications while an aircraft is flying past the antenna is the change in signal strength per degree of azimuth. Statistical data showed that approximately 10 percent of the perturbations in the pattern of the 50- and 100-MHz vertical dipoles were greater than 5 dB/degree in the area between 330° and 60° azimuth (area of

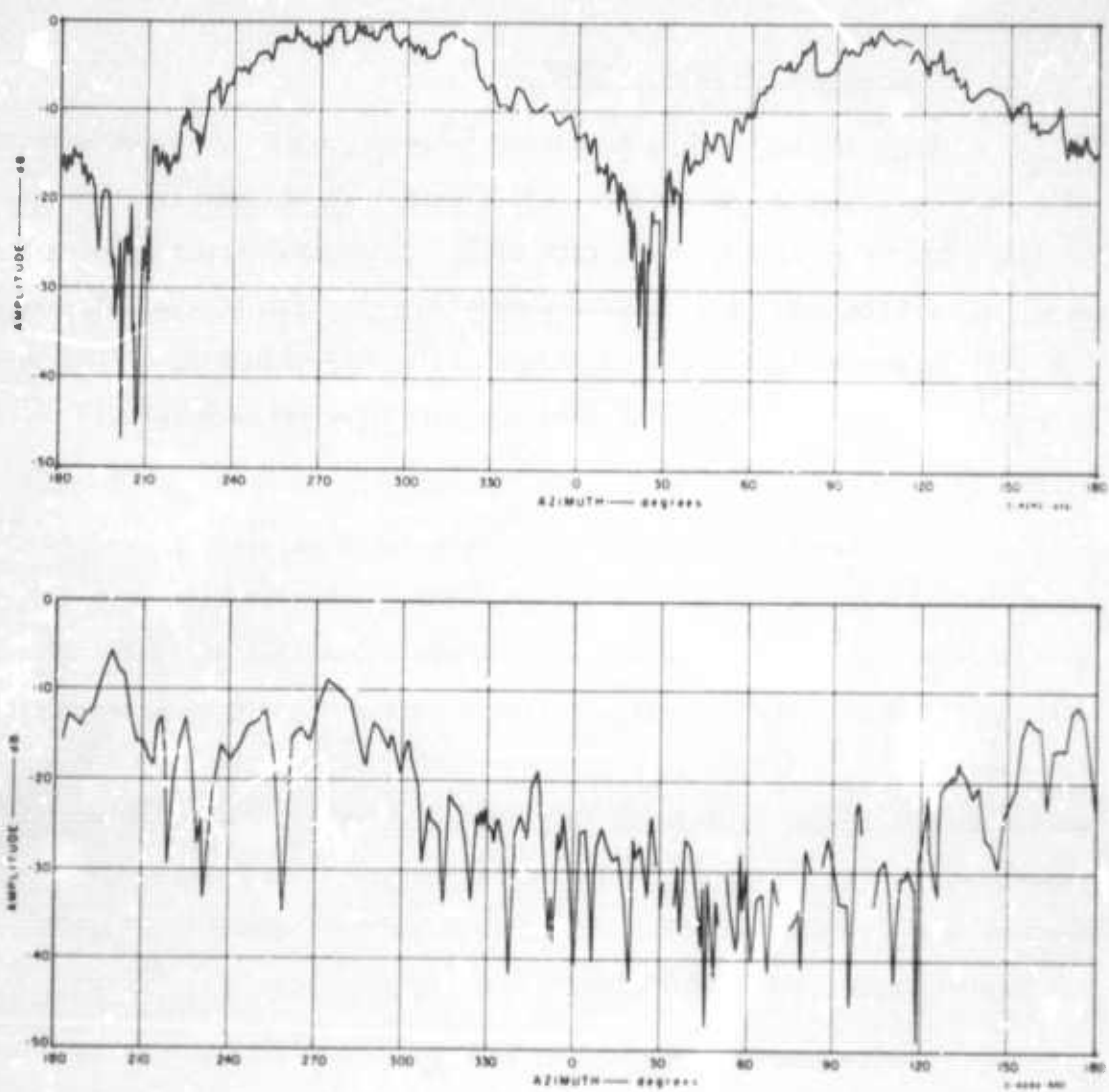


FIGURE III-27 MEASURED AMPLITUDE VERSUS AZIMUTH ANGLE OF 50-MHz VHF ANTENNAS IN A EUCALYPTUS GROVE—8° ELEVATION

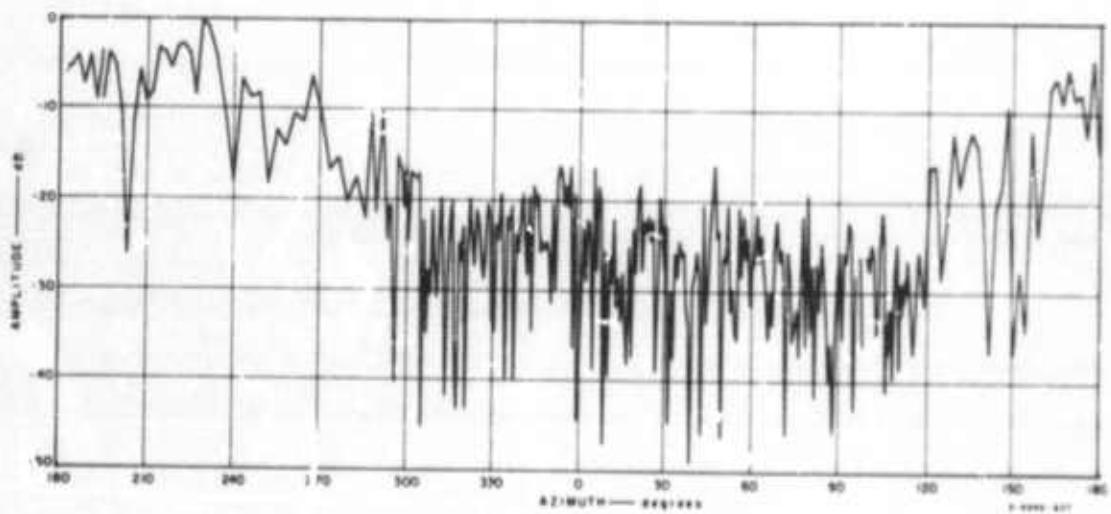
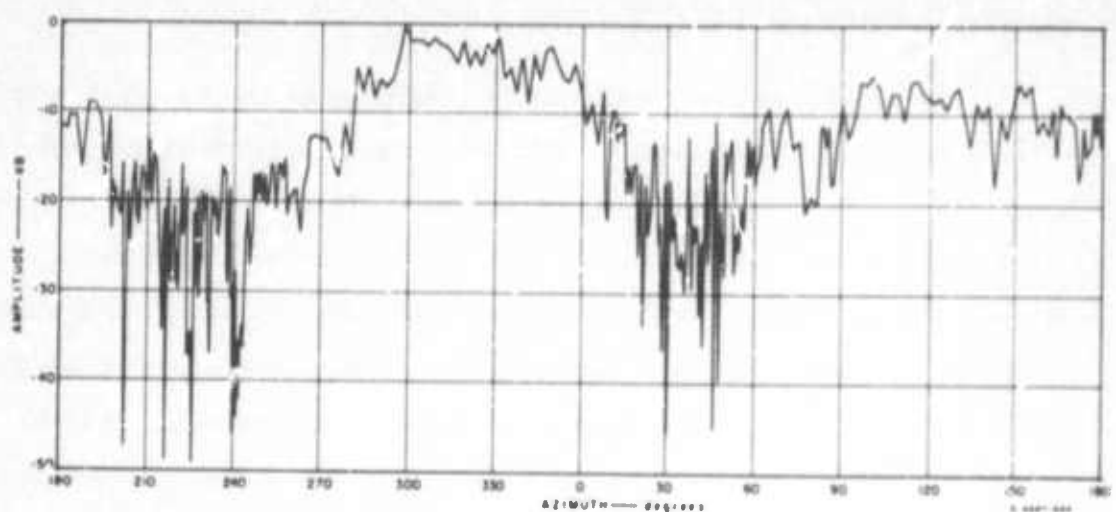


FIGURE III-28 MEASURED AMPLITUDE VERSUS AZIMUTH ANGLE OF 100-MHz VHF ANTENNAS IN A EUCALYPTUS GROVE—8° ELEVATION

greatest tree population), but less than 2 percent of the perturbations were greater than 3 dB/degree for the sector between 150° and 240° azimuth (area of least tree population).

The data from the measurements conducted at Ban Mun Chit were processed to provide estimators within 10°-azimuth sectors of the following parameters: (1) median signal strength, (2) standard deviation of samples below the median (nulls), (3) standard deviation of samples above the median (peaks), (4) mean signal strength, (5) standard deviation of samples below the mean (nulls), (6) standard deviation of samples above the mean (peaks), (7) standard deviation about the mean, and (8) the difference between the median and the mean. The estimators of the median signal strength for the 10° azimuth sectors were contoured to provide equal-area azimuth projection of the measured data as was done with HF data, and the standard deviation data were tabulated in increments of 10° of azimuth by 5° of elevation. An example of a measured pattern (along with calculated data) is presented in Figures III-32 and III-33, and more will be presented in STR 39D.

The difference between the median and mean signal strengths for each antenna was compared and it was found that this difference exceeded 2 dB for less than 5 percent of the 10-degree azimuth sample populations for any one antenna pattern. Thus, one can assume that the mean and median signal strengths are approximately equal but must remember that the samples are not Gaussian--as is shown by the inequality of the estimated standard deviations of the peaks and nulls.

6. Summary

The radiation patterns of selected HF field-expedient antennas were measured using the Xeledop technique when the antenna were erected

over an open, flat field near Lodi, California, in a pine forest near Almanor, California, and in a tropical forest near Ban Mun Chit, Thailand.

The measured HF dipole directivity patterns show that generally the E_θ (vertical polarization) patterns tend to be affected more by the scattering from surrounding vegetation than do the E_ϕ (horizontal polarization) patterns. But for either polarization, the relative response of the antennas tends to be enhanced at low elevation angles when the antennas were measured at the two forested sites. When considering the dipole antenna (and other simple antennas) one should not rely on only the primary polarization but should consider both polarization components and their effect on the total radiated power. It has been shown that the dipole antenna actually has an almost omnidirectional power pattern near the zenith and, in some cases (especially for very low antenna heights and for measurement frequencies below resonance), the E_θ response of the antenna is the stronger component. The E_ϕ component typically exceeded the E_θ component by about 3 dB for resonant dipoles.

The measured patterns of the monopole antennas indicate that the location of the maximum response of these antennas tended to occur at higher elevation angles when the antennas were situated in the forests. The E_θ and the power patterns of the 30° slant-wire antenna show that the maximum response of the antenna is slightly down from the zenith and--contrary to what is often commonly assumed--the direction of maximum gain is in the direction of the counterpoise, which acts as an active part of the antenna. The E_θ response of this antenna typically exceeded the E_ϕ response by about 8 dB.

The relative gains for all of the measured HF antennas were tabulated. When the antennas were located in the forest, the horizontal dipoles placed $\lambda/8$ or more above ground exhibited the greatest relative gain. The dipoles typically were followed by the 2:1 inverted L, 5:1

inverted L, 30° slant wire, monopoles, and loops in that order. This is essentially the same result that was obtained with the ionospheric sounder when used to measure the relative gains at the zenith (see Section III-E). The relative gain data obtained for measurement frequencies a few MHz off the design frequency indicate the rather extreme penalty to be paid for not employing an antenna of the proper design.

The measurements of VHF antenna patterns indicated that the forest at Ban Mun Chit was apparently more isotropic than the forest considered at Newark, California. Although there were pattern perturbations and fairly rapid fading was observed in the data from Ban Mun Chit, these fadings (presumably caused by the predominantly vertical tree trunks) were not as extensive as those observed at Newark where, it might be noted, the forest was composed primarily of tall vertical tree trunks.

The VHF data from Thailand were processed so as to provide statistical estimates over 10° azimuth sectors, as derived from the measured signal strength as a function of azimuth angle. The statistical estimators show that the mean and median signal strength are quite similar for these data. The radiation-pattern data indicate that the median signal strength is generally representative of that expected for the antenna structures. The pattern data from the dipole antennas indicated that the maximum signal strength occurred at higher elevation angles when the antennas were located in the forest (as was the case with the HF antennas) than when located in the clearing. The patterns of the vertical-sleeve dipoles and the vertical dipole antennas, which should have a fairly omnidirectional pattern in azimuth, became quite perturbed when located in the forest.

D. Comparison of Measured Antenna Radiation Patterns in Forests with Model Predictions (STRs 16, 39D, 45D)

1. Objective

In order to better understand the effects of forest on antenna patterns and to evaluate the mathematical models, pattern data calculated by the model described in Section III-A were compared to the measured radiation pattern data described in Section III-C.

2. Background

The mathematical model of an elementary dipole antenna situated in a forest has been described in Section III-A. In this section, measured and computed radiation pattern data are compared. Previous work that is related to this section is as follows:

- (1) Development of the mathematical model of a dipole in a forest and preliminary comparison of the calculated patterns with measured HF data from open, flat terrain and forested terrain (STR 16).
- (2) Measurement of radiation patterns of full-scale HF antennas over open, level terrain (STR 10).
- (3) Measurement of radiation patterns of full-scale HF antennas located in a U.S. conifer forest (STR 25).
- (4) Measurement of the radiation patterns of full-scale HF antennas located in a Thailand tropical forest (STR 35).

- (5) Comparison of HF pattern measurements from open, flat terrain, U.S. conifer forest, and a Thailand tropical forest with calculated patterns (STR 45D).
- (6) Measured and calculated patterns of full-scale VHF antennas located in a Thailand tropical forest (STR 39D).

3. HF Antennas

The mathematical model described in Section III-A was used to calculate the expected radiation patterns of selected HF dipole antennas measured at Lodi, Almanor, and Ban Mun Chit. The ground and foliage electrical constants were estimated for the computations of the Lodi and Almanor patterns, and the measured data from the open-wire transmission-line probe used at Ban Mun Chit (Section III-B) were used for the calculations of the patterns for that site.

Figure III-29 shows a comparison of the measured and computed effective lengths for the 23-ft-high, 8-MHz horizontal dipole. The measured values were taken from measurements performed at Lodi (no forest) and Almanor (forest). The foliage electrical constants used for the model of the antenna at Almanor were estimated from experimental measurements made in a similar conifer forest in the State of Washington. Of particular interest is the cross-over of the directivity functions from the case with no forest (solid curve) to the case with the forest (dashed curve), and the similar behavior for the measured values. Note also that the measured directivity pattern was enhanced at the lower elevation angles when the antenna was measured in the forest, as was predicted by the model.

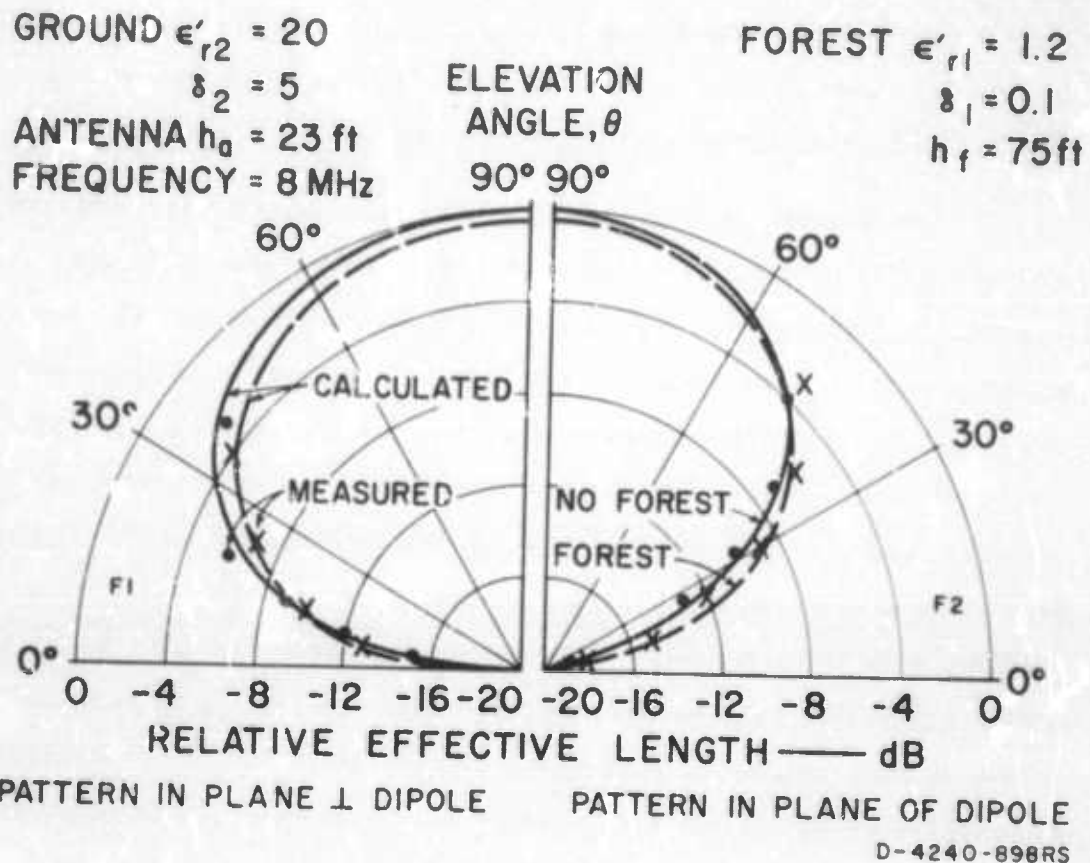


FIGURE III-29 COMPARISON OF MEASURED AND CALCULATED EFFECTIVE LENGTHS FOR DIPOLE IN FOREST AND IN OPEN

The model was used to predict the expected radiation patterns of the dipole antennas measured at Ban Mun Chit, Thailand. The ground and foliage electrical constants used in the model were based on the measured data presented in Figures III-8 and III-15. These constants were $\epsilon_r = 1.2$, $\delta = 0.09$ for the forest. These parameters are defined in Section III-A. For modeling purposes, the forest height (h_f) at Ban Mun Chit was assumed to be 65 ft; only 2 percent of the trees at this site exceeded 65 ft.

Sufficient data points were calculated so that the computed patterns could be plotted on the measured radiation contour plots. In order to facilitate comparison of the calculated patterns with the measured patterns, the computed data were normalized by adding a constant value to the calculated values so that the lower elevation angle of the calculated 3-dB contour would align itself with the estimated mean elevation angle of the lower portion of the 3-dB contour of the measured data (this was estimated by visual inspection of the contour plot of the measured data in each case). Physically, this procedure is similar to adding a constant gain to the antenna through the use of an amplifier, or a loss of gain because of a matching circuit or an impedance mismatch. Figures III-30 and III-31 are examples of the calculated and measured data. The solid curves are the contours of the measured data and the dashed curves are the contours of the computed data. Other examples will be presented in STR 45D. The data to be presented in STR 45D showed that the model would not predict the pattern distortion that occurred below resonance. This distortion is presumably caused by currents in the antenna feedline and the model does not account for antenna feed lines. Also, the patterns of balanced dipoles were predicted more accurately than those of unbalanced dipoles--particularly for frequencies other than the resonant frequencies of the antennas--because of the feed lines not being accounted for in the model.

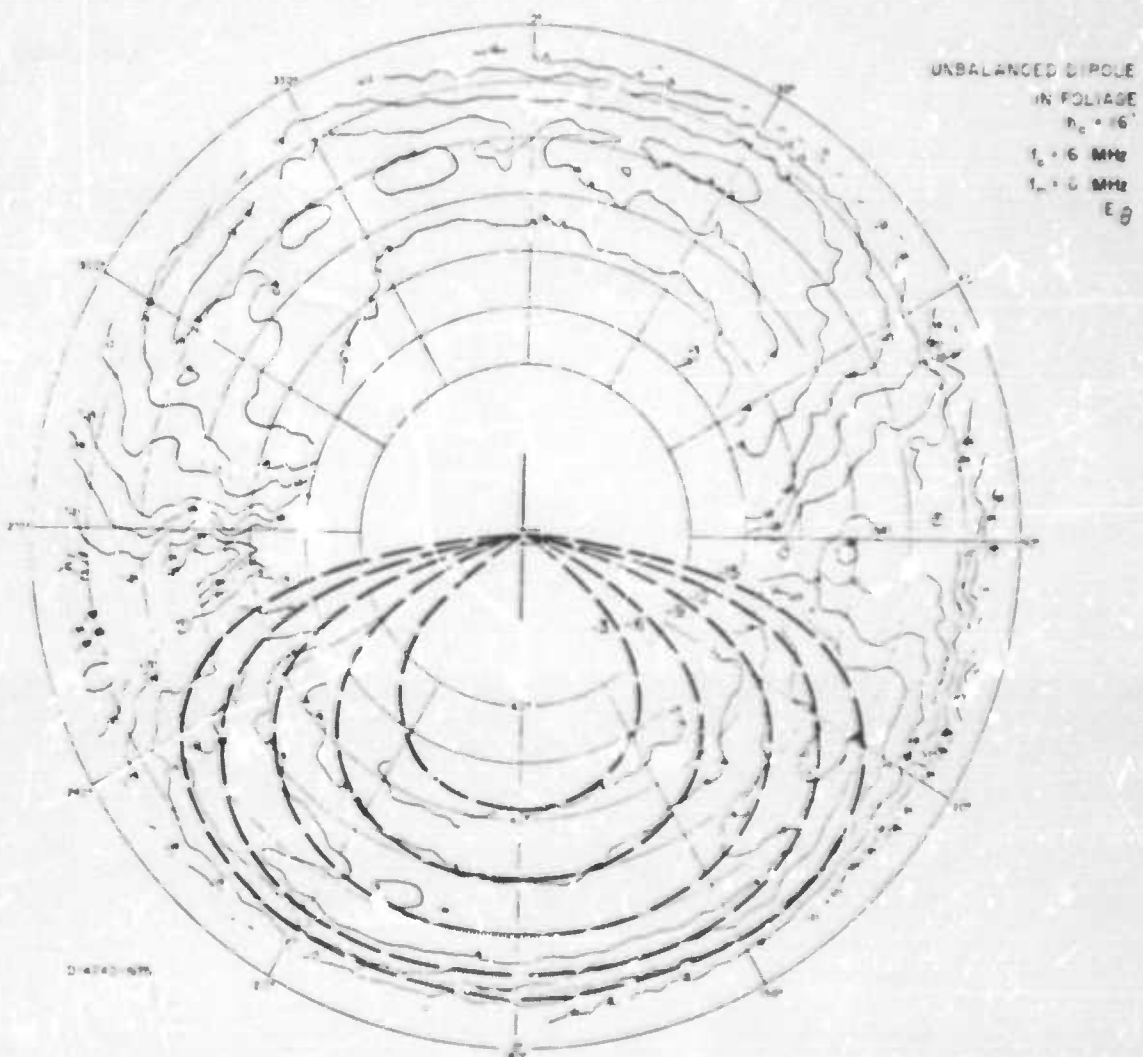


FIGURE III-30 COMPARISON OF MEASURED AND CALCULATED MEDIAN RADIATION PATTERNS FOR THE 16-ft HIGH 6 MHz UNBALANCED DIPOLE IN THE FOLIAGE AT BAN MUN CHIT— E_0 AT 6 MHz

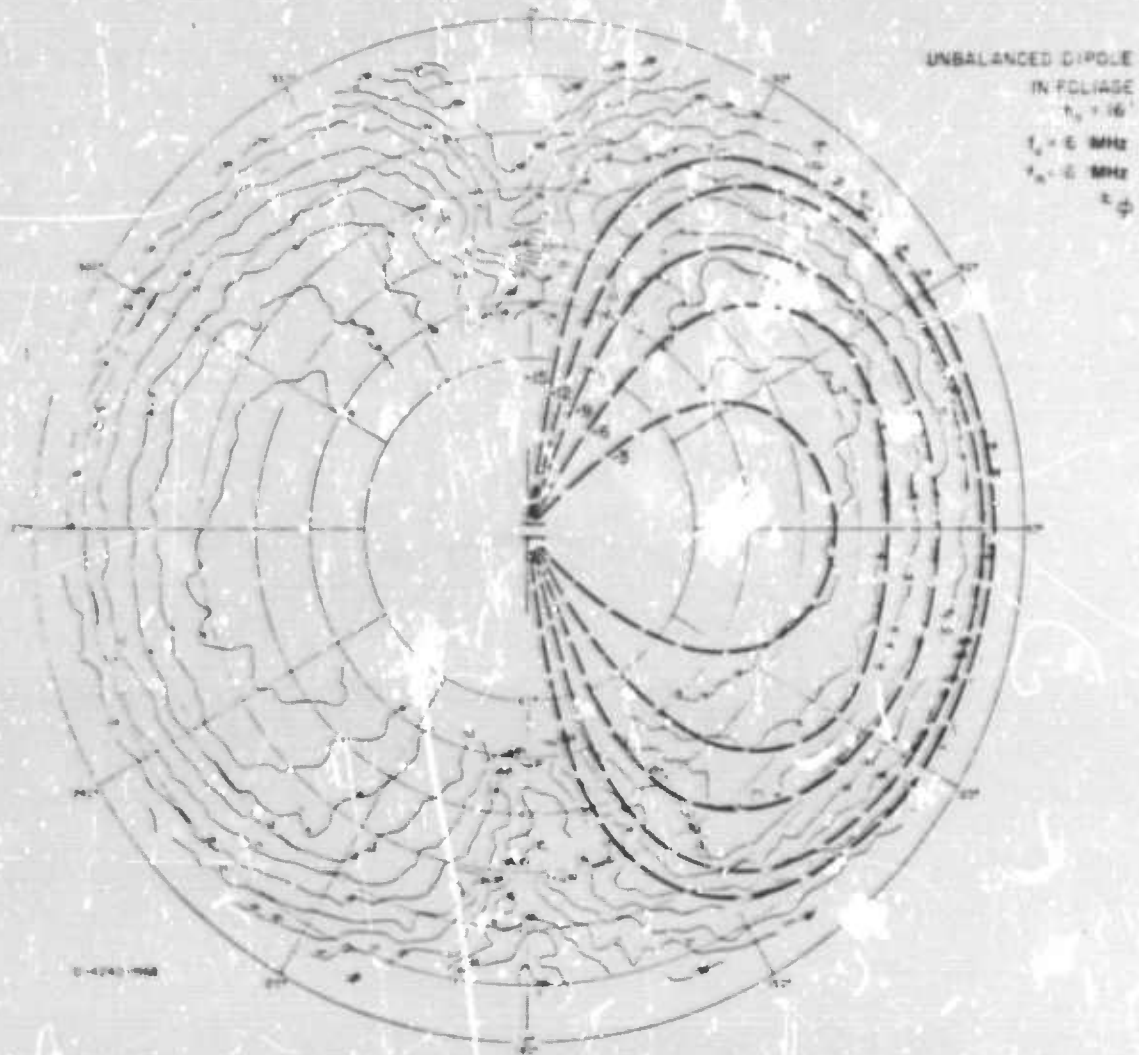


FIGURE III-31 COMPARISON OF MEASURED AND CALCULATED MEDIAN RADIATION PATTERN FOR THE 16-FOOT HIGH 6 MHz UNBALANCED DIPOLE IN THE FOLIAGE AT SAN MUN CHIT— E_ϕ AT 6 MHz

4. VHF Antennas

The computer model described in Section III-A was used to calculate the expected radiation patterns of the VHF horizontal dipole antennas measured at Ban Mun Chit. The ground and foliage electrical constants used in the model were derived from the open-wire line, and the calculated patterns were normalized in the same manner in which the HF patterns were normalized.

Examples of the calculated and measured patterns are shown in Figures III-32 and III-33. Although the calculated patterns did not duplicate the median measured VHF patterns as well as they did the HF patterns, the calculated and median measured data were generally within 3 to 6 dB of each other. From the examples of calculated and measured patterns available, it appears that the slab model can predict the average patterns of simple VHF dipoles to ± 3 dB in some cases. But more example cases should be studied before any definite conclusions can be made. Obviously, the model cannot predict the "fine structure" of the pattern, but if more data were available, it appears that one could place a figure of merit on the model regarding the prediction of the macroscopic (average) effects of the forest. In the absence of a more refined model based on empirical data, a standard deviation on the scattering caused by the macroscopic features of the forest could be employed to complete the model, so that the probability of the signal strength exceeding a certain level at a given range in a solid angle from a transmitting antenna, could be predicted.

5. Summary

The radiation patterns calculated with the multilayer slab model were compared to the measured radiation pattern data. This comparison shows that the measured and modeled data compare quite favorably

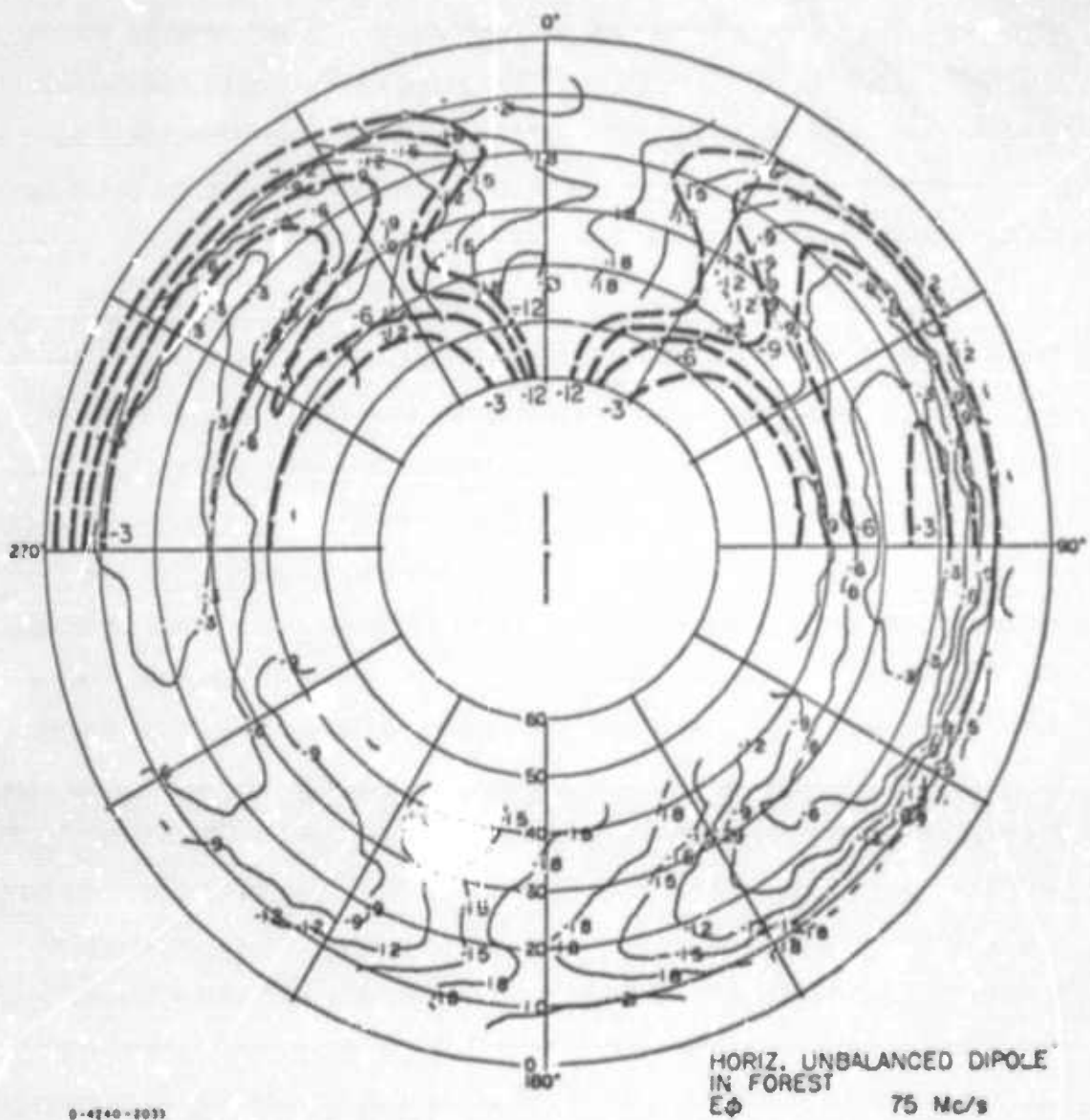


FIGURE III-32 COMPARISON OF MEASURED AND CALCULATED MEDIAN RADIATION
 PATTERN FOR THE 75 MHZ UNBALANCED DIPOLE IN THE FOREST
 AT BAN MUN CHIT.— E_Φ AT 75 MHZ

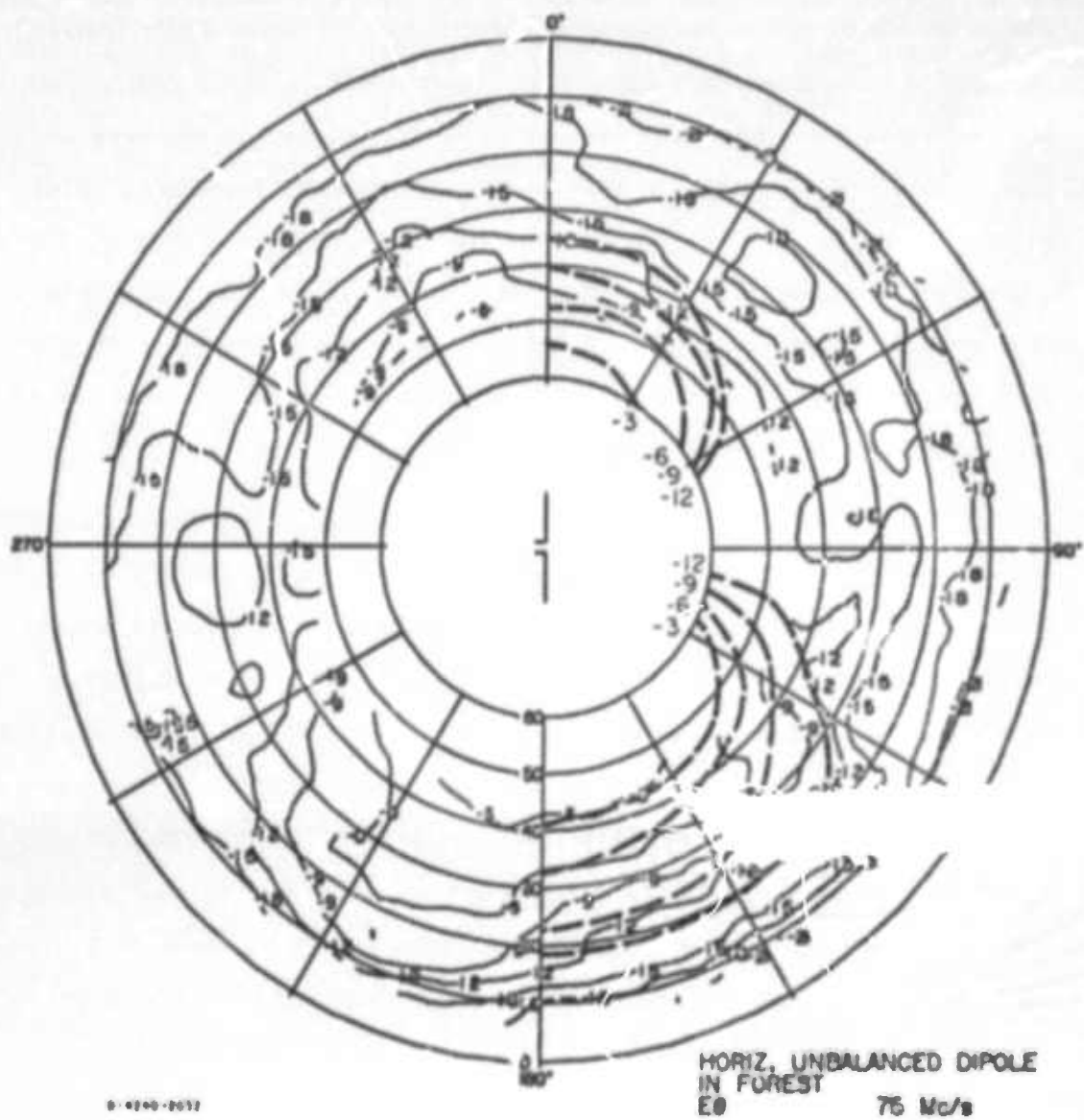


FIGURE III-33 COMPARISON OF MEASURED AND CALCULATED MEDIAN RADIATION PATTERN FOR THE 75 MHZ UNBALANCED DIPOLE IN THE FOREST AT BAN MUN CHIT--E₀ AT 75 MHZ

5

for the resonant frequencies of the HF antennas. However, the comparison deteriorates for frequencies below resonance, although the measured and calculated results should be quite similar for frequencies below resonance, since the model assumes an electrically short dipole. Part of the dissimilarity between the measured and calculated patterns can possibly be explained by the presence of the antenna feed line, which becomes an active part of the antenna when the antenna is used at frequencies other than resonance; the computer model does not take this into consideration. The patterns of the balanced dipole were predicted more accurately than those of the unbalanced dipoles--again a possible indication of the feed line distorting the measured pattern.

Although the model was developed for predicting the radiation patterns of HF antennas in a homogeneous, isotropic forest, it was used with the parameters to define the forest and horizontal dipole antennas measured at VHF in the Thailand tropical forest at Ban Mun Chit. The resulting calculated patterns compare favorably with the measured median patterns for the unbalanced dipole antennas. The greatest discrepancies between measured and modeled patterns resulted from the 75-MHz antennas. Although the model will calculate the average pattern, further development is required before it will predict the rapid variations in the patterns or a statistical estimator (or distribution function) for the variations caused by scattering at VHF.

E. Antenna Relative-Gain Measurements with Vertical-Incidence Sounders (STRs 18, 38D)

1. Objectives

The objectives of the sounder tests on field-expedient antennas were:

- (1) Measure their relative response toward the zenith
(applicable to short HF ionospheric skywave paths);
- (2) Estimate the absolute power gain of these antennas;
- (3) Obtain relative-gain data on antennas located in
and out of forests.

2. Background

It has been known since the early part of World War II, through the research of Herbstreit and Crichtlow¹ and others, that the HF skywave offers one solution to the problem of communication with low-power manpack radios in mountainous or heavily forested terrain over ranges greater than those readily achieved via groundwave (ranges greater than a few miles). For short ranges, say less than 50 miles, the HF skywave path is practically straight up to the ionosphere and back down to the receiver. Consequently, the gain toward the zenith is an excellent measure of usefulness of antennas designed for use with pack sets on short paths. Under this contract, SRI has developed a technique for measuring this relative gain toward the zenith by using ionospheric sounders (STRs 18, 38D).

Prior to the start of field tests in Thailand (Bangkok and Ban Mun Chit in 1966 and Chumphon in 1967), some measurements had been made on tactical antennas in the United States (STR 18). These tests provided a background for the later tests in a tropical environment. The actual antenna structures tested at Ban Mun Chit (SAR 6) were similar to those tested with the sounders in open terrain in the United States, whereas, the antennas measured with the sounders at Chumphon included also the HF antenna structures whose directivity patterns had been measured with the airborne Xeledop system (STRs 10, 25, 35, 45D).

Details of the antenna structures are provided in the above referenced SAR and STRs. The types of antennas were:

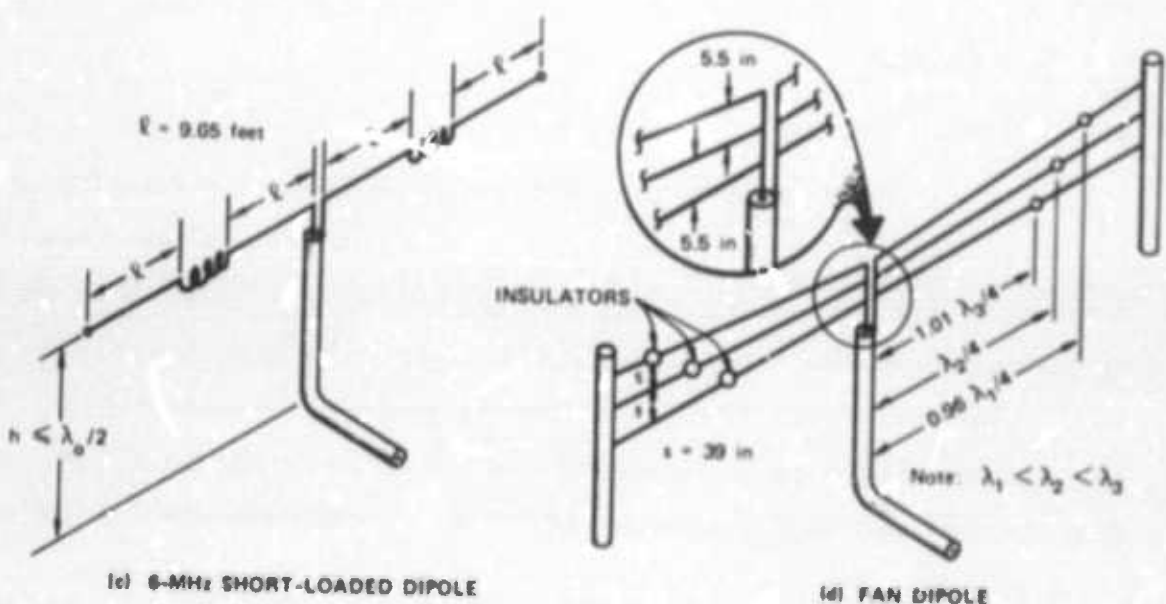
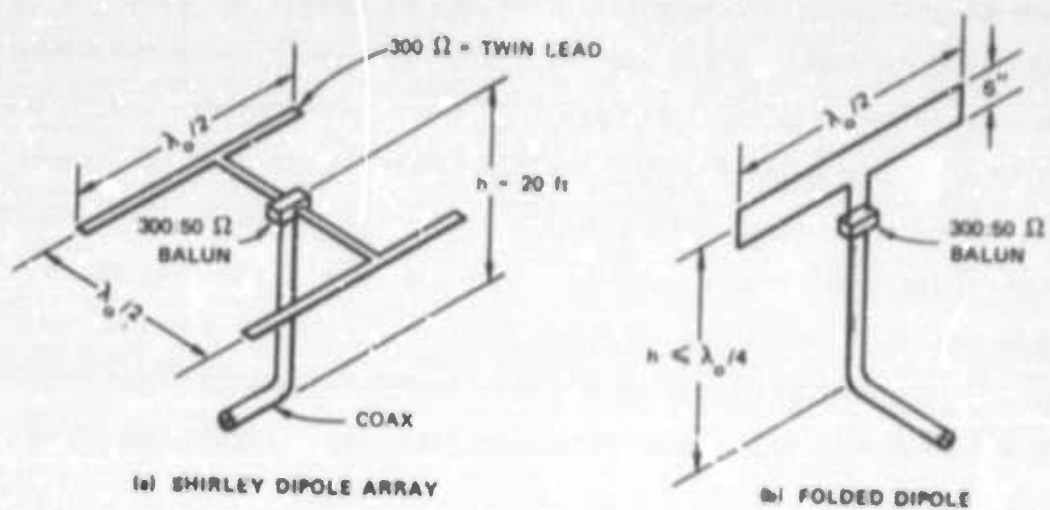
- (1) Horizontal dipoles
 - (a) Half-wave resonant
 - (b) Folded
 - (c) Short loaded
 - (d) Short
 - (e) Sleeve
 - (f) Fan¹⁵
 - (g) Shirley-folded¹⁶
- (2) Inverted-L
- (3) Slant wire
- (4) 16.5-ft untuned vertical monopole
- (5) Vertical plane loop.

Most of these antennas are sketched in Figure III-18, but some of the dipole antennas are described in Figure III-34.

3. Measurement Technique

The technique involves the use of three antennas--a transmitting antenna, a reference antenna, and a test antenna. These three antennas were placed on a north-south line,* as close together as

* At low altitudes the correlation distance is much greater in the magnetic meridian than orthogonal to it because of field-aligned ionospheric irregularities.



TA-810522-6

FIGURE III-34 SKETCHES OF SPECIAL DIPOLE CONFIGURATIONS FOR RELATIVE GAIN MEASUREMENTS

practical but not so close as to cause significant mutual coupling. A series of pulses were transmitted up to the ionosphere and received first on the reference antenna and then on the test antenna, where the switching between reference and test antennas was accomplished rapidly enough to resolve the ionospheric fading. The difference in received amplitudes in dB corresponds to the relative gain of the test antenna. Even though fading was present, usable records were obtained when the difference between the echo amplitudes received on the two antennas remained constant. It was not practical to use this technique when sporadic E or spread F were present because of the resultant poor correlation of the signals received on the test and reference antennas.

4. Results

a. CONUS

The results of the CONUS tests indicated that relative to a half-wave horizontal dipole at $\lambda/8$ above ground, the response toward the zenith of a 5:1 inverted-L was down about 9 dB, a 30° slant wire was down about 14 dB, and a 16-ft whip was down more than 20 dB. A measurement of the height-gain function of the dipole indicated that at $\lambda/10$ above ground, the response toward the zenith was down only about 3 dB from the maximum observed response (which occurred between $\lambda/8$ and $\lambda/4$ above ground). The rate of decrease of gain with height became much greater for heights lower than $\lambda/10$. A low-loss balun transformer was observed to have relatively little effect upon the performance of half-wave dipoles, and a ground screen made little difference in the relative gain toward the zenith. The effects of a sloppy setup of the dipole were investigated. It was determined that the radiating elements of a nominally horizontal $\lambda/2$ dipole can sag as much as 45° before the gain decreases more than 1 dB (provided the feed is elevated to $\lambda/10$ or greater),

and for greater sag angles the gain decreases rapidly. Decreasing the angle between the dipole radiating elements and the vertical section of transmission line by displacing the feed line in the plane of the dipole had little effect upon the antenna response until the angle exceeded about 45 degrees. These tests of element sag and of feed-line displacement were repeated in the forest at Chumphon, Thailand, and the above conclusions remain valid when the dipole is located in the forest.

b. Ban Mun Chit

The relative gains of selected field-expedient antennas were measured in the clearing and in the forest at Ban Mun Chit, Thailand, the site of the airborne pattern measurements, and the same antenna types as used for the CONUS measurements were tested at 6.05 MHz. The reference antenna was a dipole at 20 ft above ground--about $\lambda/8$. Two forest sites were used for these tests: the north site with a dense canopy and little undergrowth, and the south site with less canopy and more dense undergrowth. The results of these tests are summarized in Table III-3.

Table III-3

RELATIVE GAIN AND JUNGLE LOSS
FOR 6.05-MHz ANTENNAS AT BAN MUN CHIT

Antenna Type	Gain Relative to $\lambda/2$ Dipole $\lambda/8$ above Ground in Clearing (dB)			Effective Jungle Loss (dB)	
	Clearing Area	North Jungle	South Jungle	North Jungle	South Jungle
$\lambda/2$ Dipole	0.0	-1.7	-1.2	+1.7	+1.2
5:1 Inverted-L	-10.2	-12.5	-10.7	+2.3	+0.5
30° Slant Wire	-11.8	-14.2	-13.5	+2.4	+1.7
16.5-ft Whip	-31.7	-25.2	-25.0	-6.5	-6.7

The gain of the 16.5-ft whip was down about 32 dB relative to the dipole in the clearing and only about 25 dB relative to the dipole in the forest. Presumably the null at the zenith was filled in somewhat by scattering from the trees, or possibly the whip was not truly vertical when installed in the forest, but this effect was not observed at Chumphon. The effective jungle loss--the difference in relative gain toward the zenith between clearing and forest was about 1 to 2 dB for the antennas other than the whip. Since the dipole exhibited the greatest response toward the zenith, additional tests were made with this antenna at 6 MHz, including a height gain test. The results of this test indicate that the dipole could be lowered to only a foot or two above the relatively dry ground ($\epsilon_2 \approx 4$ mho/m) before its gain becomes comparable with the next best antenna structure tested--the inverted L.

c. Chumphon

Relative-gain tests were also made with the sounder at a field site near Chumphon, Thailand on the Malay Peninsula about 300 miles south of Bangkok. The Chumphon forest was classified as a fresh water swamp forest and there was often water standing on the ground. The forest was about 15 feet tall and had a well-formed canopy.

The main test frequency used at Chumphon was 6.05 MHz and most of the antennas tested were designed to operate on this frequency. A few antennas were designed to operate on 4.05 MHz (30° slant wire) and 8.10 MHz (2:1 inverted L), to be compatible with the airborne Xeledop directivity-pattern measurement program (STRs 10, 25, 35, 43b). The discussion in this section pertains to the results of tests made on the design frequencies of the antennas tested for relative gain at the zenith.

The results of the 6.05-MHz relative-gain tests are presented in Table III-4. The data have been corrected for cable losses but not for mismatch losses or balun insertion losses. Recall that the reference antenna was a half-wave resonant horizontal dipole placed at 32 ft above ground in the clearing--the height giving a feed-point impedance of $50 + j0$ ohms. Since the receiver input was padded to 50 ohms and a 50-ohm coaxial cable was used (RG-8), there were no mismatch losses associated with the reference antenna.

Tests at 4.05 MHz were made on an unbalanced dipole, the fan dipole, and a 30° slant wire. The results of these tests are summarized in Table III-5. The reference antenna was a half-wave horizontal dipole at 41 ft above ground in the clearing--the height giving a feed-point impedance of $50 + j0$ ohms.

Tests were made at 8.10 MHz on an unbalanced dipole, the fan dipole, and a 2:1 inverted L. The results of these tests are summarized in Table III-6. The reference antenna was a half-wave horizontal dipole at 23 ft above ground in the clearing--the height giving a feedpoint impedance of $50 + j0$ ohms.

The relative response toward the zenith observed for the 30° slant wire and whip in the clearing at Chumphon were about the same as in CONUS and at Ban Mun Chit, but the relative response of the 5:1 inverted L was about 6 dB greater than at the other sites (i.e., down only 4 dB relative to the dipole). A 2:1 inverted L was measured and it was only about 2 dB worse than the dipole when in the clearing. Perhaps the improved performance of the inverted L antennas at this site is due to the improved effectiveness of the ground rod because of the greater RF conductivity of the surface soil (see Figure 11J-16). The effective jungle loss for all these antennas was about 2 to 5 dB

Table III-4
RELATIVE GAIN DATA FOR 6-MHz ANTENNAS AT CHUMPHON

Antenna	Relative Gain (dB)	
	Clearing	Jungle
$\lambda/2$ Unbalanced Single-Wire Dipole	+1.0	-2.8
$\lambda/2$ Balanced Single-Wire Dipole	+0.5	-3.7
Folded Dipole	-0.2	-1.0
Short Loaded Dipole	-3.0	-5.2
Sleeve Dipole	-32.1	-28.3
Fan Dipole at 15 ft	-0.4	-5.1
Fan Dipole at 12 ft	-2.4	-5.6
Fan Dipole at 9 ft	-4.9	-8.1
Shirley Folded Dipole	+3.0	-0.3
2:1 Inverted L	-0.6	-2.8
3:1 Inverted L	-0.8	-3.3
4:1 Inverted L	-1.6	-5.8
5:1 Inverted L	-2.6	-6.3
30° Slant Wire	-10.1	-14.8
60° Slant Wire	-11.8	-14.8
$\lambda/4$ Monopole with Ground Plane	-19.1	-34.0
10-ft Square Loop	-24.1	-25.3

Notes: (1) Relative-gain values corrected for cable losses and mismatch loss of reference antenna (0 dB since $Z = 50 + j0$), but not for mismatch losses or balun insertion losses of the test antennas.

(2) All dipoles at 18 ft above ground except sleeve dipole (on ground) and fan dipole.

Table III-5

RELATIVE GAIN DATA FOR 4-MHz ANTENNAS AT CHUMPHON

Antenna	Relative Gain (dB)	
	Clearing	Jungle
Unbalanced Dipole at 41 ft	0.0	-7.3
Unbalanced Dipole at 61 ft ($\lambda/4$)	-0.5	-
Fan Dipole at 15 ft	-1.2	-3.7
Fan Dipole at 12 ft	-2.2	-5.2
Fan Dipole at 9 ft	-4.2	-6.7
30° Slant Wire	-17.0	-19.8

Table III-6

RELATIVE GAIN DATA FOR 8-MHz ANTENNAS AT CHUMPHON

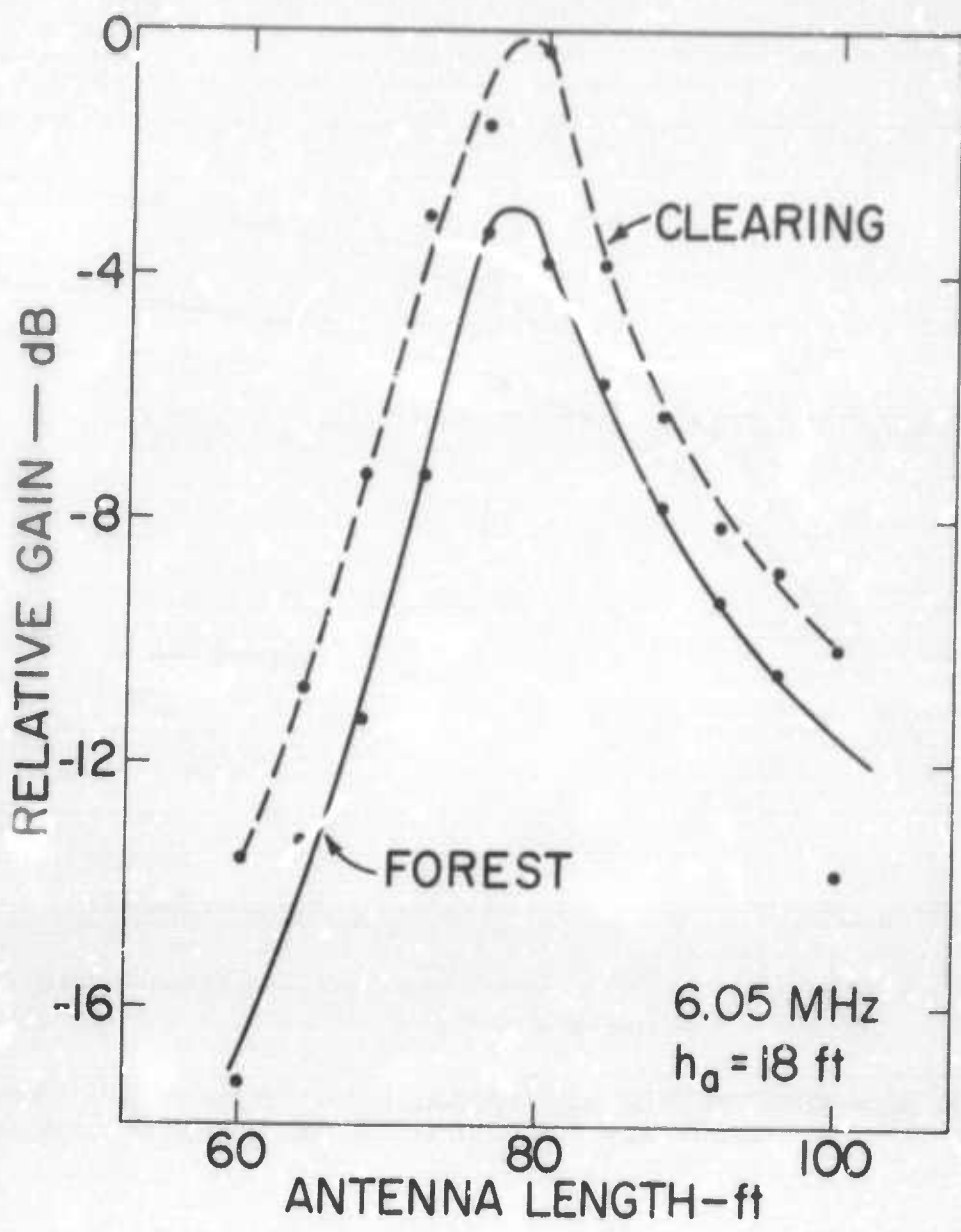
Antenna	Relative Gain (dB)	
	Clearing	Jungle
Unbalanced Dipole at 23 ft	0.0	-3.1
Unbalanced Dipole at 30 ft ($\lambda/4$)	-0.3	-3.6
Fan Dipole at 15 ft	-1.0	-7.0
Fan Dipole at 12 ft	-4.5	-9.0
Fan Dipole at 9 ft	-7.0	-11.5
2:1 Inverted L	-3.1	-6.1

at 6 MHz. The enhanced gain of the whip in the forest was not observed at this site.

Figure III-35 shows the relat.v. gain of a horizontal dipole at 18 ft above ground as a function of antenna length. The gain measurements were made as the total dipole length was decreased in 4 ft increments, and the results include the effects of mismatch loss and increase in cable loss as VSWR increased (the measurement cable was several hundred feet of RG-8). Notice that the effective jungle loss is slightly greater than that observed at Ban Mun Chit, Table III-3, and that the maximum gain occurs for a slightly shorter length when the dipole is in the forest.

Data also were obtained with the sounder at Chumphon, on the response of a 16.5-ft whip on a jeep relative to the response of a half-wave horizontal dipole at 15 ft above ground in the clearing. Supplementary data were obtained with the whip mounted on a Land Rover and on a wire cage constructed to simulate the jeep. The results of the relative response tests are given in Ref. 17.

The height gain of a 6-MHz dipole was measured at Chumphon in the clearing and forest. Measurements were also made of the ground constants and vegetation constants using open-wire transmission-line techniques (see Section III-B). These values were used in a 3-layer slab model for a dipole in a forest (see Section III-A) to calculate the dipole height-gain function. The vector effective length of a Hertzian dipole was computed and the results were assumed to apply to a half-wave dipole. Figure III-36 shows the excellent agreement obtained between model predictions and measured values when the measured relative gain data are forced to agree with calculated absolute-gain values for the dipole at 18 ft above ground in the clearing where we



D-4240-1695S

FIGURE III-35 RELATIVE DIPOLE GAIN AS A FUNCTION OF ANTENNA LENGTH

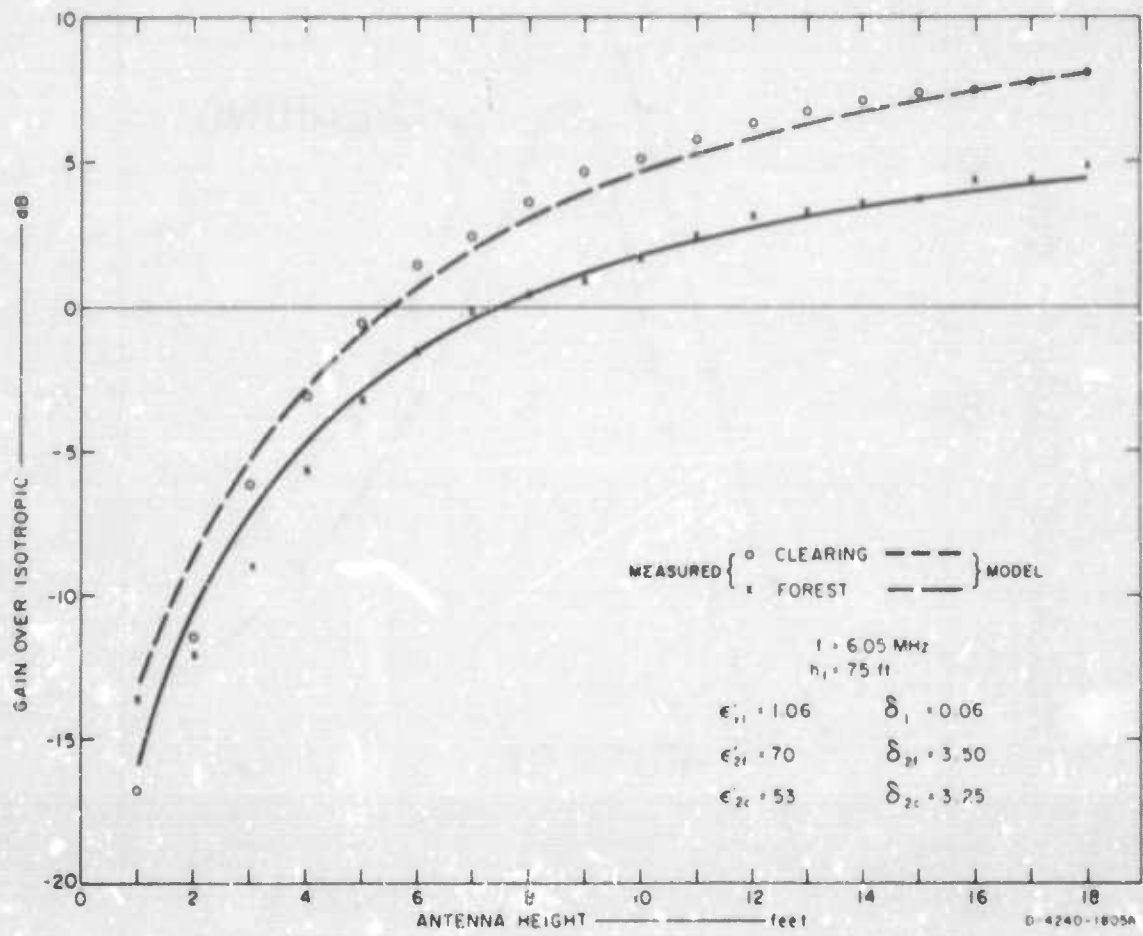


FIGURE III-36 COMPARISON OF COMPUTED AND MEASURED DIPOLE GAIN TOWARD THE ZENITH AS A FUNCTION OF ANTENNA HEIGHT IN CLEARING AND FOREST

have the greatest confidence in the model. Measured impedance values were used to calculate the gain and to correct the relative gain values for mismatch loss.

5. Summary

In summary, it was possible to use ionospheric sounders to measure relative gain at the zenith for HF tactical antennas in the frequency range 4 to 8 MHz. The technique is useful over the range of frequencies for which the ionosphere provides propagation support at vertical incidence. The horizontal dipole at a height of $\lambda/8$ had the greatest gain, and the height of this antenna could be reduced significantly before its performance became equal to the next best alternative, the inverted L. The 2:1 inverted L had slightly more gain than the 5:1 inverted L, which was superior to a 30° slant wire. The vertical whip antenna was the worst antenna tested for gain at the zenith, having a gain 25 to 55 dB below the half-wave dipole at 15 ft above ground. The results of the antenna directivity pattern measurements indicate that the dipole and inverted L exhibit their maximum gain at the zenith, whereas the maximum gain of the slant wire occurs at an angle slightly lower than the zenith and whip has a null at the zenith. The 6-MHz relative response results are summarized in Figure III-37. The absolute gain of a 6-MHz half-wave horizontal dipole relative to an isotropic radiator was calculated for several other sites where height gain data were obtained using the ionospheric sounder technique. The results are summarized in Figure III-38. The gain values obtained in the clearing at Chumphon and in the Bangkok rice paddy are very similar; this is reassuring since the ground conductivity was very high at both sites (25 to 125 mmho/m). Notice that the gain of the dipole toward the zenith reaches isotropic level at about 6 ft \pm 2 ft ($\lambda/25$) above ground even for the relatively poor ground

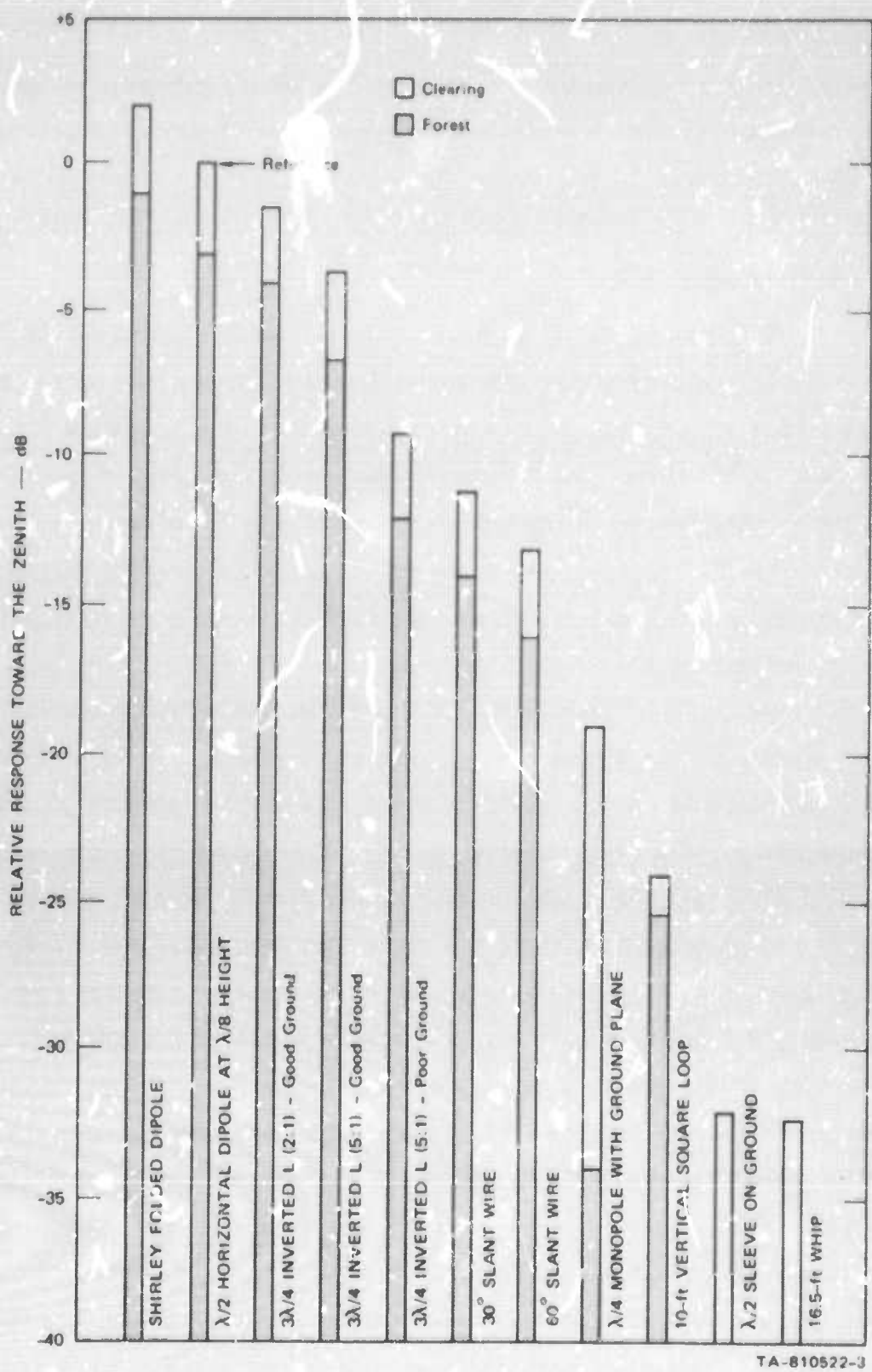


FIGURE III-37 TYPICAL RELATIVE RESPONSE TOWARD THE ZENITH OF 6 MHz FIELD-EXPEDIENT ANTENNAS

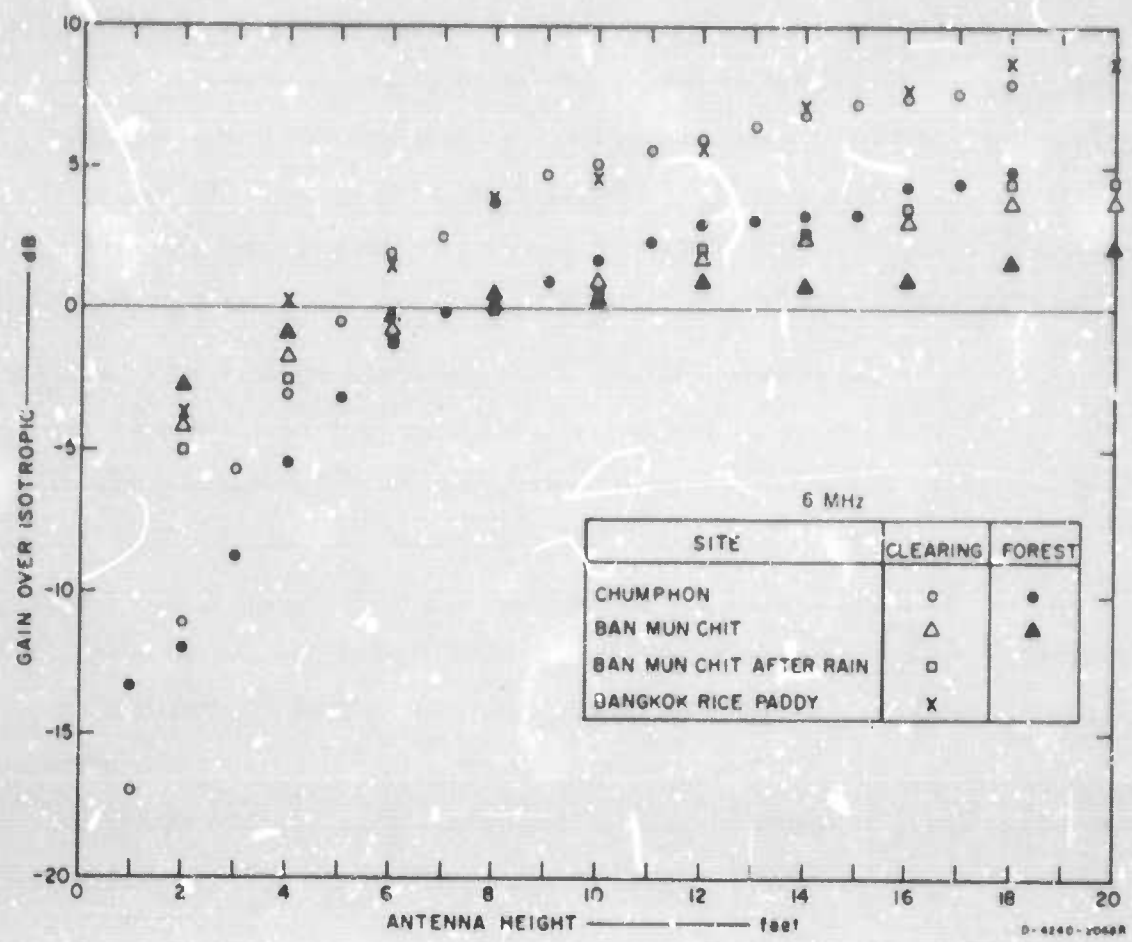


FIGURE III-38 MEASURED DIPOLE GAIN TOWARD THE ZENITH AS A FUNCTION OF ANTENNA HEIGHT—AT SEVERAL SITES

at the Ban Mun Chit site. This implies that a 6-MHz half-wave dipole is a relatively efficient antenna for use on short HF skywave paths in cleared or forested terrain even when elevated only about as high as a man can reach. This is contrary to the commonly held view that a dipole must be placed one-quarter wavelength above ground in order to be an efficient radiator toward the zenith. Indeed, our data (STR 18) have shown that the dipole is more effective (by about 1 to 2 dB) as a radiator toward the zenith when placed at $\lambda/8$ above ground than when placed at $\lambda/4$.

The measured values of dipole height-gain tend to confirm the use of the 3-layer slab model presented in Section III-B when the input data to the model are known or are derived from measurements of ground and vegetation constants using open-wire transmission-line techniques.* Since the model was formulated to predict gain of the dipole relative to an isotropic radiator, the model equations can be used to estimate the absolute gain of the dipole when used as a reference antenna. This model for the dipole provides a way to convert the measured relative gains to absolute gains, including converting the measured directivity plots obtained with the airborne Xeledop system to absolute-gain plots.

* Recall from the discussion of Section III-A that antenna height was the only really significant variable affecting dipole gain toward the zenith. Both the model predictions and the data summarized in Figure III-38 indicate that refined estimates of ground and forest parameters can improve such gain calculations only by about 3 dB for antenna heights greater than $\lambda/40$.

F. Antenna Impedance Results (STR6D, RM7, STRs 10, 18, 25, 26, 35, 36
39D, 41, 45D, 46D)

1. Objective

The objective of this section is to present some examples of measured impedances and some conclusions about the effects of forests on driving-point impedance.

2. Background

The feed-point impedance of field-expedient antennas is required by engineers designing equipments or calculating antenna gain for system calibrations (or performance evaluations). The impedance of antennas near ground is difficult to compute,* and until recently very few measured data were available on antennas located in forests. During the course of this project a great deal of impedance data have been taken on antennas both in and out of forests as part of various measurement programs:

- (1) Early HF impedance measurements (RM 7)
- (2) HF airborne Xeledop measurements (STRs 10, 25, 35, 45D)
- (3) VHF airborne Xeledop measurements (STR 39D)
- (4) VHF manpack Xeledop measurements (STRs 26, 46D)
- (5) HF sounder measurements of gain toward the zenith
(STRs 18, 38D)
- (6) Sounder propagation studies (STR 38D)

* The recently developed technique of Andreasen¹⁸ shows some promise for computation of the impedance of arbitrary wire antennas.

(7) Single tree studies (SAR 6, STR 41;
see Section III-II of this report).

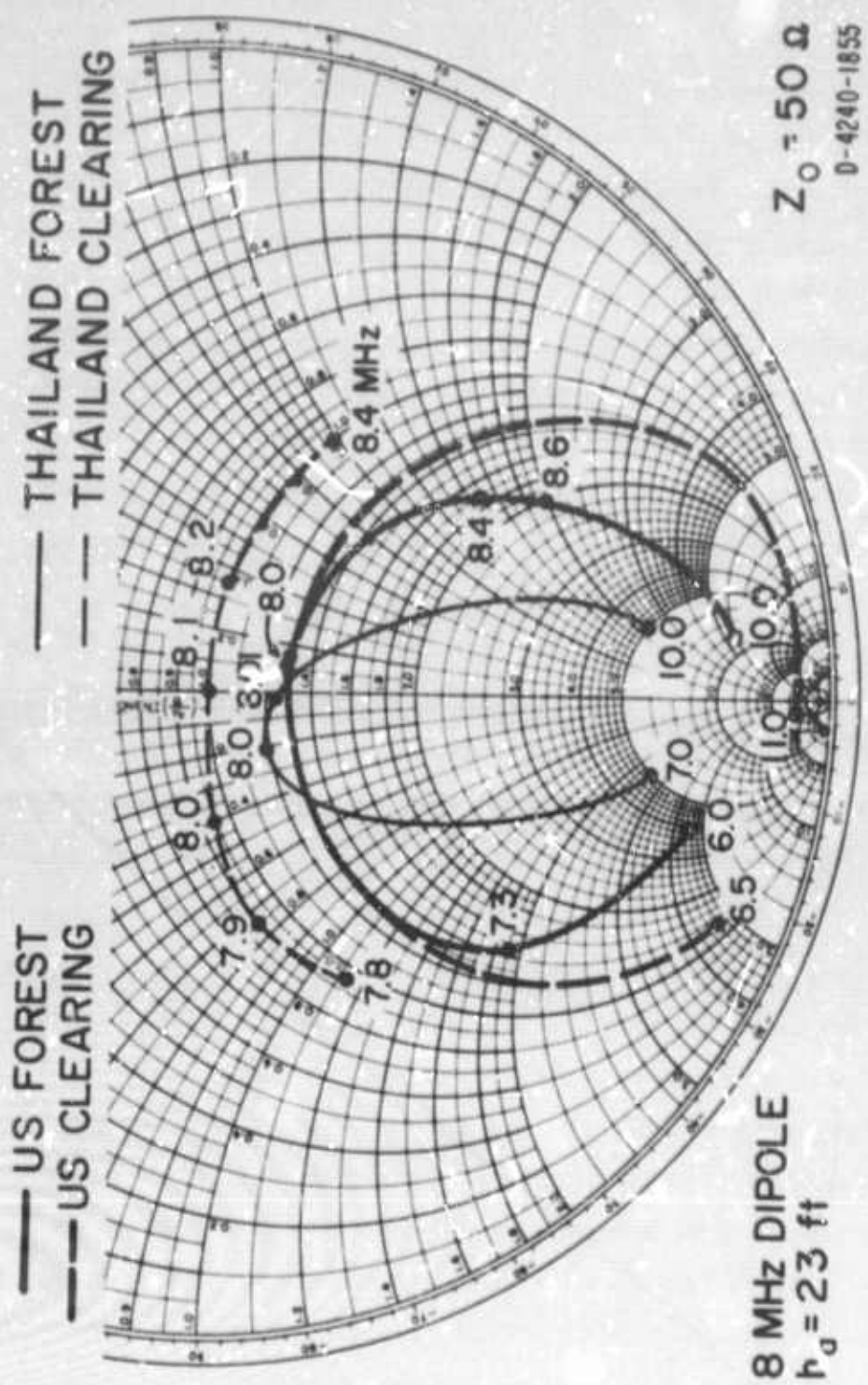
Sketches of the antenna types measured are shown in Figure III-18. The details of the antennas are given in the referenced reports. The measurement sites are described in detail in the referenced reports and in STR 43. A brief summary of the Thailand sites is given in Appendix A.

3. HF Results

a. Horizontal Dipoles

One of the standard test antennas used during the airborne Xeledop tests was a dipole cut to half-wave resonance at 8 MHz and located at 23 ft above ground. The feed-point impedance of this antenna is shown as a function of frequency in Figure III-39. The U.S. clearing was at Lodi, California (STR 19), the U.S. forest was at Lake Almanor, California (STR 25), the Thailand clearing was at Chumphon (STR 38D), and the Thailand forest data were obtained at Ban Mun Chit (STR 35). * Notice that the data for the forested sites lie inside the values for the cleared sites on the Smith chart and that the curvature of the plot near resonance increases for the data from the Thailand site (more dense vegetation). This implies that the impedance bandwidth of the dipole increased when the antenna was placed in the forest. As expected, the site with the best ground (Chumphon--where there was standing water) produced the lowest input resistance at resonance. The variation in reactance at 8.0 MHz from site to site is not significant

* The measurement sites will not be described in this section of the report but complete descriptions can be found in the referenced STRs.



MEASURED IMPEDANCE OF 8-MHz HORIZONTAL DIPOLE IN CLEARING AND FOREST—AS A FUNCTION OF FREQUENCY

because physically different antennas were employed and the antenna lengths were not necessarily identical.

The effect of the forest on the impedance of antennas of the same length can be observed in Figure III-40. This figure shows the feed-point impedance at 6 MHz, of a center-fed dipole located at 18 ft above ground at the Chumphon site as the antenna length was varied from 100 ft to 60 ft in 4-ft increments (i.e., 2 ft off each end after each measurement). The important thing to notice is that for a given antenna length the impedance is higher for the antenna located in the forest, and the reactive part is shifted in a clockwise manner on the Smith chart corresponding to a decrease in the resonant frequency as the "same" antenna is moved from the clearing to the forest. The square of the ratio of the resonant length in the clearing to the resonant length in the forest gives a rough estimate of the real part of the effective relative dielectric constant of the forest. In this case, $(78.8/72.2)^2 \approx 1.04$, which checks reasonably with the value of about 1.05 determined with the open-wire transmission-line technique described in Section III-B-1.

Figure III-41 shows the impedance of a 6-MHz dipole as a function of height as it is lowered from 18 ft to 1 ft in the clearing from 18 to 0.5 ft in the forest. Notice again the clockwise shift on the Smith chart, of the reactive part and the higher impedance level for a given height for the antenna in the forest. The impedance begins to drop as the antenna is lowered from 18 ft to about 6 to 9 ft, where the impedance starts to rise again. This is perhaps better illustrated in Figure III-42, which is a plot of the real part of the dipole feed-point impedance as a function of height above ground. The pair of curves on the left were taken in the clearing at Chumphon with and without a balun, and the pair on the right side were taken in the forest. Consider first

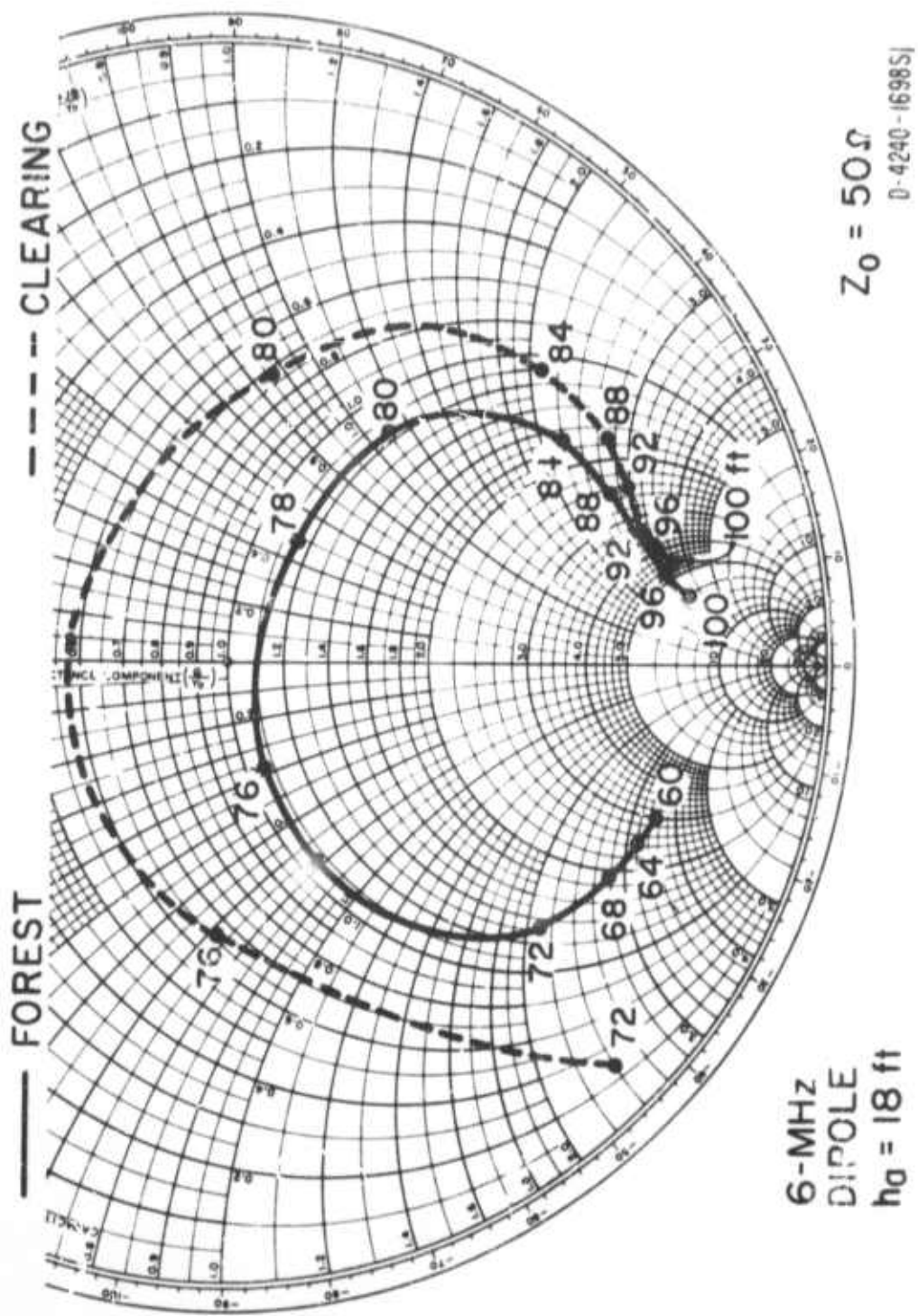


FIG. IRE III-40 MEASURED IMPEDANCE OF 6-MHz HORIZONTAL DIPOLE IN CLEARING AND FOREST—AS A FUNCTION OF LENGTH

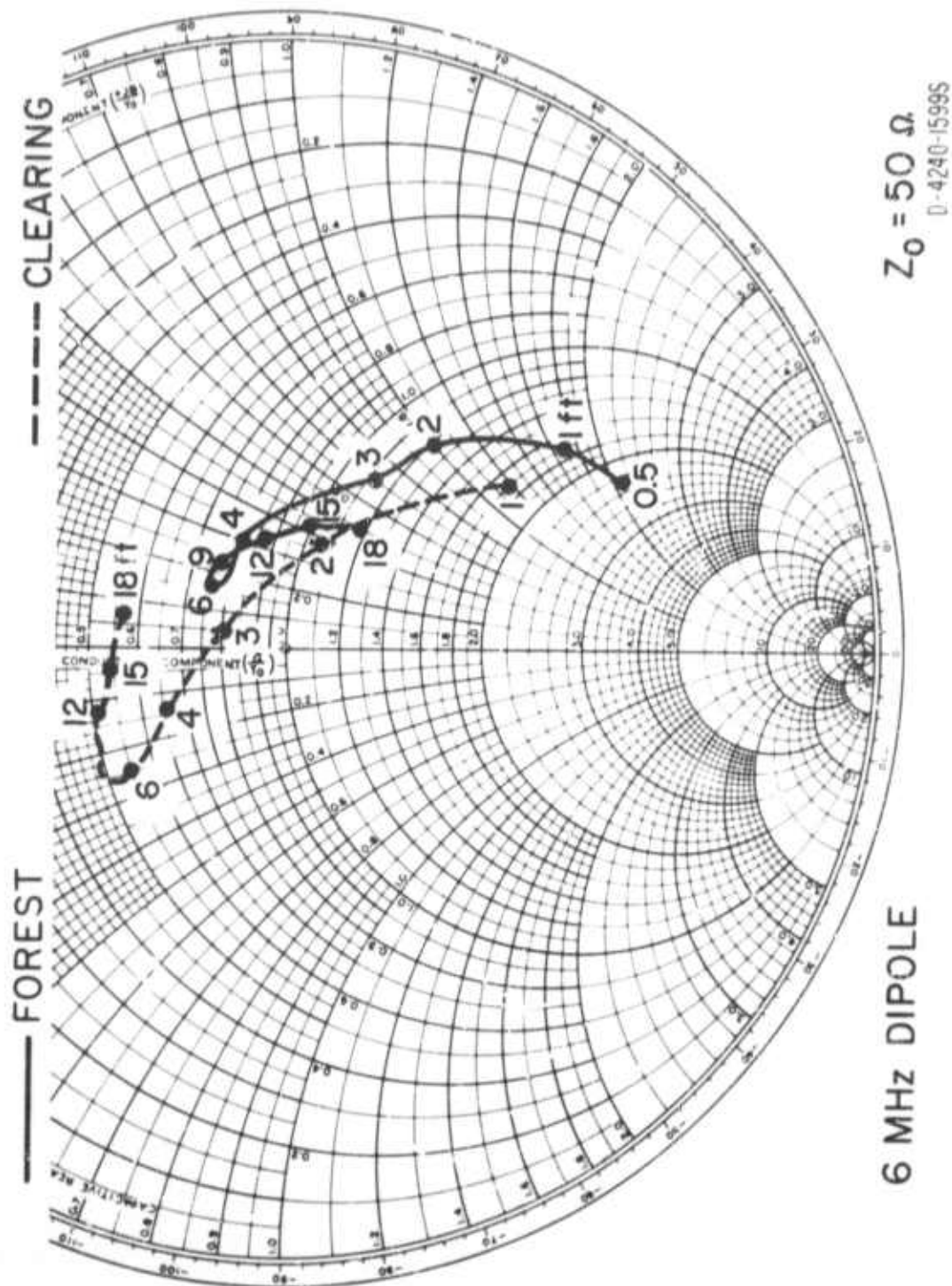
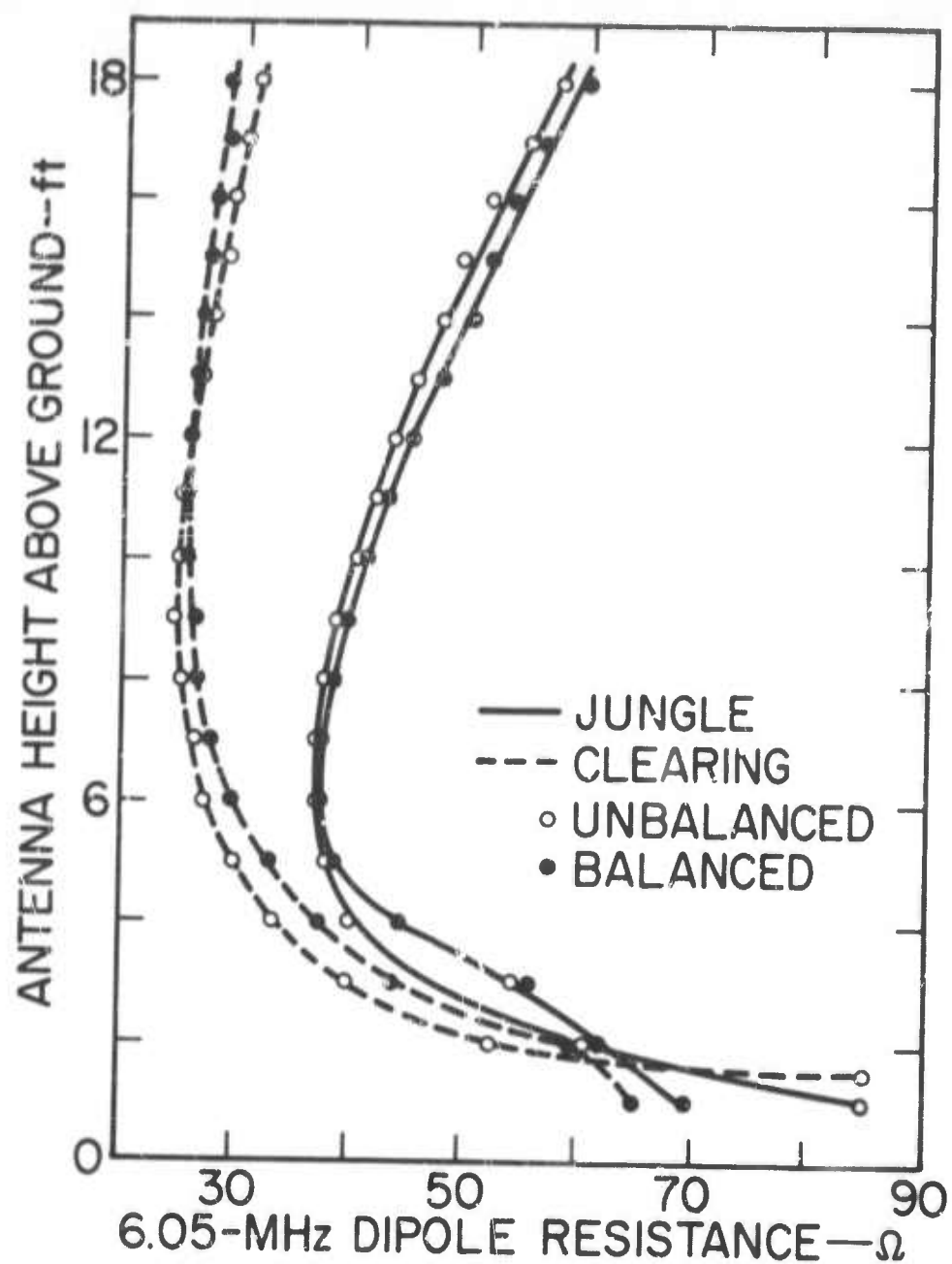


FIGURE III-41 MEASURED IMPEDANCE OF 6-MHz HORIZONTAL DIPOLE IN CLEARING AND FOREST—AS A FUNCTION OF HEIGHT



DB-4240-461S

FIGURE III-42 MEASURED RESISTANCE OF BALANCED AND UNBALANCED 6-MHz HORIZONTAL DIPOLES IN CLEARING AND FOREST—AS A FUNCTION OF HEIGHT

the curves for the dipole in the clearing. If the ground had infinite conductivity, we would expect the resistance of the dipole to drop down toward zero as the antenna is lowered toward the ground. The driving-point resistance can be defined as the sum of a radiation resistance and a loss resistance. The height at which the impedance begins to rise corresponds to the height at which the radiation resistance is about equal to the effective loss resistance. Notice also that the low-loss ferrite-core balun transformer, which had a 1:1 turns ratio, had a very small effect on the dipole resistance.

b. 30° Slant Wire

The various 30° slant-wire antennas studied all resonated very near 50 ohms. Figure III-43 shows the results of measurements at Chumphon. Measurements also were made on a 60° slant wire, which showed essentially the same trends. The effect of increasing the angle of the slant wire is to cause the feed-point impedance on the Smith chart to shift counterclockwise, with the real part staying essentially constant.

c. Inverted Ls

Impedance measurements were also made on inverted-L antennas designed so that the combined length of the vertical and horizontal wire sections was three quarters of a wavelength. These antennas were fed against a 1-1/2-ft copper ground rod. When the ratio of the lengths of the horizontal section to the vertical section was 2:1, the feed-point impedance at resonance ranged between about 125 and 200 ohms, typically being greater in the forest than in the clearing. As the ratio of horizontal to vertical sections was increased from 2:1 to 5:1, the impedance dropped for antennas in both clearing and forest and the observed impedance of a 5:1 inverted L at resonance ranged from about

$$Z_0 = 50 \Omega$$

D-4240-1706RS

30° SLANT WIRE

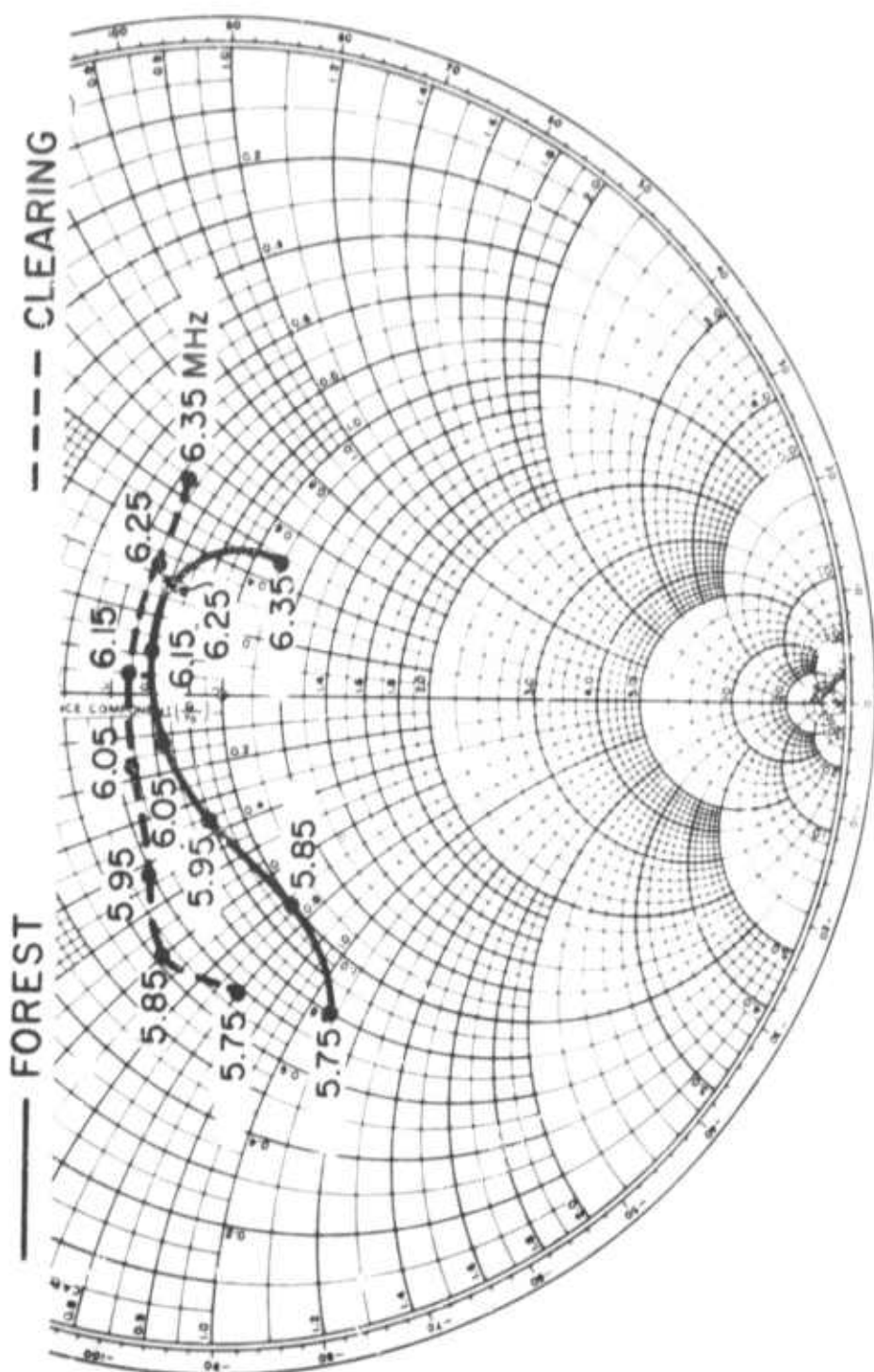


FIGURE III-43 MEASURED IMPEDANCE OF 6-MHz, 30° SLANT WIRE IN CLEARING
AND FOREST—AS A FUNCTION OF FREQUENCY

50 to 150 ohms. Figure III-44 shows the driving-point impedance versus frequency for a 5:1 inverted L at Chumphon. Notice again the increase of impedance in the forest and lower resonant frequency in the forest.

d. Vertical Monopole

The impedance of a 15.6-ft monopole with a 50-ft-diameter ground screen was measured in an open plowed field at Lodi, California (STR 10) and in a pine forest at Lake Almanor, California (STR 25). The results of these measurements are shown in Figure III-45. The impedance of the monopole near resonance is slightly higher in the forest than in the clearing. The impedance bandwidth of this antenna appears to be about the same in clearing and forest. This same antenna with a matching network was set up at Ban Mun Chit, Thailand (STR 35) and measured at 6 MHz in the clearing, at the edge of the forest and in the forest. For these tests the antenna was fed through a 50:300-ohm balun and resonated in each location with a ferrite slug inductor in series with the monopole element. The results of these tests are given in Figure III-46. Notice the decrease in impedance at resonance as the antenna is moved from clearing to forest. This reduction possibly is due to mutual coupling to nearby tree trunks.

e. Concluding Comments

The results of measured feed-point impedance discussed above indicate that the impedance of a simple field-expedient antenna typically increases as the antennas are moved from clearing to forest, and the antenna structure resonates at a slightly lower frequency in the forest. The change in resonant frequency for a given horizontally polarized antenna is related in an approximate manner to the real part of the relative dielectric constant of the forest by the square of the

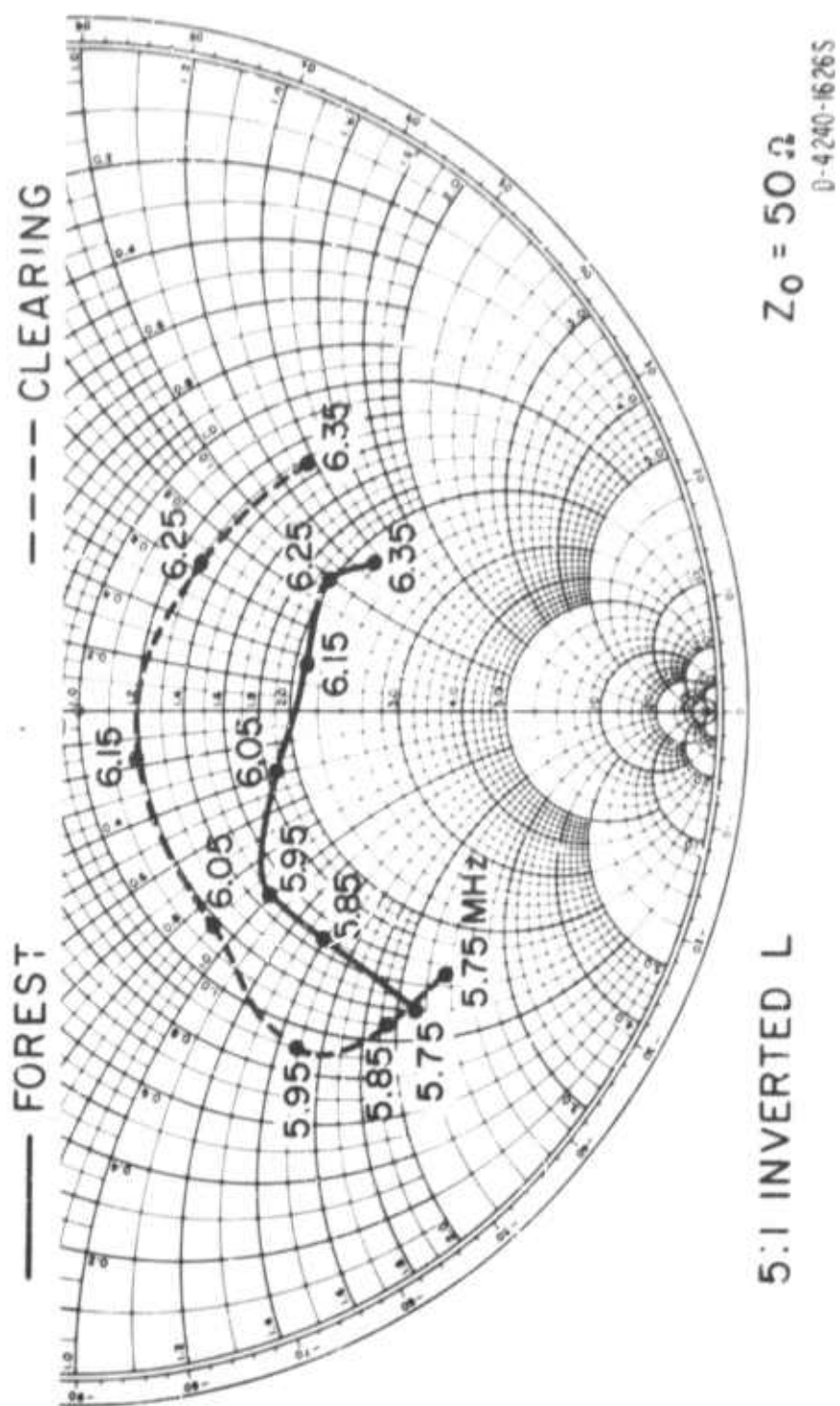


FIGURE III-44 MEASURED IMPEDANCE OF 6-MHz 5:1 INVERTED L IN CLEARING AND FOREST—AS A FUNCTION OF FREQUENCY

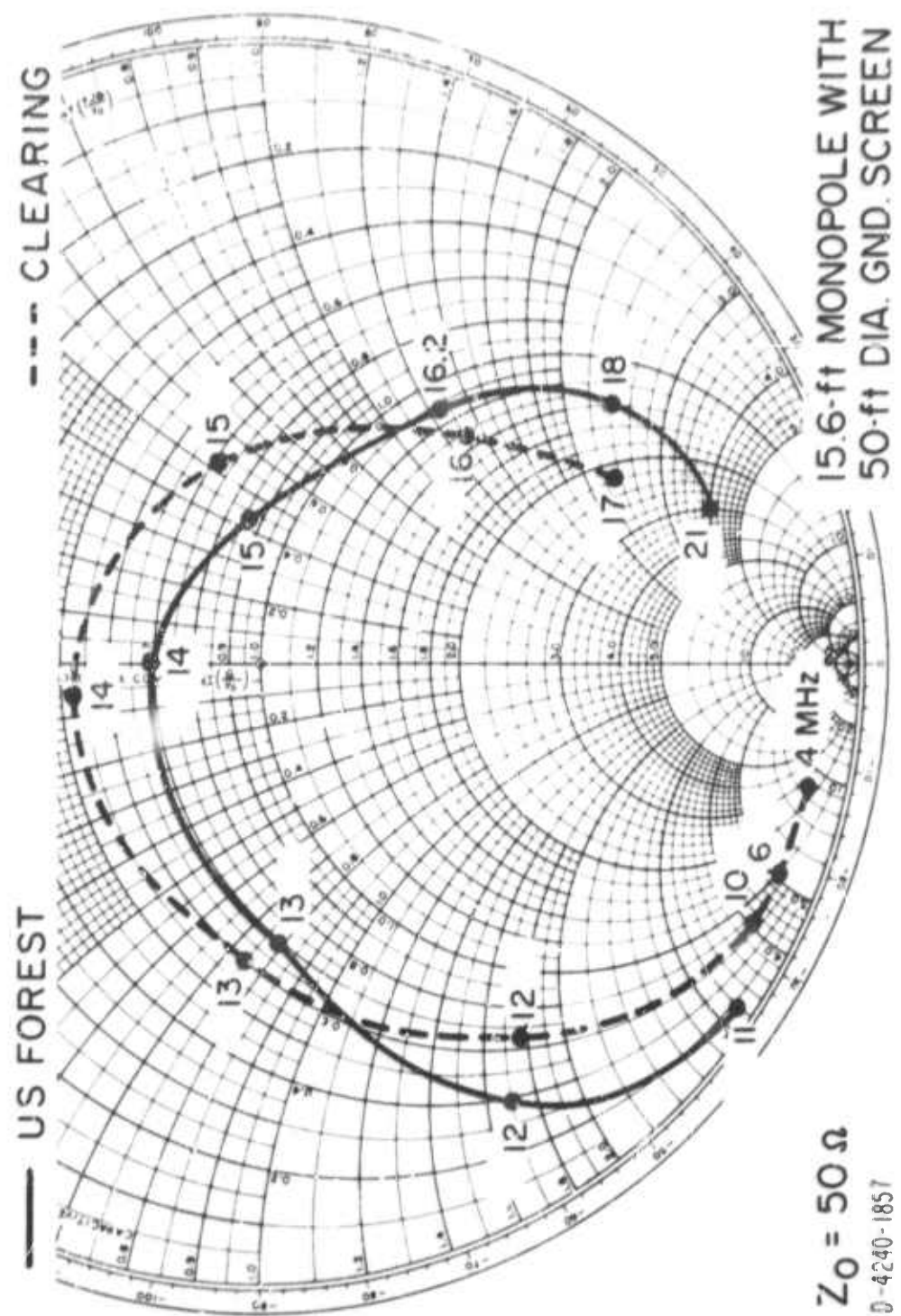


FIGURE III-45 MEASURED IMPEDANCE OF 15.6-FOOT MONPOLE IN CLEARING AND FOREST—AS A FUNCTION OF FREQUENCY
0-4240-1857

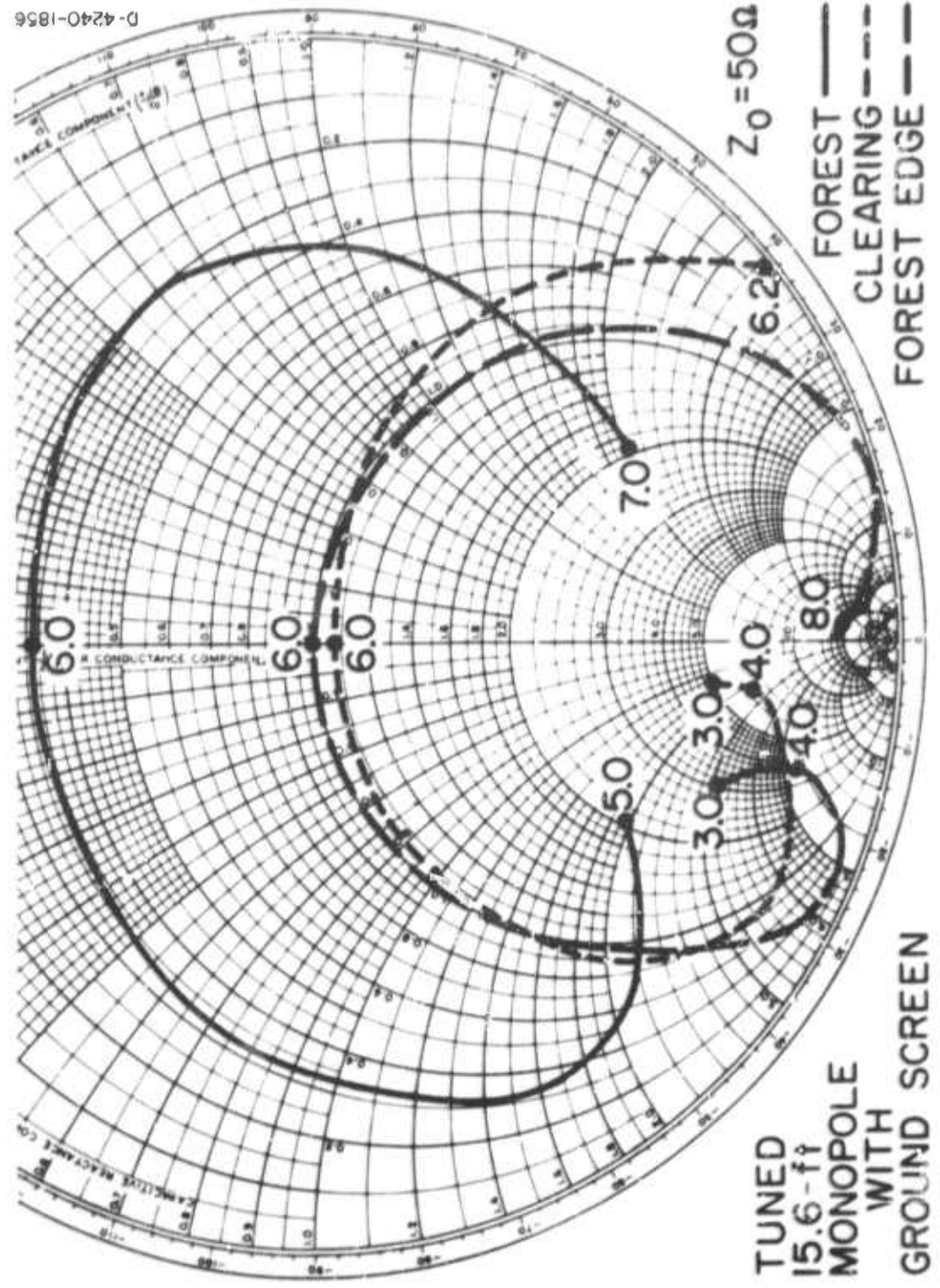


FIGURE III-46 MEASURED IMPEDANCE OF TUNED 15.6-FOOT MONPOLE IN CLEARING AND FOREST—AS A FUNCTION OF FREQUENCY

ratio of the resonant frequencies in clearing and forest or by the square of the ratio of length required for resonance in clearing and forest.

The impedance bandwidth of a half-wave horizontal dipole increases as the antenna is moved from the clearing to forest and this increase is enough to compensate for the shift of resonant frequency just discussed. In other words, an HF dipole designed for operation in the clearing with a system requiring a VSWR of less than, say, 3:1 would probably be able to meet this VSWR specification even when the antenna was operated in the forest, whereas this might not be the case for a vertical monopole placed too near a tree trunk in the forest. Indeed, the impedance bandwidth of a monopole may be reduced when it is taken from a clearing into a forest.

4. VHF Results

a. General Comments

Impedance data were obtained at VHF as part of the man-pack and airborne Xeledop programs and as part of the single-tree studies. This section will cover the Xeledop impedance data, and the single-tree data will be covered in Section III-H. The feed-points of the antennas were 10 ft above ground unless otherwise stated.

b. Airborne VHF Xeledop--Ban Mun Chit

The horizontal (balanced and unbalanced) and vertical (sleeve) dipole antennas employed at this site are described in STR 39D. The impedance data obtained at resonance for the horizontal dipoles in the clearing were typically about 50 ohms compared with 150 ohms for the vertical sleeve dipole. In general, the driving-point resistance of the

horizontal dipoles in the forest was about 5 to 10 ohms higher than for the same type of antenna in the clearing, whereas, the resistance of the vertical sleeve dipoles generally was substantially lower (e.g., 50 ohms lower) in the forest.

c. Manpack Xeledop

The antennas used for this study were balanced half-wave dipoles constructed of telescoping automobile antennas adjusted to resonance while the antenna was horizontally polarized at the open-delta site near Bangkok. The resulting antenna lengths were: 112.5 inches at 50 MHz, 77.0 inches at 75.1 MHz and 60.5 inches at 100 MHz. These lengths were used throughout the program. A North Hills model 1100EBB (1:1) VHF balun transformer was mounted at the feed, and the transmission line was brought away from the radiating elements at right angles for at least the first 2 ft. The measured impedance data obtained at the delta and beach sites (STR 26) were very consistent: 46, 60, and 56 ohms resistive (to within 10 percent) at 50, 75, and 100 MHz respectively.

Additional data were obtained with unbalanced half-wave dipoles adjusted for zero reactance at each site. These antennas were used as part of the manpack Xeledop calibration procedure. Data were obtained in the delta, at the beach, at Chantaburi (rubber plantation), and in the clearing and in the forest at Chumphon. The antenna was placed at 10 ft above the open ground and over a 10-by-10-ft chicken-wire ground screen. The results of these tests were quite consistent. Data also were obtained over the open ground with the feed at 5 ft and at 20 ft. For all the 10-ft and 20-ft test configurations, feed-point resistance was in the range 60 to 80 ohms for all frequencies and sites for both polarizations. At 5 ft above ground the range was 55 to 115 ohms, with

the higher values occurring for vertical polarization at 50 MHz and the lower values occurring for horizontal polarization at 100 MHz.

G. VHF Xeledop System Loss Measurements

1. Manpack Xeledop (MPX) Tests (STRs 19, 26, 36, 46D)

a. Objective

The objective of this work was to study short-range (ground-to-ground) VHF propagation in various tropical terrains.

b. Background

The VHF Airborne Xeledop transmitter described in the previous section was adapted for use in a backpack configuration. This unit was carried along surveyed trails at several sites over ranges of 0 to 0.5 miles:

- (1) Eucalyptus grove--Fremont, California
(SA 5, STR 19)
- (2) Open delta--Bangkok, Thailand (SA 6, STR 26)
- (3) Sandy beach--Laem Chabang, Thailand
(SA 6, STR 26)
- (4) Coastal brush--Laem Chabang, Thailand
(SA 6, STR 26)
- (5) Wet-dry second growth tropical forest--
Ban Mun Chit, Thailand (SA 7, STR 46D)
- (6) Fresh-water swamp (rain) fores.
Chumphon, Thailand (STRs 36, 46D)

(7) Rubber plantation--Chantaburi, Thailand
(STR 36)

(8) Bamboo forest--Chantaburi, Thailand
(STR 36).

2. Results

The results of the initial tests with MPX system in open terrain and in the coastal brush were reported in STR 26. Example analog records from the fresh-water swamp, bamboo forest, and rubber plantation were published in STR 36 and in Reference 19. Figure III-47 shows the effect of a rubber plantation on received signal level as the MPX was carried into the forest. A standing-wave pattern can be observed at the clearing forest interface.* The major results obtained in the wet/dry forest at Ban Mun Chit and the fresh-water swamp at Chumphon will be reported in STR 46D, and this report (which will be printed on Contract No. DAAB07-070-C-0220, USAECOM, Fort Monmouth, New Jersey) will include:

- (1) A calibration of the MPX system
- (2) A summary of the MPX results from all sites
- (3) A comparison of the measured data with propagation model predictions of median signal strength versus frequency, transmitter-receiver separation, and antenna polarization and height

* This interface effect also was observed at Chumphon (see Figures 21-23 of STR 36) where the spatial fading pattern in the clearing was much more pronounced for horizontal polarization.

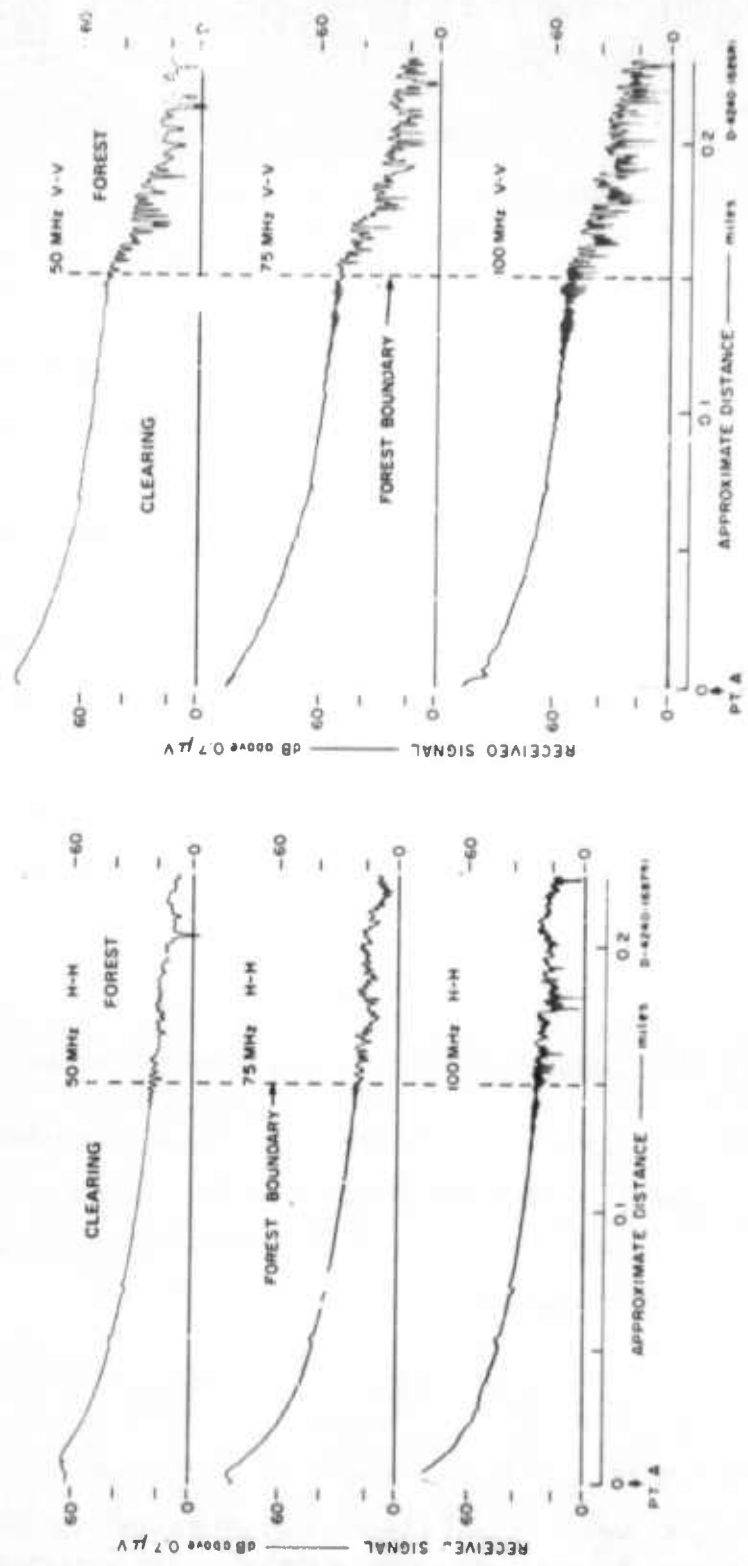


FIGURE III-47 EFFECT OF RUBBER PLANTATION ON RECEIVED SIGNAL AS MPX IS CARRIED INTO FOREST

- (4) A study of the fading characteristics as a function of distance down the trail and radio frequency
- (5) A comparison of MPX measurements with data taken with AN/PRC-25s in open and forested terrain.

3. Balloon-Borne Xeledop Tests (STR 46D)

a. Objective

The objective of this work was to measure VHF height-gain functions in the forest, with possible application to balloon-borne relays.

b. Background

A light-weight version of the VHF MPX (transmitting on 50, 75.1, and 100 MHz) in both vertical and horizontal polarized configurations was constructed for use with an aerodynamic balloon (Kytoon). This unit was used successfully to make height-gain measurements up to several hundred feet at the Chumphon, Thailand site (fresh-water swamp forest).

4. Results

The results of this work will be reported in STR 46D.

H. Single-Tree Studies (STR 41)

1. Objectives

The objectives of this work were to study at VHF:

- (1) The variation in received signal level as a function of transmitter location in proximity to a single tree
- (2) The input impedance of an electric dipole as a function of distance from the tree trunk
- (3) The scatter pattern of an isolated tree
- (4) The radiation pattern of such a tree when shunt-fed as a grounded vertical antenna in order to better define the effect of vegetation on radio-wave propagation and antenna/vegetation interaction.

2. Background

The first group of experiments was designed to determine the variation of signal strength and the impedance of an antenna in the neighborhood of an isolated tree. From these measurements, the maximum distance between tree and antenna for which there is significant effect upon received signal level and antenna impedance can be determined. The second group of experiments was designed to determine an equivalent radius of the tree in terms of the radius of the aluminum mast. With the equivalent radius, the cross section and the scatter pattern of the tree can be evaluated theoretically. If the properties of a single tree are known, then a model of propagation of radio waves in a jungle might then be based on the distribution of the nearest-neighbor distance of trees in that forest and the principle of superposition. The last experiment was to determine the directivity of an isolated tree shunt fed as a grounded vertical radiator. The bulky shape of such a radiator suggests it will have significant directivity, and this is a possible factor to offset the low efficiency of a tree antenna as reported by Dickinson.¹²

Two isolated trees were chosen at Iaem Chabang. One of them was a rubber tree, for convenience called tree "A." The height of Tree A was approximately 65 feet. The diameter of the trunk at the point just above the ground was 26.8 inches and reduced to 19.2 inches at 4 feet above the ground. The area within 300 feet of the tree was absolutely cleared. The second tree ("B") was a mango, having a height of 30 feet and a trunk diameter of 20.2 inches at the point just above the ground. Some bushes less than 5 feet high were at a distance of 130 feet from Tree B. However, the area within 130 feet of the tree was cleared.

3. Signal Level and Antenna Impedance Tests

Data obtained on the feed-point impedance of half-wave vertical dipoles in the vicinity of vertical tree trunks demonstrated a variation with separation distance similar to that of dipole above a lossy plane surface (such as the earth). Consequently, it was decided to try to model the mutual impedance using equivalent plane-wave reflection coefficients determined from the standing-wave pattern of the MPX records as the MPX was walked past the tree. Examples of received signal level as the MPX was walked up to (and past) a single tree are given in Figure III-48. Notice especially the periodic fading in the direct path, and also the drop in level in the shadowed path. It is possible to scale this type of record for the amplitude (null depth) and phase (null location) of an equivalent plane wave reflection coefficient.* The average results obtained from three trees (the smallest of which was 30 ft tall) are summarized in Table III-7.

* These reflection coefficients apply only to the direct path (positive distance from tree in Figure III-48).

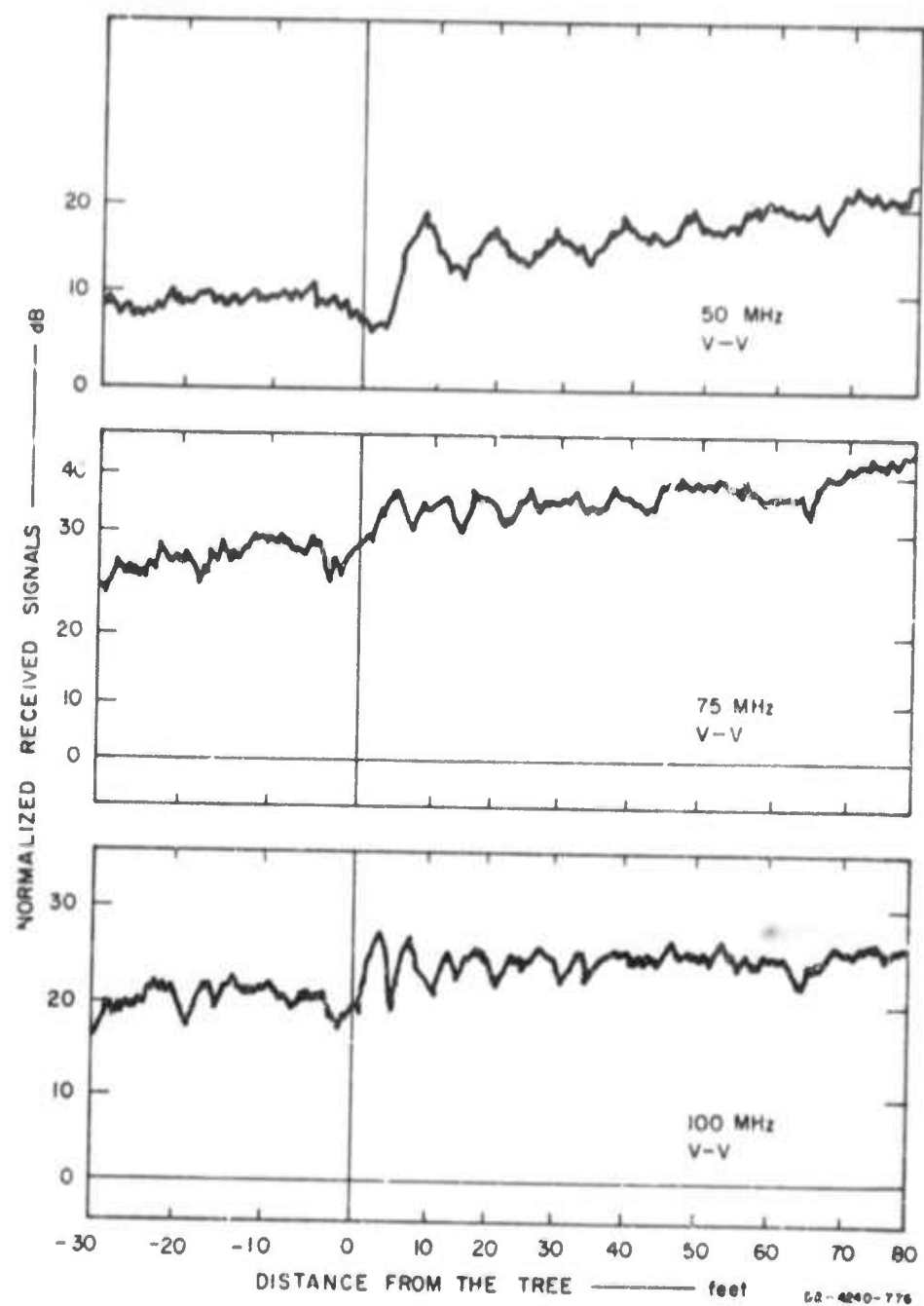


FIGURE III-48 SAMPLES OF THE RECEIVED SIGNALS IN THE PRELIMINARY STUDY OF THE SCATTERING PROPERTIES OF AN ISOLATED TREE

Table III-7
AVERAGE REFLECTION COEFFICIENTS FOR THREE TREES

Frequency (MHz)	Reflection Coefficient
50	0.32/ <u>180</u> [°]
75	0.27/ <u>180</u> [°]
100	0.38/ <u>145</u> [°]

Based on these values of the reflection coefficients at each frequency, the comparison of the theoretical and experimental values of the input impedance in the vicinity of an isolated tree was performed and reported in STR 41. An example is shown in Figure III-49. Agreement between the experimental and model values is good.

4. Scatter Pattern of an Isolated Tree

A model for the theoretical scatter pattern of an isolated tree was developed in STR 41. An example of the computed and observed scatter patterns for a 20-ft aluminum cylinder of radius 2 in are given in Figure III-50 along with measured results for Tree A and Tree B. The agreement between the measured and modeled data is "reasonable."

5. Use of a Tree as a Shunt-Fed, Grounded Vertical Antenna

An isolated 41-ft tree was used successfully as the antenna for one end of a 500-km communication link operating on 9 MHz by driving the tree with a shunt feed attached to a nail driven into the trunk several feet above ground (STR 41). The conclusion from this work was that, while trees will not replace wires as antenna elements, more study of their use as antenna elements seemed justified. A subsequent test at VHF indicated that the directivity of such a driven tree was not omnidirectional but that the maximum measured radiation occurred on the feed side of the tree.

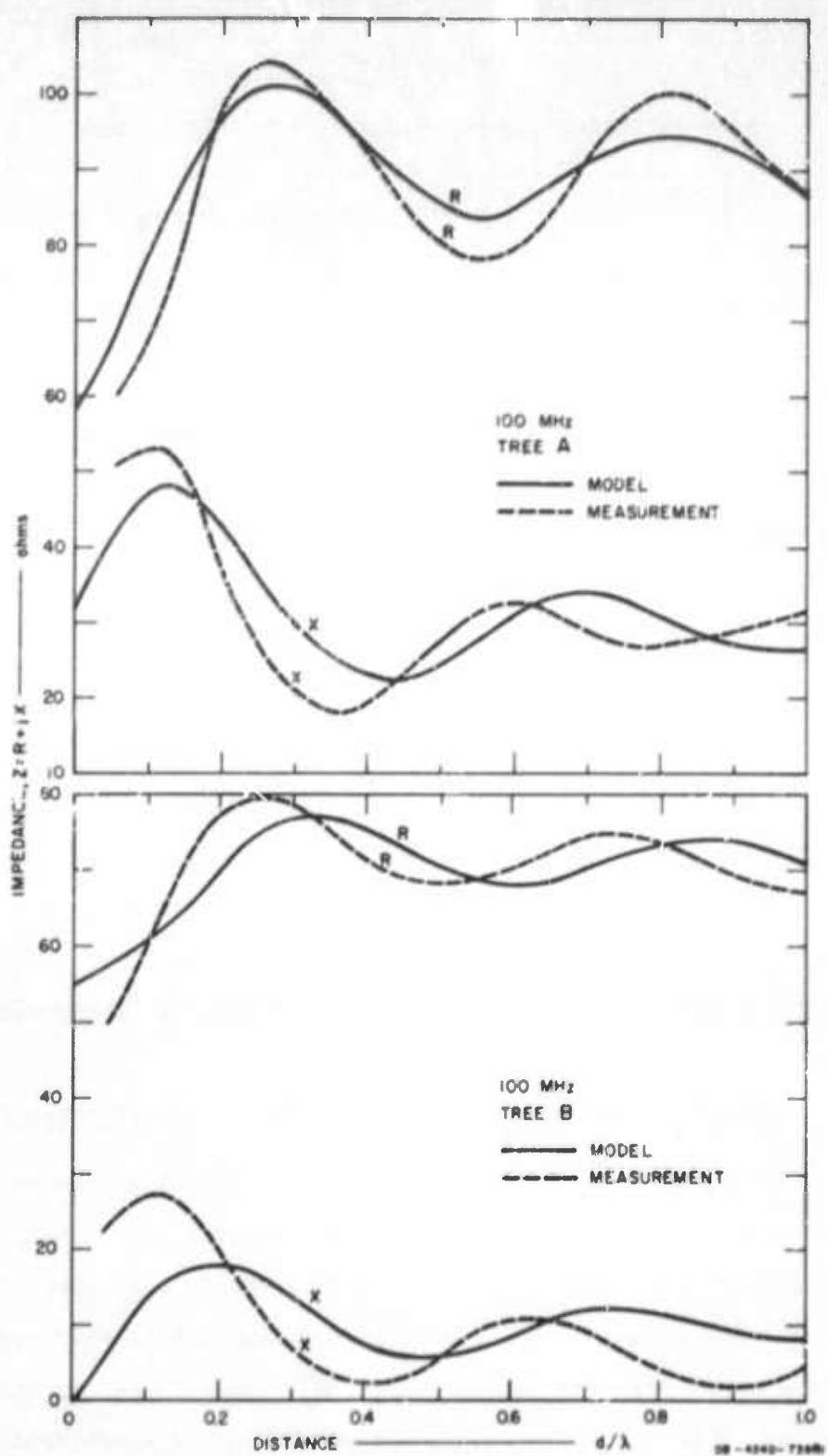


FIGURE III-49 MEASURED AND CALCULATED INPUT IMPEDANCE OF 100-MHz $\lambda/2$ DIPOLE VERSUS DISTANCE FROM TREES (HEIGHT = 6.56 FEET)

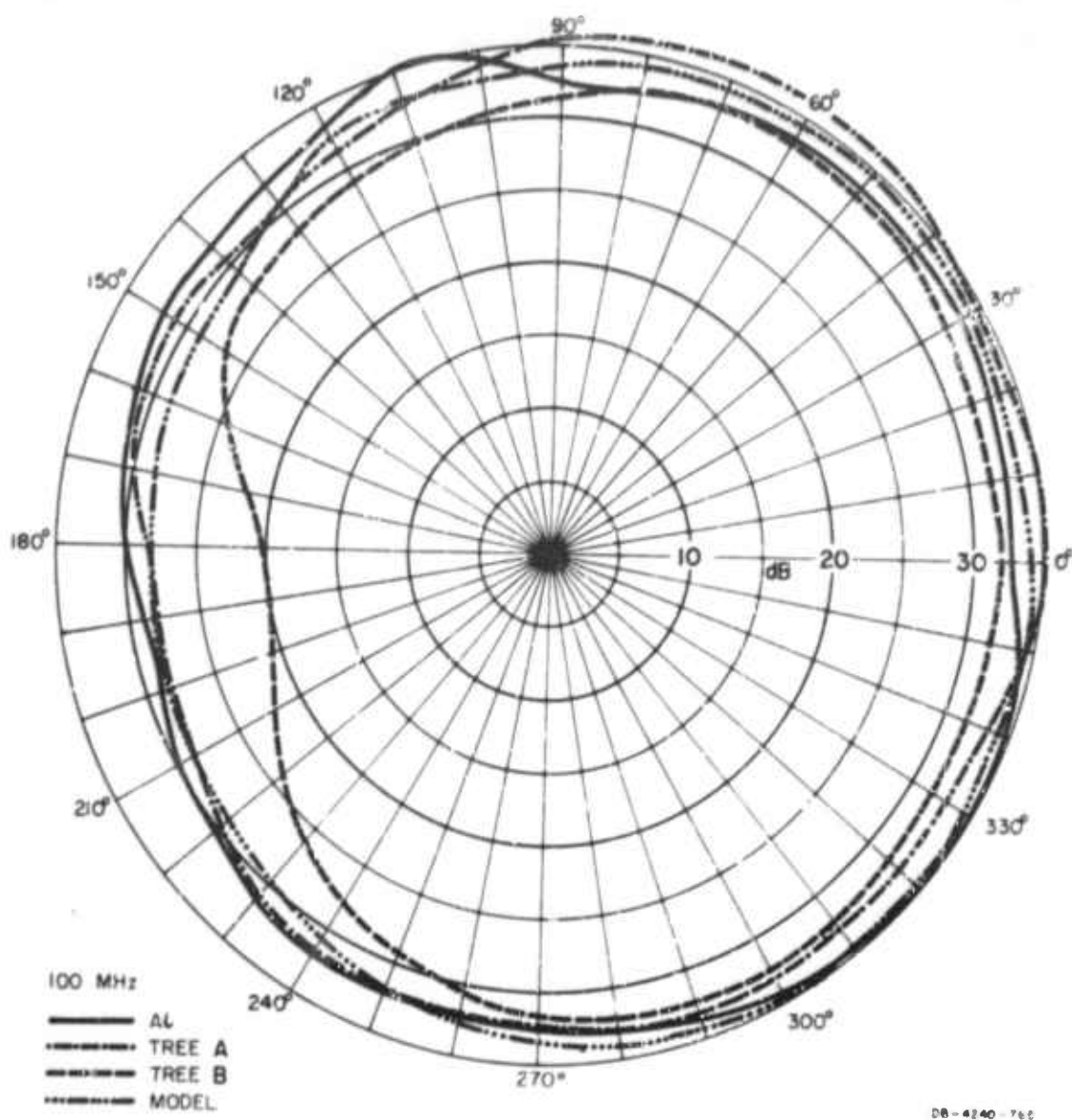


FIGURE III-50 COMPARISON OF THE THEORETICAL AND EXPERIMENTAL SCATTER PATTERNS OF AN ISOLATED TREE AND MAST

"PRECEDING PAGE BLANK-NOT FILMED".

IV TASK B: IONOSPHERIC AND FREQUENCY-SPECTRUM INVESTIGATING

A. Frequency Prediction

1. foF2 Predictions at Bangkok (STRs 15, 28, 40)

a. Objective

An objective of this work was to compare several available prediction techniques of the monthly median vertical-incidence critical frequency ($foF2$) with observations made at Bangkok with a C-2 vertical-incidence sounder, to determine the best prediction source and document its quality, and to consider whether a locally generated correction function would improve the predictions sufficiently to justify such additional effort. A second objective of this work was to determine the lowest useful tuning range for HF manpack radios intended for use on short ionospheric skywave paths in Southeast Asia.

b. Background

The C-2 ionospheric sounder began operation at the MRDC-EL site in Bangkok in September 1963, and the sounding results have been published in monthly ionospheric data bulletins (IDB) through the present. The monthly median observed values of $foF2$ for the period September 1963 through March 1965 were compared with predictions from the U.S. National Bureau of Standards (NBS) in Boulder, the Indian National Physical Laboratory (NPL) in New Delhi, and from SRI (SRI/RPA)--based on work done by SRI for the U.S. Army Radio Propagation Agency (RPA). This comparison (STR 15) indicated that the best predictions

were those of NBS --although the quality of these predictions did not greatly exceed those by NPL and SRI/RPA (see Figure IV-1 for an example comparison). It might be noted that a basic limitation of any of these prediction methods is the lack of accuracy of sunspot number predictions. The remainder of the effort was devoted primarily to the study of the NBS predictions (STRs 28,40).

c. Results

The yearly median error functions (predicted-minus-observed monthly median values of f_{oT2}) for the ESSA predictions for 1964 through 1967 together with quartile bounds, are shown in Figure IV-2. The error is almost always positive (prediction exceeds observation) and less than about 2 MHz. The predictions for 1967 are noticeably better than in previous years. There are two possible causes for this improvement:

- (1) ESSA began incorporating C-2 data from Bangkok into the predictions;
- (2) ESSA improved their prediction program (by changing coordinates for their numerical maps).

Let us consider for a moment the accuracy of the measured values that we are checking against the predictions. During two intervals a Granger Model 911 step-frequency sounder was operated at Bangkok concurrently with the C-2. The Granger sounder data were scaled in Menlo Park and plotted against the Bangkok-scaled C-2 data for the

* The Central Radio Propagation Laboratory (CRPL) of the NBS has since become part of the Environmental Science Services Administration (ESSA).

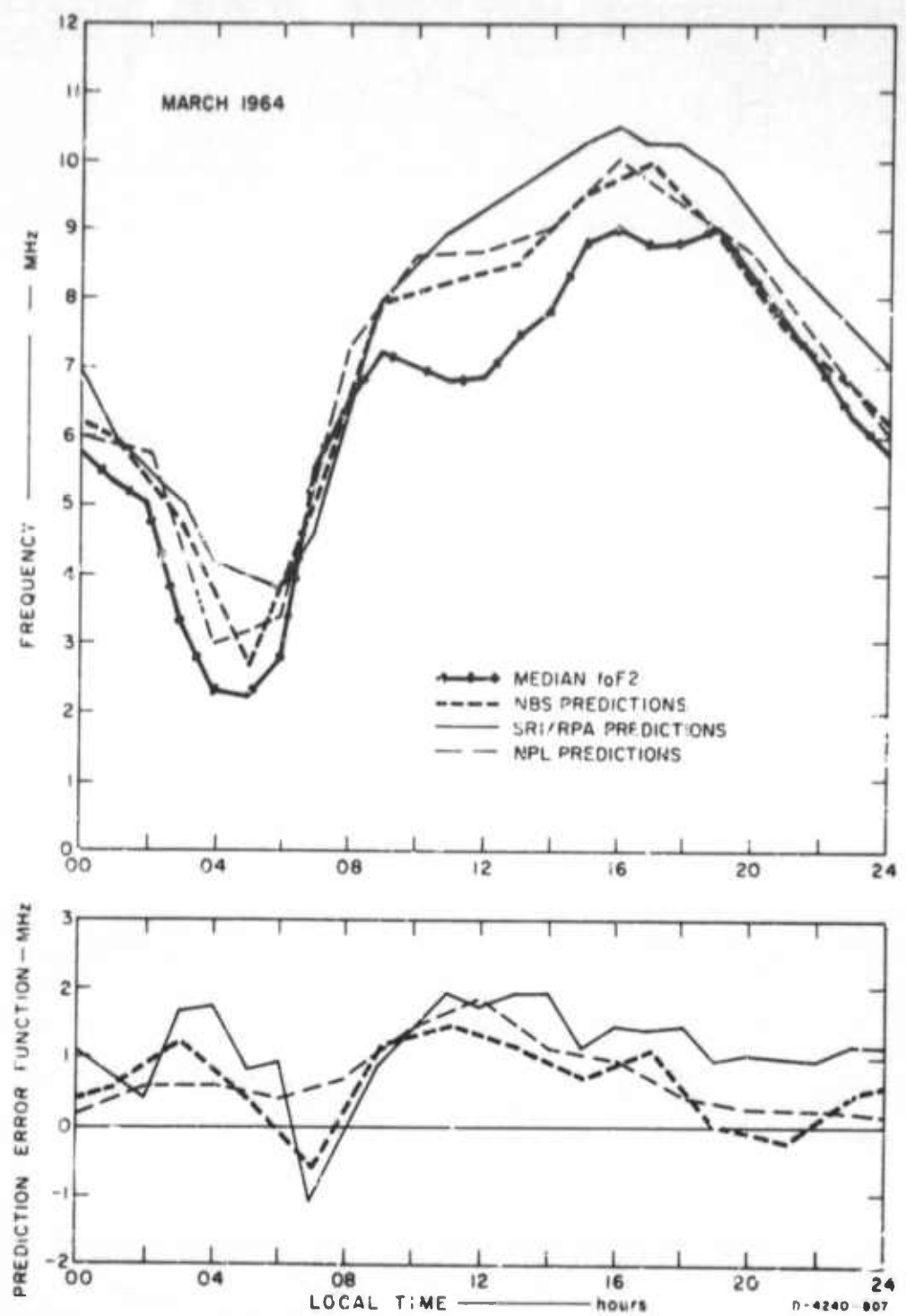


FIGURE IV-1 COMPARISON OF OBSERVED AND PREDICTED MONTHLY MEDIAN f_{oF2} FOR A TYPICAL MONTH

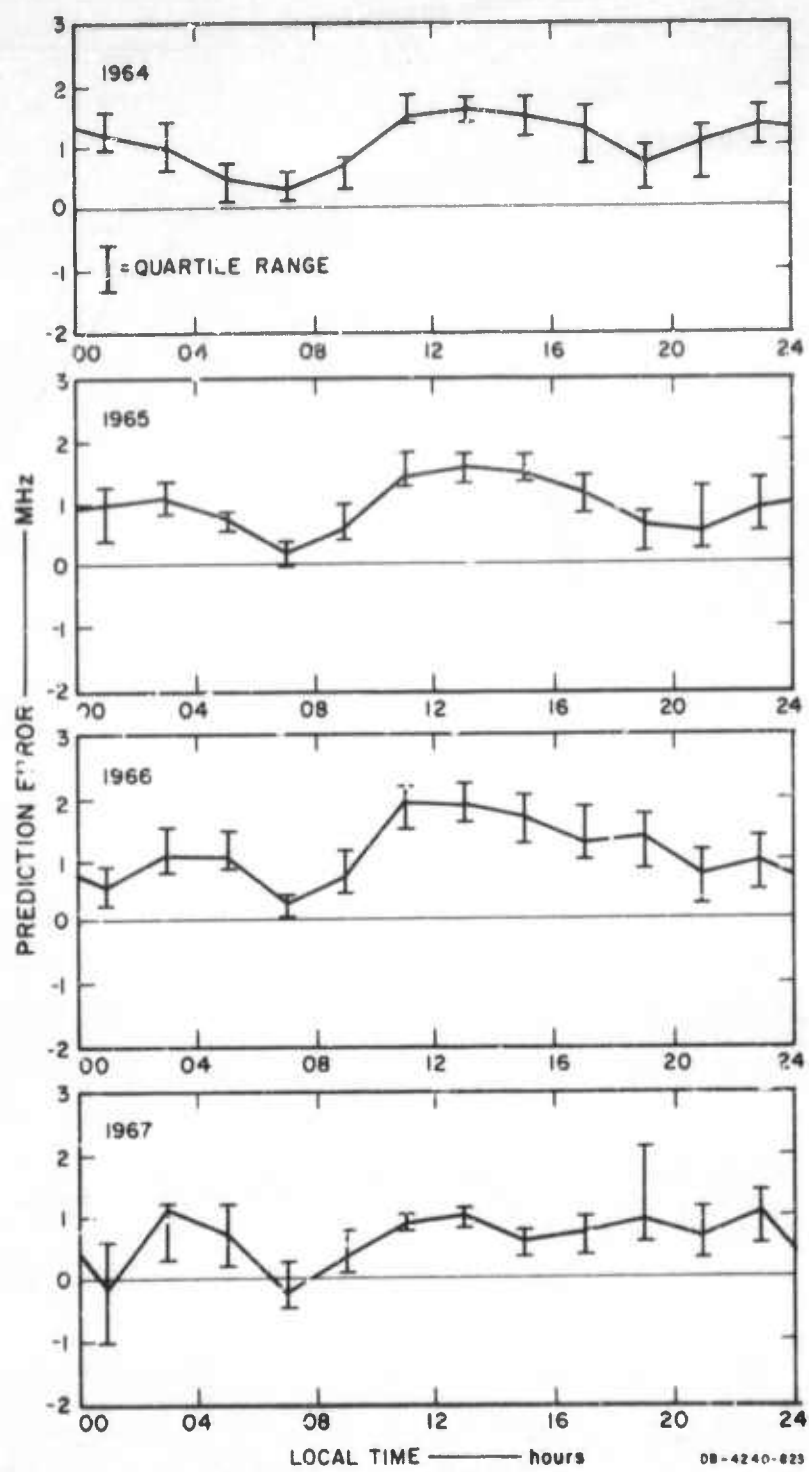


FIGURE IV-2 MEDIAN AND QUARTILE VALUES OF ERROR FUNCTIONS OF ESSA foF2 PREDICTIONS FROM 1964 THROUGH 1967

same hour (see Figure IV-3). It is not possible to say which of these sounders produced the more accurate data, but the results of this test indicate a typical ambiguity of somewhat less than 1 MHz on any given reading.

The percentage of the time a proposed operating frequency for a short-path (less than 50 km) would have exceeded an estimate of the maximum observed frequency (MOF) for such a path (based upon C-2 sounder data)* also was tabulated for the interval September 1963 - March 1965--a period of low sunspot number (see Figure IV-4). The determination of MOF included the effects of sporadic E.

d. Conclusions

The ESSA predictions of monthly median foF2 are the best available. So long as Bangkok C-2 data are used by ESSA to generate the predictions, the predicted values should be within 1 MHz of the actual observed monthly median values most of the time. This accuracy probably is sufficient to preclude the need for locally generated correction functions--should the MRDC-EL (or some other group) decide to disseminate frequency predictions within Thailand.

A lower design frequency of 2 MHz for HF manpack radios probably should be sufficient to ensure about an 80-percent chance for the existence of an operating frequency below the MOF during the hour of lowest MOF (about 0430 hours, local time) during a period of minimum solar activity. Outage during any given day due to not being able to operate below the MOF should occur less than 1.5 percent of the time

* Here the assumption is made that foF2 values observed at vertical incidence by the C-2 sounder closely approximate the MOF values that would have been observed over the short oblique path had oblique-incidence sounders been used.

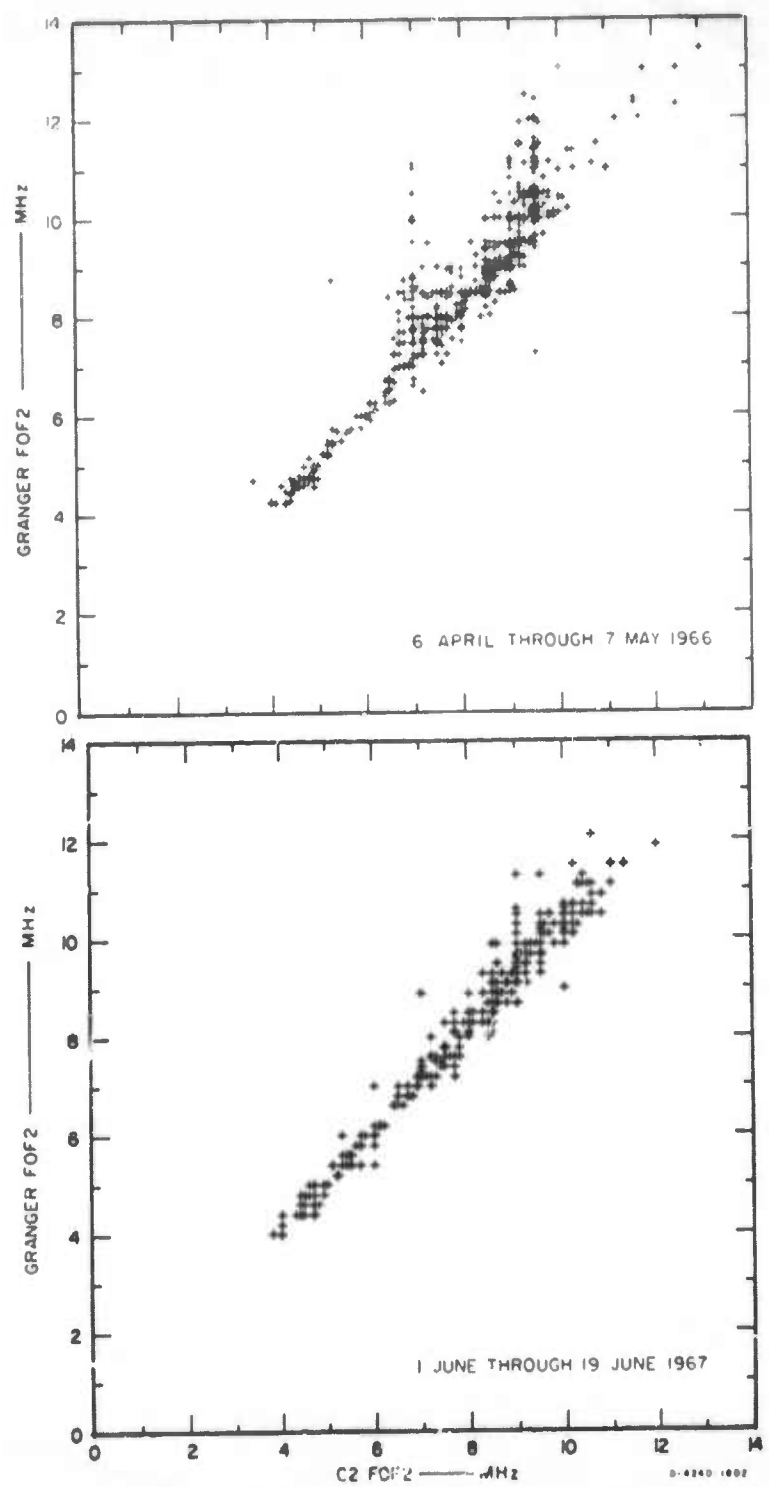


FIGURE IV-3 C-2 VERSUS GRANGER foF2 READINGS AT BANGKOK, THAILAND

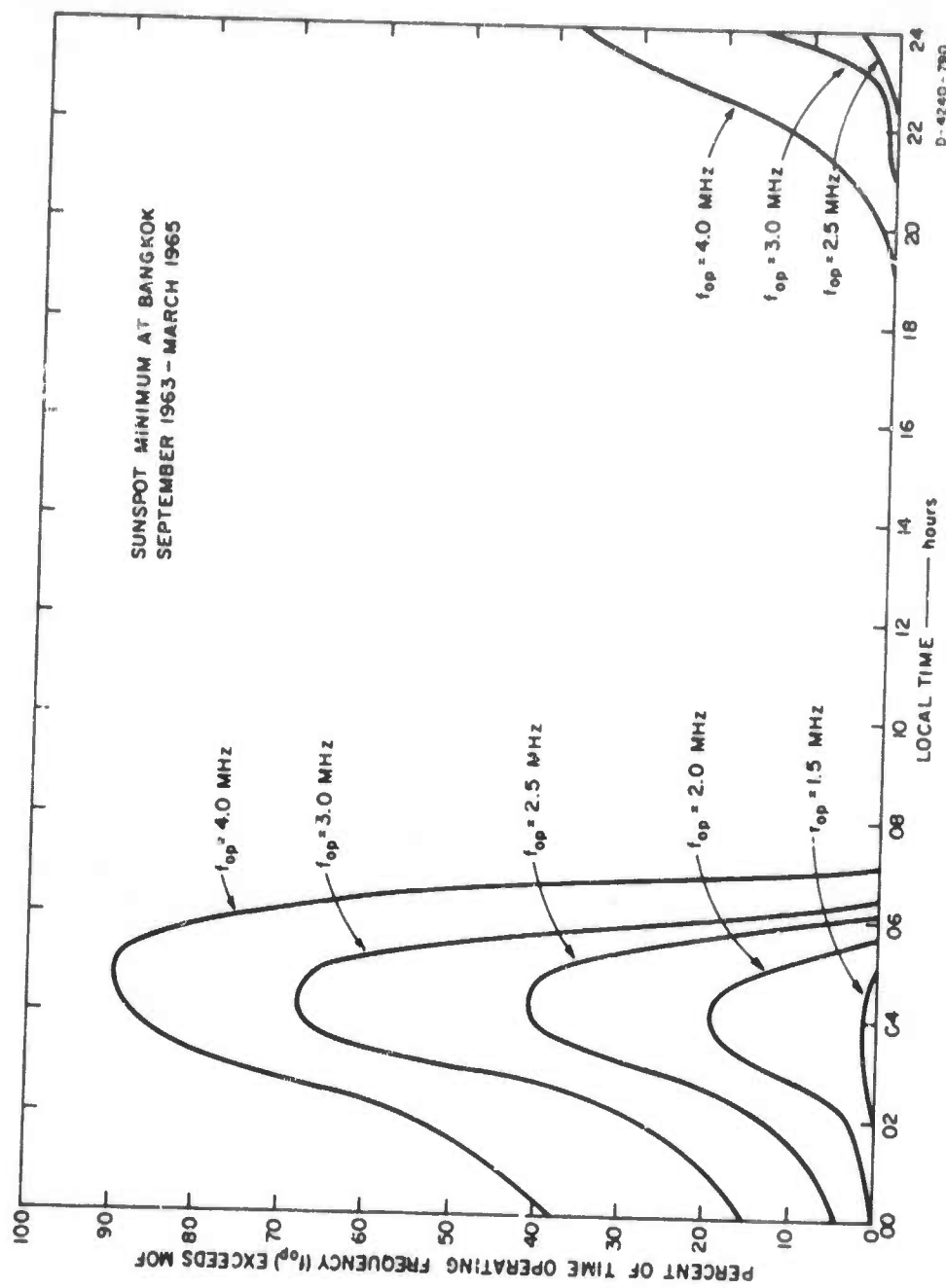


FIGURE IV-4 PERCENT OF TIME THE OPERATING FREQUENCY EXCEEDS MOF ON A PATH OF LENGTH LESS THAN 50 km

during sunspot minimum; and when the whole 11-year solar cycle is considered this lower design limit seems most adequate. It should be noted in passing that frequency management difficulties (i.e., obtaining frequency assignments) may preclude the use of the channels just above 2 MHz.

2. Ionospheric Sounding Tests in Thailand over Oblique Paths from 230 to 1320 km (SARs 7, 8, STR 48D)

a. Objectives

Two Granger Associates Model 911 oblique-incidence sounders with a capability of sounding from 4 to 64 MHz were used at vertical and oblique incidence at six sites throughout Thailand (see Figure IV-5) to obtain data pertinent to frequency prediction on short and intermediate length paths (SARs 5-8). The major objectives of the ionospheric sounding part of this study were to measure the following for at least one month on each path as a function of time of day:

- (1) The vertical-incidence critical frequencies (f_{oF2}) at sites remote from and at Bangkok, and the maximum observed frequency (MOF) on oblique-incidence paths in order that a MOF factor (ratio of MOF to f_{oF2}) for the F2 layer based on data from the C-2 sounder at Bangkok could be determined;
- (2) The lowest observed frequency (LOF) on these same paths;
- (3) The maximum multipath spread observed with the sounder system (see Section IV-B-1 for these results);

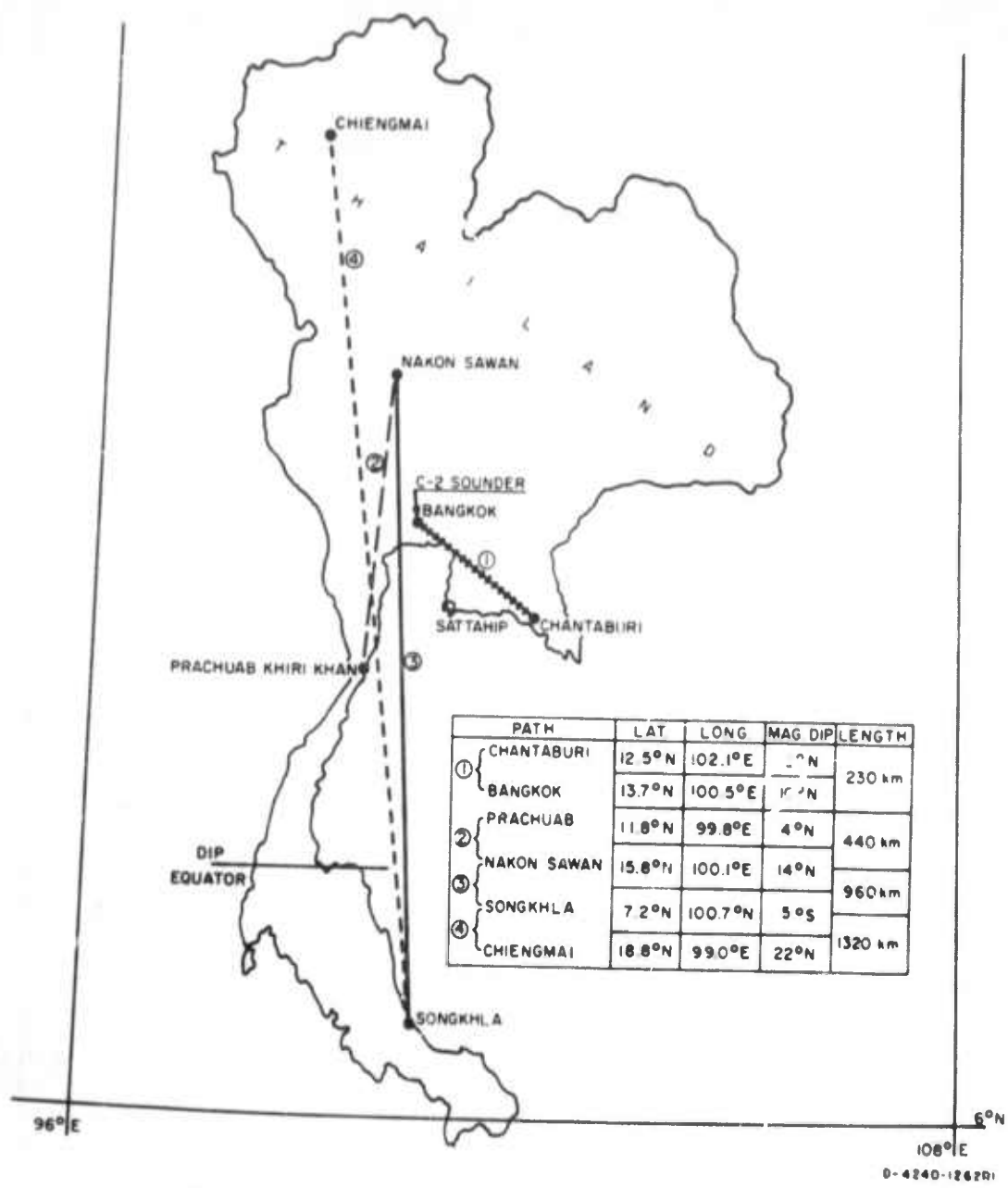


FIGURE IV-5 MAP OF SOUNDER SITES IN THAILAND

(4) The occurrence of anomalous layers such as spread F and sporadic E (these results are discussed in Section IV-C).

b. Sounder Site Operating Schedule and Procedure

A chronological description of field site activity is given in Table IV-1. The sounders and auxiliary equipment were in relatively continuous operation during this eleven-month period, although some interruption of the oblique soundings and communication tests was inevitable during times when changes in site were being made. The oblique-incidence sounders were operated on a 30-minute schedule, whereas the C-2 was operated on a 15-minute schedule.

Table IV-1
SOUNDER SITE OPERATING SCHEDULE

Site	1966											1967	
	Month												
	Apr	May	June	July	Aug	Sept	Oct	Nov	Dec	Jan	Feb		
Bangkok	*	1											
Chantaburi	1	1											
Prachuab			2	2	2								
Nakon Sawan			2	2	2	3	3						
Songkhla						3	3	4	4	4	4		
Chiengmai								4	4	4	4		

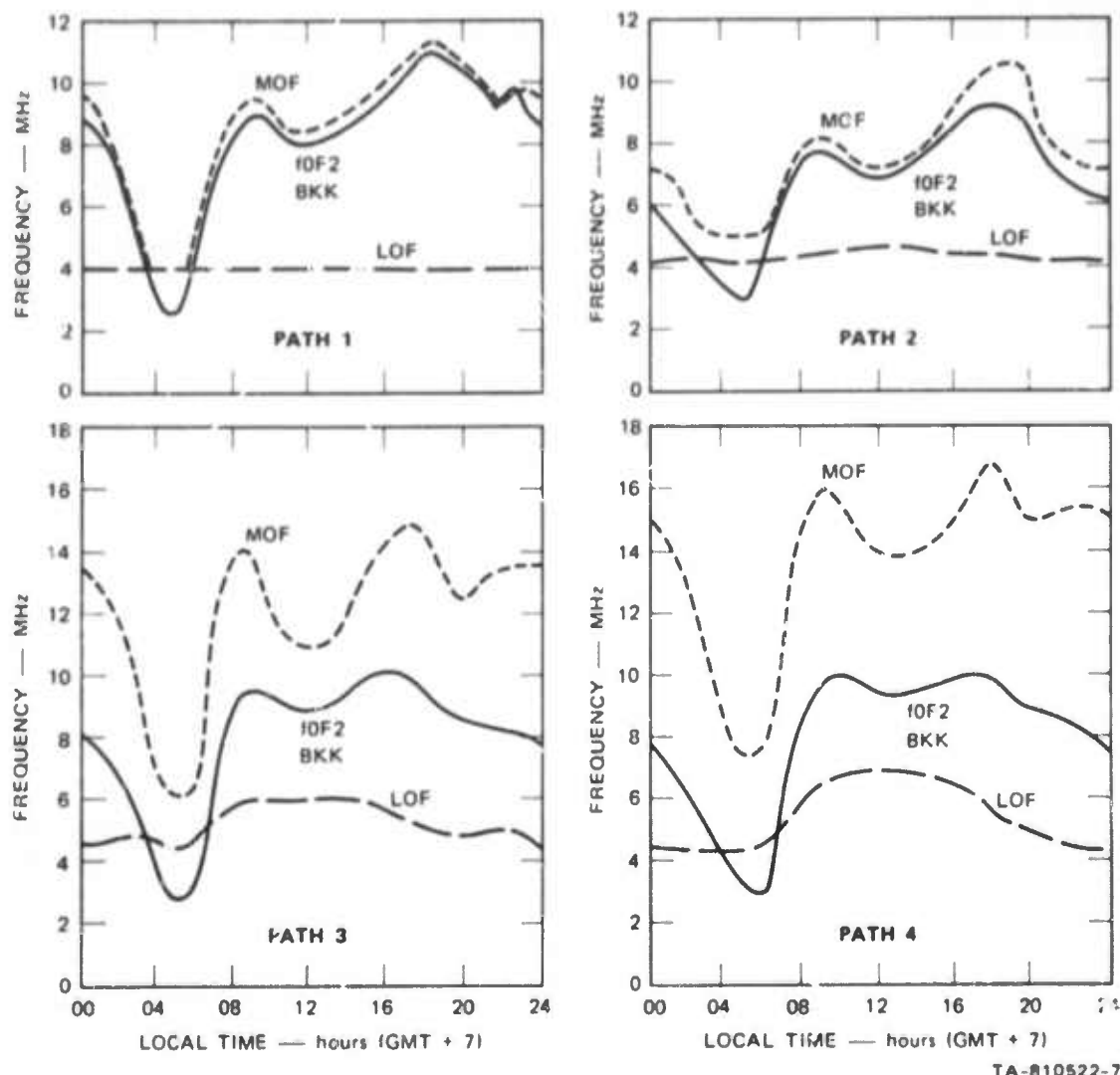
* Numbers refer to paths shown in Figure IV-5.

c. Results

Figure IV-6 presents the time-block median MOFs and LOFs for the paths of Table IV-1 as a function of local time.* Only the north-to-south paths were scaled, since the south-to-north data proved to be essentially identical. Also included for comparison are the median values of foF2 for the observation period (see Table IV-1) at Bangkok.[†] Let us define a MOF factor (for use in Thailand only) that is the ratio of the F-layer MOF to the value of foF2 from the Bangkok C-2. This MOF factor (see Figure IV-7) was calculated as a function of local time using monthly median values to illustrate the relative usefulness of Bangkok C-2 data to estimate the MOF on longer paths. These data indicate that foF2 at Bangkok is an excellent estimator of MOF on the 440-km north-south path (path 2) and a good estimator of the 320-km east-west path (path 1). On longer paths the MOF factor could be used (in the absence of ionospheric predictions) for the oblique path. The peak in MOF factor between 0400 and 0600 hours apparently results from a sharper decrease in foF2 (pre-dawn dip) than in MOF on the oblique path.

* The MOFs shown are the F-layer values and do not include the effects of sporadic E. Sporadic E was primarily a daytime phenomenon with sunrise and sunset MOFs of about 8 MHz on these paths and noon maxima of about 6, 12, 16, and 20 MHz on paths 1-4, respectively. The LOFs on paths 1 and 2 are limited by the lower frequency limit of the sounders (4 MHz).

† The detailed (hourly) vertical-incidence sounding results from both the Granger sounders and the C-2 are presented in data bulletins (see Appendix C). The detailed oblique sounding results are tabulated in an appendix of STR 48D, but this report was not printed for distribution.



TA-810522-7

FIGURE IV-6 RESULTS OF OBLIQUE-INCIDENCE IONOSPHERE IC SOUNDINGS

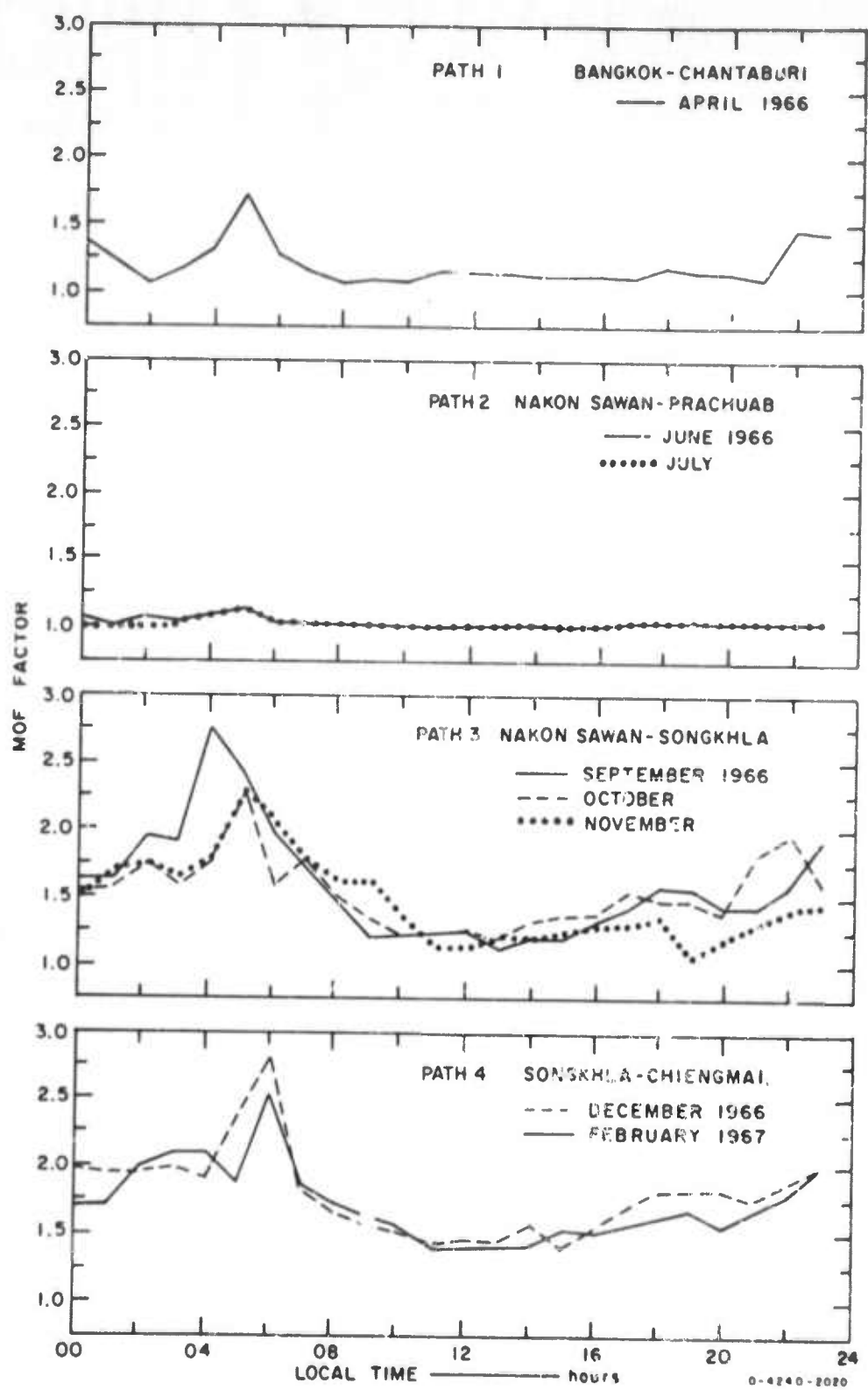


FIGURE IV-7 MOF FACTOR AS A FUNCTION OF LOCAL TIME

B. Ionospheric Signal Strength

1. HF Propagation and Communication Tests in Thailand over Oblique Paths from 440 km to 1320 km (SAR 8, STR 48D)

a. Objectives

Communication equipments (CW system and FSK teletype system) were operated on the same paths as the sounders (Section IV-A-2) in auxiliary experiments. The major objectives of the auxiliary experiments were to measure as a function of local time:

- (1) Signal strength and S/N ratio on north-south (N-S) and east-west (E-W) dipoles,
- (2) Envelope correlation of signal on N-S and E-W dipoles,
- (3) Time-delay spread (actually measured with the sounder but reported and discussed here),
- (4) Doppler spread, and
- (5) FSK system performance,

for paths 2 through 4 (see Figure IV-5) where the propagating ionospheric modes had been documented by the sounders.

b. Description of the CW Tests

CW transmissions (400 W) were made into half-wave length horizontal dipoles oriented at 45 degrees to the earth's magnetic field and located at the height above ground yielding a driving-point impedance of 50 ohms (roughly 25 ft). N-S and E-W dipoles adjusted to 50-ohm height were used for receiving, and the receiver bandwidth was 100 Hz. The receiving and recording system employed is shown in Figure IV-8. The SRI Correlation Computer²⁰ was used to generate a continuous record

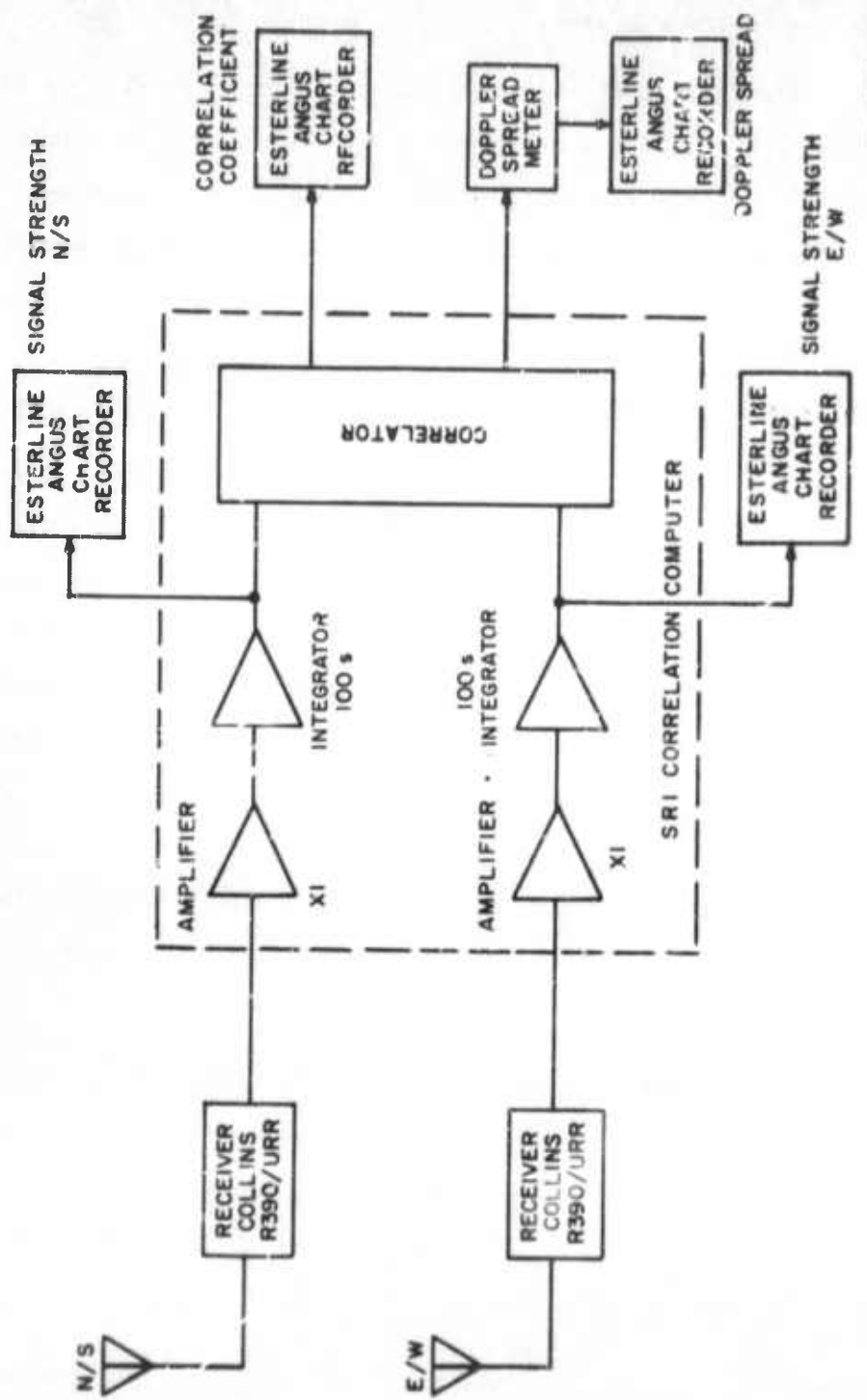


FIGURE IV-8 BLOCK DIAGRAM OF CW EXPERIMENT RECEIVING AND RECORDING SYSTEM

of the normalized cross-correlation of the input signals. The SRI Doppler Spread Meter²¹ was used to measure frequency dispersion of the CW signal (a distortion measure).

The CW transmitter operated continuously except for being turned off for 5 minutes twice an hour (at the time of the ionospheric sounding described in the previous section) in order to provide positive signal identification and an opportunity to observe the background noise level.

c. Results of the CW Tests

The received signal strength values on both N-S and E-W dipoles--as well as the envelope correlation--are presented in Figures IV-9 through IV-14 for path 2. Plots for the other paths are generally similar. The E-W dipole generally produced the greater signal strength by about 5 dB. Decile bounds on the received signal strength are shown. Note the pre-dawn decrease in signal level and increase in decile bounds when the operating frequency is above the MOF. The propagation is via a scatter mode during this period. The correlation coefficient was essentially zero (signals uncorrelated)^{*} except during midday or other times when sporadic E was significant in supporting the propagation mode.

The signal-plus-noise-to-noise ratio [(S + N)/N, see Figure IV-15] was computed by subtracting the observed noise level (in dB) from the observed signal (plus noise) level. It was not possible

* The SRI Correlation Computer is inherently not very accurate for uncorrelated signals, and correlations between ± 0.2 (see dashed lines in Figures IV-10, 12, and 14) can be assumed to be essentially zero.

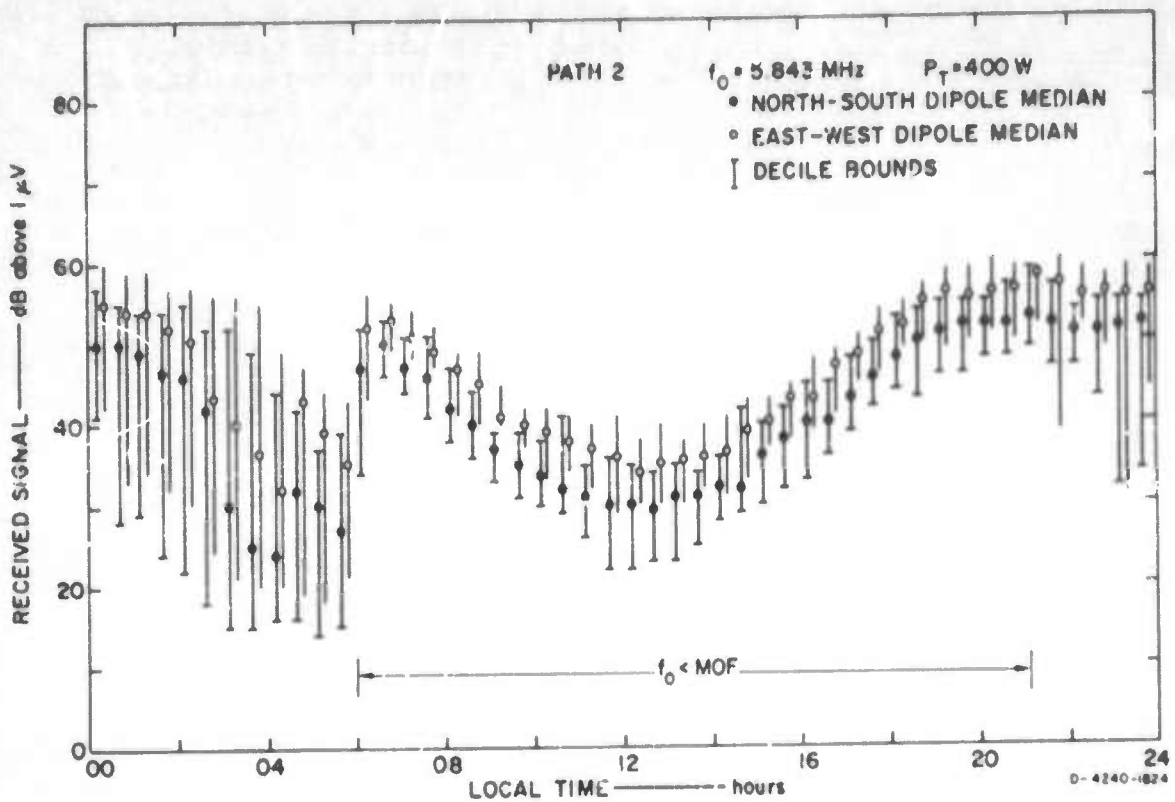


FIGURE IV-9 CW RECEIVED SIGNAL STRENGTH AT PRACHUAB

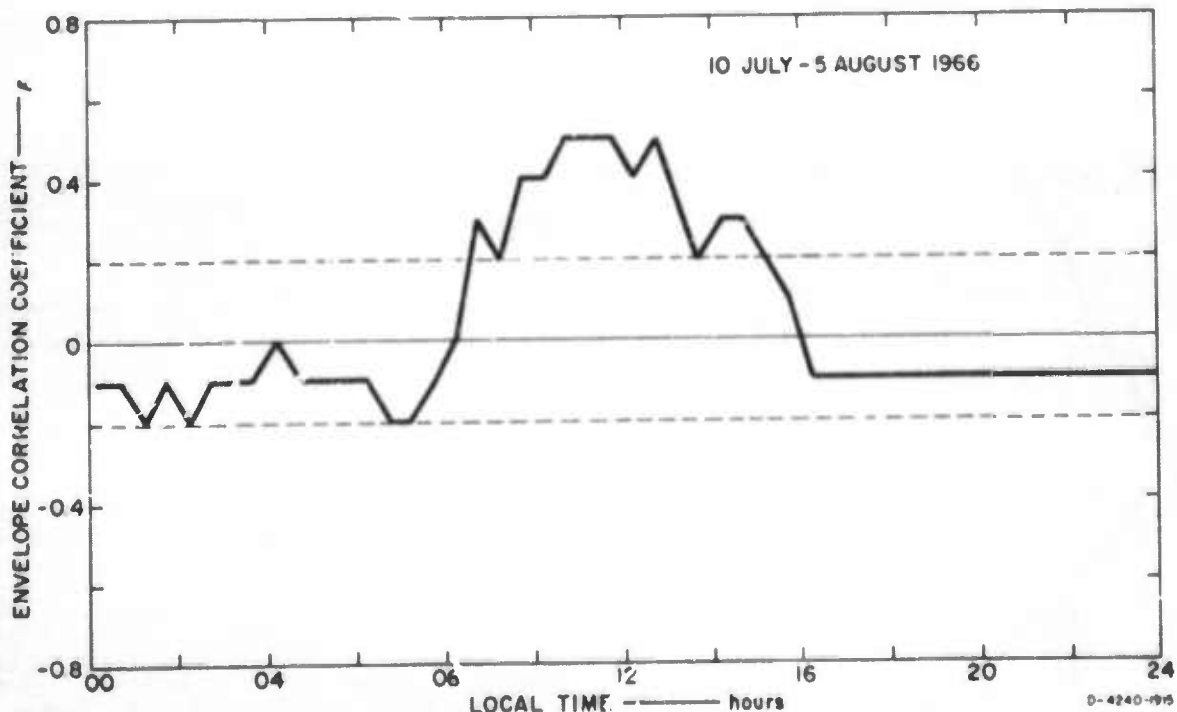


FIGURE IV-10 ENVELOPE CORRELATION COEFFICIENT OF SIGNALS RECEIVED AT PRACHUAB

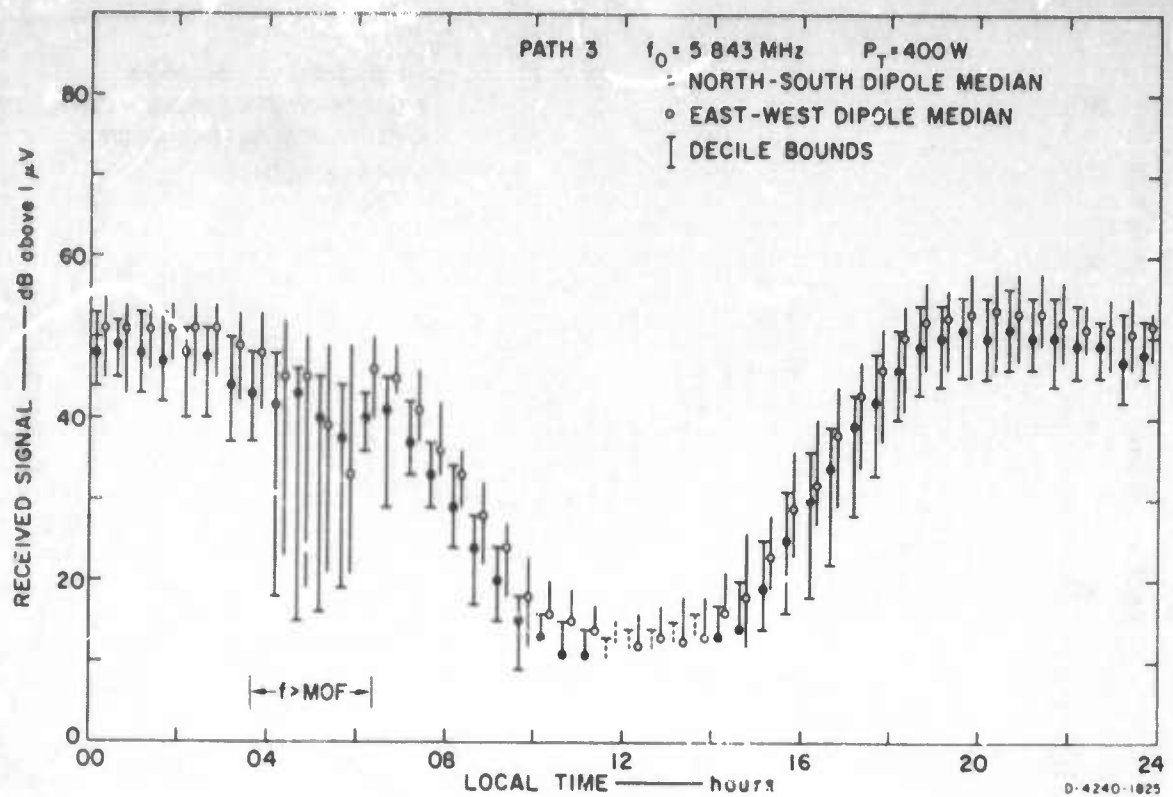


FIGURE IV-11 CW RECEIVED SIGNAL STRENGTH AT NAKON SAWAN

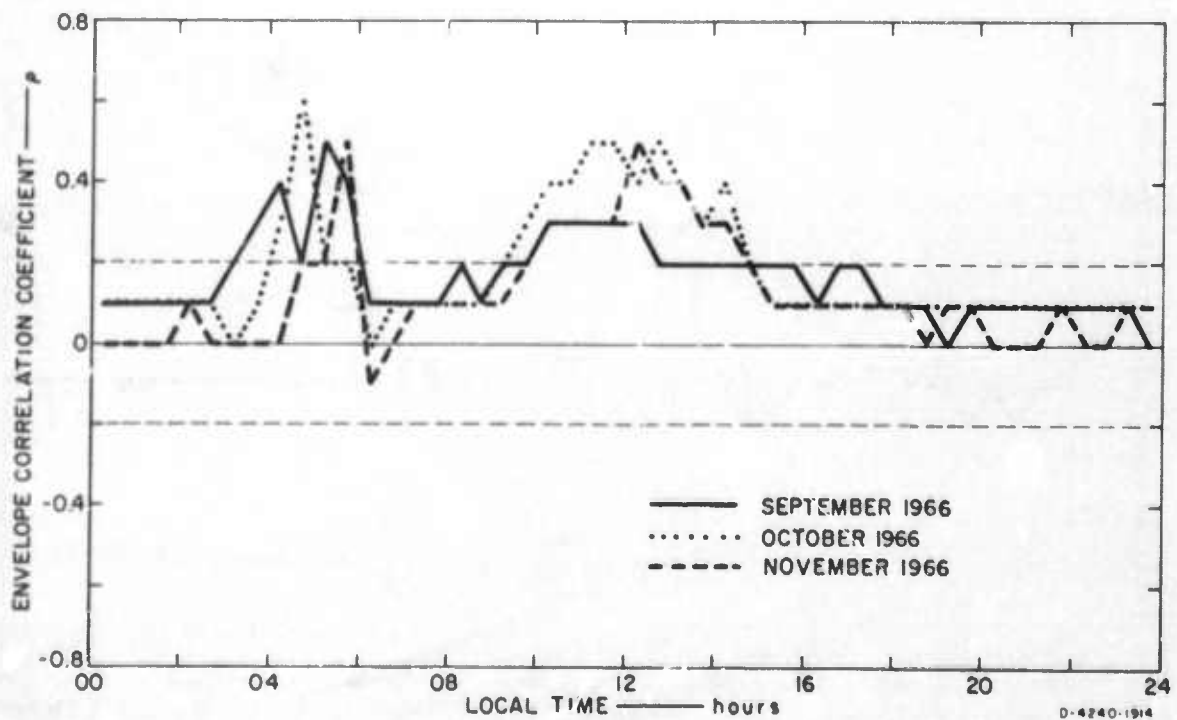


FIGURE IV-12 ENVELOPE CORRELATION COEFFICIENT OF SIGNALS RECEIVED AT NAKON SAWAN

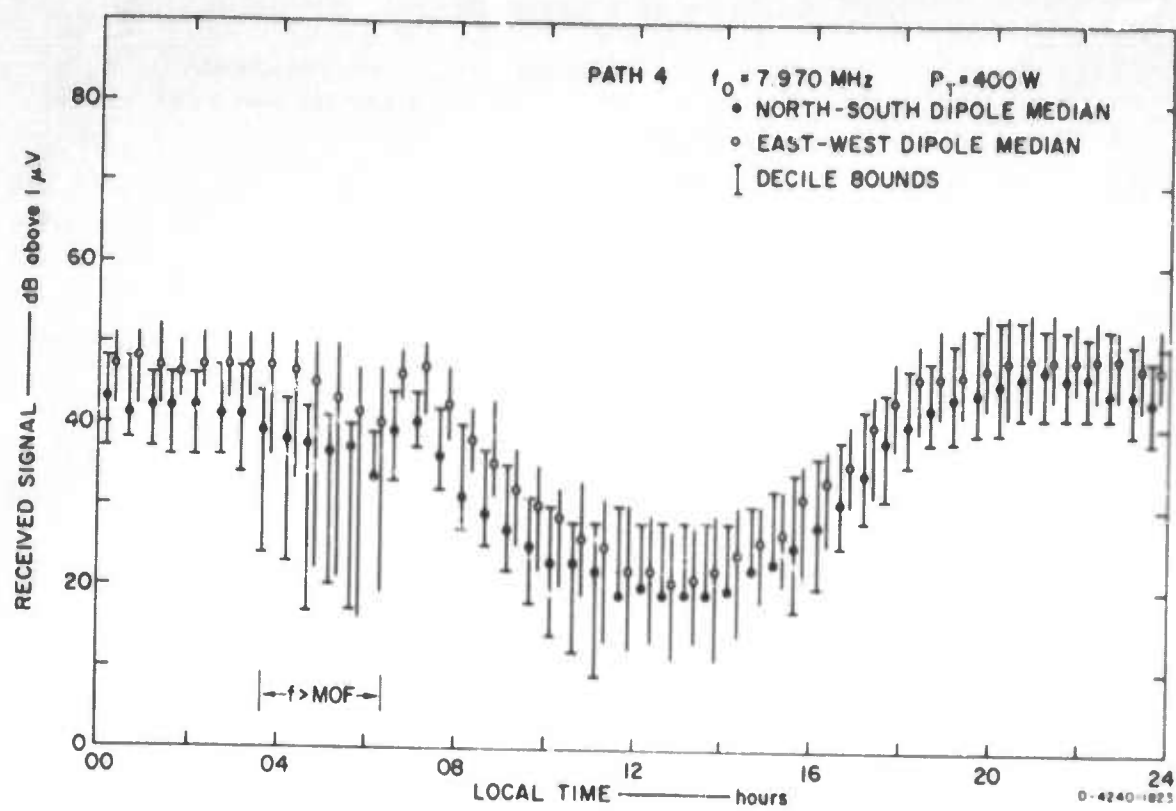


FIGURE IV-13 CW RECEIVED SIGNAL STRENGTH AT CHIENGMAI

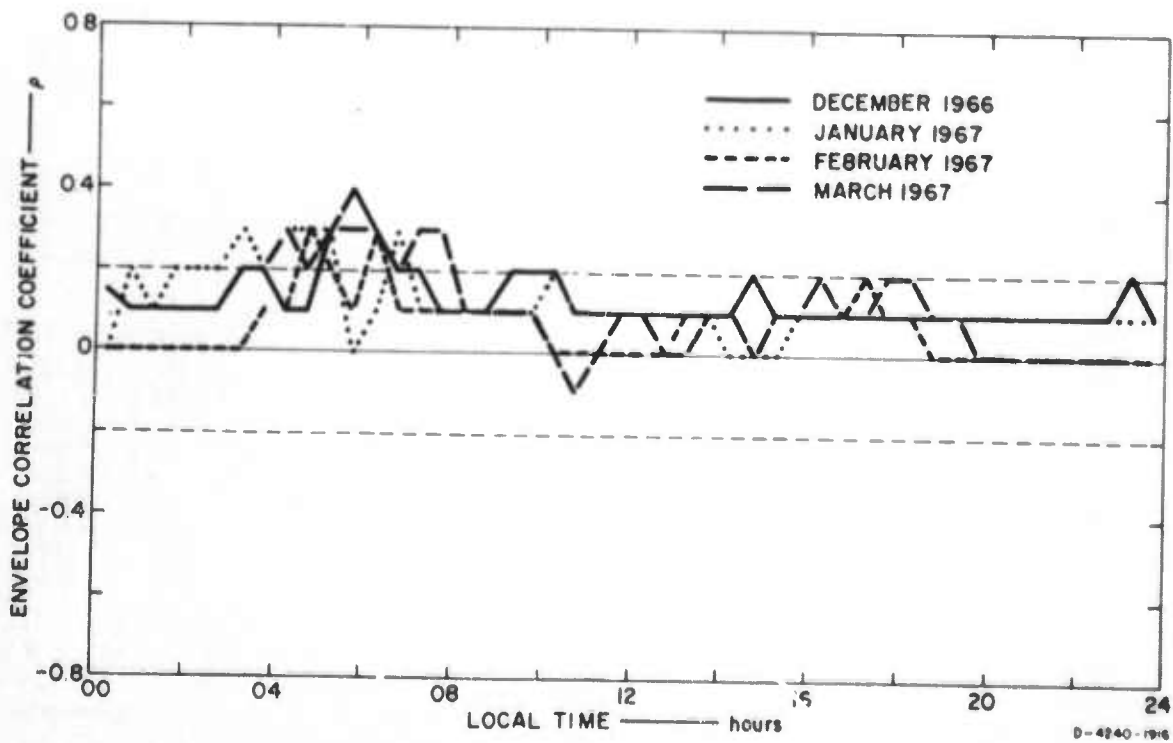


FIGURE IV-14 ENVELOPE CORRELATION COEFFICIENT OF SIGNALS RECEIVED AT CHIENGMAI

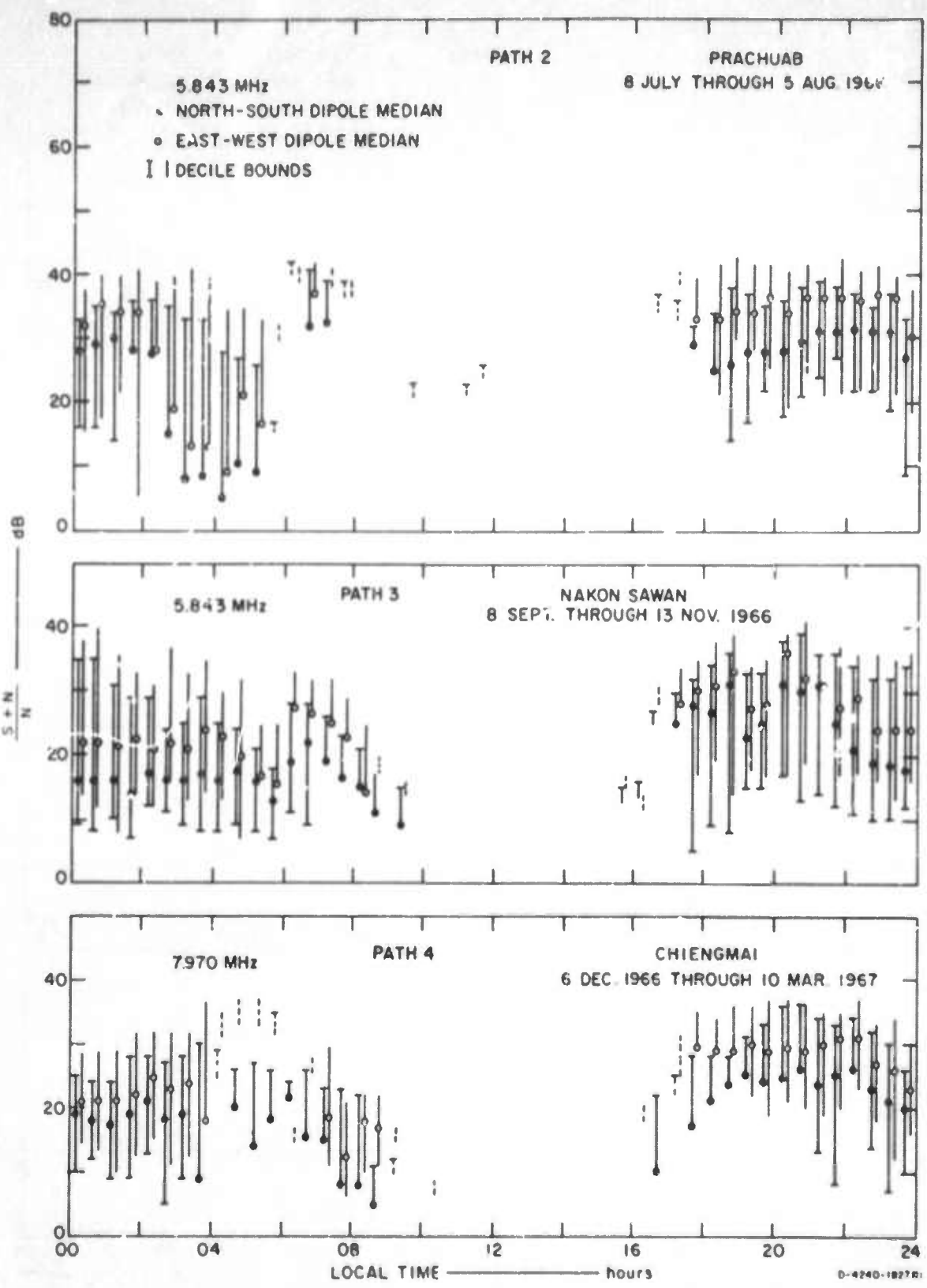


FIGURE IV-15 S/N RATIO ON PATHS 2, 3, AND 4 AS A FUNCTION OF LOCAL TIME

to compute $(S + N)/N$ during much of the day because the noise values were not available (see Section VII of STR 47). The $(S + N)/N$ values were about 5 dB higher for the E-W dipoles, but the noise picked up by the N-S and E-W dipoles was essentially the same. This same conclusion regarding the lack of sensitivity of dipoles' noise to dipole orientation in the tropics was reached when the noise on horizontal dipoles was studied independently at another site in Thailand (STR 47).

Time-delay spread was estimated by measuring the spread of the echoes observed from the oblique sounding records. These results are presented in Figure IV-16. Frequency-spread values observed over these paths with the SRI Doppler Spread Meter are given in Figure IV-17.

d. RTTY Tests

An AN/MRC-95 teletype unit was operated over path 2. Figure IV-18 gives the observed character error rate as a function of local time. The number of errors is high at night due to low signal-to-noise (plus interference) ratio. The effect of the decreased daytime $(S + N)/N$ around noon also can be observed. The data sample is very small, however. A similar test during daytime (0700 to 0900 and 1500 to 1900 hours) on path 3 during October 1966 indicated that the probability of character error often was between 3×10^{-1} --and typically about 10^{-1} . On path 4 the probability of character errors typically was 10^{-2} to 10^{-1} between 0500 and 0800 and between 1500 and 1700.

In general, the $(S + N)/N$ (and interference--especially at night) seemed the controlling factor in performance of the AN/MRC-95 on the paths tested. The effect of Doppler spread was not significant, but time-delay spreads in excess of 2 ms seemed to be the controlling factor for $(S + N)/N$ greater than about +15 dB. Reduction of the frequency shift of the AN/MRC-95 from 850 Hz to a value about one-tenth as

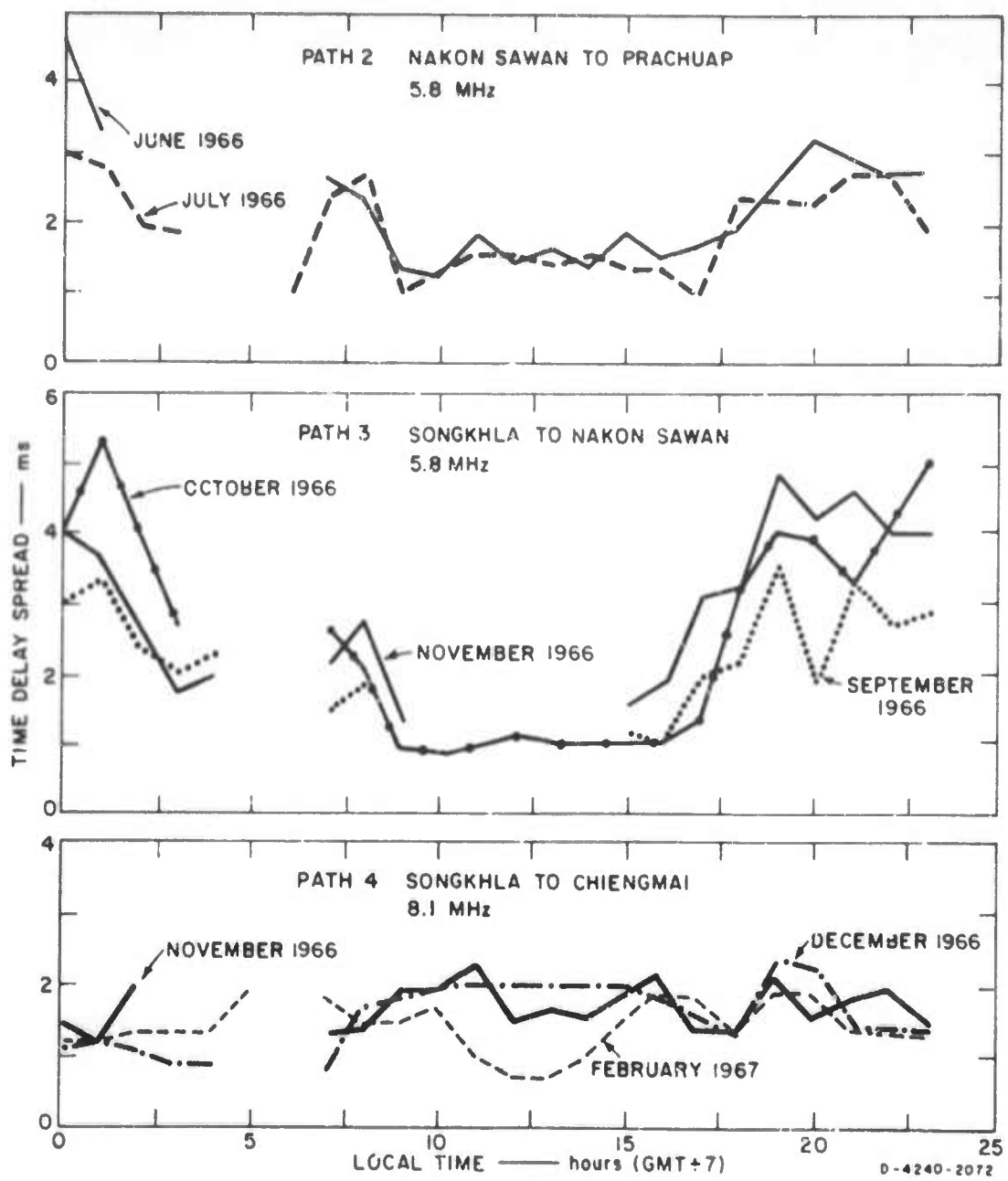


FIGURE IV-16 TIME DELAY SPREAD ON PATHS 2, 3, AND 4 AS A FUNCTION OF LOCAL TIME

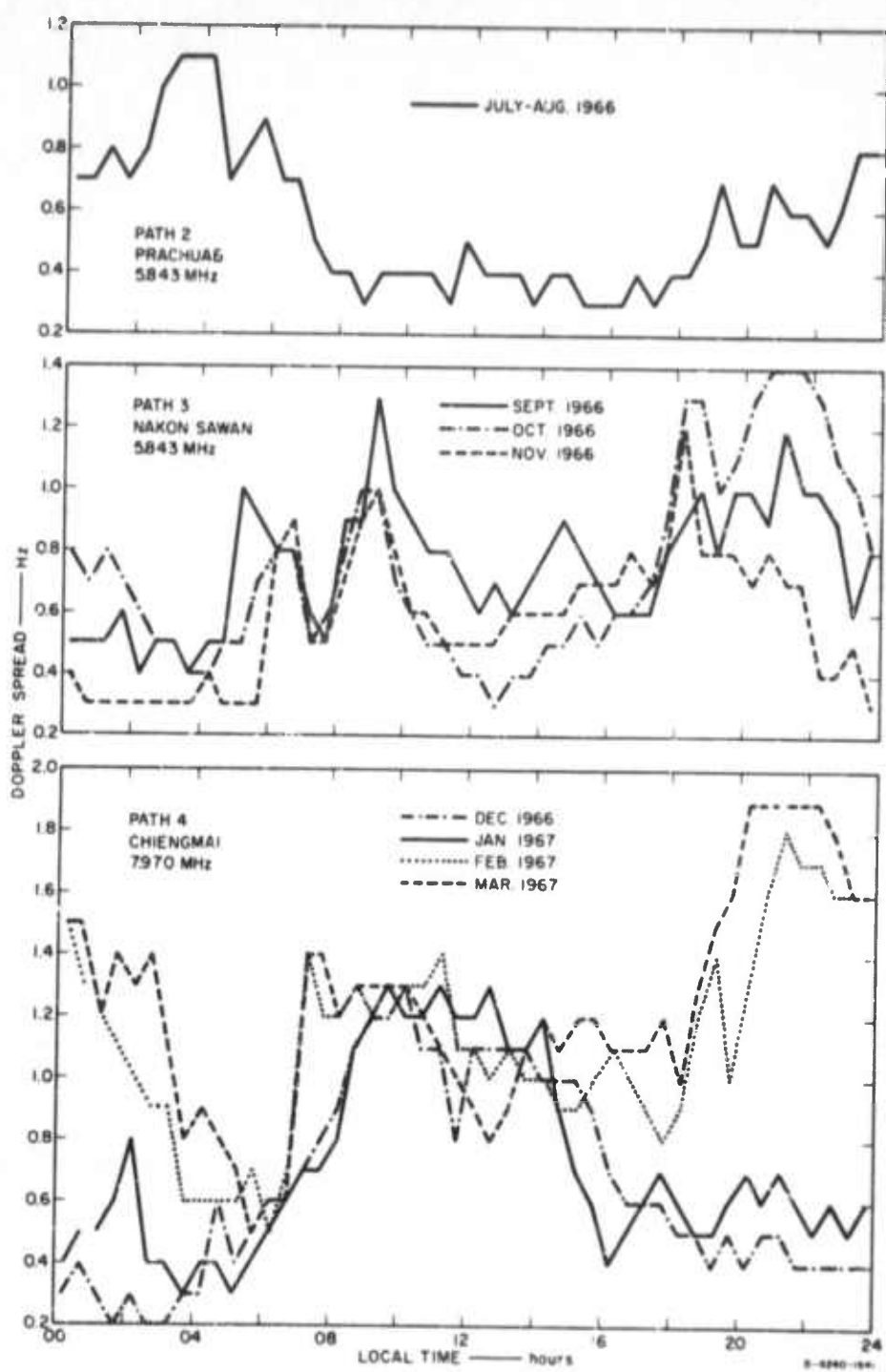


FIGURE IV-17 DOPPLER SPREAD ON PATHS 2, 3, AND 4 AS A FUNCTION OF LOCAL TIME

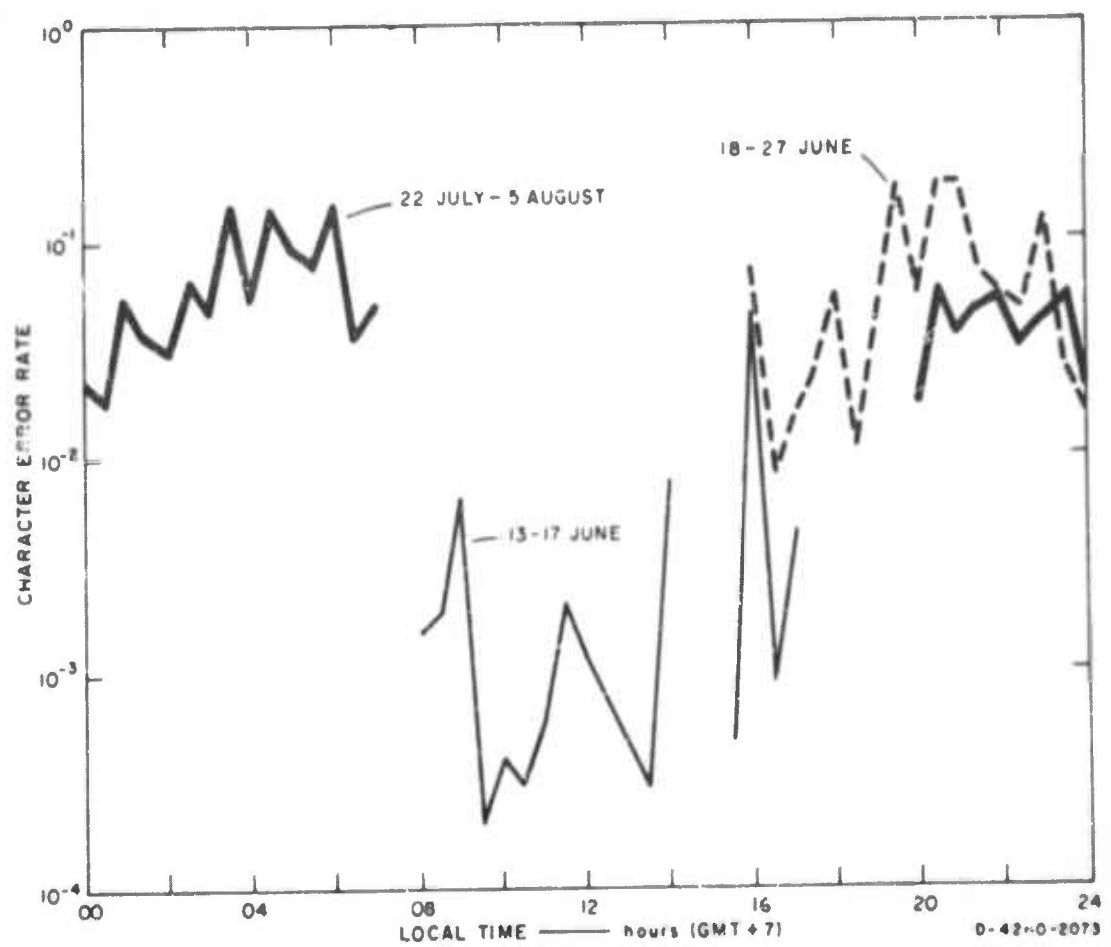


FIGURE IV-18 CHARACTER ERROR RATE ON PATH 2 AS A FUNCTION OF LOCAL TIME

large should provide an improvement in performance over short skywave paths. The envelope correlation data suggest that a further improvement might be obtained by providing for a dual diversity capability and using N-S and E-W dipoles in the orientation-diversity mode. The AN/MRC-95 system performance should be modeled for binary error rate, * however, and the model validated by lab simulation and field test before firm recommendations for changes in the system can be made.

2. Dipole Orientation Effects (RM5, RM5R, STR 9, STR 31)

a. Objective

The objective of the dipole orientation study was to determine the effect of antenna alignment upon received signal level on short-range skywave paths.

b. Background

When dipoles are used for point-to-point HF communications and when the bearing of the other station is known, it is common practice to align dipoles at right angles to the direction of intended propagation (i.e., broadside alignment for main-beam-to-main-beam coupling). When such an antenna (dipole) orientation is used on long ionospheric skywave paths, the result is to maximize the received signal (see Section IV-B-1); but, generally speaking, dipole orientation is relatively unimportant on short skywave paths of less than about 100 km. This is because the

* There is no simple relationship between binary errors (which are easily computed) and character errors (which are easily measured) for the AN/MRC-95. Hence, it would be desirable to measure binary errors in a future field test, even though this would require special instrumentation, if model validation is attempted.

signal path is almost straight up to the ionosphere and back down and the dipole is essentially an omnidirectional antenna for directions near the zenith when placed at heights of $\lambda/4$ or less. An exception to this general rule for short paths exists at low geomagnetic latitudes, where a preferred orientation exists because of the nature of the ionospheric reflection. The magnetoionic theory predicts²² that a N-S alignment should be used for linear antennas (e.g., dipoles) on both ends of a short skywave link regardless of the bearing angle between the stations when operating sufficiently near the geomagnetic dip equator (RM 5, RM 5R, STR 9, STR 31). The path geometries for which N-S alignment is better than other possible alignments may be determined from the magnetoionic theory with reasonable accuracy (see RM 5R and STR 31), but the exact amount of superiority of the N-S alignment is difficult to compute because of lack of accurate, detailed knowledge of the collision and plasma frequency height profiles--especially for the region below about 90 km. Consequently, a field measurement program was conducted in Thailand to check the existence and magnitude of the "dipole orientation effect."

c. Results of Theoretical and Experimental Investigations of Dipole Orientation Effects in Thailand

1) Theoretical Considerations

The details of the theory are given in RM 5, RM 5R, STR 9, and are repeated in STR 31. The discussion here will center on the results of the theoretical study.

The geometry of the ray path (actually the wave normal) relative to the earth's magnetic field at the point of entry into the lower part of the ionosphere is of primary importance in determining whether it is advantageous to align dipoles N-S for use on short

skywave path. If the angle between the wave normal and the earth's static magnetic field, θ , is a right angle (transverse propagation), then one can usually obtain larger received signals using N-S dipoles. But this special geometry exists only on a few paths, so the logical question arises: "How far from the purely transverse geometry, $\theta = 90^\circ$, at entry into the ionosphere can the path get before the advantages of dipole orientation are lost?" If the path is nearly transverse, the same propagation equations apply as for the transverse case, and the condition is said to be "quasi-transverse"--(i.e., QT).²² The angle for which the QT condition applies is a function of many variables, but for a given geographical location the main variation is with radio frequency. Figure IV-19 shows how far off the purely transverse condition the path can be in Thailand and still satisfy the QT criterion. There is still some benefit of N-S alignment until the "quasi-longitudinal" (QL) condition is reached--at which point there is no preferred orientation for dipoles on short paths. Figure IV-19 also shows θ_L as a function of frequency. The process of determining θ_T and θ_L for a given path is rather involved and will not be dealt with here. An example is given in Appendix B of RM SR, however.

2) Measurement Results

Data were obtained during December 1963 and January 1964 between Bangkok and two remote receiving sites: Ayudhaya (about 66 km to the north) and Nakorn Pathom (about 66 km to the west). CW transmissions of 400 W were made from Bangkok on 1.7, 3, 5, and 10 MHz and received at the remote sites. At each site two dipoles (N-S and E-W) were employed at $\lambda/6$ above ground for each test frequency and all four combinations of transmitting and receiving antennas were used. The results of these tests are summarized in STR 31 and Figures IV-20 and IV-21 show an example of the results.

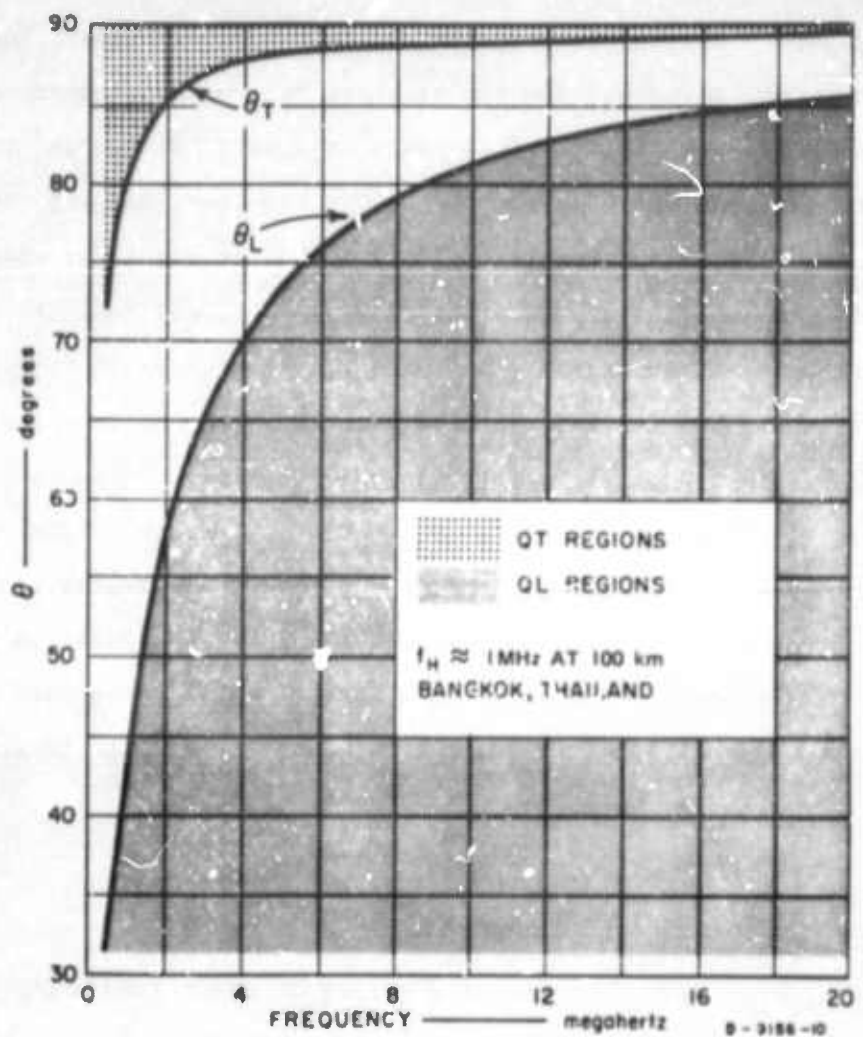


FIGURE IV-19 CL AND QT REGIONS

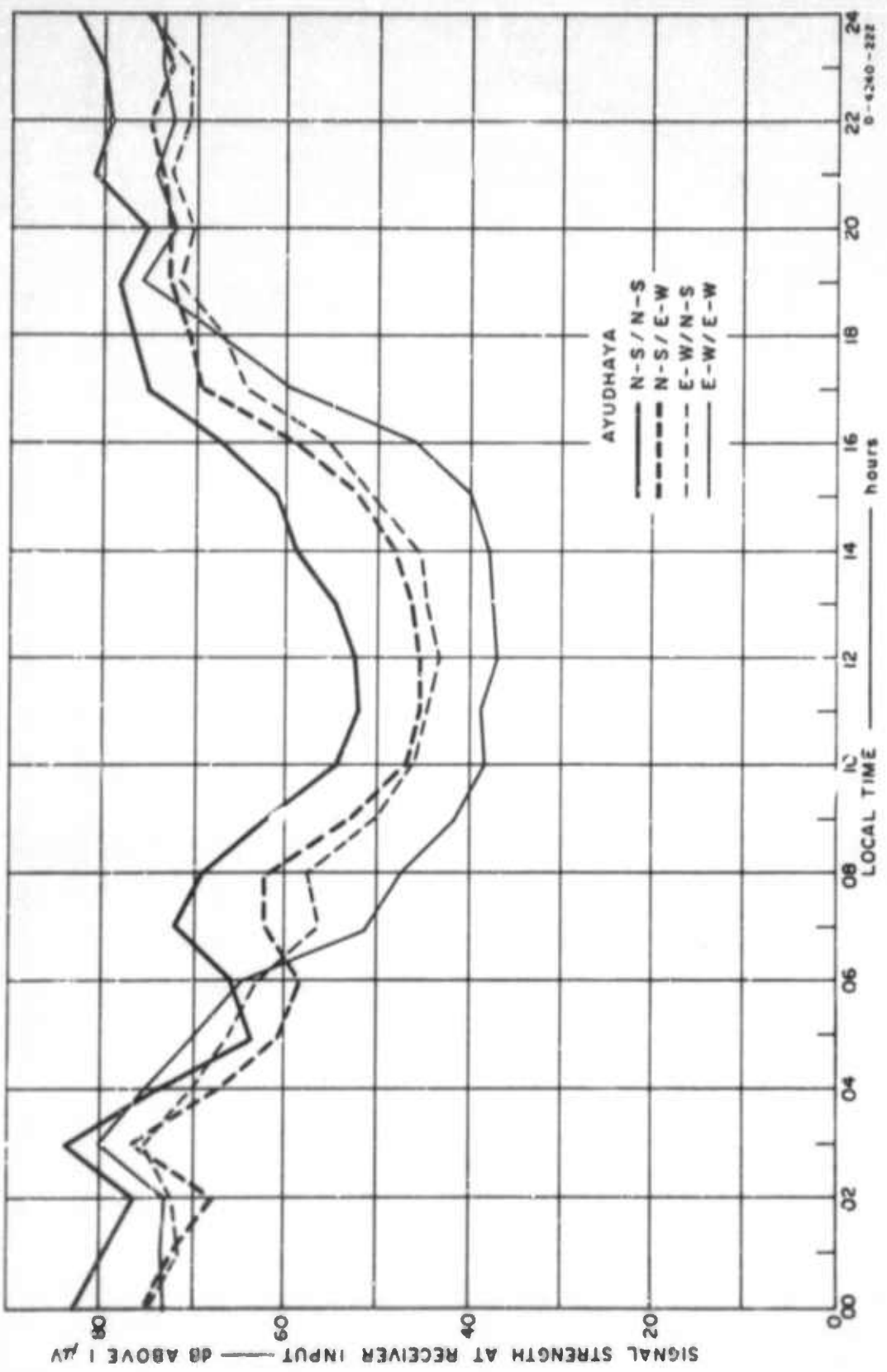


FIGURE IV-20 AYUDHAYA: 1.7 MHz CW, ALL TRANSMITTING/RECEIVING ANTENNA COMBINATIONS

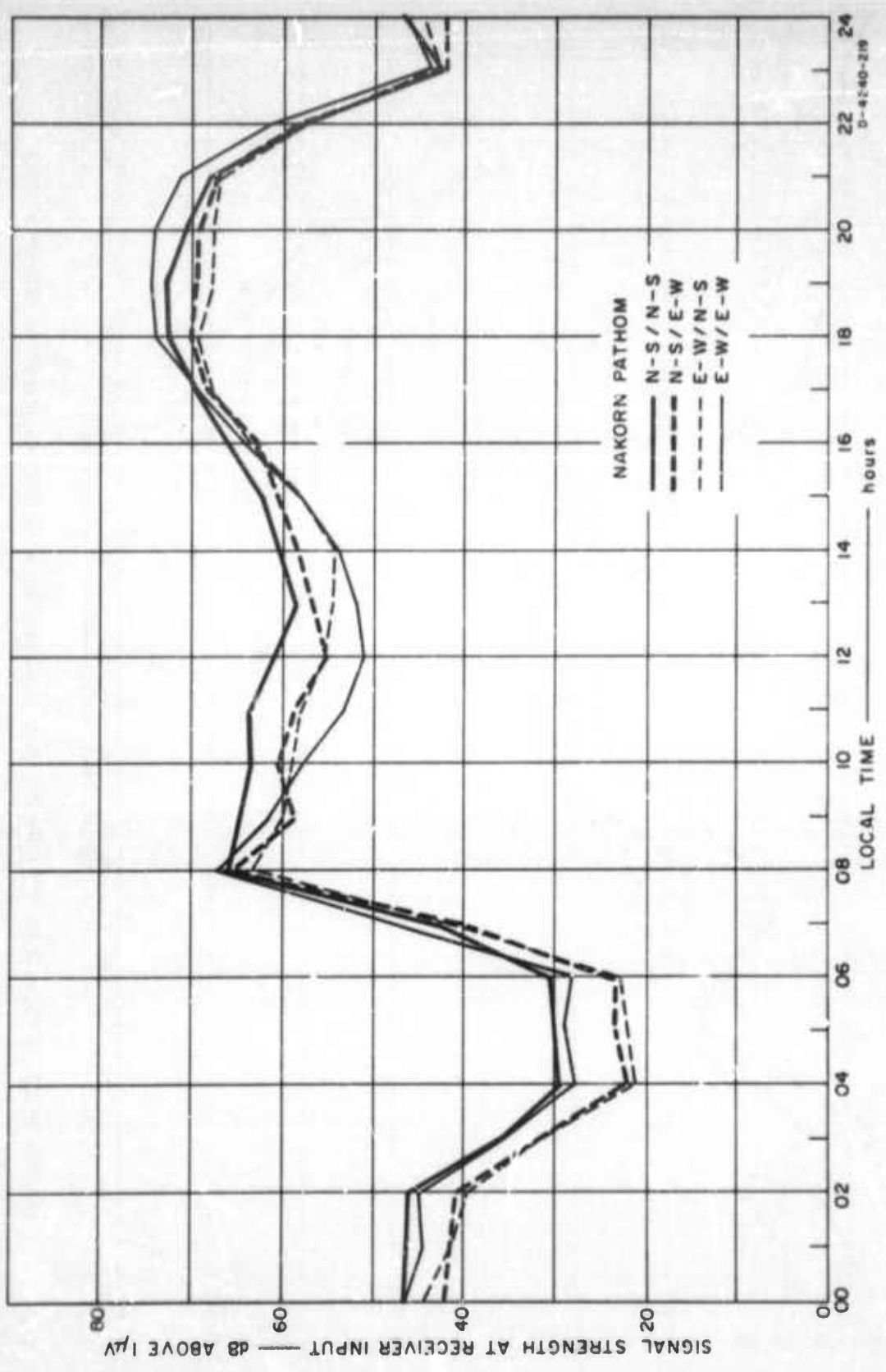


FIGURE IV-21 NAKORN PATHOM: 5 MHz CW, ALL TRANSMITTING/RECEIVING ANTENNA COMBINATIONS

It was shown that the N-S/N-S antenna combination produced the greatest received signals on both paths most of the time, as predicted. Hence, the predicted dipole orientation effect is seen to exist. But the mean received signals on the other antenna combinations are not too far down from those for the N-S pairs, and this suggests the possibility of a diversity receiving system employing a pair of dipoles (one N-S and the other E-W) located very close together so as to achieve magnetoionic-component diversity.

A test of this diversity idea was made on the Bangkok-Ayudhaya path during March 1965. The 3.95-MHz transmitting dipole at Ayudhaya was oriented NE-SW so as to generate both magnetoionic components.* The signal received at Bangkok on N-S and E-W dipoles was recorded--as well as the output of an SRI-made post-detection diversity combiner and the SRI Correlator. An example of the results of this test is shown in Figure IV-22. Notice that the envelope correlation varies rapidly about zero, and that the combiner greatly reduces the fading.

Similar tests were made on longer paths (up to 1320 km) as part of another test series (see Section IV-B-1), and the envelope correlation usually had a zero average even though the QT approximation was not valid. When sporadic E was present the mean correlation rose as high as 0.5, but even with this degree of correlation, diversity reception should provide significant improvements over a single channel.

* Note that at a field installation employing this type of diversity it might be more convenient to drive a N-S and an E-W dipole in phase while transmitting rather than to put up a third dipole for transmitting--especially if a T/R switch can be used to separate the dipole feeds on receive.

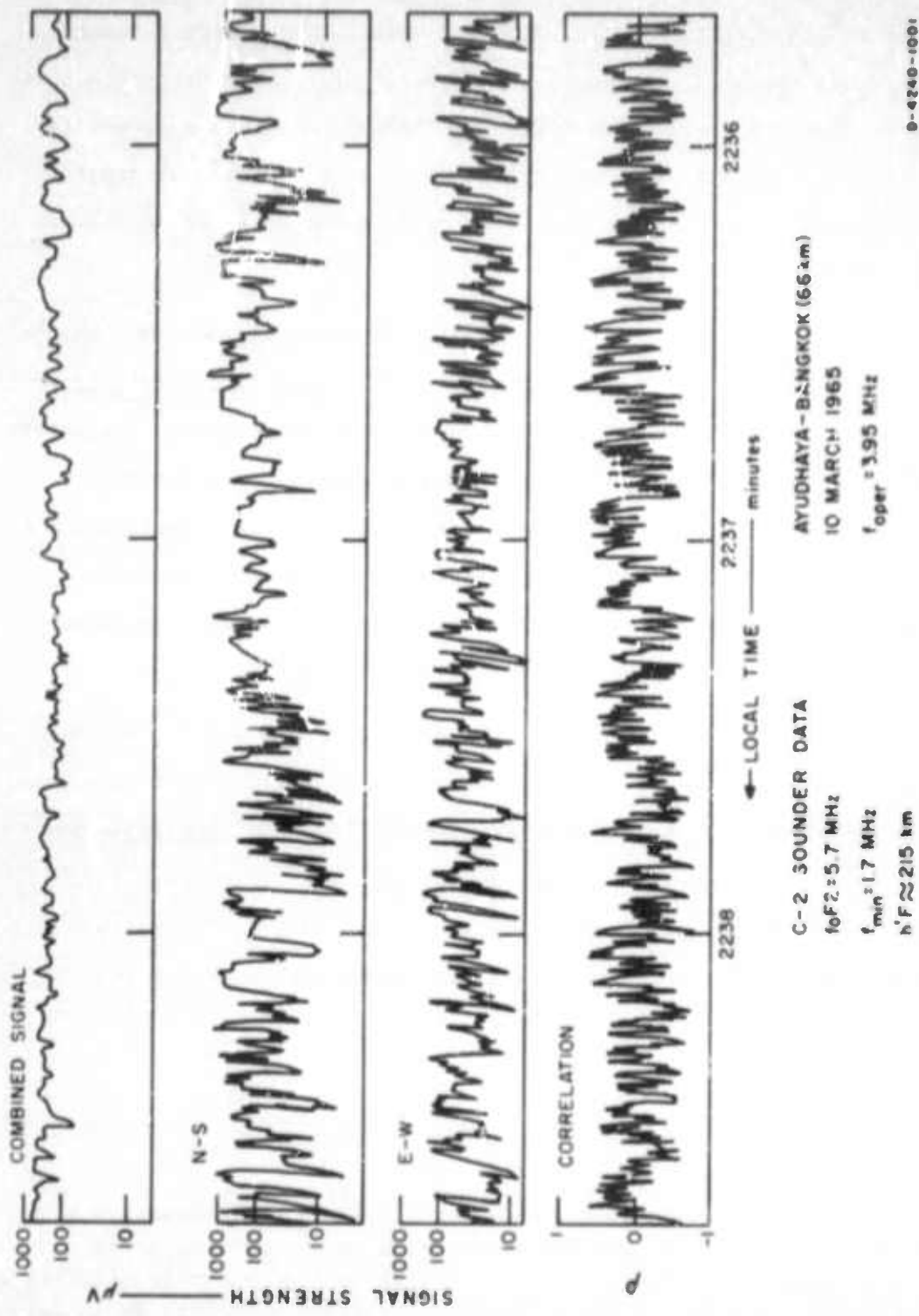


FIGURE IV-22 EXAMPLE OF RESULTS OF POLARIZATION DIVERSITY TEST—AYUDHAYA TO BANGKOK

3) Conclusions

The predicted orientation effect exists, but its magnitude cannot be accurately computed without better electron content and collision frequency profiles below 90 km than currently are available. For operation in the field on short ionospheric skywave paths near the magnetic equator, it may be advantageous to align the linearly polarized antenna (e.g., dipole) north-south, but it probably will be more important to have a center fed horizontal dipole trimmed to the half-wave resonant length and elevated at least $\lambda/10$. The availability of antenna supports to elevate the antenna probably will be more important than the alignment. At base stations, however, it probably will be advantageous to put up both N-S and E-W dipoles. The better antenna for a given path can then be selected on observed performance, and the option of orientation diversity is available.

C. Special Ionospheric Studies

1. Faraday Rotation Studies (STRs 14, 33, 34)

a. Objectives

The Faraday rotation studies were primarily of a scientific nature. The objectives of this work were:

- (1) To document total ionospheric electron content as a function of local time, season, and solar ionizing flux;
- (2) To study the equatorial anomaly;
- (3) To study the use of satellite Faraday rotation data to estimate vertical-incidence critical frequency;

- (4) To study the use of Faraday rotation records to measure the dip angle of the earth's magnetic field.

b. Background

Transmissions from three satellites, Transit IV-A, San Marco 84-A, and S-66, were recorded at Bangkok in order to study the total electron content between the satellite and the recording station as deduced from the Faraday rotations. The main data analysis efforts were devoted to Transit IV-A (STR 14) and S-66 (STR 34). The rotation-rate method of analysis was used to determine total content at about 14.2°N latitude near Bangkok, and the total-rotations method was used to determine content as a function of distance away from about 14.2°N latitude along the essentially N-S track of the satellite. The analysis of total content as a function of latitude was extended by the use of data from satellite receiving stations to the north and south of Bangkok (Singapore and Hong Kong in a cooperative study of Transit IV-A recordings, and Songkhla and Chiangmai in an MRDC-EL study of S-66 recordings). The analysis of the recordings from these low-latitude stations was facilitated by the fact that most of the records showed a distinct signature when the line from the satellite to the receiver was orthogonal to the earth's magnetic field. In addition to permitting the use of relatively simple instrumentation and data reduction techniques, the time of occurrence of this event (termed T_0) could be used along with the satellite ephemeris to estimate the dip angle of the earth's magnetic field (STR 33).

c. Results

The major analysis effort was devoted to the S-66 records. Figure IV-23 shows the total electron content for descending (north-to-

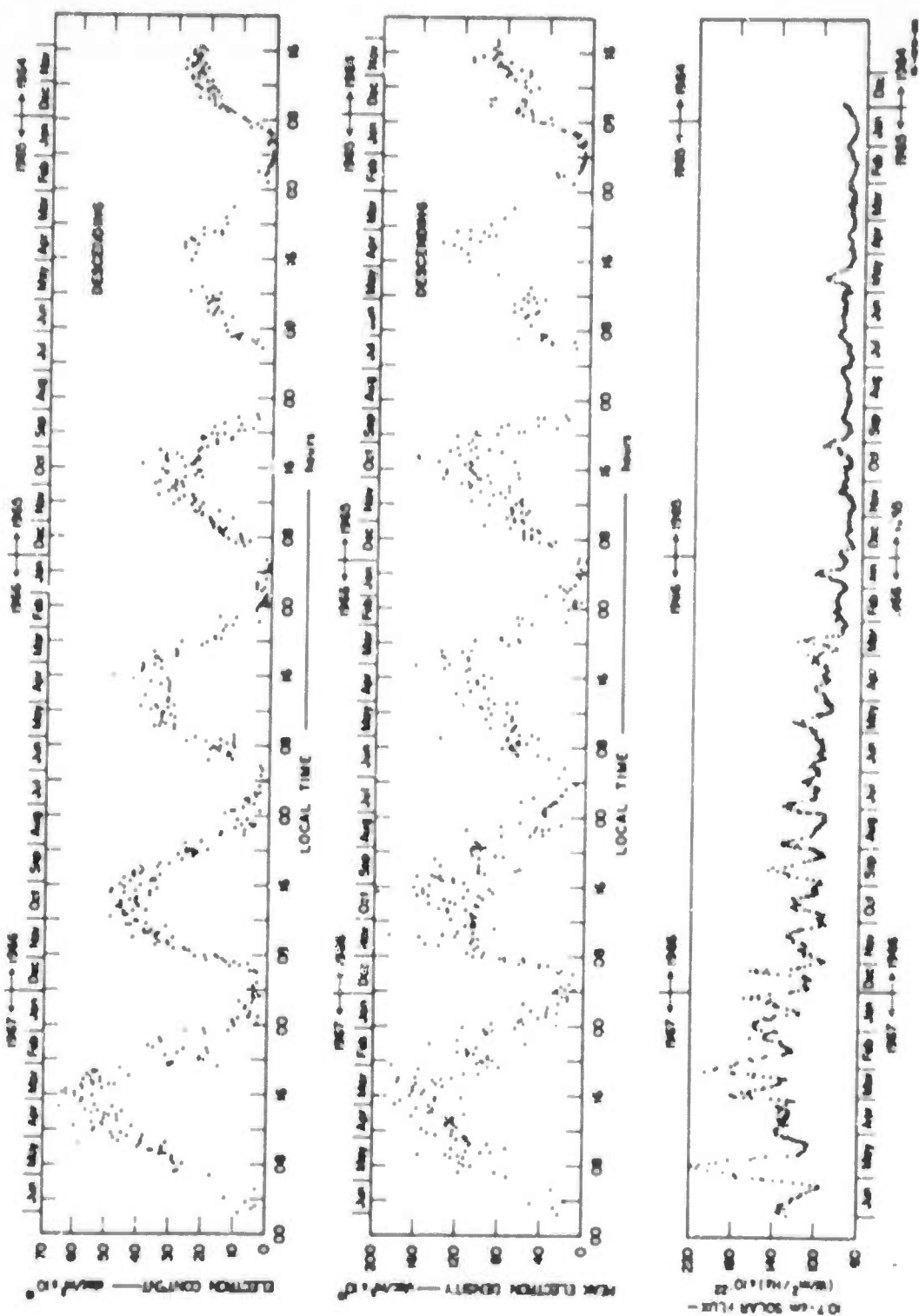


FIGURE IV-23 DIURNAL VARIATION OF ELECTRON CONTENT AND F-LAYER PEAK ELECTRON DENSITY AND SOLAR FLUX—DESCENDING PASSES

south) passes of S-66, the peak electron density of the F2 layer computed from C-2 data, and 10.7-cm solar flux. The diurnal variations of both total content and peak electron density are clearly visible. The relationship between peak total content and solar flux was essentially linear up to flux levels of $1.6 \times 10^{-20} \text{ sr}^{-1} \text{ Hz}^{-1}$. The seasonal variation of peak electron content is illustrated in Figure IV-24, which also includes 1964 data from Transit IV-A. As expected, the seasonal peaks in total content occur during equinoctial periods.

The variation of total content with latitude and time of day in Figure IV-25 (Transit IV-A data) shows a daytime minimum centered on the magnetic dip equator. A similar variation in peak content (and hence foF2) occurs, and this phenomenon is known as the equatorial anomaly. A nighttime anomaly of this type was observed from the S-66 data (STR 34). The ionospheric dynamics causing these anomalies are still under active study by scientists working on equatorial aeronomy. Data of the type presented above are useful in checking proposed dynamic models of the ionosphere.

The ratio of total content (from Faraday records) to peak density (from C-2 records) can be used to compute the equivalent slab thickness of the ionosphere. Figure IV-26 shows the diurnal variation of the equivalent slab thickness (and the related quantity, the equivalent scale height) of the ionosphere near Bangkok. By assuming that the equivalent slab thickness is independent of latitude near the dip equator,* one can use the value of slab thickness for Bangkok and

* This proved to be a reasonable assumption for the ranges of latitude considered here.

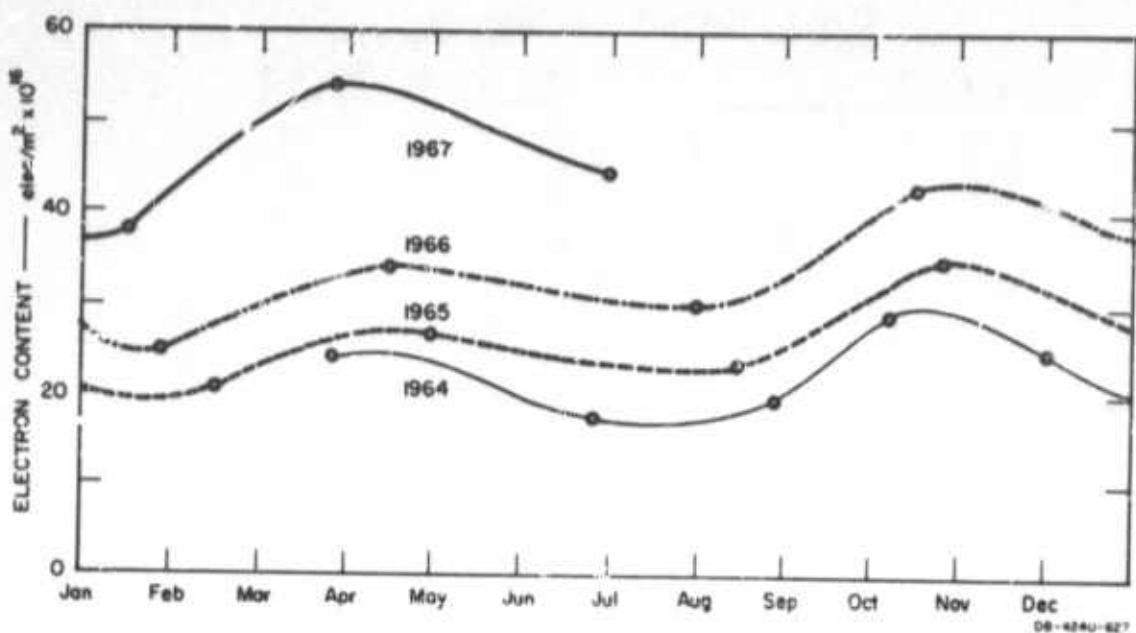


FIGURE IV-24 SEASONAL VARIATION OF PEAK ELECTRON CONTENT

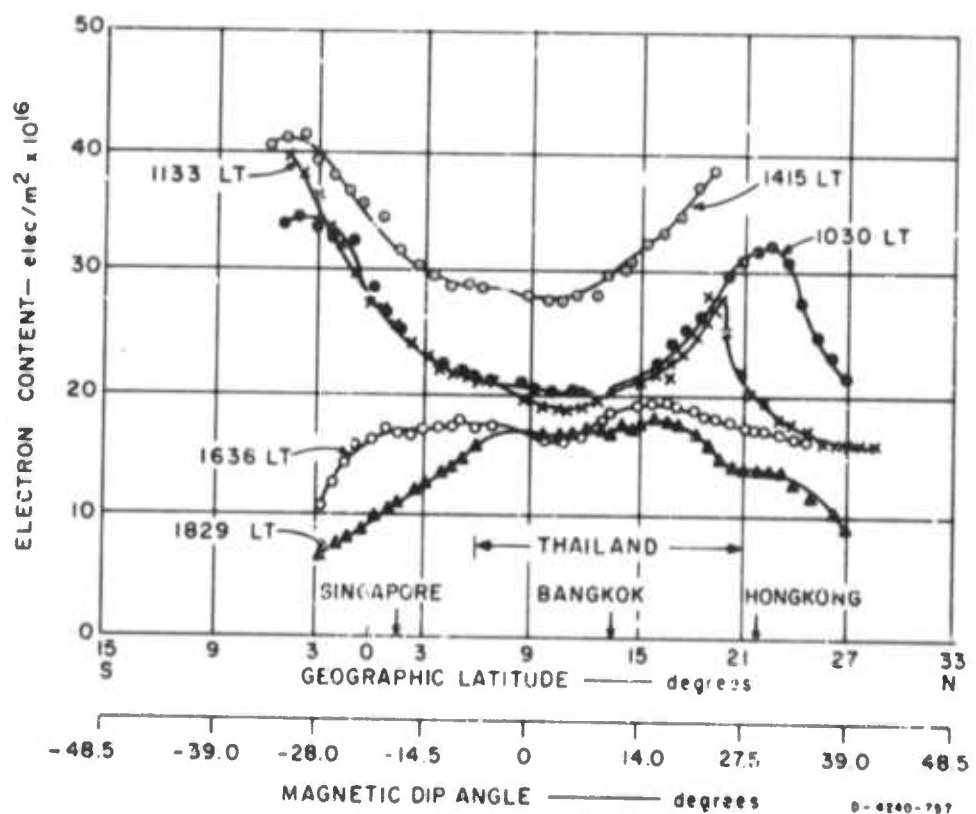


FIGURE IV-25 LATITUDINAL VARIATION OF ELECTRON CONTENT

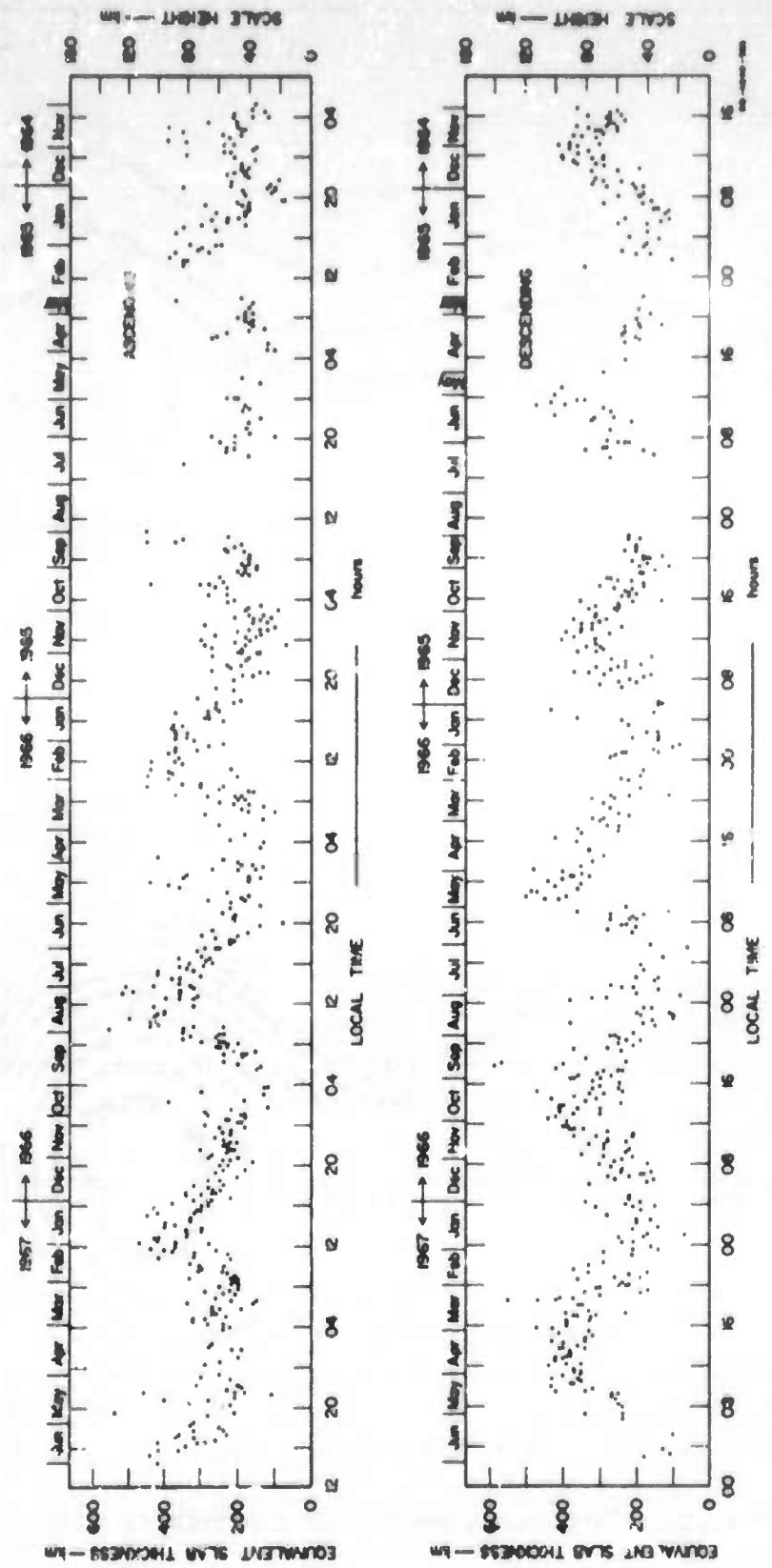


FIGURE IV-26 DIURNAL VARIATION OF EQUIVALENT SLAB THICKNESS AND MEAN SCALE HEIGHT—ASCENDING AND DESCENDING PASSES

total content data for sites remote from Bangkok to estimate the peak electron density (and hence foF2) for the remote sites. Such foF2 estimates were made for Songkhla and Chiengmai, and the resulting values agreed typically to within 10 percent or better with vertical-incidence soundings made at these remote sites between November 1966 and March 1967 (STR 34). It might be noted that data from a topside (satellite) sounder could also yield data on foF2 versus latitude, and data from such a source should be considered in any future studies of this type.

The results of magnetic field dip angle estimates made from the $\frac{f_o}{\text{times}}$ of Faraday rotation records obtained at Bangkok, Songkhla, Nakhon Sawan, and Chiengmai indicate that the magnetic dip equator (at ionospheric heights) crosses the Kra Peninsula of Thailand at about 9.30°N . This result is in good agreement with other measurements and maps (STR 33).

2. Sudden Ionospheric Disturbances (STR 50D)

a. Objective

The objective of this work was to study the Bangkok C-2 sounder records of foF2 and f_{\min} during the time immediately after a solar flare to determine whether the usable frequency spectrum (defined for the purposes of this discussion as foF2 minus f_{\min}) was affected.

b. Results

The interval of this study was September 1963 through December 1966--a period of relatively low solar activity. One hundred and ninety-six flares of importance 2 or greater occurred during this interval, and eighty-seven produced sudden ionospheric disturbances (SIDs) detected on the various instruments at MRDC-EL. Forty-one of these SIDs caused a change in the usable frequency spectrum as observed

on the hourly sounder scan immediately after the SID. For flares of importance 2 or greater the effects occasionally were still noticeable during the second hour after the SID. In almost all cases the usable spectrum decreased from its monthly median value by 20 to 70 percent, although the effects ranged from a slight increase to a complete fade out.

3. Magnetic and Ionospheric Storms (STR 50D)

a. Objective

The objective of this brief study was to observe the effect of magnetic and ionospheric storms on foF2 and on HF atmospheric noise.

b. General Comments

Magnetic storms are disturbances of the earth's magnetic field which may last from a few hours to several days. The observed intensity of the disturbance depends upon--among other things--the observing station's location. The increased ionospheric currents associated with the storms tend to be concentrated in the auroral zones. The earth's field fluctuates over wider limits during a disturbance than it does in normal conditions: about seven-tenths of one percent at Bangkok versus about one-tenth of one percent during a normal period. Magnetic storms are generally classified as either of two types: sudden commencement (SC) or gradual commencement. The SC storms begin abruptly and almost simultaneously all over the earth. During a solar flare a large quantity of energy is emitted from the solar atmosphere. Among the many geophysical phenomena associated with this outburst of energy are SC-type geomagnetic storms and ionospheric disturbances. The solar

radio outbursts of low-frequency energy can be related to SC-type geomagnetic storms, while the higher frequency energy (X-ray) is closely connected with SIDs.²³

Ionospheric storms often accompany magnetic disturbances as described above. The ionospheric storms may last from a few hours up to four or five days. There are several ionospheric phenomena which may occur during an ionospheric storm. Among these are radio blackouts, enhanced sporadic E, decrease in the occurrence of spread F (for low-latitude stations), and depression of the daytime critical frequencies of the F2 layer immediately after the storm begins.

c. Results

The planetary magnetic range index (K_p) was used as the source for determining when a magnetic storm occurred.* The ionospheric storms considered were associated with magnetic storms that had a K_p index of 6 or greater. The start time of the ionospheric storms was taken as the hour nearest in time to the start of the magnetic storm. The start time of the ionospheric storm is easily found when the storm is associated with a sudden-commencement-type magnetic storm. However, it is more difficult to determine accurately the start time of magnetic storms that do not have a sudden commencement. Sixty-one of the 137 principal magnetic disturbances observed at Bangkok between September

* After the installation of the rubidium-vapor magnetometer at the Bangkok laboratory in 1965, it also was used successfully to document the occurrence of such storms. Magnetograms of the three most disturbed days during each month in 1966 was reproduced in the quarterly geomagnetic data bulletins (see Appendix A for a list of these reports).

1963 and June 1967 were of the sudden-commencement type. The change of the total field intensity during the storms had a range of from 35 gamma up to 300 gamma.

The average variation of foF2 during 37 of the largest storms is shown in Figure IV-27. The percent change in foF2 was found by comparing the values on the storm days to the foF2 on a quiet day nearest in time to the storm day. In general, the foF2 increases during the storm except for a period of about 1 to 3 hours just after the beginning of the storm and again about 30 hours later when a decrease is seen. The change is typically less than 10 percent and hence, on the average, should not be too significant for most operational radio circuits.

A statistical analysis of the 5-MHz atmospheric noise at Laem Chabang as a function of storm time for the same 37 storms indicated that the noise is generally slightly lower during an ionospheric storm; however, the variation is almost negligible from a radio system standpoint (typically less than 3 dB).

4. Solar Eclipse Observation (STR 32)

a. Objective

The main objective was to monitor with vertical-incidence sounders the ionospheric changes over Bangkok during the 23 November 1965 partial eclipse of the sun (maximum obscuration of 88 percent at 1017 hours local time).

b. Description of the Experiment

Ionogram data were obtained from the C-2 ionosonde and a Granger sounder operating at the MRDC-EL. Another Granger sounder was used in the fixed-frequency mode (7.05 MHz) to measure the variation

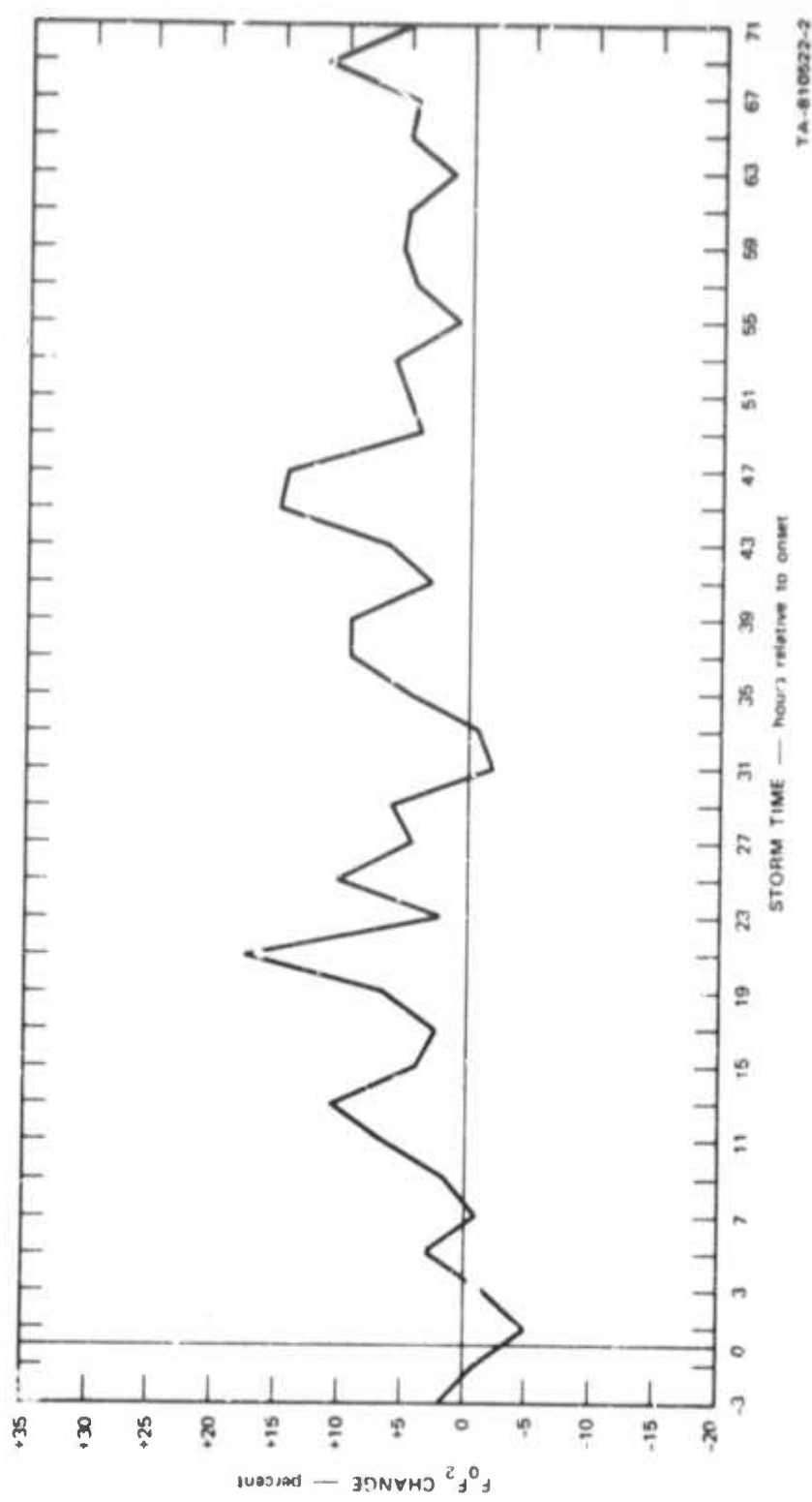


FIGURE IV-2/ PERCENTAGE CHANGE OF $f_0 F_2$ DURING IONOSPHERIC STORMS

TA-810622-2

in signal strength of echoes from the F layer. Data also were obtained with a rubidium-vapor magnetometer at the same site.

c. Results

The main feature of the ionogram observations was a stratification of the F layer. The critical frequency of the F1 layer (f_{oF1}) decreased during the eclipse, but an "F1.5" layer was observed to form during the latter half of the eclipse. Also, the regular F2 layer experienced a rapid and significant virtual height increase.

The 7.05-MHz signal strength increased during the first part of the eclipse due to a decrease of nondeviative absorption in the D layer (which, in the absence of the solar ionizing flux, had begun to recombine). Later, the signal strength decreased rapidly due to deviative absorption in the F region as the critical frequency approached 7.05 MHz, but recovery was very rapid as the stratification disappeared and the new F2 layer again supported the propagation path. An eclipse can cause enough loss of HF skywave signal from deviative absorption to result in communication outage on short paths at low latitudes for a brief period (less than an hour), but the frequency of occurrence of eclipses is so low that as a practical matter for radio operators this effect is not important.

The diurnal variation of the total geomagnetic field intensity (F) was only about one-third its normal value--presumably because of reduced current amplitude in the solar-driven E region.

5. Anomalous Ionospheric Reflections (STR 15, IDBs)

a. Objective

The objective of this scientific work was to document the occurrence of sporadic E and spread F in Thailand.

b. Sporadic E

The diurnal and seasonal variations of sporadic E (E_s) at Bangkok during a period of minimal solar activity are presented in Figure IV-28, which shows the percentage of the time foE_s exceeds 3 MHz. It is apparent from this figure that E_s is more prevalent during the day. The latitudinal variation and percent occurrence of foE_s at noon are shown in Figure IV-29, and the higher values of both foE_s and percent occurrence are observed nearer the dip equator. This is due to the greater system sensitivity of the Granger sounder. Figure IV-30 shows a mass plot of simultaneous observations of foE_s using both sounders at Bangkok from 4 April until 7 May 1966. Notice that the C2 data of Figure IV-29 fall below the Granger sounder data. There is considerable scatter to the points, but it appears that the more sensitive Granger system shows a higher observed value by about 2 ± 2 MHz.

Two types of E_s were observed. The higher latitude sites (Chiengmai and Nakhon Sawan) generally exhibited "L" type sporadic E, whereas the southern-most site (Songkhla) showed almost entirely "q" type sporadic E. These two types of E_s are defined as follows:

1(L) A flat E_s trace at or below the normal E-region minimum virtual height in the day or below the E-region minimum virtual height at night.

q(Q) An E_s trace that is diffuse and nonblanketing over a wide frequency range, the spread being most pronounced at the upper edge of the trace. (This type is common in daytime in the vicinity of the magnetic equator.)

Intermediate sites (see Figure IV-5) showed a mixture of the two types. Bangkok predominantly L type and Prachuap predominantly q type.

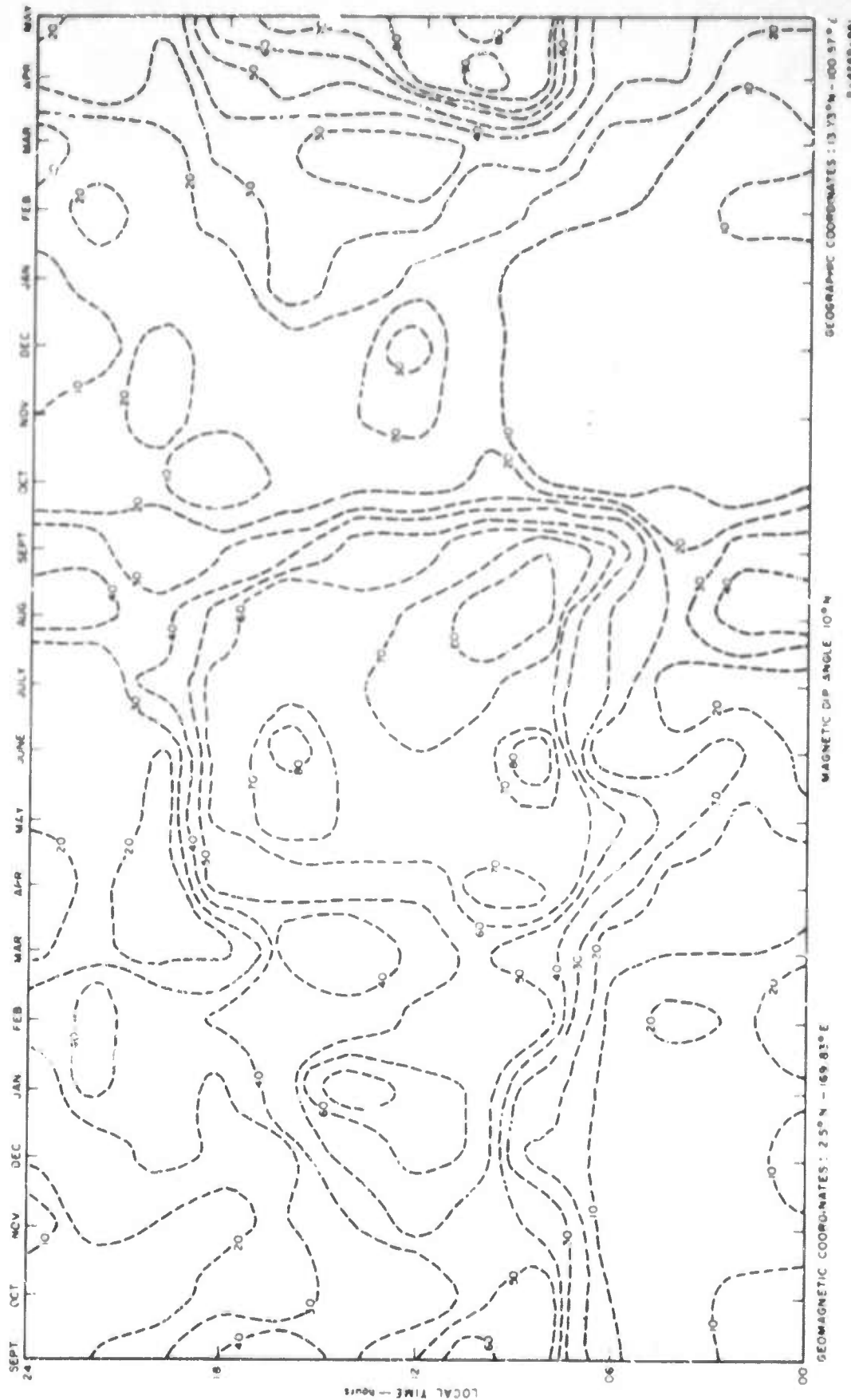


FIGURE IV-28 DIURNAL VARIATION OF PERCENT OF TIME FOR MAGNETIC DIP ANGLE EXCEEDS 3 MHZ—SEPT 1963—MAY 1965
AT BANGKOK

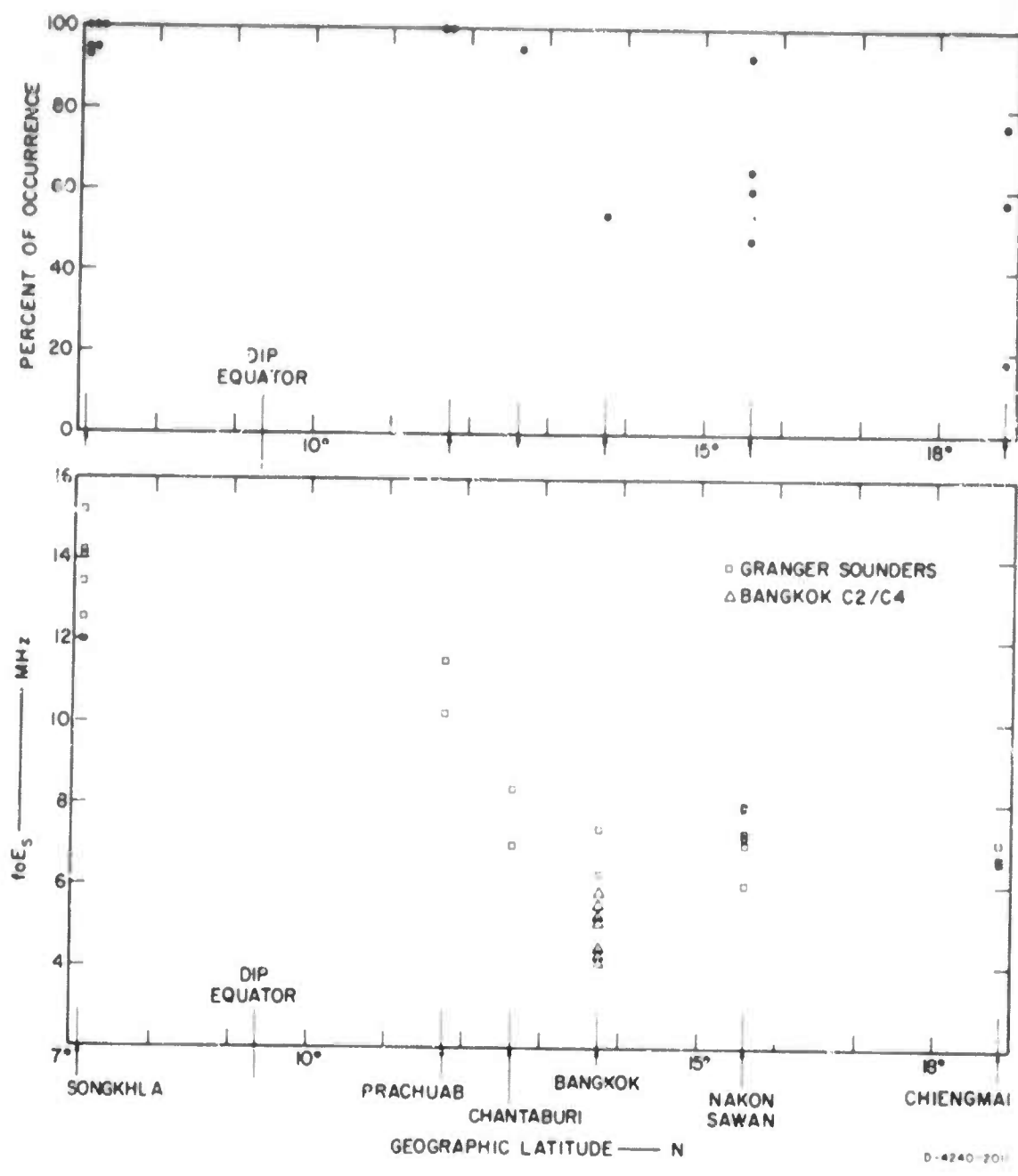


FIGURE IV-29 f_{0E_s} AND PERCENT OCCURRENCE OF SPORADIC E AT LOCAL NOON AS A FUNCTION OF LATITUDE IN THAILAND

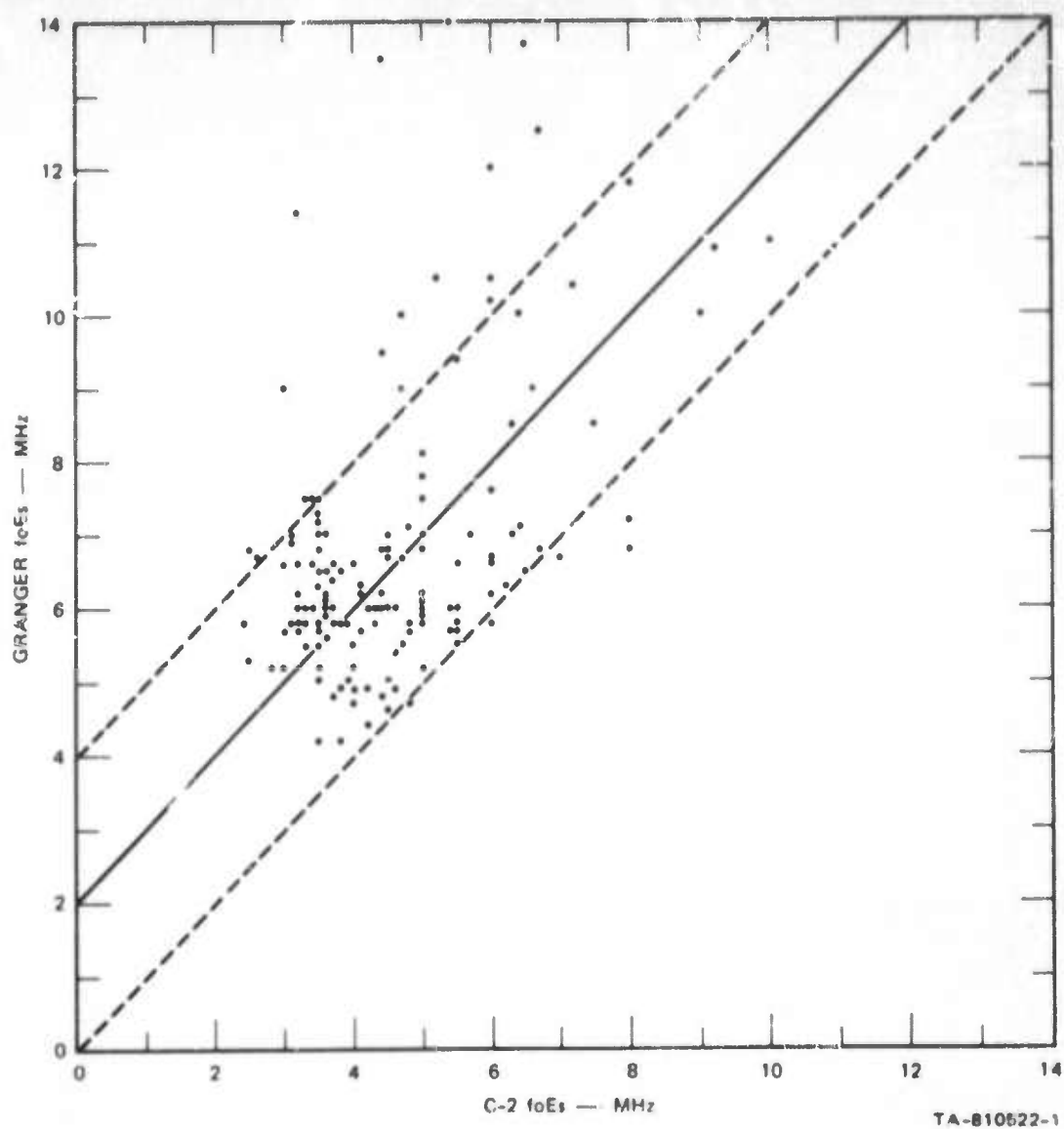


FIGURE IV-30 MASS PLOT OF f_{oE_s} AS A FUNCTION OF FREQUENCY OF THE C-2 AND GRANGER SOUNDER AT BANGKOK

The virtual height of the E_s remained relatively constant between 100 and 110 km through the time period of observation and at all sites.

c. Spread F

The lengthening of the received echoes from the F2 layer referred to as spread F was also observed at these sites. Our observation of spread F confirmed what has previously been reported. At the lower latitudes the spread F is primarily a nighttime phenomenon beginning around 2000 hours local time as the E_s begins to disappear. It tends to increase in likelihood of occurrence throughout the night to a maximum of around 80 percent just prior to the dawn, at about 0500 local time. Figure IV-31 shows a typical plot of percent occurrence of spread F and sporadic E at a low-latitude site.

There also appears to be a seasonal variation, the incidence being markedly lower in the winter months of November and December.

D. Noise and Interference

1. ARN-3 Studies (STR 27, 37, 47)

a. Objectives

The objectives of the MF and HF atmospheric radio noise studies using the ARN-3 noise-measuring equipment in Thailand were to:

- (1) Document the noise received on a vertical monopole antenna and compare the results with values predicted by the CCIR noise maps.

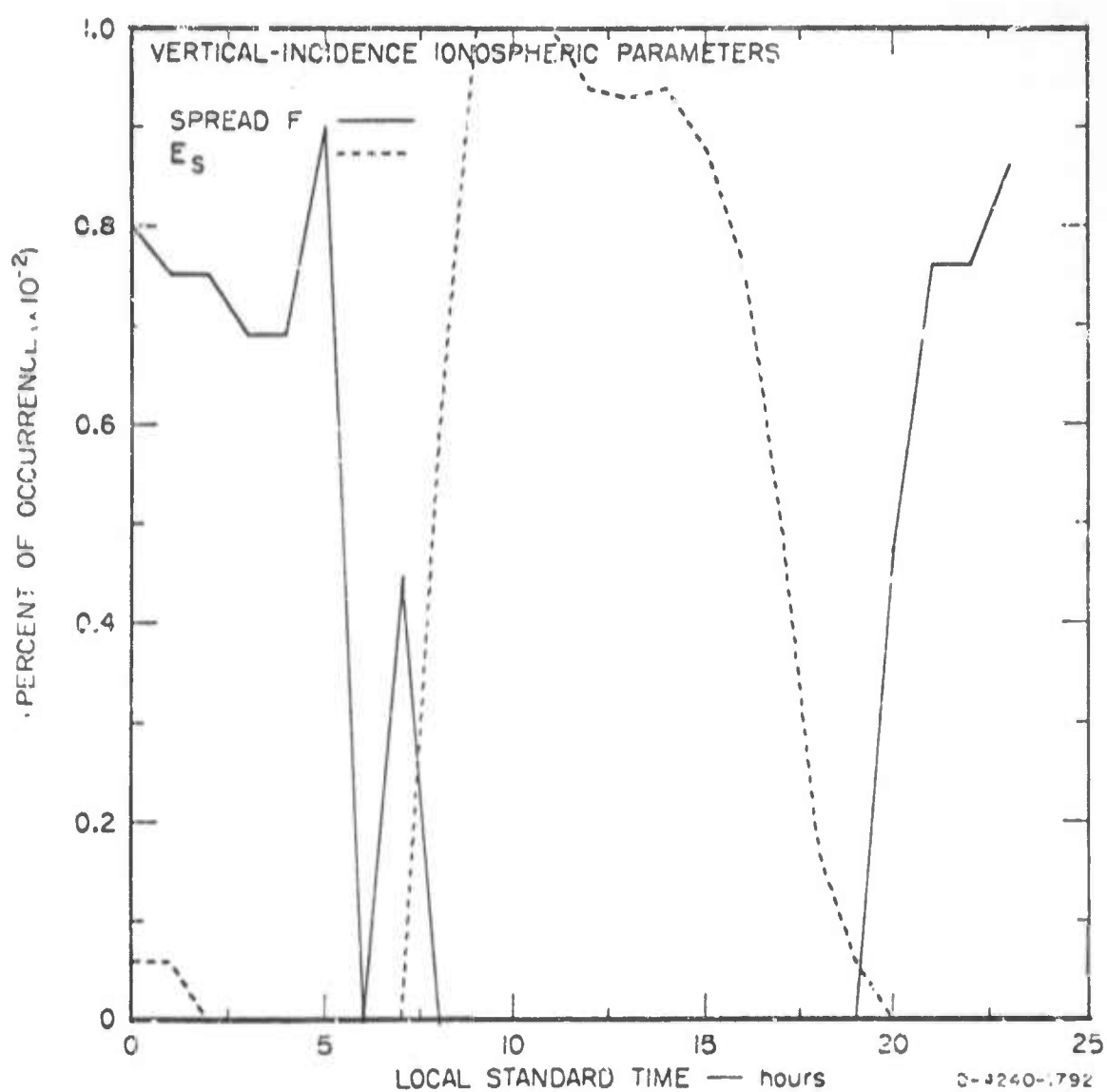


FIGURE IV-31 PERCENT OCCURRENCE OF SPREAD F AND SPORADIC F-1
SONGKHLA, FEBRUARY 1967

- (2) Compare the noise received on horizontal dipoles with the monopole results and with CCIR predictions.
- (3) Observe the increase in average noise power during local storms.

b. Background

Noise, in one form or another, provides the ultimate limitation on the performance of any radio system. The principal type of noise affecting MF and HF radio communication systems in the tropics is (in the absence of interfering signals) the atmospheric noise resulting from lightning discharges.

Significant progress in documenting atmospheric radio noise has been made during the last decade (from the International Geophysical Year to the present). A worldwide network of identical atmospheric radio noise recorders (designation ARN-2),²⁴ developed and operated under the supervision of the U.S. National Bureau of Standards, has provided data on the vertical component of mean noise power at sixteen locations,²⁵ and these data have been used to improve existing noise maps²⁶ based on meteorological data and previous noise data. The noise maps describe the vertically polarized components of the incident noise field upon a given receiving site as a function of site location, radio frequency, time of day, and season of the year.

A two-year measurement program was undertaken in March 1966 at Laem Chabang, Thailand (13.05 N, 100.9 E on the Gulf of Thailand--about 90 km southeast of Bangkok) with equipment having essentially the same technical specifications as the ARN-2 and called ARN-3 (STR 27) to obtain data for comparison with the values given in the International Radio Consultative Committee (CCIR) Report 322.²⁷ Later in the

measurement program the equipment was modified to enable additional measurements with horizontal dipole antennas. This section presents the results of these measurements along with a comparison between the observed values and the CCIR Report 322 predictions, and a comparison of noise measured at the same site on vertically and horizontally polarized antennas. The effect of local electrical storms on the observed noise levels (not considered in CCIR Report 322) is discussed in connection with the lightning-flash counter (local storm detector--see STR 49) work in Section IV-D-3.

e. Description of Equipment

The ARN-3 was designed to measure two noise parameters useful in estimating the amplitude probability distribution (APD) of the noise: F_a and V_d . The effective antenna noise factor F_a^* represents the mean noise power available from the terminals of a hypothetical lossless antenna relative to the thermal noise power available from a passive resistance at $T_0 = 288.4^\circ$ Kelvin. The voltage deviation, V_d , is the ratio (in dB) of the mean-squared noise voltage to the square of the average voltage of the noise envelope, where both voltages are measured after linear detection [i.e., $V_d = 20 \log_{10} (V_{rms}/V_{avg})$]. Of course, $(V_{rms})^2$ is proportional to the mean noise power.

The ARN-3 equipment was described in detail in STR 27, and the modifications to facilitate measurements with the dipole antennas were described in STR 47. The ARN-2 monopole antenna was constructed from drawings supplied by the U.S. Environmental Science Services

* The units of F_a are dB above $kT_0 b$, where k is Boltzmann's constant and b is the equivalent noise bandwidth of the device observing the noise.

Administration (ESSA), Boulder, Colorado, and is identical to the antenna used with the U.S. National Bureau of Standards (NBS) ARN-2 atmospheric noise recorder.²⁴ Two trapped dipoles (for magnetic orientations N-S and E-W), approximating half-wave horizontal dipoles at 2.3, 5.0, and 10.0 MHz were constructed for horizontal-antenna noise measurements. The receiving equipment was time shared with 12 minutes of each hour on the monopole, the two dipoles, and a dummy load.

d. Results

1) Observed Values

The median values of F_a observed with the standard monopole during each 3-month season/4-hour time block (denoted F_{am}) for the period March 1966 through February 1968 are presented in STR 37 (see Figure IV-32). The corresponding values of V_{dm} (median values of V_d) are given in Figure IV-33. A study of the data from each frequency (showing each hour's median for a given month) indicated that the noise power generally increases from day to night by approximately 25 dB and that the average decile range of noise power variation about the month's hourly median is typically 20 dB. It should be noted that data for a two-year period are not sufficient to define seasonal variations with any confidence. Nevertheless, seasonal variations of up to 10 dB were observed for a given hour with maxima in the spring and fall.

The monthly median values of F_{am} observed each hour with the N-S and E-W dipoles from August 1967 through February 1968 are presented in STR 47, and an example is given as Figure IV-34. The monthly-median atmospheric noise power observed in the lower part of the HF band during nighttime with horizontal dipoles at 23 ft above ground is relatively independent of frequency and season--in direct contrast to observations of noise on a vertical monopole at the

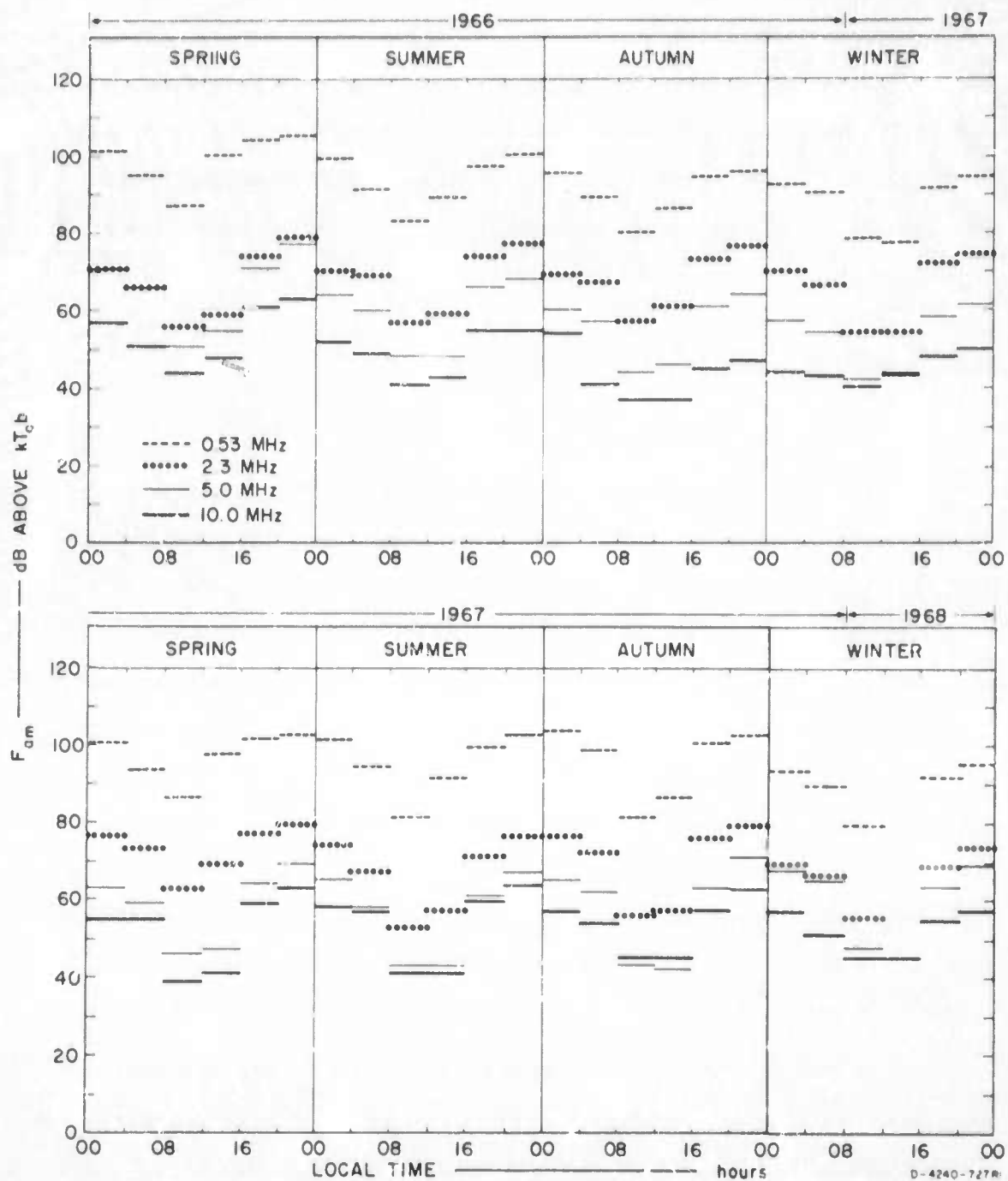


FIGURE IV-32 QUARTERLY TIME BLOCK MEDIAN OF NOISE POWER (F_{am}) OBSERVED AT LAEM CHABANG DURING THE PERIOD MARCH 1966 THROUGH FEBRUARY 1968

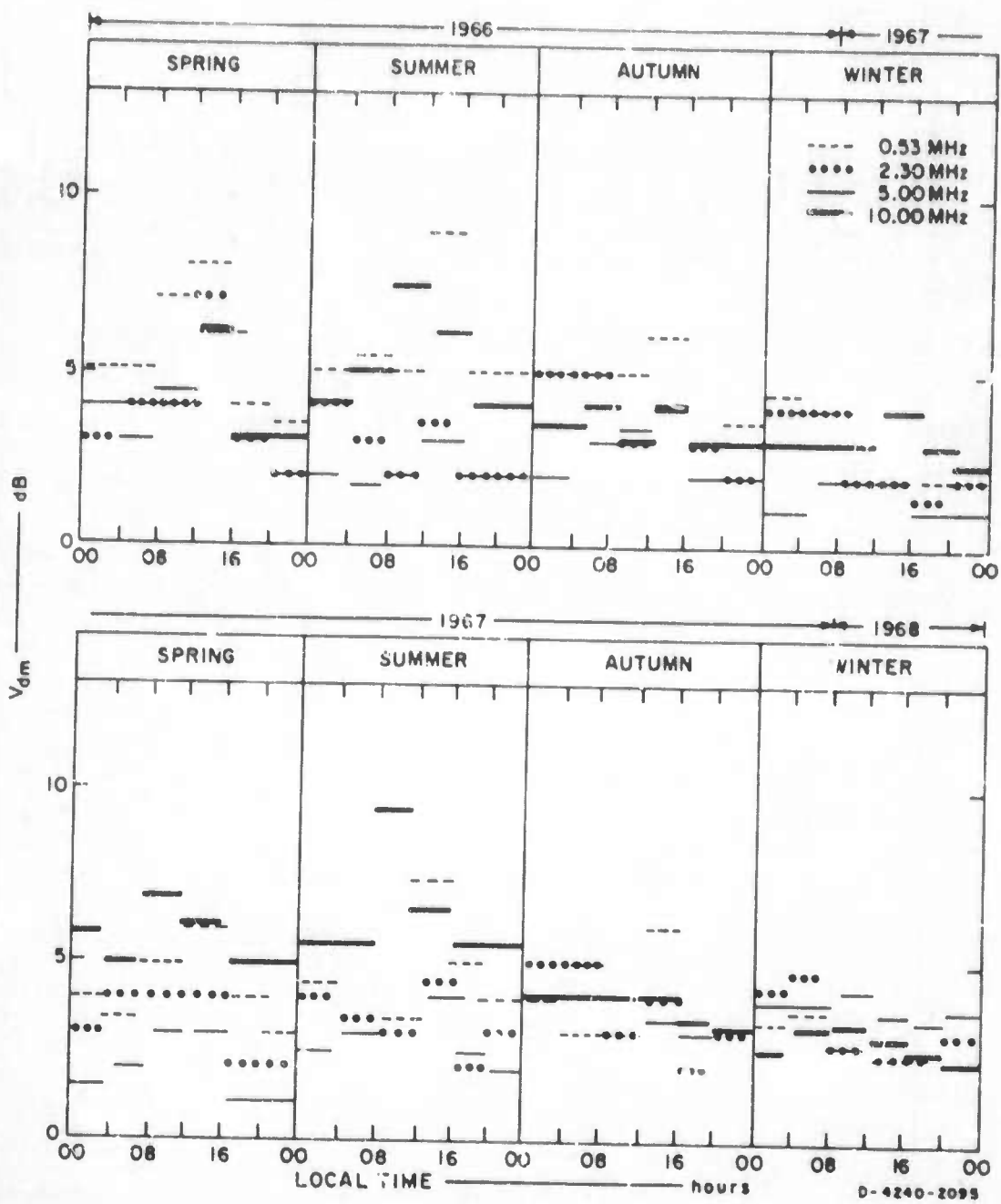


FIGURE IV-33 QUARTERLY TIME BLOCK MEDIAN OF NOISE VOLTAGE DEVIATION (V_{dm}) OBSERVED AT LAEM CHABANG DURING THE PERIOD MARCH 1966 THROUGH FEBRUARY 1968

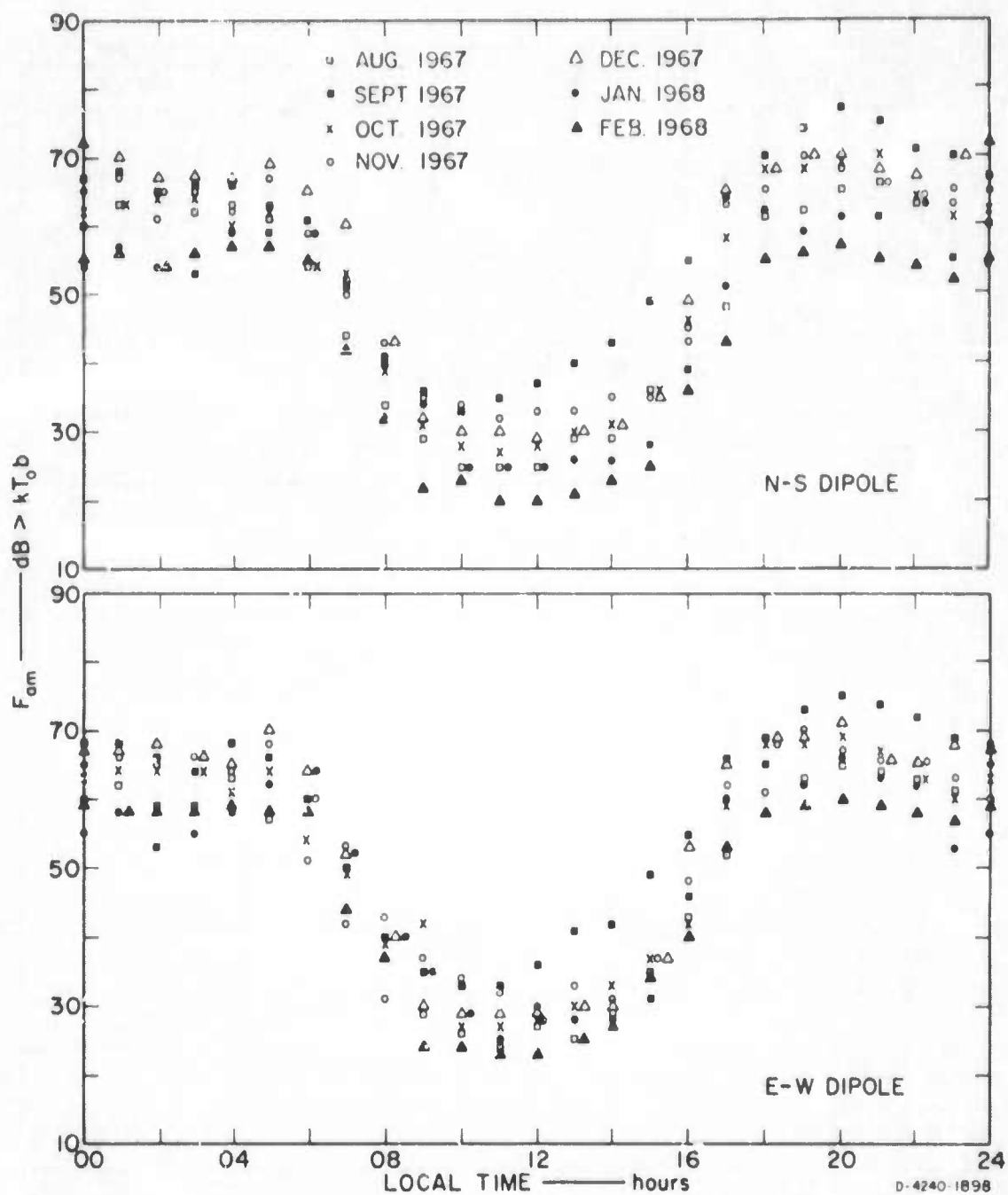


FIGURE IV-34 MONTH-HOUR VALUES OF EFFECTIVE ANTENNA NOISE FACTOR FOR 5.0-MHz TRAPPED DIPOLES AT LAEM CHABANG

same site. Typical nighttime values for the dipoles lie between about 55 and 70 dB (to the nearest 6 dB) above kT_b . There is a significant daytime variation of the noise in the frequency range 2.3 to 10 MHz, with a minimum in observed power occurring between about 1000 and 1100 hours local time.

2) Comparison of Vertical Monopole Data with CCIR Report 322 Predictions

Expected values of atmospheric noise power F_a for any geographical location and any time block and season can be determined from contour maps and conversion curves contained in CCIR Report 322. Using the CCIR report, a complete set of expected noise values for Laem Chabang for all seasons and time blocks and the four frequencies of measurement (0.53, 2.3, 5.0, and 10.0 MHz) was generated. The corresponding expected and measured values of noise power were then compared. This comparison showed that the observed noise was always higher than predicted, a result that is in agreement with a conclusion reached by Ibukun²⁷ in his study of noise in Nigeria. The discrepancies between Thailand observations and predictions are shown in Table IV-2 and an example comparison is given in Figure 1V-35.

The simplest reasonable correction to the CCIR curves would be to add 10 dB to each predicted atmospheric noise value at MF or HF regardless of time of day, season, or frequency. This correction could be improved upon by taking season and time of day into consideration as follows:

- (1) For winter add 14 dB to all predictions.
- (2) For the other seasons, add 14 dB to predictions between 0800 and 1800 local time, and add 7 dB to the predictions for other times.

Table IV-2

DISTRIBUTION OF DIFFERENCE (Δ) * BETWEEN
OBSERVED AND PREDICTED NOISE POWERS

Ranges of the Difference (Δ)	Fraction of Data in Each Range of Δ - %				
	Spring	Summer	Autumn	Winter	Average
$\Delta \leq 5$	27	35	52	12	35
$5 < \Delta \leq 10$	42	38	21	34	33
$10 < \Delta \leq 15$	19	17	17	17	17
$15 < \Delta \leq 20$	8	8	6	21	10
$20 < \Delta$	4	2	4	16	5

* $\Delta = F_{\text{am}} \text{ (measured)} - F_{\text{am}} \text{ (predicted)}$, in dB.

Examination of detailed data from Singapore and New Delhi, as well as limited data from Northern Thailand and CCIR prediction curves reveals that the Laem Chabang data cannot be applied directly to other parts of Thailand. However, geographical corrections, given in Table VI of STR 37, can be applied and should yield predictions that are adequate for engineering purposes.

In addition to measurements of atmospheric noise power F_a , data were obtained on the voltage deviation V_d . Observations of the mean voltage deviation V_{dm} were almost always lower than the predictions of CCIR Report 322. The closest agreement was obtained at 10 MHz (typically within 2 dB), and the poorest agreement was obtained at 5 MHz (typically within 4 dB). The observed values were never greater than the predicted values on 5 MHz, and they were seldom more than 1.5 dB greater than the predictions for any of the other measurement frequencies. The observed diurnal variation of V_{dm} followed the predicted trend best at 10 MHz during all seasons, but the agreement was only

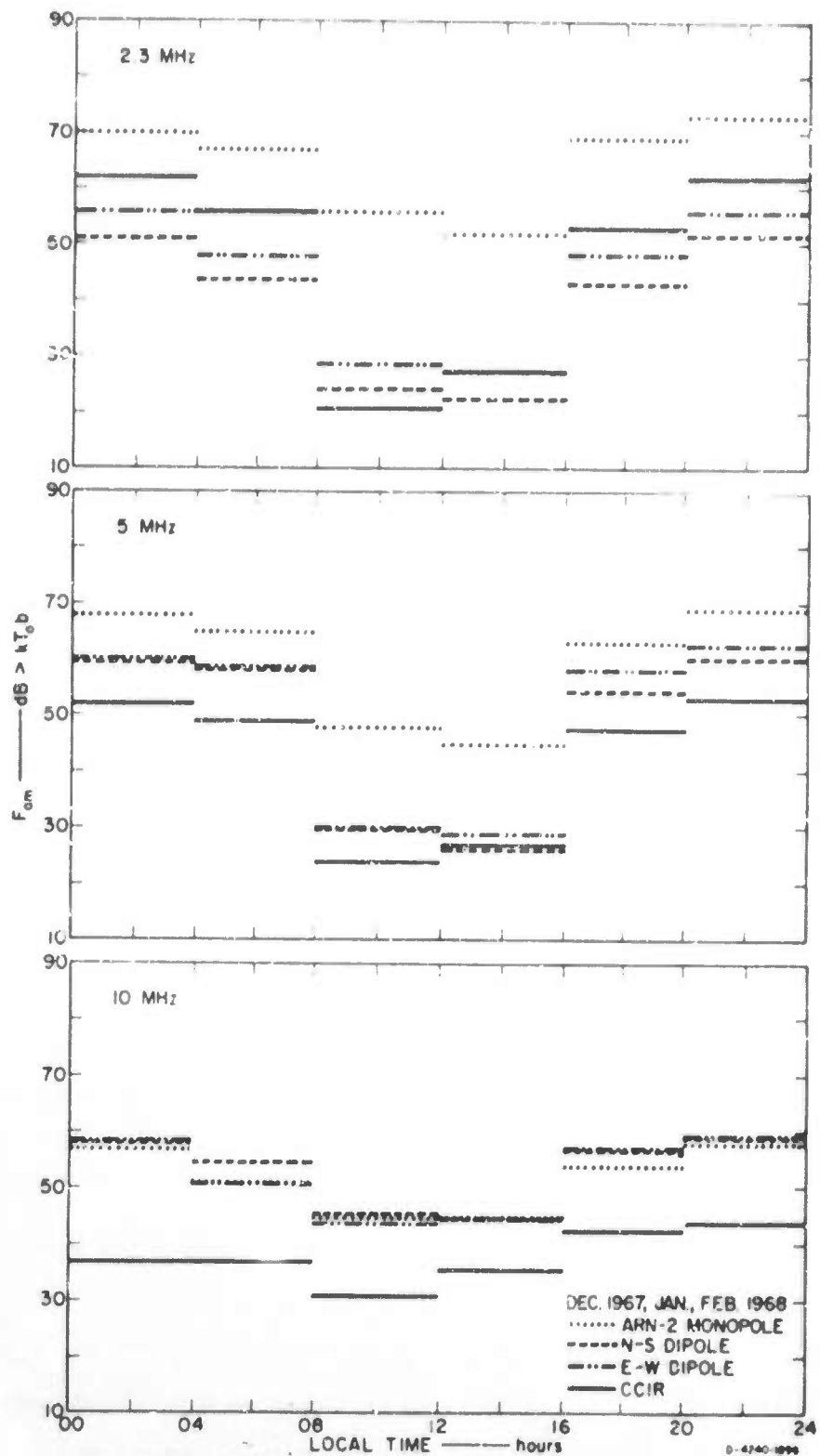


FIGURE IV-35 COMPARISON OF ARN-2 MONOPOLE AND TRAPPED DIPOLE OBSERVED NOISE WITH CCIR REPORT 322 PREDICTIONS, LAEM CHABANG, THAILAND, WINTER 1967-1968

fair for the other measurement frequencies during summer and poor for other seasons. The seasonal variation (for both predicted and observed values) indicated a loose correlation with local storminess--the smaller values of V_{dm} occurring during winter (when there were fewer local storms). The CCIR predictions indicated a decrease in V_{dm} with increasing frequency for all times except winter days, and this variation was not observed. The values at 0.53 MHz typically were larger than or comparable to the values at 10 MHz, but the values at 5 MHz (and often 2.3 MHz) were usually lower than the values at 10 MHz. Possibly more interference was experienced on 2.3 and 5 MHz than at 0.53 or 10 MHz.

3) Comparison of Horizontal Dipole Data with CCIR Predictions

Data from the trapped dipoles at Laem Chubang and from the unbalanced dipoles at other sites in Thailand were compared with the CCIR Report 322 predictions for the standard ARN-2 monopole (see Figure IV-35), and an approximate correction function was generated. Figure 20 of STR 47 shows these corrections as a function of frequency for day and night.

At 10 MHz, when applied directly to our horizontal dipoles, the CCIR predictions for the monopole gave values that were too low by 5 to 10 dB during day and by 15 to 20 during night. The noise maps give reasonable estimates of the noise power available from horizontal dipole antennas located at $\lambda/4$ to $\lambda/8$ above good ground for the frequency range 5 to 6 MHz during daytime; the map values were too low by about 5 to 10 dB at night. The maps yield values too high when applied to 2.3-MHz horizontal dipoles at one-sixteenth wavelength above ground by about 0 to 5 dB during day and 5 to 10 dB at night.

4) Comparison between Dipole and Monopole Results

The noise power from a horizontal dipole at 23 ft above ground was significantly less than the noise power from a vertical monopole in the lower part of the HF band.* This difference is greatest during daytime but tends to decrease as frequency increases, becoming negligible at 10 MHz (see Figure 17 in STR 47). The average variation of noise from day to night generally is greater on the dipoles than on the monopoles, as may be expected considering their directivity patterns and ionospheric absorption. The noise on the N-S dipoles is essentially the same as on the E-W dipoles.

2. Ratio of Signal-Plus-Noise to Noise on HF Field-Expedient Antennas

a. Objective

It was our objective to observe the signal-plus-noise-to-noise ratio $(S + N)/N$, on selected HF field-expedient antennas operated on a short (100-km) skywave path, to determine the best antenna from a signal-to-noise standpoint.

* The actual values are applicable only for dipoles at 23 ft above ground, however, and a correction for antenna height-gain effects would be required to obtain estimates of the dipole-mono, i.e. difference for other antenna heights ($h < \lambda/4$) above good ground. Extrapolation to dipole heights greater than one-quarter wavelength probably would not be too reliable because of significant changes in the directivity pattern of the dipole, whereas extrapolation to lower heights involves primarily antenna efficiency.

b. Background

Although the relative gains of selected HF field-expedient antennas for the desired signal have been measured using the ionospheric sounders and the airborne Xeledop system, it was decided to make a brief check of the $(S + N)/N$ when receiving on a short path. A 50-watt transmitter operating on about 6 MHz was set up at Bangkok to drive an efficient half-wave horizontal dipole on a 10-minute key-up/key-down cycle. At Laem Chabang, the following receiving antennas were used: $\lambda/4$ monopole, 30° slant wire, 5:1 inverted L, and a $\lambda/2$ dipole at $\lambda/8$ above ground. The test was performed around noon on two successive days during January 1968.

c. Results

The dipole exhibited the greatest $(S + N)/N$. The average $(S + N)/N$ on the slant wire typically was 2 to 4 dB below that on the dipole, whereas the inverted L was typically 6 to 8 dB worse than the dipole. As expected, the $(S + N)/N$ on the monopole was significantly lower--about 26 dB below the dipole. The noise picked up by the inverted L was typically only about 0.5 dB greater than the dipole noise, whereas the noise on the slant wire and monopole was typically 2 to 3 dB greater than the dipole noise. Evidently the difference in signal gain was more important than the noise pickup in determining the difference in $(S + N)/N$. The performance of the monopole relative to the dipole is about as one would deduce from vertical-incidence sounder relative gain measurements, but the slant wire and inverted L, while down in performance from the dipole, exhibited an inverse relationship to that deduced using the sounders. The presence of a counterpoise on the slant wire--as well as proper alignment (elevated section pointing away from Bangkok)--contributed to the superior performance of this antenna over the inverted L (used without counterpoise) at this dry, sandy site. Also, as the

path length increases from 0 km (vertical incidence) to 100 km (Laem Chabang to Bangkok), the gain of the properly aligned slant-wire antenna increases whereas the gain of the inverted-L antenna decreases--as revealed by the airborne Xeledop measurements (see Section III-C).

Information on the signal-plus-noise (and interference) to noise (and interference) ratio on a path of this length may be inferred from the 50-mile data obtained during the HF manpack tests over varied terrain during sunspot minimum (RM 3). These results at 3.6 MHz for the 15-watt HC-162 (AN/PRC-74) indicated roughly a 20-percent chance of communication with whips, a 50-percent chance with 30° slant wires, and a 75-percent chance with $\lambda/2$ dipoles at $\lambda/10$ above ground--during any 24-hour period (see Section V-A).

3. Lightning-Flash Counter Studies (STR 49)

a. Objectives

The objectives of the lightning-flash counter (LFC) work in conjunction with noise recordings were to:

- (1) Better establish the characteristics of the disturbance caused by local thunderstorms.
- (2) Assess the relationship (for use in noise predictions) between local thunderstorm intensity and such long-term climatological parameters as the thunderstorm day.
- (3) Establish some basic thunderstorm information for Thailand.

b. Background

It might be noted that there are two separate groups of engineers interested in the counting of lightning flashes, each with different objectives. Radio engineers are troubled by radio noise generated by lightning flashes, which interfere with radio communications. In order to estimate the interference, information on global thunderstorm activity is necessary, the lightning-flash counters can assist in supplying this information. Also, electrical engineers engaged in the construction of surface power lines need to decide what measures--if any--of protection from lightning strikes are desirable. The cost of installing various kinds of protective devices has to be balanced against the likelihood of strikes. Accordingly, knowledge of the incidence of lightning as a function of geography is desirable. Both electrical and radio engineers have based much of their work upon the meteorological statistic of the thunderstorm (T/S) day. This is any day during which thunder is heard; it is noted as a routine at most meteorological stations. For example, Figure 18 of STR 49 is a map of annual occurrence of thunderstorm days in Thailand.

Although the T/S-day statistic is useful, its applicability is limited. There is no indication, for example, of the violence of the activity on a day with thunder. Also, especially regarding the needs of radio engineers, the T/S-day statistic yields no information on the diurnal trend of lightning activity or the variation of diurnal trend with season. This type of information is potentially available from lightning-flash counters (LFCs). Although the data presented in this section are of value to both electrical and radio engineers, the emphasis in the remainder of this discussion will be based primarily on the needs of the radio engineer.

In a tropical country such as Thailand, radio noise has two main components:

- (1) High background due to noise signals propagated from the major centers of thunderstorm activity
- (2) Noise that is due to local lightning activity.

In this section we deal with the second source. Details are provided in STR 49.

c. Equipment

A CCIR-type counter (peak response at 10 kHz and down 6 dB at 1.5 and 40 kHz) was installed at Bangkok and was operated with a 5-m vertical antenna and a 6-volt threshold from May 1964 through November 1967.

A lightning-flash analyzer (LFA) was designed to work off the 7-m standard ARN-2 vertical monopole employed with the ARN-3 at Laem Chabang. This unit was intended to give data in the CCIR (VLF) pass band and the ERA^{*} (ELF, nominally between 6-dB points of 200 Hz and 2 kHz) pass band for threshold levels of 1, 3, and 10 volts. Equipment design problems reduced the utility of this instrument, which was operated from September 1966 through October 1967.

Finally, an ERA-type counter (on loan from Prof. S. A. Prentice, University of Queensland, Brisbane, Australia) was employed

* British "Electrical Research Association."

at the Laem Chabang site during the last three months of 1967. The counter sensitivity was adjusted so that the counter was triggered when the field developed at the antenna ("within the bandwidth of the counter) exceeded 5 V/m (threshold voltage of about 3 V).

d. Results

The results of the lightning-flash counter studies are detailed in STR 49. Here we mention only some of the highlights as follows:

- (1) The seasonal trend of lightning activity, as measured by mean daily count per month (D_m), is similar to seasonal trends (10-year average) in thunderstorm activity as measured by T/S days. A close correlation was not observed, however, and should not be expected because D_m varies considerably from year to year. The median daily count with the Bangkok instrument was 4.
- (2) The distribution of daily counts is approximately log-normal with a standard deviation of 20 dB about the median, but departures are noted for high daily counts.
- (3) Peak activity occurs between 0600 and 1200 in the early months of the year, 1200-1800 during spring, and 1800-2400 during late summer and fall. Activity from 2400 to 0600 is low except during autumn and winter. The results are consistent with meteorological data.

(4) A general relationship between mean daily counts and long-term average T/S day per month (T_m) was established empirically for the Bangkok instrument as

$$D_m = 2 T_m \quad \text{for } T_m \leq 3$$

$$D_m = (2/3) T_m^2 \quad \text{for } T_m \geq 3$$

(5) It was possible to obtain an approximate relationship between the intensity of local lightning activity (in counts per hour as monitored with lightning-flash counters) and the increase in atmospheric noise over the monthly median background level for that hour (in dB as observed with the ARN-3 system).

This is discussed in STRs 37, 47, and 49.

Typically, a local thunderstorm increases noise power at 0.53 MHz by some 15 dB.

(6) The results have been extended, through the use of T_m data obtained at many sites by the Thai Meteorological Department, to permit an estimate of the probability of a local storm (and hence the probability of a several-hour period of communication difficulty at MF and HF) for any location in Thailand as a function of month and time of day.

(7) The ERA-type counter is more suitable than the CCIR-type when the main objective is to document the occurrence of "local" electrical storms. The antenna height-threshold voltage

combination should be adjusted to yield a fairly short effective range (e.g., 20 km), and this effective range should be verified by observation to the extent practical.

4. Interference Considerations

a. Objectives

The main objective of this work was to observe spectrum occupancy in the HF band, and a secondary objective was to note the occurrence of radio-frequency interference (RFI) at HF and VHF.

b. Background

Although spectrum occupancy studies in Southeast Asia were not an official part of the SRI SEACORE program, some data of this type were obtained. Interference observations were made as part of the HF manpack radio tests (RM 2, RM 3), and the lower part of the HF spectrum (2-12 MHz) was monitored at MRDC-EL (SAR 4). Other occurrences of RFI were noted.

c. Results

The following results were obtained:

- (1) Interference from other transmitters was observed during the HF manpack radio tests, and it was concluded that flexibility in choice of operating frequency is highly desirable.
- (2) The HF spectrum from 2-12 MHz was monitored at Bangkok during the summer of 1964, and

peak signal occupancy was observed around 6 MHz with a minimum in the 2-12 MHz band during local afternoon (period of maximum ionospheric absorption).

- (3) Local interference limited the performance of the Bangkok C-2 sounder at the low-frequency end of its sweep (below about 3.5 MHz).
- (4) It was observed (but not documented) that some local stations did not meet International Telecommunication Union (ITU) and U.S. Federal Communications Commission (FCC) specifications regarding bandwidth, frequency tolerance and stability, and spurious emissions.²⁸
- (5) Severe interference at VHF was observed from automobile and power boat ignition systems (apparently few vehicles in Thailand employ interference suppression devices). Communication sites should be located several kilometers from such sources where possible, and special interference precautions^{*} should be taken when this is not practical.

* For example, it was found necessary to employ carefully balanced horizontally polarized electric dipoles at the MRDC-EL site in Bangkok in order to obtain useful data on 20 and 40 MHz during the Faraday rotation experiment discussed in Section IV-C-1.

- (6) Sufficient noise at VHF was observed to originate from local electrical storms (when present) so as to change the quieting of an AN/PRC-25.
- (7) The impulse noise data of Figure 41 in SAR 8 was identified as atmospheric noise subsequent to the publication of that report.

V TASK C: SYSTEM TEST FORMAT
AND PROCEDURE INVESTIGATIONS

A. Early Tests with HF Manpack Radios (RMs 2, 3)

1. Objective

The objective of the early HF manpack tests was to document and rank order the performance of selected sets in several tropical terrains.

2. Background

Performance tests with the AN/GRC-9, AN/TRC-88, TRP-4, and HC-162 were carried out over ranges out to about 25 miles in three types of terrain (delta, forest, and mountain), and similar tests were also performed over varied terrain (one terminal in mountains and the other in the delta) out to 50 and 100 miles. The significant test variables were the type of set, the type of antenna, the communication range, and the time of day. The test frequency was nominally 3.6 MHz for these tests.

The antennas used were an improved half-wave dipole (doublet) elevated to about $\lambda/10$, a $\lambda/5$ 30° slant wire, and a 15-ft vertical whip.

Random number lists, ten digits long, were employed as test messages. These test messages were transmitted both ways on a fixed frequency every two hours for two days, and the resulting data were tabulated to indicate the communication success during the 48-hour period.

3. Results

The results of voice comparison tests (see Figure V-1) indicated that the two more modern, higher powered sets (HC-162 and AN/TRC-88) were significantly better than the other sets tested (in order of decreasing overall performance: 77-AM, TRP-4, and AN/GRC-9). The old AN/GRC-9 was clearly the poorest set. The advantage of the frequency flexibility permitted by the synthesizer of the HC-162 (now the AN/PRC-74) was noted with regard to avoiding interference. The half-wave horizontal dipole at $\lambda/10$ above ground proved the best antenna regardless of set type.

The data on the performance of the HC-162 in jungle and mountainous terrain were combined and smoothed as a function of range and antenna type (see Figure V-2). The ordinate of Figure V-2 approximates the probability of successful communication--defined here as the average probability of correctly communicating a random digit (without repeating) during a 24-hour period. The dipole operated primarily via skywave and provided reasonable performance relatively independent of range or time of day. The whip was definitely inferior to the dipole for ranges of 5 miles or greater. It operated primarily via groundwave from dawn until early afternoon and with decreasing success out to ranges of 10 to 20 miles. For greater ranges, the whip began to operate via skywave with increasing effectiveness as the antenna directivity for the skywave path increased. The slant wire represents a compromise between the dipole and whip: it is better than the whip for groundwave, but it is inferior to the dipole for skywave. Its overall performance is inferior to the dipole for ranges of 5 miles or greater.

Diurnal effects are also important. Regardless of the type of terrain or set used, the best time for communication on 3.6 MHz was during the day, typically between 0700 and 1700 hours, and the worst

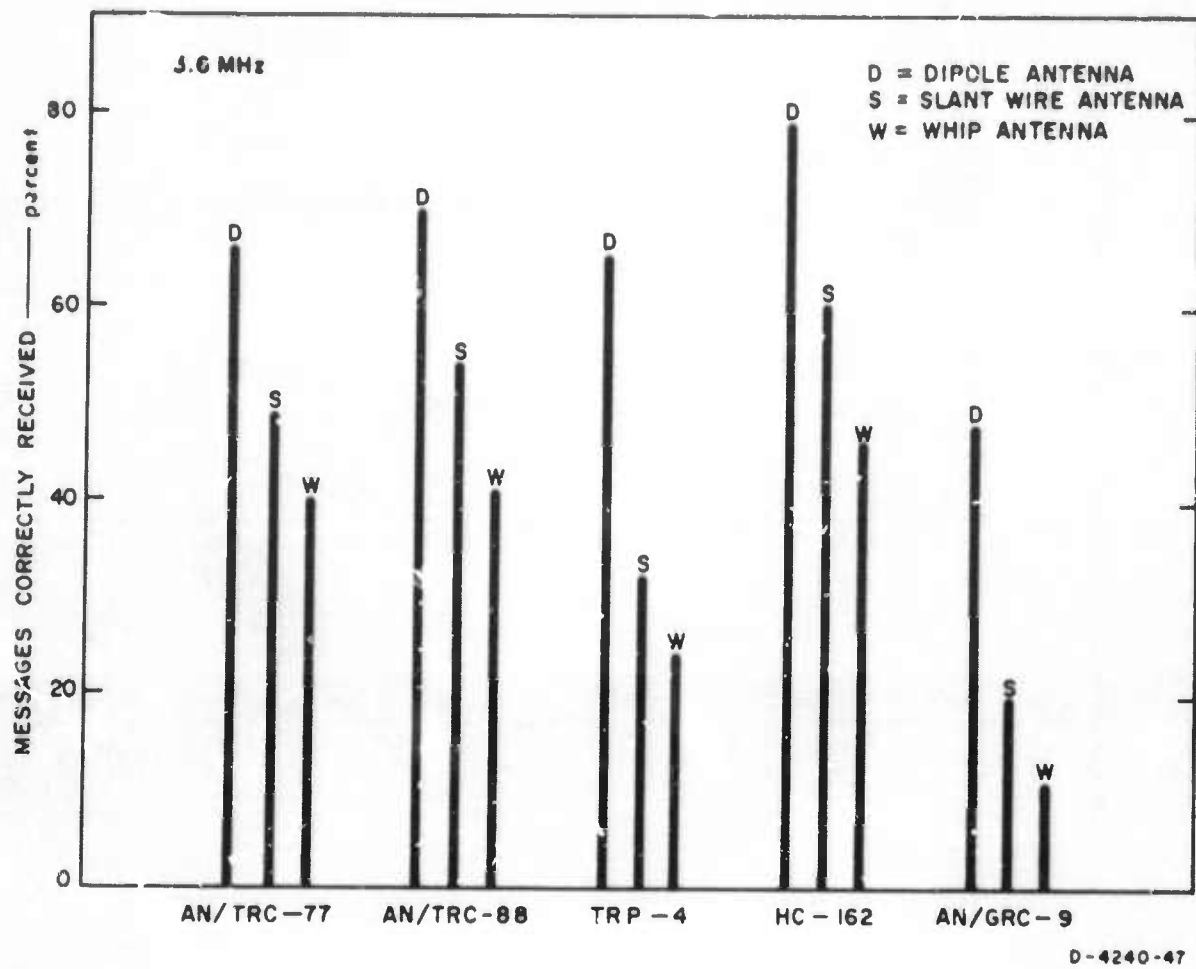


FIGURE V-1 COMPARISON OF PERFORMANCE OF SETS USING DIPOLE, SLANT-WIRE, AND WHIP ANTENNAS—ALL TESTS IN THAILAND (SPRING AND SUMMER, 1963)

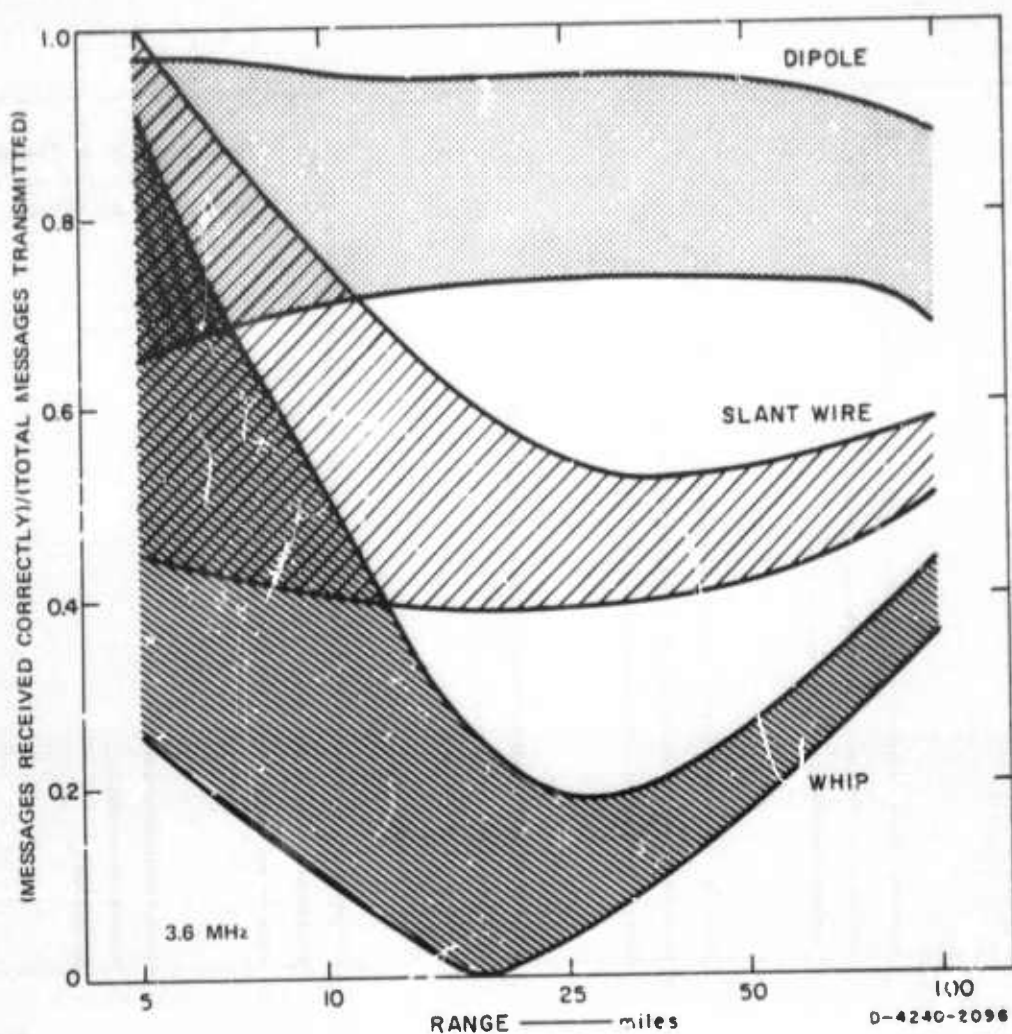


FIGURE V-2 COMMUNICATION SUCCESS AS A FUNCTION OF RANGE FOR HC-162 (AN/PRC-74) IN MOUNTAINOUS AND VARIED TERRAIN—INCLUDING JUNGLE

period typically was from midnight to dawn. The best four hours for groundwave were between about 0900 and 1300 hours and for skywave, between 0700 and 0900 hours in the morning and between about 1500 and 1700 hours in the afternoon.

Brief CW tests in the delta, in the mountains, and over varied terrain generally confirmed the results obtained with the voice tests. These tests, like the voice tests, had significant limitations, which are discussed in detail in RM 3. Small differences in performance are not meaningful. The best results were obtained with the HC-162, followed by the 77-AM, AN/TRC-88 (misaligned for this test), TRP-4, and the AN/GRC-9--which was significantly worse than the others. The HC-162 did have the narrowest bandwidth (2.7 kHz), but it should be noted that none of the sets tested had the capability for reducing the IF bandwidth for CW operation. Therefore, this potential advantage of CW over voice was not realized.

B. Tests with VHF Manpack Radios

1. Forest Test near Bang Sapan, Thailand (RMs 2, 3)

a. Objective

The objective was to test two available types of VHF manpack radios over the same paths as the HF tests described above.

b. Description of Test

AN/PRC-10 and AN/PRC-25 sets were tested on 40 MHz during March 1963 at the forest site used for the HF tests described above. Tests were made using both 3-ft and 10-ft whip antennas, near ground level and elevated. Random digits were used as test messages.

e. Results

Using their long whip (10-ft) antennas, both the AN/PRC-10 and AN/PRC-25 generally worked well at ranges up to 3 miles in moderately forested areas; although during one test, conducted through extremely dense undergrowth, total loss of signal occurred at less than one-half mile. Elevation of one or both antennas produced decided range increases. Use of a base-station antenna height of 30 feet (bamboo mast only) resulted in about 3 miles of "effective range" in communication with a manpaek unit in moderate to dense undergrowth. With both antennas elevated to 70 ft, excellent results were obtained with both sets out to 5 miles. No diurnal effects were observed. It was estimated that the sets were operating near the threshold of the FM detector. No signals were received at 10 or 22 miles. No significant difference in performance between sets was observed, although the frequency drift of the AN/PRC-10 was a nuisance.

2. Delta Tests near Bangkok, Thailand (STR 8)

a. Objective

The objective of these tests was to obtain a measure of the effective range of selected VHF radios in the dry paddy fields near Bangkok.

b. Description of the Tests

Tests were made during April 1964 with the AN/PRC-25 (with and without a power amplifier that could be adjusted for 15 or 35 watts), with the experimental AN/PRC-35 (XC-3), and with the Motorola Handie-Talkie (Model H21DCN-1000). The base of each set was elevated 2.5 ft above ground. The separation distance between the sets was

increased until the carrier-plus-noise ($C + N$) decreased to a level 10 dB above the noise voltage measured with no carrier present, and the corresponding range was termed the effective range. Concurrent voice intelligibility tests--both simple counting tests and the more elaborate Fairbanks Rhyme tests--indicated that this definition of effective range corresponded to a word intelligibility of about 50 to 70 percent.

c. Results

The results of these tests along with the set characteristics are summarized in Table V-1. It was also observed that at the range limit, elevating both the transmitting and receiving sets from 2-1/2 to 10 ft restored the signal strength to a usable level.

Increasing the transmitter power of the AN/PRC-25 with the auxiliary amplifier from 2 watts to 15 or 35 watts provided observed range increases slightly greater than those predicted when assuming a $(1/d)^2$ variation of field strength. Increasing the transmitter power from 15 to 35 watts, however, produced observed range increases somewhat less than those computed in the same manner. Nevertheless, it should be possible to use the $(1/d)^2$ law to compute range changes corresponding to power changes in open delta terrain to within 25 percent.*

3. Forest Tests near Rayong, Thailand (STR 11)

a. Objectives

The main objective of these tests was to obtain additional operating experience with VHF manpack radios in jungle to facilitate writing a test plan for future testing of such sets in the forest environment. Secondary objectives were the subjective determination of operating range and observation of electromagnetic effects that affected set performance in the jungle.

* Note that a $(1/d)^2$ law for field strength corresponds to a $+0 \log_{10}(d)$ variation for power.

Table V-1
CHARACTERISTICS AND EFFECTIVE RANGES FOR RADIO SETS TESTED IN DELTA

Set	Weight (lb)	Antenna Length (ft)	Average Noise (μ V)	Frequency (MHz)	Power Output (watts)	Effective Range (miles)
AN/PRC-35 (XC-3)	10.5	3	0.2	35	0.8	2.0
				51	0.7	1.2
AN/PRC-25	17.0	10	0.3	65	0.7	1.4
				35	2.0	4.2
AN/PRC-25, with 15-W amplifier	31.7	10	0.3	51	1.9	5.4
				65	1.7	3.4
AN/PRC-25, with 35-W amplifier	31.7	10	0.3	35	15.0	8.0
				51	15.0	12.0
Motorola Handie-Talkie	2.3	1.5	0.08	50.7	1.5	1.2

b. Results

Subjective range tests with the AN/PRC-10 made on 50 MHz near Rayong (Southeastern Thailand) during late 1964 and early 1965 indicated maximum ranges of between 1.5 and 2.5 miles when the long (10-ft) whips were employed at backpac height. Significant fading was observed for ranges beyond about 1/4 mile, and this was attributed to scattering rather than detuning of the antenna by the vegetation (SAR 4). This scatter (multipath) was observed to produce partial cancellation of the field in a quasi-periodic manner as well as partial depolarization of the transmitted signal. These observations indicated that a statistical definition of the range is required for VHF manpack radios operating in forests.

4. Forest and Varied-Terrain Tests near Chumphon, Thailand

a. Objectives

The main objective of these tests (November 1967) was to field check operating suggestions for improving marginal VHF manpack communications in forests. A secondary objective was to observe the range limits of the AN/PRC-10 and the AN/PRC-25 at this site.

b. Forest Tests of Operating Techniques

The following suggestions were proved valid for improving communications when operating with the short (3-ft) whip in forested terrain. They are listed in an order determined by considering both the ease of implementation and the probability of success.

- (1) Tilt antenna to 45° away from the set.
- (2) Rotate tilted antenna or rotate set and antenna set up as in (1) above.

- (3) Move around 5 to 15 feet.
- (4) Change to long antenna (or other antenna) or elevate set plus antenna up to 10 or 12 ft, whichever is easier.
- (5) Move out into a clearing or up on a hill-top (or hillside, preferably the side toward the other terminal) if the tactical situation will permit.
- (6) Elevate antenna or set plus antenna as high as possible--if auxiliary center-fed dipole with feed cable is available, consider elevating it (horizontally polarized) and rotate it for maximum received signal.
- (7) Change frequency--preferably to the highest frequency you can--only as a last resort and only if you have some communication and can arrange the change or if it has been prearranged.

c. Range Tests in Varied Terrain

A fixed site was established in a cleared area at the Chumphon field site, and other sites were established along the trail to the highway. Two AN/PRC-10s using the 10-ft whips and two AN/PRC-25s using 3-ft and 10-ft whip antennas were employed. The terrain was rather flat with a few low hills covered primarily with second growth (as contrasted with the primary forest at the Chumphon site). Much of the area had been cleared for agricultural purposes, and the main crops were tapioca, bananas, and rice.

The range achieved by the AN/PRC-25 using short (3-ft) whips was about 3 miles on 30, 50, and 75 MHz. At 3.3 miles, changing to the 10-ft whip on the transmit end restored marginal communications at 30 MHz and excellent communications at 75 MHz. This change did not restore communications at 50 MHz, but changing to the 10-ft whip on the receive end also restored excellent communications on all three test frequencies. The maximum range achieved with the long whips over this varied-terrain path was not defined, but it was somewhat greater than 5 miles.

A range of about 4 miles was achieved with the AN/PRC-10 operating with long (10-ft) whips at either 38 or 51 MHz over the same trail.

5. Antenna Substitution Tests with AN/PRC-25 (STR 46D)

Several substitution tests were performed with the short (3-ft) and long (10-ft) whips to determine the improvement to be obtained by switching from a pair of the more convenient short whips to the longer whips. Transmitter-receiver separations of one-tenth mile or greater were employed, and the sets were located at backpack height. The results of these tests are summarized in Table V-2. These data are reasonably consistent; however, they do not represent a statistically significant sample.

The data given in Table V-2 for the rain forest in Chumphon apply when both transmitting and receiving antennas are located in the forest and when both are in the clearing. A larger improvement (up to 10 dB more) was observed when changing to the long whips when the receiving antenna was located about 0.15 mile out in the clearing and the transmitting antenna was located in the forest. This is a most puzzling result and it is not currently understood.

Table V-2

TYPICAL IMPROVEMENT IN AN/PRC-25 SYSTEM GAIN
OBTAINED BY CHANGING FROM SHORT TO LONG WHIPS

Frequency (MHz.)	Short-to-Long-Whip Improvement (dB)		
	Open Delta	Sandy Beach	Rain Forest
50	21	15	21
75	9	10	7

C. Definition of Range of VHF Manpack Radios (STRs 8, 11)

1. Objective

The objective of this work was to formulate a meaningful definition of the "range" for VHF manpack radios.

2. Background

The effective range of a manpack radio set is defined as the maximum range over which it can be used to perform its tactical function adequately. There are several problems in arriving at the effective range of a VHF manpack radio:

- (1) A reasonable measure of usability must be defined, and limits must be placed upon this measure in terms of the tactical scenario.
- (2) The measure of usability must be related to range.

3. Results

A direct approach to this problem was taken in STR 8 where word intelligibility was considered to be a good measure of usability for voice communications. Intelligibility was measured as a function of range in open delta terrain, and a typical result is reproduced in Figure V-3. If it is assumed that a word intelligibility of about 50 percent was adequate for a given tactical scenario, then the effective range for the set and test condition studied would be about 2 km. But it is impractical to measure intelligibility vs. range for each case of interest. A more germane question is this: What is the probability of achieving a given word intelligibility for a given percentage of the time as a function of range for different tactical scenarios, and how can this be computed? These problems were considered in STR 11 where the concept of a statistical definition of range was discussed and an example computation was made.

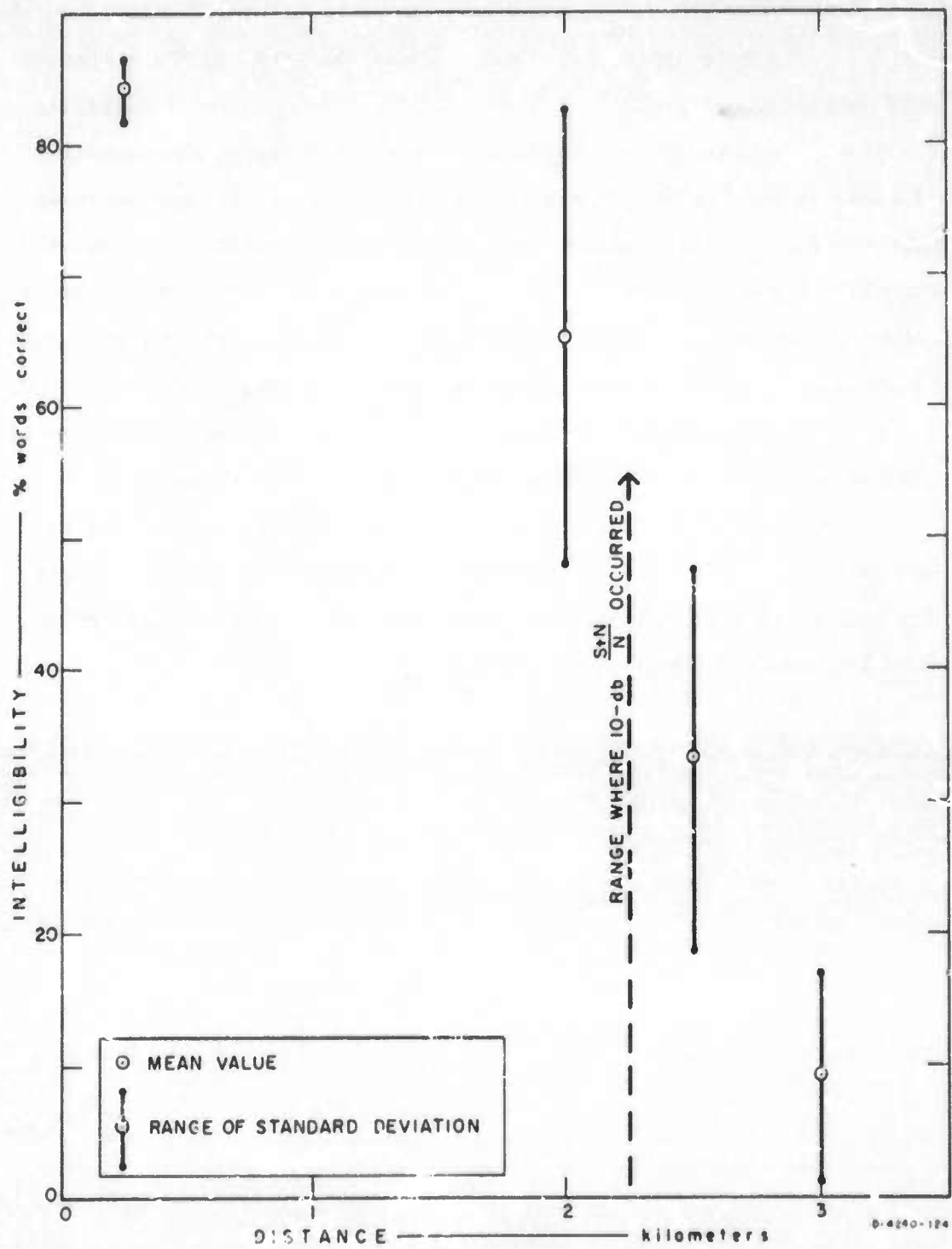


FIGURE V-3 INTELLIGIBILITY VERSUS DISTANCE FOR AN/PHC-35(XC-3)—65 MHz

VI RECOMMENDATIONS

A. Technical Recommendations

The technical findings of the work described in this report are summarized in Section II. We recommend that the findings be incorporated into future designs and operational procedures to improve radio communications in the tropics.

B. Future Work

The following recommendations are offered for future work on radio communications in tropical areas:

- (1) The information generated under the SEACORE Program is presently available in numerous (over 100) technical reports and data bulletins generated by several contractors.

We recommend that:

- The available information on antenna performance and radio propagation in a tropical environment be briefly summarized in a single volume written for engineers and physicists. This document should include data from all available sources--including other jungle programs (e.g., radar studies).
- Operational suggestions should be made available to field communicators in the form of a simplified handbook. (A draft version of such a handbook was prepared under this project.)

(2) The lossy dielectric slab model of air-forest-ground proved useful for predicting the median value of radio system loss, but the model is of decreasing usefulness above about 100 MHz. We recommend that:

- The upper frequency limit of applicability of the slab model for forest propagation be better defined by checking existing data against model predictions.
- Models be generated and are applicable at frequencies above the useful upper frequency limit of the slab model.
- Propagation models should be generated for situations which include mixed-path terrains (i.e., jungle-clearing etc.)
- Models be improved to include some statistical description of the variations in signal level--especially the localized spatial variations about the median value predicted by the slab model.
- These models be worked into a format for handy reference and use by radio engineers for computation of propagation effects for both ground-to-ground and air-to-ground propagation paths.
- Techniques for measuring the conductivity and permittivity of the jungle for frequencies above 100 MHz be devised. Concentration should be centered on obtaining two-point correlations measurements as well as measurements for determining any inhomogeneity or anisotropy.

(3) The possibility of improving communications through the use of diversity techniques for HF and VHF tactical radios has been demonstrated by propagation measurements. Space diversity appears attractive for mobile VHF communications in forests and magneto-ionic component diversity (using crossed horizontal dipoles or the equivalent) looks promising for short HF skywave paths near the magnetic dip equator--and possibly at higher latitudes. We recommend that:

- Breadboard equipments be developed and tests conducted to demonstrate that the postulated improvements can be achieved in practice.

(4) Data on the actual performance of tactical radio equipment in a tropical environment have been rather meager, however, enough data exist to construct propagation channel simulators. We recommend that:

- Existing channel simulators be reviewed (and, if necessary, additional simulators be developed) for use in signal design and system testing. Field performance tests with actual equipments should be performed to validate the simulation.
- Field tests be conducted that document the operational aspects of system performance.

(5) In the absence of satellites or other relays, high frequency (HF) skywave will be required for ranges greater than about 20 miles when employing low-powered equipments. HF propagation effects are reasonably well understood and documented. We recommend that:

- Future work on HF focus on the frequency-management aspects of HF usage.
- A single ionospheric sounder be considered for use in a tactical area to facilitate near real-time frequency control of tactical communication networks. Not only should the ability of the ionosphere to support propagation be measured, but also the noise and interference levels in potential communication channels should be ascertained.
- The procedures for network control should be revised as required to facilitate taking advantage of the flexibility that such data, properly employed, would permit.

Appendix A

DESCRIPTIONS OF FORESTED MEASUREMENT SITES IN THAILAND

Appendix A

DESCRIPTIONS OF FORESTED MEASUREMENT SITES IN THAILAND

The various measurement programs under this contract that involved forested environments were conducted primarily at five sites in Thailand: Ban Mun Chit, Pak Chong, Laem Chabang, Satun, and Chumphon (see Figure I-2 for the locations of these sites). Although Pak Chong and Satun were sites operated by Jansky and Bailey for path-loss measurements, some SRI programs were conducted at these sites and the sites are described in this appendix.

More detailed descriptions of the forests can be found in STR 43 or in the reports describing the programs that were conducted at these sites.

1. Ban Mun Chit

The forested site used for airborne and manpack Xeledop measurements was located near the village of Ban Mun Chit, about 25 km southeast of Chonburi, in the province of the same name.

A detailed description of the site is provided in an environmental survey done by the Environmental Sciences Division of MRDC (MRDC-ES). Briefly, there were about ten square kilometers of trees, bordered on the southwest by tapioca fields, where much of the controlled measurements were taken for the several experimental programs at the site. The grove had been subject to selective logging for many years, so that the remaining older trees of the population were interspersed with second-growth members, and there was dense undergrowth everywhere rising

often as high as 7 meters, where it merged with the lower story of tree crowns. The tree-crown canopy in this dry evergreen forest was often three-storied. The upper story, quite discontinuous, grew between 25 and 34 meters high. The middle story, containing more species, grew from 15 to 24 meters high. The lowest story was of young trees that had attained heights between 6 and 14 meters. In many places, especially the areas bordering the tapioca field, the forest canopy was two-storied. Here, the upper story lay between 15 and 30 meters, the lower between 6 and 15. The ground was only 60 percent covered by canopy and the dense undergrowth associated with the open canopy made penetrability on foot very poor.

A soil survey was made, indicating a surface composed of humus layer, leaf litter, and decomposed remains of trees. Earth-resistivity measurements (dc) made in the forest, together with the soil survey conducted under the direction of the MRDC-ES, show that the earth was heterogeneous near the surface, which was mostly brown sand, having a moisture content of about 10 percent by weight and dc conductivity of 1.7 to 3.4 mmho/meter down to about 3 meters, where a deeper stratum having higher dc conductivity (perhaps 100 mmho/m) seemed to begin.

2. Pak Chong

The Jansky and Bailey forest site near Pak Chong is described in detail in Reference 3. The main camp was in a large valley in the Khao Yai National Forest supporting dry evergreen forest similar in many respects to the forest at Ban Mun Chit.

The forest at this site usually had its crown canopy in two stories: the lower between 1.5 and 18 meters and the upper between 6 and 41 meters. The crown canopy covered approximately 60 percent of the ground area. This is quite similar to the canopy coverage estimated

for the forest near Ban Mun Chit. However, since the lower canopy at the Pak Chong site was closer to the ground, it blocked more light, and the undergrowth at this site, though dense, was not so luxuriant as that at the Ban Mun Chit site. We were able to walk about at Pak Chong without cutting a path. As with the forest at Ban Mun Chit, much of the Khao Yai forest at Pak Chong was secondary growth, not virgin stand.

Earth resistivity measurements (dc) were made in the open near the J & B transmitter tower for estimation of subsurface conductivity stratification at the site. Together with results of a soil survey done there under the direction of the MRDC-ES, they show that the earth conductivity decreased uniformly with depth, from a surface value of about 8 mmho/m (dc) to less than one mmho/m (dc) at 3 meters down; that the soil moisture content above a depth of one meter was between 24 and 33 percent by weight; and that the surface in the vicinity was composed of either silty or sandy clay (USGS terminology) containing fragments of red stone.

3. Laem Chabang

The coastal brush and other environment on the beach near the SRI Laem Chabang low-noise site have been described in STRs 26 and 43. True trees are scarce at that location, and none taller than 10 meters was found there. The vegetation is mostly scrub growth classified as evergreen beach forest though it is composed of shrubs, bushes, climbers, and thorny herbs (including cactus). This growth presents a dense tangled mass that provides poor penetration and visibility. It is quite similar

* It should be emphasized that the soil moisture content data (obtained two years before) do not seem compatible with the electrical-constant data--which indicate a soil moisture content of 5 to 10 percent.

to what has been referred to as undergrowth at other sites, usually growing up to at least 2.5 meters and sometimes as much as 6. The median growth height was about 3.5 meters. The growth was quite evenly distributed.

4. Satun

This J & B test site was on the western coast of the Malay Peninsula near Satun in an evergreen tropical rain forest. Thunderstorms are prevalent in this area, usually being heard on more than 100 days each year, and bringing torrential rain that produces the succulent growth commonly associated with the word jungle. Indeed, the Khuan Karlong forest at the site was the last stand of a once-rich wilderness; but it had lost many of its valuable trees to the axe, so that its upper-canopy story was discontinuous, though regular in height, having trees between 24 and 30 meters tall. The greatest numbers of trees were from the middle-story canopy, 15 to 23 meters high, in a seemingly continuous horizontal layer. There was a lower-canopy story composed of young trees between 8 and 14 or more meters high that formed a sort of height continuum with the middle story; the result was complete canopy coverage of the ground beneath the forest. The irregular undergrowth lived on filtered light except where rare breaks occurred in the cover. There, in the direct sunlight, the undergrowth resembled what we saw at the other sites: dense shrubs, climbers, and herbs reaching up between 3 and 7 meters, barely penetrable on foot.

Results of earth resistivity measurements (at dc) made in the middle of the clearing, along the airstrip, indicated subsurface conductivity stratification at the site. They show that the earth conductivity varied markedly with depth: there was a 0.3-meter-thick surface layer of conductivity 2 mmho/meter (dc), a 4.3-meter-thick mid-layer of conductivity 0.4 mmho/meter (dc), and a region below that having dc

conductivity 15 mmho/meter. Results of a soil survey done there under the direction of the MRDC-ES show the average moisture content of the sandy soil above 2 meters was 29 percent by weight.

5. Chumphon

The SRI test site on the isthmus of Kra southwest of Chumphon was in a low valley inundated by water during the continual rains, often to a depth of 30 cm. Some types of vegetation thrive under these conditions, forming a fresh-water swamp forest such as the Wisai Nua forest at Chumphon. The tree growth there was almost uniform throughout the forest stand. Its canopy was three-storyed as usual, but here the upper story was almost horizontally continuous, between 25 and 36 meters high. The middle story was 15 to 24 meters high. The lowest story contained about 60 percent of the trees, these between 7 and 14 meters high. The lowest trees were heavily suppressed by the continuous canopy above them, yet there was considerable undergrowth present.

The undergrowth was quite uniform, in two layers, the upper composed of tree seedlings and shrubs growing to 4 meters; the lower layer, only 0.3 meters high, had mostly herbs. Below these, the soft, muddy forest floor was covered with a layer of humus several centimeters thick.

The soil at the Chumphon site was silty clay with gravel interspersed. The clay in the forest was grey, having a mixture of humus that improved its water-holding capability (average surface moisture content 70 percent); most of the clay in the clearing was reddish, and often dried at the surface between rains (average surface moisture content 25.4 percent). At a depth of 2 to 15 cm in the clearing, the soil was water-saturated at all times. The surface soil at some locations remained saturated with water during the entire summer, being low-lying areas fed by a stream.

"PREVIOUS PAGE BLANK-NOT FILMED".

Appendix B

PROJECT PERSONNEL

Appendix B

PROJECT PERSONNEL

The personnel listed below (by primary location and affiliation) participated in this project at various times from its initiation in 1962 through its completion in 1970.

A. Stanford Research Institute, Menlo Park, California

W. R. Vincent	Supervisor
G. H. Hagn	Project Leader
A. O. Williams	Administrator
E. T. Fierce	Staff Scientist
H. W. Parker	Physicist
G. E. Barker	Research Engineer
T. S. Cory	Research Engineer
N. E. Goldstein	Research Engineer
J. D. Hice	Research Engineer
E. M. Kreinberg	Research Engineer
W. A. Ray	Research Engineer
J. M. Yarborough	Research Engineer
C. Barnes	Development Engineer
A. Fuller	Development Engineer
S. S. Martensen	Programmer
M. Brushberg	Programmer
B. E. Frank	Programmer
W. A. Hall	Programmer
K. A. Posey	Research Assistant

B. Bangkok, Thailand

1. Stanford Research Institute

R. E. Leo	Technical Director (1963-1965)
E. L. Younker	Technical Director (1965-1967)
G. D. Koehrsen	Administrator (1963-1966)
J. J. Balestrini	Administrator (1966-1967)
D. J. Barnes	Senior Research Engineer
R. L. Brown	Senior Research Engineer
R. Daniel	Field Engineer
D. J. Lyons	Field Engineer
J. E. van der Laan	Field Engineer
R. J. Ratliff	Field Engineer
W. N. Ward	Field Engineer

2. Montana State University

C. L. Rufenach	Research Engineer
N. K. Shrawan	Research Engineer

3. Pan Supplies

Ponsak Buasri	Research Engineer
Prajuab Nimityongskul	Research Engineer
Rangsit Chindaphorn	Research Engineer
Vichai Thepgoonhanimitta	Research Engineer
Vichit Lorcharachoonkul	Research Engineer
Withnn Makarabhiromya	Research Engineer
Boonsong Punyarat	Data Supervisor

4. Vitro Corporation

J. W. Chapman	Field Engineer
K. L. Taylor	Field Engineer
F. J. Phillips	Field Engineer

5. Military Research and Development Center

Prapat Chandaket, Captain R.T.N., Communications Program
Manager (1963-1967)

Termpoon Kovattana, Wing Commander, R.T.A.F., Project Officer
(1963-1965)

Deputy Communications Program Manager (1965-1967)

Paibul Nacaskul, Commander, R.T.N., Project Officer (1963-1967)
Acting Director, MRDC-EL (1968-present)

Udom Suwanpramott, Major, R.T.A., Project Officer
Jammong Sowanna, Lieutenant Commander, R.T.N., Project Officer
Sukdichai Nivatmaraka, Flight Lieutenant, R.T.A.F., Project Officer
Chaikamol Lumjiak, Flying Officer, R.T.A.F., Project Officer
Manit Dowkhanon, C.P.O., R.T.N., Radio Technician
Charerm Deosang, C.P.O., R.T.N., Radio Technician
Vichcha Kanitchaya, S/SGT., R.T.A.F., Radio Technician
Rangsan Panthalanondthaka, S/SGT., R.T.A.F., Radio Technician
Sopin Viriyapanaporn, S/SGT., R.T.A.F., Communications

C. University of South Carolina, Columbia, South Carolina

John Taylor	Lead, Electrical Engineering
Gerald Bright	Student Engineer
Ching Chun Han	Student Engineer
Robert Padowicz	Student Engineer
Harry Smoak	Student Engineer
Chung Lien Tien	Student Engineer

"PRECEDING PAGE BLANK-NOT FILMED".

Appendix C

TECHNICAL REPORTS PREPARED UNDER THIS CONTRACT

Appendix C

TECHNICAL REPORTS PREPARED UNDER THIS CONTRACT

This appendix describes the various types of reports prepared under this contract and lists the reports.

1. Description of Types of Reports

a. Final Reports

Three reports prepared under this contract carry the name "Final Report":

- (1) Final Report--Vol. I. This report covers work performed under both Task I and Task II through 24 February 1964.
- (2) Final Report--Task I. This report covers work performed under Task I through the completion of this task in 1965.
- (3) Final Report--Task II. This is the present report covering the work performed under Task II through the completion of this task in 1969.

b. Semiannual Reports

Eight semiannuals have been prepared under this contract covering the period 1 September 1962 through 31 March 1967. The purpose of these reports was to document on a chronological basis the work performed, present a discussion of work planned for the following six-month period, present preliminary results of work that would be treated in more detail

in Research Memoranda and Special Technical Reports (see below), record work done that was of such a nature as not to warrant special technical reporting, and give selected administrative information (e.g., project personnel). The first three of these reports covered both Task I and Task II, whereas the remainder covered only Task II.

c. Research Memoranda and Special Technical Reports

These reports were prepared when subtasks were completed or when significant research plateaus had been reached. During the course of this contract 50 reports in these categories were initiated. These reports generally were numbered in sequence according to the preparation date of their first drafts, and no distinction was made between Research Memoranda (the earlier designation for this type of report) and Special Technical Reports (the later designation) or between reports prepared under Task I or Task II.

A few of these reports exist only in draft form. These report drafts have been referenced in order to credit the authors in this report whose work was summarized for this report, but the letter D has been added as a suffix to each of these report numbers to indicate that these reports are not available. Four of these reports (STRs 39D, 42D, 45D, and 46D) will be completed with support from USAECOM under Contract DAAB07-70-C-0550.

d. Geophysical Data Reports

Four types of data reports were prepared under this contract:

- (1) Ionospheric Data Reports. Twenty-five monthly data bulletins were prepared to report the results of vertical-incidence ionospheric soundings with a C-2 sounder at Bangkok from the beginning of sounder

operation in September 1963 through September 1965, when the operation of this sounder was undertaken by MRDC and USAECOM.* One report summarizing the vertical-incidence data obtained in Thailand with two oblique-incidence sounders between April 1966 and March 1967 also has been published.

- (2) Faraday Rotation Data Reports. Five reports, each covering about six months' observations at Bangkok of signals from Transit 4-A and S-66 between November 1964 and June 1967, have been published.
- (3) Atmospheric Radio Noise Data Reports. Eight quarterly reports on MF and HF atmospheric radio noise observed in Thailand between March 1966 and February 1968 on a standard ARN-2 vertical monopole have been published.
- (4) Magnetometer Data Reports. Four quarterly reports on the data obtained in Bangkok with a rubidium-vapor magnetometer during 1966 have been published.

e. Handbook Drafts

Draft versions of two types of "handbooks" have been prepared to assist the U.S. and Thai governments in converting the scientific and technical information gathered under Task II of this contract into a form more usable by personnel faced with the task of radio communication in the tropical environment:

*The MRDC has continued to operate the sounder and to publish these monthly data bulletins through the present. Inquiries about these later bulletins should be addressed to: Commanding General, Military Research and Development Center, Soi Kloy Nam Thai (42), Rama IV Road, Bangkok, Thailand.

- (1) "Questions and Answers about Field Radio Communications in the Tropics." This handbook draft is a source book of about 150 questions and answers about field communications in the tropics based upon SEACORE research and selected materials from other available sources. It was not within the scope of the current effort to generate a comprehensive field communications handbook. Rather, our goal has been to provide useful supplementary information for improving HF and VHF short-path communications in tropical areas.
- (2) "Instructor's Supplement to 'Questions and Answers about Field Radio Communications in the Tropics.'" This draft volume contains references to SRI SEACORE reports--by question number.

f. Monthly Letter Reports

Sixty-three Monthly Letter Reports were prepared under this contract to document project progress, approximate expenditures, and information on travel, visitors, etc. These reports covered the period 1 September 1962 through 31 December 1967--the period from the beginning of the contract through the end of SRI technical directorship of the MRDC-EL. They are not listed in this appendix.

2. List of Technical Reports

a. Final Reports

"Research-Engineering and Support for Tropical Communications," Final Report--Volume 1, covering the period 1 September 1962 through 29 February 1964 (September 1964), AD 480 594.

* York Lucci, "Countersurgency Communications Requirements in Thailand (U)," Final Report--Task I, CONFIDENTIAL (December 1966), AD 380 555.

G. H. Hagn, draft of "Questions and Answers about Field Radio Communications in the Tropics" (February 1970).

G. H. Hagn, draft of "Instructor's Supplement to 'Questions and Answers about Field Radio Communications in the Tropics'" (February 1970).

G. H. Hagn and G. E. Barker, "Research Engineering and Support for Tropical Communications," covering the period 1 September 1962 through 15 February 1970 (February 1970).

b. Semiannual Reports

W. R. Vincent, "Research-Engineering and Support for Tropical Communications," Semiannual Report 1, covering the period 1 September 1962 through 28 February 1963 (March 1963), AD 480 589.

"Research-Engineering and Support for Tropical Communications," Semiannual Report 2, covering the period 1 March through 3 August 1963 (September 1963), AD 480 590.

"Research-Engineering and Support for Tropical Communications," Semiannual Report 3, covering the period 1 March through 31 August 1963 (October 1964), AD 458 523.

R. E. Leo, G. H. Hagn, and W. R. Vincent, "Research Engineering and Support for Tropical Communications," Semiannual Report 4, covering the period 1 September 1964 through 31 March 1965 (October 1965), AD 474 163.

G. H. Hagn, H. W. Parker, and E. L. Younker, "Research-Engineering and Support for Tropical Communications," Semiannual Report 5, covering the period 1 April through 30 September 1965 (May 1966), AD 486 466.

* Prepared under Task I, Operations Analysis Program.

G. H. Hagn, E. L. Younker, and H. W. Parker, "Research-Engineering and Support for Tropical Communications," Semianual Report 6, covering the period 1 October 1965 through 31 March 1966 (June 1966), AD 653 608.

E. L. Younker, G. H. Hagn, and H. W. Parker, "Research-Engineering and Support for Tropical Communications," Semianual Report 7, covering the period 1 April through 30 September 1966 (September 1966), AD 653 615.

E. L. Younker, G. H. Hagn, and H. W. Parker, "Research-Engineering and Support for Tropical Communications," Semianual Report 8, covering the period 1 October 1966 through 31 March 1967 (May 1967), AD 675 459.

c. Special Technical Reports and Research Memorandums

*Kenneth Dimmick, "Communications Systems Implications of Thai Speech," Special Technical Report 1 (June 1965), AD 473 557.

W. R. Vincent, "Voice Tests on Man-Pack Radios in a Tropical Environment," Research Memorandum 2 (July 1963), AD 480 591.

W. R. Vincent, "Field Tests on Man-Pack Radios in a Tropical Environment," Research Memorandum 3 (July 1963), AD 473 860.

T. S. Cory, "Scale-Model Measurements on a Sloping-Wire Antenna," Research Memorandum 4 (June 1963).

George H. Hagn, "Orientation of Linearly Polarized HF Antennas for Short-Path Communication via the Ionosphere near the Geomagnetic Equator," Research Memorandum 5 (August 1963, revised June 1964), AD 418 497 and AD 480 592.

Douglas J. Barnes, Gary E. Barker, and George H. Hagn, "Measured Impedances of Simple Field-Expedient Antennas in Open and Forested Terrain," Special Technical Report 6. (This report exists only in draft form. The major results of this study are given in Section III-F).

Terry S. Cory and William A. Ray, "Measured Impedances of Some Tactical Antennas near Ground," Research Memorandum 7 (February 1964), AD 480 593.

*Prepared under Task I, Operations Analysis Program.

N. K. Shreuger, "Field Tests of VHF Man-Pack Radios," Special Technical Report 8 (April 1965), AD 480 587.

George H. Hagn, "Absorption of Ionospherically Propagated HF Radio Waves under Conditions where the Quasi-Transverse (QT) Approximation Is Valid," Special Technical Report 9 (September 1964), AD 480 588.

William A. Ray, "Full-Scale Pattern Measurements of Simple HF Field Antennas," Special Technical Report 10 (May 1966), AD 487 494.

George H. Hagn, "The Use of Ground Wave Transmission-Loss and Intelligibility Test to Predict Effective Range and Performance of VHF Manpack Radios in Forests," Special Technical Report 11 (September 1966), AD 672 069.

George H. Hagn and Kenneth A. Posey, "Survey of Literature Pertaining to the Equatorial Ionosphere and Tropical Communication," Special Technical Report 12 (February 1966), AD 486 800.

G. H. Hagn, K. A. Posey, and H. W. Parker, "Subject Index for Survey of Literature Pertaining to the Equatorial Ionosphere and Tropical Communication," Special Technical Report 12--Addendum (October 1966), AD 805 545.

H. W. Parker and G. H. Hagn, "Feasibility Study of the Use of Open-Wire Transmission Lines, Capacitors, and Cavities to Measure the Electrical Properties of Vegetation," Special Technical Report 13 (August 1966), AD 489 294.

C. L. Rufenach, Vichai T. Nimit, and R. E. Leo, "Faraday Rotation Measurements of Electron Content near the Magnetic Equator Using the Transit IV-A Satellite," Special Technical Report 14 (January 1966), AD 486 729.

Clifford L. Rufenach and George H. Hagn, "Comparison of C-2 Ionospheric Sounder Data with Frequency Predictions for Short-Range Communication with Man-Pack Transceivers in Thailand," Special Technical Report 15 (August 1966), AD 662 065.

John Taylor, "A Note on the Computed Radiation Patterns of Dipole Antennas in Dense Vegetation," Special Technical Report 16 (February 1966), AD 487 495.

John Taylor, Kenneth A. Posey, and George H. Hagn, "Literature Survey Pertaining to Electrically Small Antennas, Propagation through Vegetation, and Related Topics," Special Technical Report 17 (January 1966), AD 624 155.

George H. Hagn, Jan E. van der Laan, David J. Lyons, and Edwin M. Kreinberg, "Ionospheric Sounder Measurement of Relative Gains and Bandwidths of Selected Field-Expedient Antennas for Skywave Propagation at Near-Vertical Incidence," Special Technical Report 18 (January 1966), AD 489 537.

George H. Hagn, Gary E. Barker, Harold W. Parker, James D. Nice, and William A. Ray, "Preliminary Results of Full-Scale Pattern Measurements of Simple VHF Antennas in a Eucalyptus Grove," Special Technical Report 19 (January 1966), AD 484 239.

*Anton D. Levandowsky, "Human Factors in Thai Counterinsurgency Communications," Special Technical Report 20 (January 1966), AD 825 327L.

Sven E. Wahlstrom, "Controller's Data Display Mark II--Instruction Manual," Special Technical Report 21 (June 1966), AD 486 799.

*Donald A. Price, "Survey of Existing Communications Systems in Thailand (U)," Special Technical Report 22 (May 1966), CONFIDENTIAL, AD 377 365.

*J. A. McLeod and R. E. Morse, "Communications in Low-Intensity Counterinsurgency: A Study of the Border Patrol Police in Thailand (U)," Special Technical Report 23 (May 1966), SECRET, AD 383 804L.

*Angelo Gualtieri, "Communications Traffic Requirements to Support Counterinsurgency Operations Against Medium-Level Insurgency in Thailand (U)," Special Technical Report 24 (May 1966), CONFIDENTIAL, AD 377 364.

William A. Ray, Gary E. Barker, and Sandra S. Martensen, "Full-Scale Pattern Measurements of Simple HF Field Antennas in a U.S. Conifer Forest," Special Technical Report 25 (February 1967), AD 653 165.

* Prepared under Task I, Operations Analysis Program.

N. K. Shrauger and K. L. Taylor, "Initial VHF Propagation Results Using Xeledop Techniques and Low Antenna Heights," Special Technical Report 26 (December 1966), AD 653 609.

R. L. Brown, "Manual for ARN-3 Type Atmospheric Noise Measuring Equipment," Special Technical Report 27 (November 1966), AD 653 780.

Clifford L. Rufenach, "Evaluation and Prediction of Maximum Usable Frequency (MUF) over Bangkok," Special Technical Report 28 (January 1967), AD 655 566.

Termpoon Kovattana, "Electrical Ground Constants of Central, Eastern, and Northeastern Thailand," Special Technical Report 29 (February 1967), AD 661 058.

N. E. Goldstein, H. W. Parker and G. H. Hagn, "Three Techniques for Measurement of Ground Constants in the Presence of Vegetation," Special Technical Report 30 (March 1967), AD 672 496.

Lt. Cdr. Paibul Nacaskul, R.T.N., "Orientation Measurements in Thailand with HF-Dipole Antennas for Tactical Communication," Special Technical Report 31 (June 1967), AD 675 460.

J. E. van der Laan, "Ionospheric and Magnetic Observation at Bangkok, Thailand, During the Annular Solar Eclipse on November 23, 1965," Special Technical Report 32 (December 1967), AD 672 068.

Vichai T. Nimit, "Measurements of Equatorial Magnetic Dip Angle at Ionospheric Heights," Special Technical Report 33 (May 1967), AD 662 064.

Vichai T. Nimit, "Measurements of Electron Content and Latitudinal F-Layer Critical Frequency Near the Magnetic Equator," Special Technical Report 34 (December 1967), AD 675 461.

Gary E. Barker and Glenn D. Koehrsen, "Full-Scale Pattern Measurements of Simple HF Field Antennas in a Tropical Forest in Thailand," Special Technical Report 35 (February 1968), AD 647 739.

N. K. Shrauger and E. M. Kreiberg, "Selected Examples of VHF Signal Propagation Records in Tropical Terrains," Special Technical Report 36 (November 1967), AD 672 070.

Rangsit Chindahporn and E. Leroy Younker, "Analysis of Medium- and High-Frequency Atmospheric Radio Noise in Thailand," Special Technical Report 37 (May 1968), AD 681 878.

G. H. Hagn and D. J. Barnes, "Sounder Measurements of the Relative Gain of HF Field-Expedient Antennas on Short Ground and Skywave Paths in Thailand," Special Technical Report 38D. (This report exists only in draft form. The major results are given in Section III-E.)

G. E. Barker and W. A. Hall, "Full-Scale Pattern Measurements of Simple VHF Antennas in a Thailand Tropical Forest," Special Technical Report 39D. (This report will be published under Contract DAAB07-70-C-0550.)

Vichit T. Nimit, "Further Evaluation of Frequency Predictions for Short-Path Radio Communications in Thailand," Special Technical Report 40 (January 1968), AD 675 462.

Vichit Lorchirachoonkul, "A Study of the Electromagnetic Properties of an Isolated Tree," Special Technical Report 41 (February 1968), AD 687 298.

John Taylor, Ching Chun Han, Chung Lien Tien, and George H. Hagn, "Open-Wire Transmission Line Techniques for Measuring the Macroscopic Electrical Properties of a Forest Region," Special Technical Report 42D. (This report will be published under Contract DAAB07-70-C-0550.)

H. W. Parker and Wilthan Makarabhiromya, "Electric Constants Measured in Vegetation and in Earth at Five Sites in Thailand," Special Technical Report 43 (December 1967), AD 674 740.

J. E. van der Laan, D. J. Lyons, D. J. Barnes, and G. H. Hagn, "VHF Diffraction and Groundwave Propagation Tests Using Ionospheric Sounders," Special Technical Report 44 (June 1968).

Gary E. Barker, John Taylor, and George H. Hagn, "Measurements and Modeling of the Radiation Patterns of Simple HF Field Antennas over Level, Mountainous and Forested Terrains," Special Technical Report 45D. (This report will be published under Contract DAAB07-70-C-0550.)

G. H. Hagn, N. K. Shrauger and G. E. Barker, "VHF Propagation Results Using Low Antenna Heights in Tropical Forests," Special Technical Report 46D. (This report will be published under Contract DAAB07-70-C-0550.)

George H. Hagn, Rangsit Chindahporn, and John M. Yarborough, "HF Atmospheric Radio Noise on Horizontal Dipole Antennas in Thailand," Special Technical Report 47 (June 1968), AD 681 879.

D. J. Barnes, G. H. Hagn, J. W. Chapman, D. J. Lyons, and J. E. van der Laan, "Results of Ionospheric Sounding and Communication Experiments Along North-South Paths in Thailand," Special Technical Report 48D. (This report exists only in draft form. The major results of this work are given in Sections IV-A-2 and IV-B-1.)

E. T. Pierce, "The Counting of Lightning Flashes," Special Technical Report 49 (June 1968), AD 682 023.

G. H. Hagn and J. W. Chapman, "Observations of Sudden Ionospheric Disturbances in Thailand," Special Technical Report 50D. (This report exists only in draft form. The major results of this study are given in Sections IV-C-2 and IV-C-3.)

d. Data Bulletins

1) Ionospheric Data

Vichai T. Nimit, "Ionospheric Data: Bangkok, Thailand," Ionospheric Data Report, September 1963 (March 1965), AD 800 613.

Vichai T. Nimit, "Ionospheric Data: Bangkok, Thailand," Ionospheric Data Report, October 1963 (March 1965), AD 800 614.

Vichai T. Nimit, "Ionospheric Data: Bangkok, Thailand," Ionospheric Data Report, November 1963 (March 1965), AD 480 574.

Vichai T. Nimit, "Ionospheric Data: Bangkok, Thailand," Ionospheric Data Report, December 1963 (January 1965), AD 800 615.

Vichai T. Nimit, "Ionospheric Data: Bangkok, Thailand,"
Ionospheric Data Report, January 1964 (January 1965),
AD 800 616.

Vichai T. Nimit, "Ionospheric Data: Bangkok, Thailand,"
Ionospheric Data Report, February 1964 (December 1964),
AD 800 617.

Vichai T. Nimit, "Ionospheric Data: Bangkok, Thailand,"
Ionospheric Data Report, March 1964 (December 1964),
AD 800 618.

Vichai T. Nimit, "Ionospheric Data: Bangkok, Thailand,"
Ionospheric Data Report, April 1964 (November 1964), AD
800 619.

Vichai T. Nimit, "Ionospheric Data: Bangkok, Thailand,"
Ionospheric Data Report, May 1964 (August 1964), AD 800
620.

Vichai T. Nimit, "Ionospheric Data: Bangkok, Thailand,"
Ionospheric Data Report, June 1964 (September 1964).

Vichai T. Nimit, "Ionospheric Data: Bangkok, Thailand,"
Ionospheric Data Report, July 1964 (May 1965), AD 480 575.

Vichai T. Nimit, "Ionospheric Data: Bangkok, Thailand,"
Ionospheric Data Report, August 1964 (May 1965), AD 480
576.

Vichai T. Nimit, "Ionospheric Data: Bangkok, Thailand,"
Ionospheric Data Report, September 1964 (May 1965), AD
480 577.

Vichai T. Nimit, "Ionospheric Data: Bangkok, Thailand,"
Ionospheric Data Report, October 1964 (March 1965), AD
480 578.

Vichai T. Nimit, "Ionospheric Data: Bangkok, Thailand,"
Ionospheric Data Report, November 1964 (March 1965), AD
800 621.

Vichai T. Nimit, "Ionospheric Data: Bangkok, Thailand,"
Ionospheric Data Report, December 1964 (March 1965), AD
800 622.

Vichai T. Nimit, "Ionospheric Data: Bangkok, Thailand,"
Ionospheric Data Report, January 1965 (June 1965), AD
480 579.

Vichai T. Nimit, "Ionospheric Data: Bangkok, Thailand,"
Ionospheric Data Report, February 1965 (June 1965), AD
480 580.

Vichai T. Nimit, "Ionospheric Data: Bangkok, Thailand,"
Ionospheric Data Report, March 1965 (June 1965), AD 480 581.

Vichai T. Nimit, "Ionospheric Data: Bangkok, Thailand,"
Ionospheric Data Report, April 1965 (June 1965), AD 485 491.

Vichai T. Nimit, "Ionospheric Data: Bangkok, Thailand,"
Ionospheric Data Report, May 1965 (July 1965), AD 480 582.

Vichai T. Nimit, "Ionospheric Data: Bangkok, Thailand,"
Ionospheric Data Report, June 1965 (August 1965), AD 800 623.

Vichai T. Nimit, "Ionospheric Data: Bangkok, Thailand,"
Ionospheric Data Report, July 1965 (October 1965), AD 480
624.

Vichai T. Nimit, "Ionospheric Data: Bangkok, Thailand,"
Ionospheric Data Report, August 1965 (October 1965), AD
480 583.

Vichai T. Nimit, "Ionospheric Data: Bangkok, Thailand,"
Ionospheric Data Report, September 1965 (February 1966),
AD 800 625.

Bernadine E. Frank and George H. Hagn, "Vertical-Incidence
Ionospheric Data: Thailand," Ionospheric Data Report,
April 1966 to March 1967 (December 1967), AD 669 601.

2) Faraday Rotation Data

Vichai T. Nimit, Boonsong Punyarat, and Clifford L.
Rufenach, "Faraday Rotation Data: Bangkok, Thailand,"
Geophysical Data Reports--November 1964 through June 1965
(February 1966).

Vichai T. Nimit, Boonsong Puayarat, and Clifford L. Rufenach, "Faraday Rotation Data: Bangkok, Thailand," Geophysical Data Report--July 1965 through December 1965 (May 1966), AD 486 677.

Vichai T. Nimit, "Faraday Rotation Data: Bangkok, Thailand," Geophysical Data Report--January through June 1966 (July 1966), AD 488 204.

Vichai T. Nimit, "Faraday Rotation Data: Bangkok, Thailand," Geophysical Data Report--July through December 1966 (January 1967), AD 807 773.

Vichai T. Nimit, "Faraday Rotation Data: Bangkok, Thailand," Geophysical Data Report--January through June 1967 (July 1967), AD 819 257.

3) Atmospheric Noise Data

Rangsit Chindahporn, Lt. Chaikamol Lumjiak, and Prajuab Nimitpongskul, "Atmospheric Radio Noise Data, Bangkok, Thailand: March-May 1966," Geophysical Data Report (January 1967), AD 653 616.

Rangsit Chindahporn, Lt. Chaikamol Lumjiak, and Prajuab Nimitpongskul, "Atmospheric Radio Noise Data, Bangkok, Thailand: June-August 1966," Geophysical Data Report (January 1967), AD 652 685.

Rangsit Chindahporn, Lt. Chaikamol Lumjiak, and Prajuab Nimitpongskul, "Atmospheric Radio Noise Data, Bangkok, Thailand: September-November 1966," Geophysical Data Report (March 1967), AD 653 164.

Rangsit Chindahporn, Lt. Chaikamol Lumjiak, and Prajuab Nimitpongskul, "Atmospheric Radio Noise Data, Bangkok, Thailand: December 1966-February 1967," Geophysical Data Report (March 1967), AD 662 771.

Rangsit Chindahporn, Lt. Chaikamol Lumjiak, and Prajuab Nimitpongskul, "Atmospheric Radio Noise Data, Bangkok, Thailand: March-May 1967," Geophysical Data Report (October 1967), AD 663 801.

Rangsit Chindahporn, Lt. Chaikamol Lumjaiak, and Ponsak Buasri, "Atmospheric Radio Noise Data, Bangkok, Thailand: June-August 1967," Geophysical Data Report (October 1967), AD 663 802.

Rangsit Chindahporn and Ponsak Buasri, "Atmospheric Radio Noise Data, Bangkok, Thailand: September-November 1967," Geophysical Data Report (December 1967), AD 665 382.

Rangsit Chindahporn and Ponsak Buasri, "Atmospheric Radio Noise Data, Bangkok, Thailand: December 1967-February 1968," Geophysical Data Report (May 1968), AD 670 052.

4) Magnetometer Data

Douglas J. Barnes and John Chapman, "Geomagnetic Data, Bangkok, Thailand: January-March 1966," Geophysical Data Report (March 1967), AD 659 407.

Douglas J. Barnes and John Chapman, "Geomagnetic Data, Bangkok, Thailand: April-June 1966," Geophysical Data Report (June 1967), AD 667 957.

Douglas J. Barnes and John Chapman, "Geomagnetic Data, Bangkok, Thailand: July-September 1966," Geophysical Data Report (September 1967), AD 665 377.

Douglas J. Barnes and John Chapman, "Geomagnetic Data, Bangkok, Thailand: October-December 1966," Geophysical Data Report (December 1967), AD 667 958.

"PRECEDING PAGE BLANK-NOT FILMED".

REFERENCES

1. J. W. Herbstreit and W. Q. Crichton, "Measurement of Factors Affecting Jungle Radio Communications," Report ORB-2-3, Operational Research Staff, Office of the Chief Signal Officer, Washington, D.C. (November 1943). Note: This work was subsequently summarized as "Measurement of the Attenuation of Radio Signals by Jungles," in Radio Science, Vol. 68D, No. 8, pp. 903-906 (August 1961).
2. H. A. Whale, "Radio Propagation Through New Guinea Rain Forest," Report No. 8, Department of Scientific and Industrial Research Operational Research Section, Wellington, New Zealand (1944). Note: This work was subsequently summarized in Radio Science, Vol. 3, No. 10 (October 1968).
3. L. G. Sturgill et al., "Tropical Propagation Research, Final Report, Vol. I, Jansky and Bailey Engineering Division, Atlantic Research Corporation, Alexandria, Virginia (June 1966).
4. D. J. Pounds and A. H. La Grone, "Considering Forest Vegetation as an Imperfect Dielectric Slab," Report 6-53, Contract AF 19(604)-8038, Project 4603, The Electrical Engineering Research Laboratory, University of Texas, Austin, Texas (1963) AD 410336.
5. B. A. Lippmann, "The Jungle as a Communication Network," IMR-168/1, Defense Research Corp., Santa Barbara, California (1965).
6. D. L. Sachs and P. J. Wyatt, "A Conducting Slab Model for Electromagnetic Propagation Within a Jungle Medium," Technical Memorandum 376, General Research Corp. (May 1966), AD 679 171. [This work was summarized: Radio Science, Vol. 3, No. 2 (February 1968)].
7. T. Tamir, "The Role of the Skywave and Lateral Waves on Propagation in Forest Environments," Technical Report, U.S. Army Electronics Command, Fort Monmouth, New Jersey (March 1967). [An expanded version is: "On Radio-Wave Propagation in Forest Environments," IEEE Transactions on Antennas and Propagation, Vol. AP-15, No. 6 (November 1967)].

8. D. Dence and T. Tamir, "Transmission Losses in a Forest for Antennas Close to the Ground," Tech. Report ECOM-2940, U.S. Army Electronics Command, Fort Monmouth, New Jersey (1968). (This work was subsequently summarized in an expanded version: "Radio Loss of Lateral Waves in Forest Environments," Radio Science, Vol. 4, No. 4 (April 1969).)

9. J. R. Wait, "Asymptotic Theory for Dipole Radiation in the Presence Of a Lossy Slab Lying on a Conducting Half-Space," IEEE Trans. Antennas and Propagation, Vol. AP-15, No. 5, pp. 645-648 (September 1967).

10. L. G. Sturgill, et al., "Tropical Propagation Research," Semiannual Report 7, Jansky and Bailey, Alexandria, Virginia, p. A-2 (January 1960).

11. S. Sabhasri and L. E. Wood, "Forest Biomass in Thailand," Military Research and Development Center, Bangkok, Thailand (October 1967).

12. R. M. Dickinson, P. D. Potter, and W. J. Schimek, "Tree Antennas," Space Technology Applications Report 33-1, Jet Propulsion Laboratory, California Institute of Technology, Pasadena, California (May 1967).

13. E. J. Kirkscether, "Ground Constant Measurements Using a Section of Balanced Two-Wire Transmission Line," IRE Trans. Antennas and Propagation, Vol. AP-8, No. 3, pp. 307-312 (May 1960).

14. C. Barnes, Jr., "Transmitters Towed Through Air Test Antenna's Radiation Pattern," Electronics, pp. 96-101 (October 18, 1965).

15. C. Barnes, J. A. Hudick, and M. E. Mills, "A Field Guide to Simple HF Dipoles," SRI Project 6183, Contract DA 28-043 AMC-C2201(E), p. 28, Stanford Research Institute, Menlo Park, California (March 1967).

16. J. E. Shirley, "The Shirley Aerial - A Vertically Beamed Antenna for Improved Short Distance Sky Waves," Report 8/52, Operational Research Section, Far East Land Forces, Great Britain (1952).

17. G. H. Hagn and J. E. van der Laan, "Measured Relative Responses Toward the Zenith of Short-Whip Antennas on Vehicles at High Frequencies," IEEE Trans. Vehicular Technology (to be published August 1970).

18. M. G. Andreasen and F. B. Harris, Jr., "Analysis of Wire Antennas of Arbitrary Configuration by Precise Theoretical Numerical Techniques," Final Report ECOM-0631 Contract No. DAABC7-67-C-0631, U.S. Army Electronics Command (July 1968). [The model described in this report has been further developed by Technology for Communications International, Mountain View, California.]
19. W. R. Vincent and G. H. Hagn, "Comments on the Performance of VHF Vehicular Radio Sets in Tropical Forests," IEEE Trans. Vehicular Technology, Vol. VF-18, No. 2, pp. 61-65 (August 1969).
20. K. D. Felperin, D. J. Barnes, and R. T. Wolfram, "SRI Correlation Computer," Stanford Research Institute, Menlo Park, California (June 1965).
21. R. T. Wolfram, K. D. Felperin and B. C. Tupper, "SRI Doppler Spread Meter," Stanford Research Institute, Menlo Park, California (December 1965).
22. J. A. Ratcliffe, The Magneto-ionic Theory and Its Applications to the Ionosphere, (Cambridge University Press, 1959).
23. Y. Hakura, "On the Relationship Between Solar Eruptions and Geomagnetic and Ionospheric Disturbances," in Some Ionospheric Results Obtained During the IGY, ed. W.J.G. Beynon (Elsevier 1960).
24. W. H. Ahlbeck, W. Q. Crichlow, R. T. Disney, F. F. Fulton, Jr., and C. A. Samson, "Instruction Book for ARN-2 Radio Noise Recorder, Serial Numbers 1 to 10," NBS Report 5545, National Bureau of Standards, Boulder, Colorado (3 January 1958).
25. W. Q. Crichlow, C. A. Samson, R. T. Disney, and M. A. Jenkins, "Radio Noise Data for the International Geophysical Year July 1, 1957 - December 31, 1958," Technical Note 18, National Bureau of Standards, Boulder, Colorado (27 July 1959). (Quarterly Radio Noise Data after the IGY have been published as Technical Note 18-n).
26. "World Distribution and Characteristics of Atmospheric Radio Noise," CCIR Report 322, Doc. X, Plenary Assembly, Geneva, 1963 (Int. Tele. Union, Geneva, 1964).
27. O. Thukun, "Variations of Radio Noise Parameters at a Tropical Station," J. Atmos. Terr. Phys., Vol. 27, pp. 1081-1093 (1965).
28. Ardharn Kullavanijaya, "Investigation of Radio Broadcasting Interference in Bangkok," M. S. Thesis, Chulalongkorn University (April 1965).

UNCLASSIFIED

Security Classification

DOCUMENT CONTROL DATA - R & D

(Security classification of title, body of abstract and indexing annotation must be entered when the overall report is classified)

1. ORIGINATING ACTIVITY (Corporate author) Stanford Research Institute 333 Ravenswood Avenue Menlo Park, California 94025	2a. REPORT SECURITY CLASSIFICATION Unclassified
	2b. GROUP N/A

3. REPORT TITLE

RESEARCH ENGINEERING AND SUPPORT FOR TROPICAL COMMUNICATIONS

4. DESCRIPTIVE NOTES (Type of report and inclusive dates)

Final Report Covering the Period 1 September 1962 through 15 February 1970

5. AUTHORISI (First name, middle initial, last name)

G. H. Hagn

G. E. Barker

6. REPORT DATE February 1970	7a. TOTAL NO. OF PAGES 278	7b. NO. OF REFS 28
8a. CONTRACT OR GRANT NO. DA 36-039 AMC-00040(E)	8b. ORIGINATOR'S REPORT NUMBER(S) Final Report SRI Project 4240	
8c. PROJECT NO. Order No. 5384-PM-63-91	8d. OTHER REPORT NO(S) (Any other numbers that may be assigned to this report)	
8e. ARPA Order No. 371		

10. DISTRIBUTION STATEMENT

11. SUPPLEMENTARY NOTES Report on communication research in Thailand	12. SPONSORING MILITARY ACTIVITY Advanced Research Projects Agency Washington, D.C.
---	--

13. ABSTRACT

This report summarizes the results of the technical and scientific research effort on radio communications in the tropical environment conducted by the Stanford Research Institute under the SEACORE Program of the Advanced Research Projects Agency's Project AGILE [Contract DA 36-039 AMC-00040(E)]. The work included studies of HF ionospheric propagation and prediction; MF and HF atmospheric radio noise; HF and VHF propagation through tropical terrain including forests (jungle), paddy fields, and mountains; and modeling and measurement of the directivity patterns of antennas emersed in forests.

KEY WORDS	LINK A		LINK B		LINK C	
	HOLE	WT	HOLE	WT	HOLE	WT
Bangkok, Thailand						
HF and VHF Communications						
Manpack radio						
Forest (jungle)						
Slab model						
Ground electrical constants						
Vegetation electrical constants						
Dipole, inverted L, slant wire, whip						
Antenna impedance in forest						
Antenna directivity and gain						
Airborne pattern measurements (Xeledop)						
Ionospheric frequency prediction						
Ionospheric sounding						
Sporadic E						
Faraday rotation studies						
Atmospheric radio noise						
Lightning-flash counter						
SEACORE						